



**HAL**  
open science

# Transition from compression to strike-slip tectonic styles along the northern margin of the Levant Basin

Vasilis Symeou

► **To cite this version:**

Vasilis Symeou. Transition from compression to strike-slip tectonic styles along the northern margin of the Levant Basin. Earth Sciences. Sorbonne Université, 2018. English. NNT : 2018SORUS003 . tel-02078777

**HAL Id: tel-02078777**

**<https://theses.hal.science/tel-02078777>**

Submitted on 25 Mar 2019

**HAL** is a multi-disciplinary open access archive for the deposit and dissemination of scientific research documents, whether they are published or not. The documents may come from teaching and research institutions in France or abroad, or from public or private research centers.

L'archive ouverte pluridisciplinaire **HAL**, est destinée au dépôt et à la diffusion de documents scientifiques de niveau recherche, publiés ou non, émanant des établissements d'enseignement et de recherche français ou étrangers, des laboratoires publics ou privés.

# Université Pierre et Marie Curie

Ecole doctorale Géosciences, Ressources Naturelles et Environnement

*Institut des Sciences de la Terre de Paris*

## **Transition from compression to strike-slip tectonic styles along the northern margin of the Levant Basin**

Presented by:

Vasilis SYMEOU

Doctorale thesis in Geosciences

Directed by Catherine HOMBERG, Fadi Henri NADER and  
Romain DARNAULT

Presented on: 23/02/2018

Members of the Jury:

Mr. JACKSON Christopher	Imperial College London	Reviewer
Mr. SOSSON Marc	Univ. of Nice, Sophia-Antipolis	Reviewer
Mrs. ZOMENI Zomenia	Cyprus Geo. Surv. Department	Examiner
Mrs. LEROY Sylvie	Sorbonne Uni. - ISTeP	Examiner
Mr. KOKKALAS Sotiris	Petroleum Instit. Abu Dhabi UAE	Examiner
Mr. BARRIER Eric	Sorbonne Uni. - ISTeP	Examiner
Mrs. HOMBERG Catherine	Sorbonne Uni. - ISTeP	Thesis Director
Mr. NADER Fadi-Henri	IFPEN	Co-Director
Mr. DARNAULT Romain	IFPEN	Co-Director



*This PhD thesis is dedicated to the memory of my loving Mother.*

## *Acknowledgement*

First and foremost I would like to thank my supervising team and all my colleagues who aided me during these last three years. This project was launched in order to extend the knowledge of the Levant Basin towards to the east, after the first projects which started in Lebanon. With this in mind I would like to warmly thank my supervisor Fadi Nader for his initiative and Mr. Solon Kassinis, as he was the person who convinced me to pursue this PhD project.

It is with warmth and gratitude that I thank the director of my thesis, Catherine Homberg for all the assistance, methodical way of work and co-operation that helped me finalize this project. Fadi Nader is thanked for all the time he spent guiding and supporting me throughout the duration of my thesis. It is with great pleasure that I thank Romain Darnault which stood by my side and helped me understand the back stripping processes and aided me in the field. Jean-Claude Lecomte is thanked for his help with the interpretation software and the long discussions on the seismic interpretation of the data. A warm thank goes out to Jean-Marc Daniel, although we didn't work too long as he left his post at IFPE, the first steps were made easier and smoother by his experience and knowhow.

I would like to thank dearly Dr. Stelios Nicolaidis and Mrs Eleni Mavraki for their pivotal role that they played in helping me acquire a scholarship through the Ministry of Energy, Commerce, Industry and Tourism of the Republic of Cyprus.

I am indebted to Dr. Zomenia Zomeni and Dr. Efthymios Tsiolakis of the Geological Survey Department of Cyprus, for the endless efforts to help me and the valuable and constructive conversations we had together which helped me understand, even if it's a small fraction of the abundant knowledge that they have gained through years of work onshore Cyprus.

A heartfelt thank you goes out to all the new friends I had the pleasure to spend time with here in Paris. Especially Nikolas, Richard and Anouk which made my time here special, engaging in many activities with the favorite undoubtedly being the long summer night at the Seine drinking beers and discussing science, trips and our everyday lives.

Finally, I would like to extend a warm thank you to my family for always being there for me and always having my back all these years even if I am away from home. Thank you very much and it is very much appreciated.



## Table of Contents

<i>Abstract</i> .....	31
<i>Resume</i> .....	34
<i>Chapter 1</i> .....	38
<i>Introduction</i> .....	38
<i>Chapter 2</i> .....	48
<i>Geological Setting</i> .....	48
2.1 Regional geology.....	49
2.1.1 Late Permian – Early Jurassic .....	51
2.1.2 Late Jurassic – Early Cretaceous.....	55
2.1.3 Upper Cretaceous – Oligocene.....	59
2.1.4 Miocene – Present .....	64
2.2 Gravity and magnetic data.....	68
2.2.1 Gravity data .....	68
2.2.2 Magnetic data .....	73
2.3 Geology of Cyprus .....	73

2.3.1 Stratigraphic Units.....	73
2.3.2 Sedimentary basins.....	76
2.3.3 Main faults.....	85
2.3.4 Offshore Structures .....	90
2.3.5 Present-day tectonics.....	92
<i>Chapter 3</i> .....	96
<i>Offshore tectonic structure investigation</i> .....	96
3.1 Methodology .....	97
3.1.1 Data .....	97
3.1.2 Stratigraphic picking and time determinations.....	98
3.1.3 Structural interpretation on seismic profiles .....	99
3.1.4 Time to Depth conversion .....	101
Start of Article.....	102
3.2 Abstract .....	102
3.3 Introduction .....	103
3.4 Geological Setting.....	104

3.4.1 Early Triassic – Early Cretaceous .....	105
3.4.2 Upper Cretaceous – Oligocene.....	105
3.4.3 Miocene – Present .....	107
3.5 Data and Methodology .....	108
3.6 Results .....	110
3.6.1 Seismo-stratigraphy and structural domains .....	110
3.6.2 Tectonic structures and timing of deformation .....	113
3.7 Discussion .....	123
3.7.1 Miocene .....	124
3.7.2 Pliocene to Recent.....	126
3.8 Conclusions .....	128
<i>Chapter 4</i> .....	131
<i>Onshore tectonic structure investigations</i> .....	131
4.1 Surface and sub-surface data analysis .....	133
4.1.1 Borehole data analysis and sedimentary units.....	133
4.1.2 Surface data and map revisions .....	140

4.2 Polis Basin.....	140
4.2.1 Compressional structures .....	143
4.2.2 Extensional structures .....	151
4.2.3 Transpressional structures .....	154
4.3 Polemi Basin .....	156
4.3.1 Compressional structures .....	156
4.3.2 Extensional structures .....	159
4.4 Limassol Basin .....	161
4.4.1 Compressional regime .....	163
4.4.2 Extensional structures .....	172
4.4.3 Transpressional regime .....	173
4.5 Synthetic Cross sections.....	174
4.5.1 Cross sections in Polis Basin.....	175
4.5.2 Cross section in the Limassol Basin.....	190
4.6 Discussion .....	192
<i>Chapter 5</i> .....	199

<i>Discussion</i> .....	199
5.1 Regional structural offshore framework .....	200
5.2 Structural onshore framework .....	203
5.3 Regional synthesis.....	206
5.4 Assessment of impact of tectonic structures on the petroleum systems .....	215
<i>Chapter 6</i> .....	218
<i>Conclusions</i> .....	218
<i>References</i> .....	223
<i>Appendix</i> .....	238

## Table of Figures

FIGURE 1 - 1: TECTONIC MAP OF THE AEGEAN AND EASTERN MEDITERRANEAN REGION, SHOWING THE MAIN PLATE BOUNDARIES, MAJOR SUTURE ZONES, AND FAULT SYSTEMS. THICK, WHITE ARROWS DEPICT THE DIRECTION AND MAGNITUDE (MM/A) OF PLATE CONVERGENCE; GREY ARROWS MARK THE DIRECTION OF EXTENSION (MIOCENE–RECENT) (FROM REILINGER ET AL., 2006). LIGHT-GREY TONE NORTH OF THE NORTH ANATOLIAN FAULT ZONE (NAFZ) AND WEST OF THE CALABRIAN ARC DELINEATES EURASIAN PLATE AFFINITY, WHEREAS THE GREY TONES SOUTH OF THE HELLENIC, STRABO AND CYPRUS TRENCHES DELINEATE AFRICAN PLATE AFFINITY. BF, BURDUR FAULT; CACC, CENTRAL ANATOLIAN CRYSTALLINE COMPLEX; DKF, DATCA-KALE FAULT; EAFZ, EAST ANATOLIAN FAULT ZONE; EF, ECEMIS FAULT; EKP, ERZURUM-KARS PLATEAU; IASZ, IZMIR-ANKARA SUTURE ZONE; IPS, INTRA-PONTIDE SUTURE ZONE; ITS, INNER-TAURIDE SUTURE; KF, KEFALONIA FAULT; KOTJ, KARLIOVA TRIPLE JUNCTION; MM, MENDERES MASSIF; MS, MARMARA SEA; MTR, MARAS TRIPLE JUNCTION; NAFZ, NORTH ANATOLIAN FAULT ZONE; OF, OVACIK FAULT; PSF, PAMPAK-SEVAN FAULT; TF, TUTAK FAULT; TGF, TUZ GOLU FAULT; TIP, TURKISH-IRANIAN PLATEAU [FROM DILEK AND SANDVOL, [2009], AS IT WAS MODIFIED FROM DILEK [2006]. RED LINES INDICATE THE LOCATIONS OF THE THREE FIGURES THAT FOLLOW.....	44
FIGURE 1 - 2: GEOLOGICAL CROSS SECTION THROUGH THE ZAGROS FOLD AND THRUST BELT, ILLUSTRATING THE TECTONIC DEFORMATION IN THE ZAGROS REGION [AGARD ET AL., 2011].....	45
FIGURE 1 - 3: GEOLOGICAL CROSS SECTION INDICATING THE SUBDUCTION OF THE AFRICAN PLATE UNDER THE AEGEAN REGION AND SLAB ROLL BACK [DILEK AND ALTUNKAYNAK, 2009]. .....	45
FIGURE 1 - 4: GEOLOGICAL CROSS SECTION ILLUSTRATING THE COLLISION OF THE ERATOSTHENES SEAMOUNT WITH THE ISLAND OF CYPRUS [MODIFIED BY KINNAIRD, 2008 FROM ORIGINAL SAGE AND LETOUZEY, 1990].....	46
FIGURE 2 - 1: REGIONAL GEOLOGICAL MAP ILLUSTRATING THE MAIN TECTONIC ELEMENTS [GHALAYINI, 2015]. .....	50
FIGURE 2 - 2: SCHEMATIC CROSS SECTION ACROSS THE LEVANT LITHOSPHERE, SHOWING THE MAIN UNITS AND INTERFACES USED DURING THE ISOSTATIC CALCULATION. POSITION INDICATED IN FIGURE 2 - 1. [INATI, ET AL., 2016]. .....	51
FIGURE 2 - 3: SEVERAL ALTERNATIVE RECONSTRUCTIONS OF THE TETHYAN RIFTING IN THE LEVANT REGION. TWO PREVIOUSLY PROPOSED MODELS ARE: (A) AFTER DEWEY ET AL. [1973] AND STAMPFLI AND BOREL [2002], SHOWING NORTH-SOUTH EXTENSION WITH EASTERN TRANSFORM MARGIN AND (B) AFTER	

<p>GARFUNKEL AND DERIN [1984] AND GARFUNKEL [1998], SHOWING NW-SE EXTENSION WITH SOUTHERN TRANSFORM MARGIN. RECONSTRUCTIONS (C) AND (D) ARE BASED ON GARDOSH ET AL., [2010]. TETHYAN RIFTING ON THE NORTHERN MARGIN OF GONDWANA WAS PULSED AND PROGRESSED FROM THE LATE PALEOZOIC (C) TO EARLY JURASSIC (D) [FROM GARDOSH ET AL., 2010].</p>	54
<p>FIGURE 2 - 4: PALEOTECTONIC SKETCH MAPS OF THE EASTERN MEDITERRANEAN SINCE THE TRIASSIC (ER=ERATOSTHENES CONTINENTAL BLOCK, CY=CYPRUS, BD= BEYDAGLARI, HB=HERODOTUS BASIN, PB=PAMPHYLIAN BASIN, T=TAURUS, AR=ARABIA, AF=AFRICA, MR=MEDITERRANEAN RIDGE). (I) RIFTING FROM TRIASSIC TO MIDDLE JURASSIC. [FROM MONTADERT ET AL., 2014].</p>	55
<p>FIGURE 2 - 5: PALEOTECTONIC SKETCH MAPS OF THE EASTERN MEDITERRANEAN FROM LATE JURASSIC TO EARLY CRETACEOUS (ER=ERATOSTHENES CONTINENTAL BLOCK, CY=CYPRUS, BD= BEYDAGLARI, PB=PAMPHYLIAN BASIN, T=TAURUS, AR=ARABIA, AF=AFRICA). (II) BLUE ARROWS INDICATE EXTENSION AND SPREADING FROM UPPER JURASSIC TO LOWER CRETACEOUS. [FROM MONTADERT ET AL., 2014].</p>	56
<p>FIGURE 2 - 6: PALINSPASTIC RECONSTRUCTION OF THE TETHYS REGION IN LATE TRIASSIC TIMES, INDICATING THE MAIN STRUCTURAL ELEMENTS [BARRIER AND VRIELYNCK, 2008]. BLACK BOX INDICATES THE STUDY AREA. LITHOLOGY AND TECTONICS ELEMENTS AS IN FIGURE 2 - 7.</p>	57
<p>FIGURE 2 - 7: DESCRIPTION OF TECTONIC ELEMENTS, LITHOLOGY, KINEMATICS AND PALAEOGEOGRAPHY FOR THE PALINSPASTIC RECONSTRUCTION MODELS AS ILLUSTRATED IN FIGURE 2 - 6, FIGURE 2 - 8, FIGURE 2 - 9, FIGURE 2 - 10, FIGURE 2 - 11.</p>	58
<p>FIGURE 2 - 8: PALINSPASTIC RECONSTRUCTION OF THE TETHYS REGION IN MIDDLE TO LATE JURASSIC TIMES, INDICATING THE MAIN STRUCTURAL ELEMENTS AND THE NW-SE OPENING OF THE NEO-TETHYS OCEAN [BARRIER AND VRIELYNCK, 2008]. BLACK BOX INDICATES THE STUDY AREA. LITHOLOGY AND TECTONICS ELEMENTS AS IN FIGURE 2 - 7.</p>	59
<p>FIGURE 2 - 9: PALINSPASTIC RECONSTRUCTION OF THE TETHYS REGION IN EARLY CAMPANIAN TIMES, INDICATING THE MAIN STRUCTURAL ELEMENTS [BARRIER AND VRIELYNCK, 2008]. BLACK BOX INDICATES THE STUDY AREA. LITHOLOGY AND TECTONICS ELEMENTS AS IN FIGURE 2 - 7.</p>	61
<p>FIGURE 2 - 10: PALINSPASTIC RECONSTRUCTION OF THE TETHYS REGION IN MIDDLE EOCENE TIMES, INDICATING THE MAIN STRUCTURAL ELEMENTS [BARRIER AND VRIELYNCK, 2008]. BLACK BOX INDICATES THE STUDY AREA. LITHOLOGY AND TECTONICS ELEMENTS AS IN FIGURE 2 - 7.</p>	62

FIGURE 2 - 11: PALINSPASTIC RECONSTRUCTION OF THE TETHYS REGION IN PLIO-PLEISTOCENE TIMES, INDICATING THE MAIN STRUCTURAL ELEMENTS [BARRIER AND VRIELYNCK, 2008]. BLACK BOX INDICATES THE STUDY AREA. LITHOLOGY AND TECTONICS ELEMENTS AS IN FIGURE 2 - 7..... 63

FIGURE 2 - 12: PALEOTECTONIC SKETCH MAPS OF THE EASTERN MEDITERRANEAN FROM LATE CRETACEOUS TO OLIGOCENE (ER=ERATOSTHENES CONTINENTAL BLOCK, CY=CYPRUS, BD= BEYDAGLARI, HB=HERODOTUS BASIN, PAL=PAMPHYLIAN BASIN, T=TAURUS, AR=ARABIA, AF=AFRICA). (III) LATE CRETACEOUS: FORMATION OF THE CYPRUS ARC AND OPHIOLITE BELT, SUBDUCTION CONTINUING DURING PALEOGENE [FROM MONTADERT ET AL., 2014]..... 64

FIGURE 2 - 13: REGIONAL MAP OF THE EASTERN MEDITERRANEAN ILLUSTRATING THE MAIN STRUCTURAL ELEMENTS IN THE REGION. INSET MAP INDICATES THE AREA OF INTEREST ABBREVIATIONS: EAF=EAST ANATOLIAN FAULT, M=MAGHARA FOLD, Y=YELLEG FOLD, H=HALAL FOLD, G.F=FALIG ANTICLINE, G.ED=EL DIRSA ANTICLINE, MP=MITLA PASS. [MODIFIED FROM BOWMAN, 2011]. ..... 65

FIGURE 2 - 14: PALEOTECTONIC SKETCH MAPS OF THE EASTERN MEDITERRANEAN OF MIOCENE TO PRESENT (ER=ERATOSTHENES CONTINENTAL BLOCK, CY=CYPRUS, BD= BEYDAGLARI, HB=HERODOTUS BASIN, AR=ARABIA, AF=AFRICA). (IV) MIOCENE TO PLIO-PLEISTOCENE GEODYNAMIC MODEL [FROM MONTADERT ET AL., 2014]..... 67

FIGURE 2 - 15: BOUGUER GRAVITY ANOMALIES MAP, ORANGE ARCUATE LINE REPRESENTS THE CYPRUS ARC, TO REFERS TO THE TROODOS OPHIOLITE. HIGH ANOMALIES INDICATE THE OPHIOLITE BODY [FROM WOODSIDE, 1977 AS MODIFIED BY MONTADERT ET AL, 2014]. ..... 68

FIGURE 2 - 16: BOUGUER GRAVITY MAP OF THE EASTERN MEDITERRANEAN. LOCATION OF MODELLED GRAVITY PROFILES A–D SHOWN. RED DASHED LINE REPRESENTS THE CYPRUS ARC [MODIFIED FROM ERGUN ET AL., 2005]..... 69

FIGURE 2 - 17: BOUGUER GRAVITY PROFILES AND 2D MODELS. DOTS ARE OBSERVED GRAVITY, FULL LINE SHOWS MODEL VALUES, RED ARROWS SHOW LOWS WHERE THE CYPRUS ARC RUNS. DENSITIES OF LAYERS ARE GIVEN IN  $MG.M^{-3}$  [MODIFIED FROM ERGUN ET AL., 2005]. LOCATIONS OF PROFILES A AND B ARE INDICATED IN FIGURE 2 - 16..... 71

FIGURE 2 - 18: BOUGUER GRAVITY PROFILES AND 2D MODELS. DOTS ARE OBSERVED GRAVITY, FULL LINE SHOWS MODEL VALUES, RED ARROWS SHOW LOWS WHERE THE CYPRUS ARC RUNS. DENSITIES OF

LAYERS ARE GIVEN IN $\text{MG.M}^{-3}$ [MODIFIED FROM ERGUN ET AL., 2005]. LOCATIONS OF PROFILES C AND D ARE INDICATED IN FIGURE 2 - 16.....	72
FIGURE 2 - 19: MAGNETIC ANOMALIES MAP, ORANGE ARCUATE LINE REPRESENTS THE CYPRUS ARC [FROM WOODSIDE, 1977, AS MODIFIED BY MONTADERT ET AL, 2014]. .....	73
FIGURE 2 - 20: STRATIGRAPHIC CHART ILLUSTRATING THE MAIN LITHOLOGICAL UNITS IDENTIFIED ONSHORE CYPRUS, CORRELATED WITH THE MAJOR TECTONIC EVENTS IN THE EASTERN MEDITERRANEAN REGION. ....	77
FIGURE 2 - 21: LEGEND OF FIGURE 2 - 20, DESCRIBING THE LITHOLOGICAL UNITS OF THE CHART.....	78
FIGURE 2 - 22: OUTLINE GEOLOGICAL MAP OF CYPRUS ILLUSTRATING THE MAIN TECTONIC STRUCTURES AND SEDIMENTOLOGICAL FORMATIONS. AL=AKROTIRI LINEAMENT; ATFS=ARAKAPAS TRANSFORM FAULT SYSTEM; AQ=ANDROLYKOU QUARRY; GTFB=GERASA THRUST AND FOLD BELT; LB=LIMASSOL BASIN; LFB=LIMASSOL FOREST BLOCK; MB=MARONI BASIN; OTF=OVGOS TRANSFORM FAULT; PB=POLIS BASIN; PFS=PAPHOS FAULT SYSTEM; PIB=PISSOURI BASIN [MODIFIED AFTER KINNAIRD ET AL., 2011]. .....	79
FIGURE 2 - 23: LATE MIOCENE EXTENSION IN THE POLIS GRABEN FROM STRUCTURAL DATA COLLECTED BY KINNAIRD. THE FAULTS SHOWN IN THE FIGURE ARE AS MAPPED BY PAYNE AND ROBERTSON [1995], [FROM KINNAIRD, 2008].....	80
FIGURE 2 - 24: POST MIOCENE COMPRESSION EXPRESSED FROM STRUCTURAL DATA COLLECTED BY KINNAIRD FROM THE POLIS GRABEN. THIS EVENT IS CONSTRAINED TO PLEISTOCENE/RECENT TIMES. THE FAULTS SHOWN IN THE FIGURE ARE AS MAPPED BY PAYNE AND ROBERTSON [1995] [FROM KINNAIRD, 2008]...	81
FIGURE 2 - 25: DEFORMATION PHASES IN THE PISSOURI BASIN FROM STRUCTURAL DATA COLLECTED BY KINNAIRD: D1:- ~ N-S ORIENTATED FAULTS FORMED DURING TORTONIAN E-W EXTENSION; D2:- ~ NE-SW ORIENTATED FAULTS FORMED DUE TO DISSOLUTION AND COLLAPSE OF GYPSUM; AND, D3:- REACTIVATION OF D1/D2 STRUCTURES IN A DEXTRAL SENSE [FROM KINNAIRD, 2008]. .....	82
FIGURE 2 - 26: STRUCTURAL DATA COLLECTED BY KINNAIRD FROM THE MARONI-PSEMATISMENOS BASIN SHOWING EXTENSION IN THE AREA DURING LATE MIOCENE TIME. FAULTS SHOWN ARE AS MAPPED BY THE GEOLOGICAL SURVEY DEPARTMENT OF CYPRUS [FROM KINNAIRD, 2008].....	83

FIGURE 2 - 27: STRUCTURAL DATA COLLECTED BY KINNAIRD FROM THE MARONI-PSEMATISMENOS BASIN SHOWING COMPRESSION IN THE AREA DURING PLEISTOCENE TIME. FAULTS SHOWN ARE AS MAPPED BY THE GEOLOGICAL SURVEY DEPARTMENT OF CYPRUS [FROM KINNAIRD, 2008].....	84
FIGURE 2 - 28: MODELS FOR THE TECTONIC EVOLUTION OF THE MESAORIA BASIN AND KYRENIA RANGE AS PROPOSED BY DIFFERENT AUTHORS (SEEN IN TEXT), MF = MESAORIA FAULT, OF = OVGOS FAULT, KF = KYRENIA FAULT [FROM KINNAIRD, 2008].....	85
FIGURE 2 - 29: GEOLOGICAL MAP OF SOUTHWEST CYPRUS, SHOWING THE OUTCROP PATTERNS OF DIARIZOS OCEANIC BASEMENT (PART OF THE MAMONIA COMPLEX) AND THE TROODOS OCEANIC BASEMENT (TROODOS COMPLEX), SERPENTINITE (MARKING THE LOCATION OF BASEMENT FAULTS) AND THE KATHIKAS FORMATION. THE MAIN OUTCROPS OF METAMORPHIC ROCKS ARE AT: 1, LOUTRA TIS APHRODITIS; 2, GALATARIA; 3, AYIA VARVARA. PLACE NAMES REFERRED TO IN THE TEXT: KT, KATHIKAS; K, KANNAVIU; S, STATOS; MD, MAVROKOLYMBOS DAM; N, NATA; PTR, PETRA TOU ROMIOU. A CYPRUS GEOLOGICAL SURVEY BOREHOLE BH, NEAR NEOKHORION, INDICATES TROODOS OCEANIC BASEMENT BENEATH THE TERTIARY CHALKS [BAILEY ET AL., 2000].....	88
FIGURE 2 - 30: CAMPANIAN TO MAASTRICHTIAN DEFORMATION ALONG THE MAMONIA COMPLEX SUTURE ZONE. A) DEXTRAL TRANSTENSION ALONG THE SUTURE ZONE DURING THE ANTI-CLOCKWISE ROTATION OF THE TROODOS MICROPLATE IN CAMPANIAN, WITH FRAGMENTS OF THE TROODOS OPHIOLITES DETACHED AND LOCALLY JUXTAPOSED AGAINST THE MAMONIA COMPLEX. THE MONI FORMATION IS DEPOSITED ABOVE THE TROODOS OPHIOLITES INDICATIVE OF THE CLOSE PROXIMITY OF THE TWO TERRANES. B) SW DIRECTED IMPINGEMENT OF TROODOS OPHIOLITES INTO THE MAMONIA COMPLEX. BLACK ARROWS ILLUSTRATE THE RADIAL PATTERN OF SHORTENING [BAILEY ET AL., 2000].....	89
FIGURE 2 - 31: THE LOCATION OF THE AGIA MARINOUDA AND KOUKLIA FOLDS IN THE PAPHOS AREA [FROM KINNAIRD, 2008].....	90
FIGURE 2 - 32: GEOMORPHOLOGICAL MAP OF CYPRUS WITH PLATE BOUNDARIES AND RELATIVE MOTION [FROM PAPADIMITRIOU AND KARAKOSTAS, 2006]. .....	93
FIGURE 2 - 33: GRAPHICAL REPRESENTATIONS OF THE FAULT PLANE SOLUTIONS OF EARTHQUAKES IN THE AREA. THE TYPICAL SOLUTIONS OF THE THREE CLUSTERS (A, B, C) ARE DENOTED BY LARGER SYMBOLS [FROM PAPAACHOS AND PAPAIOANNOU, 1999].....	93

FIGURE 2 - 34: INTERPRETIVE GEODYNAMIC MODEL OF THE EVOLUTION OF THE NORTH-SOUTH TRENDING FIELD IN THE WESTERN ANATOLIA ALONG A SUBDUCTION-TRANSFORM EDGE PROPAGATOR (STEP FAULT ZONE, DEVELOPED IN A TEAR WITHIN THE NORTHWARD SUBDUCTING AFRICAN LITHOSPHERE [DILEK AND ALTUNKAYNAK, 2009]). ..... 94

FIGURE 3 - 1: LOCATION MAP OF THE 2D SEISMIC PROFILES AVAILABLE FOR THIS STUDY. GREY LINE DEPICTS SOME OF THE BLOCKS IN THE EXCLUSIVE ECONOMIC ZONE OF CYPRUS. BLUE LINES REPRESENT THE SEISMIC PROFILES AVAILABLE FROM THE MC2D-CYP2006 SURVEY AND ORANGE LINES REPRESENT SEISMIC PROFILES FROM THE MC2D-CYP2008 SURVEY (COURTESY OF PGS). ..... 99

FIGURE 3 - 2: DIFFERENT SEISMIC UNITS AND HORIZONS UTILIZED IN THIS STUDY. AGES AND SEISMIC UNITS ARE IN ACCORDANCE WITH PREVIOUS STUDIES [GARDOSH ET AL., 2010; HAWIE ET AL., 2013]. ..... 100

FIGURE 3 - 3: DIX FORMULA, AN EQUATION USED TO CALCULATE THE INTERVAL VELOCITIES OF FLAT OR PARALLEL LAYERS [DIX, 1955]. ..... 101

FIGURE 3 - 4: REGIONAL BATHYMETRIC MAP [EMODNET], WITH THE MAIN TECTONIC STRUCTURES. RED DASHED LINE DELINEATES THE BOUNDARY BETWEEN THE THIN CONTINENTAL CRUST (LEVANT BASIN) AND THE OCEANIC CRUST (HERODOTUS BASIN) AS IT WAS IDENTIFIED BY GRANOT [2016]. BLACK ARROWS INDICATE THE RELATIVE MOTION AND AVERAGE SLIP RATE FOR THE AFRICAN AND ANATOLIAN PLATES [MCCLUSKY ET AL., 2000]. ABBREVIATIONS: AM=ANAXIMANDER MOUNTAIN, CA=CYPRUS ARC, COB=CONTINENT-OCEAN BOUNDARY, DSTF=DEAD SEA TRANSFORM FAULT, FR=FLORENCE RISE, HA=HELLENIC ARC, LR=LATAKIA RIDGE, MDR=MEDITERRANEAN RIDGE, PTF=PAPHOS TRANSFORM FAULT, PST=PLINY AND STRABO TRENCHES. .... 106

FIGURE 3 - 5: PALEO-GEOGRAPHIC MAPS OF THE LEVANT REGION ILLUSTRATING THE TECTONIC EVOLUTION: (A) MESOZOIC RIFTING PHASE, NORMAL FAULT ACTIVITY CEASES BY MIDDLE JURASSIC TIME; (B,C) INITIAL CLOSURE OF THE NEO-TETHYS DUE TO CONVERGENCE; (D) INITIAL FOLDING ALONG THE LEVANT MARGIN; (E) WESTWARD EXPULSION OF THE ANATOLIAN MICROPLATE; AND (F) CURRENT TECTONIC REGIME [MODIFIED FROM GHALAYINI ET AL., 2017]. ..... 109

FIGURE 3 - 6: MAP OF OFFSHORE CYPRUS. MAIN STRUCTURAL ELEMENTS IDENTIFIED AFTER SEISMIC INTERPRETATION. RED DOTTED LINE DELINEATES THE TRANSITION BOUNDARY BETWEEN CONTINENTAL

AND OCEANIC CRUST [GRANOT, 2016]. BLACK THIN LINES DELINEATE THE AVAILABLE SEISMIC DATA, WHILE THE RED THICK LINES DELINEATE THE SEISMIC PROFILES ILLUSTRATED IN THIS PAPER. ABBREVIATIONS: CA=CYPRUS ARC, CB=CYPRUS BASIN, COB=CONTINENT-OCEAN BOUNDARY, EMC=ERATOSTHENES MICRO-CONTINENT, FR=FLORENCE RISE, HR=HECATAEUS RISE, LNR=LARNACA RIDGE, LR=LATAKIA RIDGE, MR=MARGAT RIDGE, PTF=PAPHOS TRANSFORM FAULT. .... 111

FIGURE 3 - 7: CHRONO-STRATIGRAPHIC CHART DEPICTING THE HORIZONS IDENTIFIED DURING SEISMIC INTERPRETATION WITH THE PROPOSED AGES, SEISMIC FACIES AND THICKNESSES. .... 115

FIGURE 3 - 8: STRATIGRAPHIC COLUMNS ILLUSTRATING THE SEDIMENTARY FILLING OF THE FOUR DIFFERENT DOMAINS, WHICH ARE EXAMINED. RED BOXES INDICATE THE LOCATION OF EACH COLUMN. SEQUENCES AS DESCRIBED IN FIGURE 3 - 7. A) LEVANT BASIN DOMAIN: THICK SEDIMENTARY INFILL ABOVE A THIN STRETCHED CONTINENTAL CRUST, B) CYPRUS BASIN DOMAIN: THIN SEDIMENTARY SEQUENCE, LACKING IN DEPOSITION OF SEVERAL SEISMIC PACKAGES, PERCEIVED TO BE FLOORED BY OBDUCTED OPHIOLITE, C) ERATOSTHENES MICRO-CONTINENT DOMAIN: CARBONATE PLATFORM OF MESOZOIC AGE COVERED BY PLIOCENE SEDIMENTS, BELIEVED TO BE FLOORED BY CONTINENTAL CRUST, D) HERODOTUS BASIN DOMAIN: INFILLED BY A VERY THICK LAYER OF PLIOCENE AND MESSINIAN DEPOSITS AND FLOORED BY AN OCEANIC CRUST. ABBREVIATIONS: L.B= LEVANT BASIN, C.B=CYPRUS BASIN, E.S=ERATOSTHENES MICRO-CONTINENT, H.B=HERODOTUS BASIN. .... 116

FIGURE 3 - 9: SEISMIC LINE 6063 TRENDING SOUTH-NORTH. LETTERS IN SQUARES ARE USED TO REFER TO A SPECIFIC ZONE IN THE TEXT. POSITION OF THIS PROFILE FOUND IN FIGURE 3 - 6. POSITION A: NORMAL FAULTS OFFSETTING THE EARLY TO MIDDLE MIOCENE SEDIMENTS, COMMENCING AT THE EOCENE UNCONFORMITY HORIZON (R4) AND DYING OUT AT THE BASE OF THE MESSINIAN HORIZON (R7). POSITION B: STRUCTURALLY HIGHER POSITION OF THE CYPRUS BASIN, INFILLED BY A THIN SEDIMENTARY SEQUENCE IN COMPARISON WITH THE LEVANT BASIN. CHANGE IN THICKNESS OF THE MESSINIAN SALT BETWEEN THE LEVANT AND CYPRUS BASINS IMPLIES THE ACTIVE NATURE OF THE LATAKIA RIDGE. POSITION C: SMALL BASIN OF MIDDLE MIOCENE AGE AS THE EARLY MIOCENE SEDIMENTS ARE INCLINED TOWARDS THE NORTH WITH THE MID MIOCENE SEDIMENTS ONLAPPING ON THE SLOPE OF THE BASIN. A3 SIZE INTERPRETED AND UN-INTERPRETED PROFILES IN APPENDIX. .... 117

FIGURE 3 - 10: SEISMIC LINE 6061 TRENDING SOUTH-NORTH. THE LETTER IN SQUARE IS USED TO REFER TO A SPECIFIC ZONE IN THE TEXT. POSITION OF THIS PROFILE FOUND IN FIGURE 3 - 6. POSITION D: PIGGY BACK BASINS CREATED DUE TO CONTINUOUS CONVERGENCE OF THE AFRICAN PLATE WITH RESPECT TO THE EURASIAN PLATE. A3 SIZE INTERPRETED AND UN-INTERPRETED PROFILES IN APPENDIX. .... 118

FIGURE 3 - 11: SCHEMATIC ILLUSTRATION OF DEPTH CONVERTED SEISMIC REFLECTORS, ILLUSTRATING THE DEPTH CONVERTED PACKAGES AS THEY WERE OBTAINED BY USING THE DIX FORMULA AND THE STACKED VELOCITIES. .... 119

FIGURE 3 - 12: SEISMIC LINE 6053 TRENDING SOUTH-NORTH. THE LETTER IN SQUARE IS USED TO REFER TO A SPECIFIC ZONE IN THE TEXT. POSITION OF THIS PROFILE FOUND IN FIGURE 3 - 6. POSITION E: THINNING OF THE SEDIMENTARY SEQUENCE AS WE MOVE TOWARDS THE WEST, IN COMPARISON WITH THE MIDDLE MIOCENE DEPOSITIONS OF PROFILE 6063. POSITION F: FLEXURAL BASIN CREATED FROM THE UPLIFT OF THE LARNACA RIDGE NORTH OF THIS SEISMIC PROFILE (AS IDENTIFIED BY CALON ET AL., [2005]). INSET IS A ZOOMED IMAGE OF THE CYPRUS BASIN, ILLUSTRATING THINNING OF THE PLIOCENE SEDIMENTS TOWARDS THE SOUTH AND ONLAPS ON THE MESSINIAN AND MIOCENE SEDIMENTS. A3 SIZE INTERPRETED AND UN-INTERPRETED PROFILES IN APPENDIX..... 121

FIGURE 3 - 13: SEISMIC LINE 6015 TRENDING SOUTH-NORTH. THE LETTER IN SQUARE IS USED TO REFER TO A SPECIFIC ZONE IN THE TEXT. POSITION OF THIS PROFILE FOUND IN FIGURE 3 - 6. POSITION G: FLEXURAL BASIN CREATED FROM THE CONVERGENCE OF ERATOSTHENES MICRO-CONTINENT WITH CYPRUS AND INFILLED BY PLIO-PLEISTOCENE SEDIMENTS. A THIN SKINNED THRUST WITH A DECOLLEMENT LEVEL NORTH OF THE BASIN PORTRAYS THE SHORTENING. A3 SIZE INTERPRETED AND UN-INTERPRETED PROFILES IN APPENDIX. .... 122

FIGURE 3 - 14: SCHEMATIC ILLUSTRATION OF DEPTH CONVERTED SEISMIC REFLECTORS THAT ELIMINATES THE LARGE VELOCITY CONTRAST BETWEEN SP8 (CLASTICS) AND SP7 (SALT) WHICH RESULTS IN A PULL-UP EFFECT AS OBSERVED IN FIGURE 3 - 13. SP3 IS NOT STEEPLY BENDING UPWARDS AND THUS A THRUST FAULT IS ILLUSTRATED WITH A DECOLLEMENT LEVEL IN THE SALT. THE CONTINUATION TOWARDS THE NORTH IS COMPLEX DUE TO THE LIMITED AND POOR IMAGING. THE SEISMIC PROFILE DOES NOT CROSS THE CYPRUS ARC, ALTHOUGH THE THRUST FAULT (DASHED LINE) IS EXPECTED TO CONNECT WITH THE CYPRUS ARC. IN-SET BATHYMETRY MAP WITH THE LOCATION OF THE SEISMIC PROFILE DISPLAYED IN RED. .... 123

FIGURE 3 - 15: TECTONOSTRATIGRAPHIC EVOLUTION OFFSHORE CYPRUS IN ACCORDANCE WITH SEISMIC INTERPRETATIONS IN THIS PAPER AND IN CONNECTION WITH PREVIOUS SEISMIC STUDIES FROM CALON ET AL., 2005A; HALL ET AL., 2005; BOWMAN, 2011; MONTADERT ET AL., 2014. A: OLIGOCENE-EARLY MIOCENE: THE LARNACA AND MARGAT RIDGES ARE ACTIVE AS THE EARLY MIOCENE SEDIMENTS ARE THINNING NORTH OF THE MARGAT RIDGE, WHILE THE LATAKIA RIDGE IS COVERED BY A THIN SEQUENCE OF EARLY MIOCENE SEDIMENTS. B: MIDDLE MIOCENE: LATAKIA AND MARGAT RIDGES ARE ACTIVE, WITH MID MIOCENE SEDIMENTS ONLAPPING ON THE INCLINED EARLY MIOCENE SEDIMENTS. NORMAL FAULTS

ARE INITIATING IN THE LEVANT BASIN. C: LATE MIOCENE: CONTINUOUS ACTIVITY OF THE LATAKIA, MARGAT AND LARNACA RIDGES AS MESSINIAN SALT IS DEPOSITED INTO SMALL DEPRESSIONS. NORMAL FAULTS IN THE LEVANT BASIN REACH FULL GROWTH RESTRICTED BETWEEN THE EOCENE UNCONFORMITY AND BASE MESSINIAN HORIZONS. D: PLIOCENE-RECENT: ACTIVE LATAKIA AND MARGAT RIDGES GIVE RISE TO POSITIVE FLOWER STRUCTURES THAT INDICATE A TRANSPRESSIVE STRIKE SLIP NATURE. ABBREVIATIONS AS IN FIGURE 3 - 6. EACH PERIOD IS ILLUSTRATED IN A3 SIZE IN THE APPENDIX.  
 ..... 129

FIGURE 4 - 1: GEOLOGICAL MAP OF CYPRUS ILLUSTRATING THE MAIN STRUCTURAL ELEMENTS, THE GEOLOGICAL SEDIMENTARY COVER OF THE INVESTIGATED BASINS AND THE LOCATIONS OF THE CROSS SECTIONS. BLACK LINES INDICATE THE TECTONIC STRUCTURES WHICH ARE GENERALLY ACCEPTED, WHILE GRAY LINES INDICATE STRUCTURES PROPOSED IN DIFFERENT STUDIES [PAYNE AND ROBERTSON, 1995; BAILEY ET AL., 2000; GEOTER, 2005]. THE INVESTIGATED BASINS SOUTH OF TROODOS OPHIOLITES ARE INDICATED, POLIS, POLEMI, PISSOURI, LIMASSOL AND MARONI/PSEMATISMENOS BASINS. ABBREVIATIONS: 1) AKAMAS CROSS SECTION, 2) POLIS CROSS SECTION, 3) LIMASSOL CROSS SECTION. ABBREVIATIONS: ATF: ARAKAPAS TRANSFORM FAULT; GFTB: GERASA FOLD AND THRUST BELT; PTF: PAPHOS TRANSFORM FAULT; OTF: OVGOS TRANSFORM FAULT..... 133

FIGURE 4 - 2: GEOLOGICAL MAP OF SOUTHERN AND WESTERN CYPRUS WITH THE AVAILABLE BOREHOLE DATA (COURTESY OF GSD CYPRUS). BLACK LINES REPRESENT THE LOCATIONS OF THE CROSS SECTIONS. MAPS ARE FROM THE GSD DATABASE BASED ON PREVIOUS MAPS OF LAPIERRE [1971], TURNER [1992], ZOMENI AND TSIOLAKIS [2008], ZOMENI AND GEORGIADOU [2015]..... 135

FIGURE 4 - 3: BOREHOLE DATA IN THE POLIS BASIN COURTESY OF THE GEOLOGICAL SURVEY DEPARTMENT OF CYPRUS (LOCATIONS IN FIGURE 4 - 2). THE DESCRIPTION OF EACH BOREHOLE IS PRESENTED ALONG WITH THE CORRESPONDING FORMATION AND AGE AS INTERPRETED HEREIN. .... 138

FIGURE 4 - 4: BOREHOLE DATA: (A) IN THE POLEMI BASIN (9-15) AS THEY ARE INTERPRETED BY GEOTER [2005] AND (B) IN LIMASSOL BASIN (16-19) AS INTERPRETED BY KINNAIRD [2008] (LOCATIONS IN FIGURE 4 - 2).  
 ..... 139

FIGURE 4 - 5: GEOLOGICAL MAP OF CYPRUS (FROM GSD, COMPILED BY THE MAPS OF LAPIERRE, 1971; TURNER, 1992; ZOMENI AND TSIOLAKIS 2008; ZOMENI AND GEORGIADOU, 2015) IN THE POLIS BASIN. THE RED

SQUARE IN THE INSET MAP DEPICTS THE POSITION OF THE POLIS BASIN ON THE ISLAND OF CYPRUS. THE POINTS INDICATE THE LOCATIONS OF EACH OUTCROP DISCUSSED IN THIS MANUSCRIPT. 1) FIGURE 4 - 6: KATHIKAS PANORAMA VIEW. 2) FIGURE 4 - 7 AND FIGURE 4 - 8: PANORAMA UNCONFORMITY. 3) FIGURE 4 - 9: ANDROLYKOU QUARRY. 4) FIGURE 4 - 10: CONTACT BETWEEN OPHIOLITES AND REEFS NEAR NEO CHORIO PAPHOU. 5) FIGURE 4 - 11: KORONIA MEMBER REEFS NEAR PERISTERONA VILLAGE. 6) FIGURE 4 - 12: GRAVITATIONAL SCARP IN PAKHNA FORMATION OR THE FOLDING LEVEL OF THE CHALKS. 7) FIGURE 4 - 13: NORMAL FAULTS IN PAKHNA FORMATION NEAR PANO AKOURDALIA VILLAGE. 8) FIGURE 4 - 14: SMALL SCALE NORMAL FAULTS IN PAKHNA FORMATION NEAR KRITOU TERA VILLAGE. 9) FIGURE 4 - 15: HORST AND GRABEN STRUCTURES IN PAKHNA FORMATION NEAR AKOURSOS VILLAGE. 10) FIGURE 4 - 16: STRIATIONS IN PAKHNA FORMATION INDICATIVE OF STRIKE-SLIP DISPLACEMENT NEAR KRITOU TERA VILLAGE. FAULT STRUCTURES AT LOCATIONS 1, 2, 3, 5 ARE PROPOSED FOR THE FIRST TIME IN THIS STUDY, AS ARE THE INFERRED THRUST FAULTS. FAULT STRUCTURES AT LOCATION 4 ARE AFTER SWARBRICK [1993] AND BAILEY ET AL., [2000]. STRUCTURE AT LOCATION 7 IS AFTER PAYNE AND ROBERTSON, [1995]. FAULTS, BED ORIENTATION AND DIPS ARE FROM THIS STUDY. .... 142

FIGURE 4 - 6: PANORAMIC PHOTOGRAPH SHOWING THE CONTACT BETWEEN THE KATHIKAS FORMATION (MAASTRICHTIAN AGE) AND LEFKARA FORMATION (MAASTRICHTIAN TO MIDDLE EOCENE AGE) TO THE SOUTH, WHICH ARE UNCONFORMABLY OVERLAIN BY THE PAKHNA FORMATION (MIDDLE MIOCENE AGE), NEAR THE VILLAGE OF KATHIKAS. THE JUXTAPOSITION OF THE KATHIKAS FM AND LEFKARA FM IS CONNECTED WITH THE ACTIVITY OF A THRUST FAULT, COMMENCING IN OLIGOCENE TO EARLY MIOCENE TIME. THE THRUST FAULT IS VERGING ROUGHLY TOWARDS THE SW. FIELD LOCATION IN FIGURE 4 - 5, POINT 1..... 145

FIGURE 4 - 7: PHOTOGRAPH SHOWING THE CONTACT BETWEEN THE OVERLYING TERA MEMBER BURDIGALIAN CHALK AND THE UNDERLYING MAASTRICHTIAN CHALK PRESUMABLY OF THE LOWER LEFKARA MEMBER, NORTH OF THE VILLAGE OF PEGEIA. THE AGES WERE OBTAINED BY BIO STRATIGRAPHIC DATING [N. PAPADIMITRIOU, PERS. COMM., 2017]. BLACK DOTTED LINE ILLUSTRATES A KARSTIFIED SURFACE INDICATIVE OF THE LIMIT BETWEEN THE TWO FORMATIONS AND THE CLOSE PROXIMITY TO THE SEA LEVEL. RED LINES ILLUSTRATE FAULTS OR CRACKS BETWEEN THE TWO FORMATIONS. OUTCROP LOCATION INDICATED IN FIGURE 4 - 5 POINT 2. .... 146

FIGURE 4 - 8: ZOOMED IN PHOTOGRAPH OF FIGURE 4 - 7 ILLUSTRATING THE DISCONTINUITIES IN THE LATE MAASTRICHTIAN CHALK FILLED WITH FRAGMENTS FROM SURROUNDING FORMATIONS, PRESUMABLY FROM THE MAMONIA COMPLEX. OUTCROP POSITION INDICATED IN FIGURE 4 - 5, POINT 2 AND FIGURE 4 - 7..... 147

FIGURE 4 - 9: PHOTOGRAPH SHOWING EARLY MIOCENE TERA MEMBER REEF DEPOSITS IN THE ANDROLYKOU QUARRY, DEPICTING LATE MIOCENE OR PLIOCENE COMPRESSION. SHEARING OBSERVED BY THE LENSES ILLUSTRATED, INDICATIVE OF THRUSTING-COMPRESSION TOWARDS THE S-SSW. OUTCROP LOCATION INDICATED IN FIGURE 4 - 5, POINT 3. FIELD BOOK USED AS SCALE. .... 148

FIGURE 4 - 10: PHOTOGRAPH DEPICTING THE CONTACT BETWEEN BRECCIATED REEFS PROBABLY OF KORONIA MEMBER (TORTONIAN AGE), WITH OPHIOLITES (UPPER PILLOW LAVAS) NEAR THE VILLAGE OF NEO CHORIO PAPHOU, IN THE AKAMAS PENINSULA. OUTCROP LOCATION INDICATED IN FIGURE 4 - 5, POINT 4..... 149

FIGURE 4 - 11: PHOTOGRAPH DEPICTING LATE MIOCENE KORONIA MEMBER REEFS NEAR THE VILLAGE OF PERISTERONA PAPHOU. BLACK LINES INDICATE THE EASTWARD DIP OF THE KORONIA REEFS. THE TILTING OF THE REEF DEPOSITS IS CONNECTED WITH A WESTWARD VERGING THRUST FAULT (NOT OBSERVED IN THIS FIGURE) OUTCROP LOCATION INDICATED IN FIGURE 4 - 5, POSITION 5..... 150

FIGURE 4 - 12: PHOTOGRAPH DEPICTING A NORMAL FAULT IN THE PAKHNA FORMATION NEAR THE VILLAGE OF PANO AKOURDALIA. THE FAULT DISPLACES CHALKS OF THE PAKHNA FORMATION, IT IS TRENDING NW-SE AND IS DIPPING EASTWARD AT ~45-50°. OUTCROP LOCATION INDICATED IN FIGURE 4 - 5, POSITION 7.151

FIGURE 4 - 13: PANORAMIC PHOTOGRAPH SHOWING A SEQUENCE OF PAKHNA CHALKS DIPPING TOWARDS THE EAST. THE RED DOTTED LINE ILLUSTRATES EITHER THE GRAVITATIONAL SURFACE THAT DISPLACES THE CHALKS, OR THE LEVEL AT WHICH THE CHALKS ARE FOLDING. OUTCROP LOCATION INDICATED IN FIGURE 4 - 5 POSITION 6..... 152

FIGURE 4 - 14: PHOTOGRAPH DEPICTING NORMAL FAULTS DISPLACING THE PAKHNA FORMATION, NEAR KRITOU TERA. DIRECTION OF FAULTS SSE-NNW. INSET IMAGE INDICATES THE STEREOGRAPHIC PROJECTION OF THE MEASURED FAULT PLANES. OUTCROP LOCATION INDICATED IN FIGURE 4 - 5, POSITION 8. .... 153

FIGURE 4 - 15: PHOTOGRAPH OF NORMAL FAULTS IN THE PAKHNA FORMATION, NEAR THE VILLAGE OF AKOURSOS. FAULT ACTIVITY IS OF MIDDLE TO LATE MIOCENE ILLUSTRATING A NE-SW EXTENSION. THE FAULT MOVEMENTS RESULT IN THE CREATION OF HORST AND GRABEN STRUCTURES WHICH IS CHARACTERISTIC OF AN EXTENSIONAL ENVIRONMENT. THE SMALL OFFSET MEASURED FROM THESE FAULTS INDICATES A RATHER LOCAL DISPLACEMENT. OUTCROP LOCATION INDICATED IN FIGURE 4 - 5, POSITION 9. .... 154

FIGURE 4 - 16: PANORAMIC PHOTOGRAPH DEPICTING A LARGE SINISTRAL STRIKE SLIP FAULT STRIKING SW-NE, IN THE PAKHNA FORMATION NEAR THE VILLAGE OF KRITOU TERA. INSET FIGURES ILLUSTRATE THE RIEDEL STRIATIONS MEASURED AT THIS OUTCROP AND THE STEREO NET PROJECTIONS INDICATE COMPRESSION (COMPRESSONAL-TRANSPRESSIONAL STRESS) IN A NNW-SSE DIRECTION AND AN EXTENSION (EXTENSIONAL-TRANSTENSIONAL STRESS) IN AN ENE-WSW DIRECTION. OUTCROP LOCATION INDICATED IN FIGURE 4 - 5, POSITION 10. .... 155

FIGURE 4 - 17: GEOLOGICAL MAP OF CYPRUS (FROM GSD COMPILED BY THE MAPS OF LAPIERRE, 1971; ZOMENI AND TSIOLAKIS 2008) IN THE POLEMI BASIN. THE RED SQUARE IN THE INSET MAP DEPICTS THE POSITION OF THE POLEMI BASIN. THE POINTS INDICATE THE LOCATIONS OF EACH OUTCROP DISPLAYED IN THIS MANUSCRIPT. 11) FIGURE 4 - 18: REVERSE FAULT IN LEFKARA FORMATION. 12) FIGURE 4 - 19 INDICATES REVERSE FAULTS IN THE LEFKARA FORMATION AND FIGURE 4 - 20 ILLUSTRATES NORMAL SYN-SEDIMENTARY FAULTS IN LEFKARA FORMATION. NORTHERN FAULT STRUCTURE IS AFTER SWARBRICK [1993] AND BAILEY ET AL., [2000]. SOUTHERN FAULT STRUCTURE IS AFTER GEOTER, [2005]. BED ORIENTATION AND DIPS ARE FROM THIS STUDY. .... 157

FIGURE 4 - 18: PHOTOGRAPH DEPICTING FOLDED LEFKARA FORMATION CHALKS NEAR THE VILLAGE OF FOINIKAS (FIGURE 4 - 17, POSITION 11). BIO-STRATIGRAPHY DATING INDICATED A PRIABONIAN AGE (LATE EOCENE, NANNO FOSSIL ZONE NP 20/19), WHICH IS ASSOCIATED WITH THE UPPER LEFKARA MEMBER CHALKS..... 158

FIGURE 4 - 19: PHOTOGRAPH DEPICTING A REVERSE FAULT DISPLACING THE CHALKS AND CHERTS OF THE LEFKARA FORMATION NEAR THE VILLAGE OF NATA (FIGURE 4 - 17, POSITION 12). THE DIP OF THE MEASURED FAULTS IS LARGE BETWEEN 40 TO 60°. .... 159

FIGURE 4 - 20: PHOTOGRAPH DEPICTING NORMAL FAULTS DISPLACING LEFKARA FORMATION CHALK AND CHERTS LAYERS (MID EOCENE AGE), NEAR THE VILLAGE OF NATA. SYN-SEDIMENTARY FAULT ACTIVITY IS IDENTIFIED FROM THE CHANGE IN THICKNESS OF THE CHALKS ON EITHER SIDE OF THE DEPICTED FAULT. THE INSET STEREOGRAPHIC PROJECTION ILLUSTRATES A NE-SW EXTENSION. OUTCROP LOCATION INDICATED IN IN (FIGURE 4 - 17, POSITION 12)..... 160

FIGURE 4 - 21: PHOTOGRAPH SHOWING NORMAL FAULTS IN THE CHALK AND CHERT MEMBER OF THE LEFKARA FORMATION (MIDDLE EOCENE AGE), NEAR THE VILLAGE OF NATA. A HORST GEOMETRY IS IDENTIFIED AT THIS OUTCROP. THE INSET STEREOGRAPHIC PROJECTION INDICATES A NW-SE EXTENSION (FIGURE 4 - 17, POSITION 12). .... 161

FIGURE 4 - 22: GEOLOGICAL MAP OF CYPRUS (FROM GSD COMPILED BY THE MAPS OF LAPIERRE, 1971; ZOMENI AND TSIOLAKIS 2008) AT THE WESTERN FLANK OF THE LIMASSOL BASIN. THE RED SQUARE IN THE INSET MAP DEPICTS THE POSITION OF THE LIMASSOL BASIN. THE POINTS INDICATE THE LOCATIONS OF EACH OUTCROP DISPLAYED IN THIS MANUSCRIPT. 13) FIGURE 4 - 23: FOLDING IN MAMONIA COMPLEX. 14) FIGURE 4 - 24: CONTACT BETWEEN LEFKARA AND MAMONIA COMPLEX. 15) FIGURE 4 - 25: FOLDING IN THE PAKHNA FORMATION INDICATING LATE MIOCENE THRUSTING. 16) FIGURE 4 - 26: S-TYPE SHEARING IN PAKHNA FORMATION. NORTHERN FAULT STRUCTURE IS AFTER SWARBRICK [1993] AND BAILEY ET AL., [2000]. SOUTHERN FAULT STRUCTURE IS AFTER GEOTER, [2005]. BED ORIENTATION AND DIPS ARE FROM THIS STUDY. .... 162

FIGURE 4 - 23: PHOTOGRAPH DEPICTING THE FOLDING OF MAMONIA COMPLEX RADIOLARIAN CHERT LAYERS, NEAR THE VILLAGE OF STAVROKONNOU. FAULT THRUSTING MOVEMENT IS TOWARDS THE SW, WITH A FOLD AXIS OF  $155^{\circ}$ ,  $04^{\circ}$  E. EXACT AGE OF DEFORMATION IS DIFFICULT TO DETERMINE DUE TO THE LACK OF SEDIMENTARY COVER. OUTCROP LOCATION INDICATED IN FIGURE 4 - 22, POSITION 13. .... 163

FIGURE 4 - 24: PANORAMIC PHOTOGRAPH SHOWING THE STRATIGRAPHIC CONTACT BETWEEN THE TRIASSIC MAMONIA COMPLEX AND THE OVERLYING LEFKARA FORMATION (MIDDLE EOCENE AGE) AT THE PETRA TOU ROMIOU (WESTERN LIMASSOL BASIN). OUTCROP LOCATION INDICATED IN FIGURE 4 - 22, POSITION 14. .... 164

FIGURE 4 - 25: PHOTOGRAPH SHOWING FOLDED PAKHNA FORMATION CHALKS (MIDDLE MIOCENE AGE) NEAR THE VILLAGE OF KOUKLIA. THRUSTING MOVEMENT IS OF QUATERNARY TIME AS FOLDED TERRACES WERE IDENTIFIED IN A TRENCH EXCAVATION [RESULTS OF GEOTER, 2005], WITH THE FOLD VERGING TOWARDS THE SW. FOLD AXIS  $125^{\circ}$ ,  $04^{\circ}$ N. OUTCROP LOCATION INDICATED IN FIGURE 4 - 22, POSITION 15. .... 165

FIGURE 4 - 26: PHOTOGRAPH DEPICTING FOLDING OF THE PAKHNA FORMATION (MID MIOCENE AGE) NEAR THE PETRA TOU ROMIOU. REVERSE FAULT DISPLACEMENT IS ENVISAGED IN MIDDLE-LATE MIOCENE, WITH A THRUSTING DIRECTION TOWARDS THE SW. A) THRUSTING AND SHEARING OF THE SEDIMENTS B) FOLDING OF CHALKS CREATING KINKS OF APPROXIMATELY  $90^{\circ}$ . BOTH OUTCROPS ARE IN THE SAME VICINITY. OUTCROP LOCATION IN FIGURE 4 - 22 POSITION 16. .... 166

FIGURE 4 - 27: GEOLOGICAL MAP OF CYPRUS (GSD COMPILED BY THE MAPS OF LAPIERRE, 1971; TURNER, 1992; ZOMENI AND TSIOLAKIS 2008; ZOMENI AND GEORGIADOU, 2015) WITH THE MAIN TECTONIC STRUCTURES IN THE EASTERN FLANK OF THE LIMASSOL BASIN. THE RED SQUARE IN THE INSET MAP DEPICTS THE POSITION OF THE LIMASSOL BASIN. THE POINTS INDICATE THE LOCATIONS OF EACH

OUTCROP DISPLAYED IN THIS MANUSCRIPT. 17) FIGURE 4 - 28: FOLDING IN THE LEFKARA FORMATION, 18) FIGURE 4 - 29: JUXTAPOSED VERTICAL BEDS OF LEFKARA FORMATION WITH TROODOS OPHIOLITES, 19) FIGURE 4 - 30: FOLDING OF THE LEFKARA FORMATION AT THE GERMASOGIA DAM, FIGURE 4 - 31: S-TYPE DEFORMATION IN THE LEFKARA FORMATION INDICATING THRUSTING ACTIVITY TOWARDS THE SW, NEAR THE GERMASOGIA DAM, 20) FIGURE 4 - 32: DEFORMATION ZONE IN THE LEFKARA FORMATION NEAR THE VILLAGE OF ARMENOCHORI, WHERE S-TYPE GEOMETRIES ARE OBSERVED INDICATING SW THRUSTING ACTIVITY, 21) FIGURE 4 - 33: NORMAL FAULTS IN THE PAKHNA FORMATION INDICATING EXTENSION IN AN EAST –WEST DIRECTION, 22) FIGURE 4 - 34: DEXTRAL STRIKE FAULT IN THE PAKHNA FORMATION IDENTIFIED FROM MEASUREMENTS OF CALCITE STEPS AND RIEDDLE STRIATIONS, 23) FIGURE 4 - 35: CONJUGATE STRIKE SLIP SYSTEM IDENTIFIED IN THE PAKHNA FORMATION. ABBREVIATIONS: GFTB=GERASA FOLD AND THRUST BELT; MTD=MASS TRANSPORT DEPOSITS. FAULT STRUCTURE AFTER EATON AND ROBERTSON, [1993]. BED ORIENTATION AND DIPS ARE FROM THIS STUDY. .... 167

FIGURE 4 - 28: PHOTOGRAPH SHOWING A TYPICAL FOLDING SEQUENCE IN THE LEFKARA FORMATION BETWEEN THE VILLAGES OF MANDRIA AND OMODOS. BANDS OF CHERTS AND THICK BEDS OF CHALK ARE DEFORMED. THRUSTING PULSE OF OLIGOCENE TO EARLY MIOCENE. INSET STEREOGRAPHIC PROJECTION ILLUSTRATES THE MEASURED PLANES (BLACK LINES), THE POLES OF THE PLANES (BLACK DOTS), THE CONSTRUCTED FOLD AXIS IS  $310^{\circ}, 02^{\circ}\text{N}$  (RED DOT) WHICH MATCHES WITH THE AXIS MEASURED IN THE FIELD  $120^{\circ}, 05^{\circ}\text{S}$ . THE LINEAR DIRECTION OF THE POLES INDICATES THE DIRECTION OF COMPRESSION IN A SW-NE DIRECTION (BLACK ARROWS). THUS THIS FOLD IS INTERPRETED AS VERGING TOWARDS THE SOUTH WITH ITS UPPER LIMBS PROBABLY ERODED (WHITE DASHED LINES). OUTCROP LOCATION IN FIGURE 4 - 27 POSITION 17..... 168

FIGURE 4 - 29: PANORAMIC PHOTOGRAPH SHOWING THE JUXTAPOSITION OF THE TROODOS MELANGE (LATE CRETACEOUS AGE, BROWN AREA) WITH THE YOUNGER LEFKARA FORMATION (PALEOGENE AGE) WITH THIS FORMATION BEING TILTED ALMOST TO A VERTICAL LIMIT (WHITE DASHED LINES) NEAR THE VILLAGE OF KAPILIO. THE FAULT THRUST (DASHED RED LINE) IS VERGING TOWARDS THE SW AND THE MOVEMENT IS PERCEIVED TO BE FROM OLIGOCENE ONWARDS. OUTCROP LOCATION INDICATED IN FIGURE 4 - 27, POSITION 18..... 169

FIGURE 4 - 30: PANORAMIC PHOTOGRAPH OF ILLUSTRATING THE FOLDED GEOMETRY OF THE LEFKARA FORMATION NEAR THE GERMASOGIA DAM. A THRUSTING MOVEMENT OF OLIGOCENE TO MIOCENE TIME IS ENVISAGED VERGING TOWARDS THE SW. THE FOLD AXIS IS CALCULATED AROUND  $120\text{-}130^{\circ}$ . OUTCROP LOCATION INDICATED IN FIGURE 4 - 27, POSITION 19..... 170

FIGURE 4 - 31: PHOTOGRAPH SHOWING A SHEARING ZONE WITH S-TYPE LENSES DEFORMATION WITHIN THE LEFKARA FORMATION NEAR THE GERMASOGIA DAM. THE THRUSTING IS VERGING TOWARDS THE SW WHICH IS IN ACCORDANCE WITH PREVIOUS OBSERVATIONS. TIMING OF DEFORMATION IS BETWEEN OLIGOCENE TO MIOCENE TIME. OUTCROP LOCATION INDICATED IN FIGURE 4 - 27, POSITION 19.....	170
FIGURE 4 - 32: PHOTOGRAPH SHOWING THE DEFORMATION IN THE LEFKARA FORMATION NEAR THE VILLAGE OF ARMENOCHORI. SHEARING ZONE WITH THE CREATION OF S-TYPE LENSES ILLUSTRATING THRUSTING ACTIVITY TOWARDS THE SW. BLACK DOTTED LINE IS USED TO ENVISAGE THE FOLDING OF THE LAYERS. OUTCROP INDICATED IN FIGURE 4 - 27, POSITION 20. ....	171
FIGURE 4 - 33: PHOTOGRAPH DEPICTING NORMAL FAULTS IN THE PAKHNA FORMATION, NEAR THE VILLAGE OF OMODOS, INDICATING EXTENSION IN AN E-W DIRECTION. OUTCROP LOCATION SHOWN IN FIGURE 4 - 27, POSITION 21. ....	172
FIGURE 4 - 34: PANORAMIC PHOTOGRAPH SHOWING STRIKE SLIP DEFORMATION IN THE PAKHNA FORMATION NEAR THE VOLLAGE OF MONAGRI. STRIKE SLIP FAULTING OBSERVED FROM RIEDEL STEPS AND CALCITE DEPOSITION ILLUSTRATING A TRANSPRESSIONAL REGIME IN A NNE-SSW WHICH COULD BE CONNECTED WITH THE CHANGE IN DEFORMATION STYLE IN LATE MIOCENE TO PLIOCENE TIME TO A STRIKE SLIP REGIME. OUTCROP LOCATION SHOWN IN FIGURE 4 - 27, POSITION 22.....	173
FIGURE 4 - 35: PHOTOGRAPH SHOWING STRIKE SLIP MOVEMENT IN THE PAKHNA FORMATION NEAR THE VILLAGE OF ALASSA. A CONJUGATE STRIKE SLIP SYSTEM IS OBSERVED ILLUSTRATING A TRANSPRESSIONAL REGIME IN A NNE-SSW WHICH COULD BE CONNECTED WITH THE CHANGE IN DEFORMATION STYLE IN LATE MIOCENE TO PLIOCENE TIME TO A STRIKE SLIP REGIME. OUTCROP LOCATION INDICATED IN FIGURE 4 - 27, POSITION 23. ....	174
FIGURE 4 - 36: GEOLOGICAL MAP OF WEST CYPRUS (FROM GSD, COMPILED BY THE MAPS OF LAPIERRE, 1971; TURNER, 1992; ZOMENI AND TSIOLAKIS 2008; ZOMENI AND GEORGIADOU, 2015) ILLUSTRATING THE LOCATIONS OF THE TWO CROSS SECTIONS. CROSS SECTION A-B CUTS THE AKAMAS PENINSULA (A) IN THE WEST AND PASSES THROUGH THE POLIS BASIN AND ENDS AT THE WESTERN FLANK OF THE TROODOS MOUNTAIN (B). CROSS SECTION C-D STARTS FROM THE COASTLINE CLOSE TO THE VILLAGE OF PEGEIA (C) AND CROSS CUTS THE POLIS BASIN THROUGH TO THE VILLAGE OF LYSOS (D), CLOSE TO THE FOOTHILLS OF THE TROODOS MOUNTAIN.....	175

FIGURE 4 - 37: STRUCTURAL CROSS-SECTIONS THROUGH THE POLIS BASIN (PAYNE AND ROBERTSON, 1995; 2000). THICK LINES DENOTE FIRST-ORDER FAULTS (DASHED = INFERRED) AND THIN LINES DENOTE SECOND-ORDER FAULTS. INSET SHOWS THE LOCATION OF THE POLIS BASIN, THE LOCATIONS OF THE CROSS-SECTIONS AND SEVERAL VILLAGES DISCUSSED IN THE TEXT BELOW. .... 176

FIGURE 4 - 38: CROSS SECTION PASSING FROM THE AKAMAS PENINSULA TO THE TROODOS OPHIOLITES ILLUSTRATING THE CONTACTS AND THE TECTONIC STRUCTURES IN THE POLIS BASIN. LOCATION OF CROSS SECTION ILLUSTRATED IN FIGURE 4 - 36 (PROFILE A-B). LOCATION AND DESCRIPTION OF BOREHOLE DATA INDICATED IN FIGURE 4 - 2 AND FIGURE 4 - 3 (BOREHOLE 8). NOTE: BASEMENT LEVEL IS ARBITRARY..... 178

FIGURE 4 - 39: RECONSTRUCTION MODEL ILLUSTRATING THE TECTONIC ACTIVITY OF THE NORTHERN PART OF THE POLIS BASIN (CAMPANIAN-MAASTRICHTIAN). RED LINES INDICATE ACTIVE THRUSTING, WHILE BLACK LINES INDICATE INACTIVITY. LOCATION OF CROSS SECTION ILLUSTRATED IN FIGURE 4 - 36 (PROFILE A-B). NOTE: BASEMENT LEVEL AND SHORTENING RATES ARE ARBITRARY. LEGEND AS IN FIGURE 4 - 38. .... 180

FIGURE 4 - 40: RECONSTRUCTION MODEL ILLUSTRATING THE TECTONIC ACTIVITY OF THE NORTHERN PART OF THE POLIS BASIN (PALEOCENE-EARLY MIOCENE). RED LINES INDICATE ACTIVE THRUSTING, WHILE BLACK LINES INDICATE INACTIVITY. LOCATION OF CROSS SECTION ILLUSTRATED IN FIGURE 4 - 36 (PROFILE A-B). NOTE: BASEMENT LEVEL AND SHORTENING RATES ARE ARBITRARY. LEGEND AS IN FIGURE 4 - 38. .... 181

FIGURE 4 - 41: RECONSTRUCTION MODEL ILLUSTRATING THE TECTONIC ACTIVITY THROUGH TIME OF THE NORTHERN PART OF THE POLIS BASIN (MIDDLE-LATE MIOCENE). RED LINES INDICATE ACTIVE THRUSTING, WHILE BLACK LINES INDICATE INACTIVITY. LOCATION OF CROSS SECTION ILLUSTRATED IN FIGURE 4 - 36 (PROFILE A-B). NOTE: BASEMENT LEVEL AND SHORTENING RATES ARE ARBITRARY. LEGEND AS IN FIGURE 4 - 38. .... 182

FIGURE 4 - 42: CROSS SECTION PASSING FROM THE PEGEIA VILLAGE TO THE TROODOS OPHIOLITES ILLUSTRATING THE CONTACTS AND THE TECTONIC STRUCTURES OF THE CENTRAL PART OF THE POLIS BASIN. LOCATION OF CROSS SECTION ILLUSTRATED IN FIGURE 4 - 36 (PROFILE C-D). LOCATION AND DESCRIPTION OF BOREHOLE DATA INDICATED IN FIGURE 4 - 2 AND FIGURE 4 - 3 (BOREHOLES 1-7). NOTE: BASEMENT LEVEL AND SHORTENING RATES ARE ARBITRARY. .... 185

FIGURE 4 - 43: RECONSTRUCTION MODEL ILLUSTRATING THE TECTONIC ACTIVITY OF THE CENTRAL PART OF THE POLIS BASIN (CAMPANIAN-MAASTRICHTIAN). RED LINES INDICATE ACTIVE THRUSTING, WHILE BLACK

LINES INDICATE INACTIVITY. LOCATION OF CROSS SECTION ILLUSTRATED IN FIGURE 4 - 36 (PROFILE C-D).  
NOTE: BASEMENT LEVEL AND SHORTENING RATE ARE ARBITRARY. LEGEND AS IN FIGURE 4 - 42. .... 187

FIGURE 4 - 44: RECONSTRUCTION MODEL ILLUSTRATING THE TECTONIC ACTIVITY OF THE CENTRAL PART OF THE POLIS BASIN (PALEOGENE-EARLY MIOCENE). RED LINES INDICATE ACTIVE THRUSTING, WHILE BLACK LINES INDICATE INACTIVITY. LOCATION OF CROSS SECTION ILLUSTRATED IN FIGURE 4 - 36 (PROFILE C-D).  
NOTE: BASEMENT LEVEL AND SHORTENING RATE ARE ARBITRARY. LEGEND AS IN FIGURE 4 - 42. .... 188

FIGURE 4 - 45: RECONSTRUCTION MODEL ILLUSTRATING THE TECTONIC ACTIVITY OF THE POLIS BASIN (MIDDLE-LATE MIOCENE). RED LINES INDICATE ACTIVE THRUSTING, WHILE BLACK LINES INDICATE INACTIVITY. LOCATION OF CROSS SECTION ILLUSTRATED IN FIGURE 4 - 36 (PROFILE C-D). NOTE:  
BASEMENT LEVEL AND SHORTENING RATE ARE ARBITRARY. LEGEND AS IN FIGURE 4 - 42. .... 189

FIGURE 4 - 46: CROSS SECTION PASSING FROM THE PARAMALI VILLAGE TO THE TROODOS OPHIOLITES ILLUSTRATING THE CONTACTS AND THE TECTONIC STRUCTURES IN THE LIMASSOL BASIN. LOCATION OF CROSS SECTION ILLUSTRATED IN FIGURE 4 - 2 (PROFILE 3). NOTE: BASEMENT LEVEL IS ARBITRARY. .... 191

FIGURE 4 - 47: SIMPLIFIED CARTOON OF THE STRUCTURAL EVOLUTION OF SW CYPRUS. RED LINES DEPICT ACTIVE THRUST FAULTS, WHILE BLACK LINES DEPICT INACTIVE FAULTS. DASHED LINES INDICATE INFERRED FAULTS IN AREAS WHERE THE OUTCROPS ARE COVERING THE STRUCTURES OR IT IS DIFFICULT TO OBSERVE THEM. GREY DASHED LINES INDICATE THE LIMIT BETWEEN THE TWO BASINS. BLACK LINES WITH NUMBERS INDICATE THE CROSS SECTIONS DISCUSSED ABOVE. ABBREVIATIONS: AKT: AKAMAS THRUST; GFTB: GERASA FOLD AND THRUST BELT; KAT: KATHIKAS THRUST; PPT: PELATHOUSA-PERISTERONA THRUST; PTF: PAPHOS THRUST FAULT..... 197

FIGURE 5 - 1: UN-INTERPRETED AND INTERPRETED SEISMIC PROFILE IN TWO WAY TRAVEL TIME (TWT) IN THE CILICIA BASIN. RED LINE IN INDEX MAP ILLUSTRATED THE POSITION OF THE PROFILE. UNIT 1 CORRESPONDS TO PLIO-PLAISTOCENE CLASTIC SEDIMENTS. UNIT 2 INDICATES MESSINIAN SALT DEPOSITS. UNIT 3 CORRESPONDS TO MIDDLE TO LATE MIOCENE HEMI-PELAGIC CARBONATES [BLANCO, 2014]..... 202

FIGURE 5 - 2: INTERPRETED SEISMIC PROFILE IN TWO-WAY-TRAVEL TIME (TWT) PASSING FROM THE ERATOSTHENES MICRO CONTINENT TOWARDS THE CYPRUS ARC SYSTEM. A FLEXURAL BASIN IS

DOCUMENTED AND A POP-UP STRUCTURE ASSOCIATED WITH THICK SKINNED DEFORMATION. [MONTADERT ET AL., 2014]. THE BLACK LINE IN THE INSET MAP INDICATES THE LOCATION OF THE SEISMIC PROFILE. ABBREVIATIONS: CA=CYPRUS ARC; ECB=ERATOSTHENES CONTINENTAL BLOCK; LR=LATAKIA RIDGE.....	203
FIGURE 5 - 3: SIMPLIFIED GEOLOGICAL CROSS SECTION THROUGH THE GERASA FOLD AND THRUST BELT, WHICH ILLUSTRATES A STRATIGRAPHIC UNCONFORMITY BETWEEN THE PAKHNA FORMAITON AND THE UNDERLYING LEFKARA FORMATION [FROM KINNAIRD, 2008 AS MODIFIED AFTER EATON AND ROBERTSON, 1993.] THE RED LINE ON THE INSET MAP INDICATES THE LOCATION OF THE CROSS SECTION [MAP MODIFIED FROM HARRISON ET AL., 2008].....	205
FIGURE 5 - 4: THE LEFKONIKO BOREHOLE AND SCHEMATIC CROSS SECTION ACROSS THE OVGOS THRUST FAULT, WHICH IS CONSIDERED AS THE BOUNDARY BETWEEN THE TROODOS SEDIMENTARY COVER AND THE KYRENIA TERRANE. TRUE DEPTH OF THE CONTACTS ARE SHOWN FOR THE BOREHOLE. INSET MAP OF CYPRUS INDICATES THE LOCATION OF THE CROSS SECTION (RED LINE). LEGEND EXPLAINS THE FORMATIONS USED IN THIS CROSS SECTION. [FROM HARRISON ET AL., 2008]. THE RED LINE ON THE INSET MAP INDICATES THE LOCATION OF THE CROSS SECTION [MAP MODIFIED FROM HARRISON ET AL., 2008].....	206
FIGURE 5 - 5: DEFORMATION CHART ILLUSTRATING THE STRESS DIRECTION, THE DEFORMATION PHASE CONNECTED WITH THE GEODYNAMIC CONTEXT THROUGH TIME. ....	207
FIGURE 5 - 6: OLIGOCENE TO EARLY MIOCENE GEODYNAMIC EVOLUTION MODEL OF THE EASTERN MEDITERRANEAN REGION. DESCRIPTION OF STRUCTURES IN FIGURE 5 - 7. ABBREVIATIONS: ATF: ARAKAPAS THRUST FAULT; EH: ERATOSTHENES HIGH; GFTB: GERASA FOLD AND THRUST BELT; HB: HERODOTUS BASIN; HR: HECATAEUS RISE; KAT: KATHIKAS THRUST; KR: KYRENIA RANGE; LB: LEVANT BASIN; LNR: LARNACA RIDGE; MR: MARGAT RIDGE; TOP: TROODOS OPHIOLITES.....	209
FIGURE 5 - 7: LEGEND EXPLAINING THE DIFFERENT FEAUTURES ILLUSTRATED IN FIGURE 5 - 6, FIGURE 5 - 8, FIGURE 5 - 9. ....	210
FIGURE 5 - 8: LATE MIOCENE GEODYNAMIC EVOLUTION MODEL OF THE EASTERN MEDITERRANEAN REGION. DESCRIPTION OF STRUCTURES IN FIGURE 5 - 7. ABBREVIATIONS: ATF: ARAKAPAS THRUST FAULT; EH: ERATOSTHENES HIGH; GFTB: GERASA FOLD AND THRUST BELT; HB: HERODOTUS BASIN; HR: HECATAEUS	

RISE; KAT: KATHIKAS THRUST; KR: KYRENIA RANGE; LB: LEVANT BASIN; LNR: LARNACA RIDGE; LR: LATAKIA RIDGE; MR: MARGAT RIDGE; TOP: TROODOS OPHIOLITES. .... 211

FIGURE 5 - 9: PLIO-PLEISTOCENE GEODYNAMIC EVOLUTION MODEL OF THE EASTERN MEDITERRANEAN REGION. DESCRIPTION OF STRUCTURES IN FIGURE 5 - 7. ABBREVIATIONS: ATF: ARAKAPAS THRUST FAULT; EH: ERATOSTHENES HIGH; GFTB: GERASA FOLD AND THRUST BELT; HB: HERODOTUS BASIN; HR: HECATAEUS RISE; KAT: KATHIKAS THRUST; KR: KYRENIA RANGE; LB: LEVANT BASIN; LNR: LARNACA RIDGE; LR: LATAKIA RIDGE; MR: MARGAT RIDGE; TOP: TROODOS OPHIOLITES. .... 212

FIGURE 5 - 10: ILLUSTRATION OF THE THROW ALONG STRIKE OF THE LATAKIA RIDGE. IN THE EAST THE LARGE THROW BETWEEN THE MIOCENE AND THE PLIO-PLEIOCENE LINES INDICATES THE TRANSITION FROM COMPRESSION TO STRIKE SLIP DEFORMATION. IN THE WEST THE LARGE THROW OF THE PLIO-PLEISTOCENE LINE INDICATES THE COLLISION BETWEEN ERATOSTHENES MICRO CONTINENT AND CYPRUS WHICH RESULTS IN THE UPLIFT OF THE ISLAND. .... 214

FIGURE 5 - 11: ILLUSTRATION OF THE THROW ALONG STRIKE OF THE MARGAT RIDGE. THE DIMINISHING THROW TOWARDS THE WEST INDICATES THAT THE STRUCTURE DOES NOT EXTEND TOWARDS THE WEST PROBABLY DUE TO THE EXISTENCE OF THE HECATAEUS RISE, A CONTINENTAL BLOCK THAT PREVENTS THE MARGAT RIDGE MIGRATING TOWARDS THE WEST. .... 214

FIGURE 5 - 12: LOCATION OF SEISMIC PROFILES UTILIZED TO CREATE THE CHARTS IN FIGURE 5 - 10 AND IN FIGURE 5 - 11. ABBREVIATIONS: CA: CYPRUS ARC; CB: CYPRUS BASIN; HR: HECATAEUS RISE; LNR: LARNACA RIDGE; LR: LATAKIA RIDGE; MR: MARGAT RIDGE; PTF: PAPHOS TRANSFORM FAULT. .... 215



## Abstract

The Cyprus Arc system is a major plate boundary in the Eastern Mediterranean, where different plates interact, namely the Arabian, African, Eurasian, as well as the Anatolian micro-plate. It constitutes the northern boundary of the Levant Basin (thin stretched continental crust) and the Herodotus Basin (oceanic crust). The Cyprus Arc is directly linked with the northward convergence of the African continental plate with respect to the Eurasian continental plate since the Late Cretaceous. The indentation of the Arabian plate and the slab pull effect of the African plate roll back in the Aegean region on the eastern and western part of the Anatolian plate respectively, lead to the westward escape of Anatolia from Late Miocene to Recent, which results in a strike-slip component along the Cyprus Arc system and onshore Cyprus.

Several scientific questions with regard to the geological setting of the region were investigated during this project. How is the deformation accommodated at the Cyprus Arc system? Is this deformation style affected by the variation of the crustal nature at each domain? How is this deformation recorded on the sedimentary pile onshore Cyprus? How does the onshore and offshore deformation connect within the geodynamic context of the region?

In order to answer these scientific questions, 2D reflection seismic data were utilized, that image the main plate structures and their lateral evolution south and east of Cyprus. Interpretation of these data lead to the identification of nine tectono-sedimentary packages in three different crustal domains south of the Cyprus Arc system: (1) The Levant Basin (attenuated continental crust), (2) The Eratosthenes micro-continent (continental crust) and (3) The Herodotus Basin (oceanic crust). Within these domains, numerous tectonic structures were documented and analysed in order to understand the mechanism and timing of deformation.

At the northern boundary of the Levant Basin domain, thrust faults verging towards the south were documented in the Cyprus Basin with the thrust movement commencing in Early Miocene time as identified on the Larnaca and Margat Ridges. On the Latakia Ridge no activity was identified during this time interval. The peak of deformation occurred in Middle to Late Miocene time, with the activity of the Latakia Ridge indicating the forward propagation of the deformation front towards the south. This southward migration was documented from the development of flexural basins and from stratigraphic onlaps in the Cyprus Basin. Successive tectonic pulses through the Late Miocene until Recent times, are evident from the angular unconformities and the piggy back basins. In Plio-Pleistocene time, the westward escape of the Anatolian micro-plate resulted in the reactivation of existing structures. The evolution to strike-slip deformation along the plate boundary is identified by the creation of positive flower structures revealing transpressive movements along the Larnaca and Latakia Ridges (eastern domains). The central domain includes the Eratosthenes Seamount which is identified as a Mesozoic carbonate platform covered by a thin sequence of sediments ranging from Miocene-Messinian to Pliocene-Pleistocene deposits. An important thrust bordering a flexural basin

infilled by Plio-Pleistocene sediments is evidence of the active compressive nature of the Cyprus Arc until Recent times and could be associated with the convergent movement of the African plate and the collision and northward subduction of the Eratosthenes Seamount under Cyprus. The South-West domain of the Herodotus Basin is characterized by thick Pliocene and Messinian salt sedimentation, which poses difficulties in the observation of deep structures. Messinian and Pliocene aged faulting is observed and could be attributed to salt tectonics. The westward change in the internal architecture of the plate boundary as well as the increase in shortening along the Cyprus Arc are in accordance with the change of the crustal nature of the Eastern Mediterranean basin.

Two field campaigns were undertaken in order to record and constrain the tectonic structures onshore Cyprus. The study area was the south and southwest Alassa and Polemi Basins respectively. Initial reconnaissance lead to a number of outcrops consisting of the following sedimentary formations: a) Triassic age Mamonnia Complex; b) Campanian age Kannaviou Formation; c) the Maastrichtian Moni and Kathikas Formations; d) the Paleogene Lefkara Formation; e) the Miocene Pakhna Formation which is divided into the i) Early Miocene Tera Member; ii) the Middle Miocene Pakhna Formation; and iii) the Late Miocene Koronia Member; and f) the Plio-Pleistocene Nicosia Formation. The main focus of the two campaigns was the Cenozoic sedimentary cover as the Late Cretaceous structures are difficult to constrain due to the debris flow and melange nature. In the Polis Basin, an Oligocene to Early Miocene thrusting movement was identified as Late Maastrichtian chalks are overlying Middle Eocene chalks and cherts. This deformation phase was also observed on the eastern flank of the Limassol Basin as Miocene Pakhna chalks are unconformably overlying the Eocene Lefkara chalks, thus indicating a regional deformation event. A second tectonic pulse of Late Miocene time was identified in the Polis Basin as Koronia Member reefs are in direct contact with the Kannaviou Formation. In the Limassol Basin the Tortonian Koronia Member reefs are overlying the Campanian Moni Formation, a large hiatus which is indicative of a regional tectonic pulse. During the Plio-Pleistocene both basins are progressively shallowing due to the collision of the Eratosthenes Seamount with Cyprus.

Based on the onshore observations, the geological maps were revised and information from existing boreholes were utilized to create cross-sections of the SW and S part of the island. Structural field data and bio-stratigraphic dating were gathered especially in the area of the Polis Basin in order to comprehend the main geometries and to obtain key information in order to constrain the timing of tectonic activity. These data are combined to propose reconstruction models at different key periods which illustrate the structural evolution of SW Cyprus since Late Cretaceous. Onshore and offshore observations highlight the deformation, in the form of

SW verging thrusts. Although it is more difficult to constrain strike-slip faults, these are inferred at least during the later stages of deformation.

Concluding three major deformation phases were identified, commencing with a compression from Oligocene to Early Miocene time. The most intense compressional phase is recorded in Middle to Late Miocene time and it is associated with propagation of the deformation front towards the south and re-activation of inland structures. The final phase is recorded in Plio-Pleistocene time and it is associated with strain partitioning and transpressive deformation. These observations were tied together by using offshore data which provide a large scale regional understanding and by correlating it with onshore data which provide a good understanding of the outcropping formations and a good constrain on the timing of deformation. In the eastern domain, the interaction between continental crust and attenuated continental crust results in strike slip deformation, while in the central domain collision between continent/continent crust results in compressional deformation.

## Resume

En Méditerranée orientale, l'arc de Chypre est une frontière géologique majeure où interagissent les plaques Arabie, Afrique, Eurasie et la microplaque anatolienne. Il constitue la limite Nord du bassin du Levant (croûte continentale amincie étirée) et du bassin d'Hérodote (croûte océanique). L'arc de Chypre est directement lié à la convergence vers le Nord de la plaque Africaine sur la plaque Eurasienne depuis la fin du Crétacé. Dans la région Egéenne, l'indentation de la plaque Arabique sur la partie orientale de la plaque Anatolienne d'une part, et l'effet « roll back » du plan de subduction africain dans la partie occidentale de la plaque Anatolienne d'autre part, ont pour conséquence l'expulsion de l'Anatolie depuis la fin du Miocène à aujourd'hui, ce qui se traduit par un décrochement le long de l'arc de Chypre, se prolongeant sur l'île de Chypre.

Plusieurs questions scientifiques concernant le cadre géologique de la région ont été étudiées au cours de ce projet. Comment la déformation est-elle intégrée dans le système de l'Arc de Chypre? La variation crustale de chaque domaine affecte-t-elle le style de déformation? Comment cette déformation est-elle enregistrée dans les sédiments de l'île de Chypre? Comment ces déformations (Onshore / Offshore) peuvent être connectées au contexte géodynamique régional?

Afin de répondre à ces questions scientifiques, des données sismiques de réflexion 2D ont été utilisées, et ont permis d'imager les structures principales et leur évolution spatiale dans les parties Sud et Orientale de Chypre. L'interprétation de ces données conduit à l'identification de neuf unités tectono-sédimentaires dans trois différents domaines de la croûte crustale au sud du système de l'Arc chypriote: (1) le bassin du Levant (croûte continentale amincie), (2) le micro-continent d'Eratosthène (croûte continentale) et (3) le bassin d'Hérodote (croûte océanique). Dans ces domaines, de nombreuses structures tectoniques ont été documentées et analysées afin de comprendre le mécanisme et le timing de la déformation.

À la limite nord du domaine du bassin du Levant, des accidents majeurs chevauchants vers le Sud ont été documentés dans le bassin de Chypre, commençant au début du Miocène et enregistrés par les failles de Larnaca et de Margat. La faille Latakia n'a quant à elle enregistré aucune activité pendant cette période. L'apogée de la déformation s'est produite du Miocène moyen jusqu'à la fin du Miocène, l'activité de la faille de Latakia indiquant la propagation vers le Sud du front de déformation. Cette migration vers le sud a été documentée à partir du développement de bassins flexuraux et des chevauchements stratigraphiques dans le bassin de

Chypre. Les pulses tectoniques successifs depuis la fin du Miocène jusqu'à aujourd'hui, sont indiquées par les discordances angulaires et les bassins piggy back. Pendant la période Plio-Pléistocène, l'expulsion vers l'ouest de la microplaque anatolienne a entraîné la réactivation des structures existantes. L'évolution de la déformation le long de la limite de la plaque est identifiée à partir de la création de structures en fleur positives révélant des mouvements transpressifs le long des failles Larnaca et Latakia (domaines orientaux). Le domaine central comprend le mont sous-marin d'Eratosthène qui se caractérise comme une plate-forme carbonatée mésozoïque recouverte d'une mince séquence sédimentaire allant des dépôts Messinien aux dépôts Pléistocène. L'un des marqueurs de l'activité de la compression à cette période est le chevauchement marquant la bordure du bassin flexural remplis de sédiments Plio-Pléistocène, qui peut être associé à la collision et à la subduction vers le Nord du mont sous-marin Eratosthène sous Chypre. Le domaine Sud-Ouest du bassin d'Hérodote est caractérisé par une pile sédimentaire épaisse d'âge Pliocène et le dépôt de sel Messinien, ce qui pose des difficultés pour l'observation des structures profondes. Une activité des chevauchements, supposée Messinienne à Pliocène, pourrait être attribuée à la tectonique salifère de cette période. La variation latérale de l'architecture interne en allant vers l'Ouest de la frontière de plaque et l'augmentation du raccourcissement le long de l'Arc de Chypre sont concordantes avec le changement de nature crustal du bassin méditerranéen oriental.

Dans ce projet, deux campagnes de terrain ont été entreprises afin de cartographier et de contraindre les structures tectoniques de la partie Sud-Ouest de Chypre (bassins d'Alassa et de Polémi). Ces deux campagnes visaient principalement la couverture sédimentaire Cénozoïque, les structures Crétacée étant difficiles à caractériser en raison de l'altération prononcée du mélange. Dans le bassin de Polis, les failles chevauchantes ont été actives depuis l'Oligocène jusqu'au début du Miocène. Cette phase de déformation a également été identifiée sur les flancs Est du bassin de Limassol, montrant ainsi qu'il s'agit d'une déformation régionale. Une seconde phase de déformation compressive a été identifiée à la fin du Miocène dans les bassins de Polis et de Limassol, indiquant une déformation d'échelle régionale. Pendant le Plio-Pléistocène, les deux bassins subsident progressivement en raison de la collision d'Eratosthène avec Chypre.

Des données structurales de terrain et des datations bio-stratigraphiques ont été entreprises dans le but de comprendre les principales géométries actuelles et reconstruire l'activité tectonique dans le temps. Ces données ont été assemblées afin de proposer un modèle de reconstruction illustrant l'évolution structural du Sud-Ouest de Chypre depuis la fin du Crétacée.

Trois phases de déformation majeures ont été identifiées, débutant avec une compression à l'Oligocène jusqu'au début du Miocène. La phase de compression la plus importante est enregistrée au Miocène moyen jusqu'à la fin du Miocène et est associées avec la propagation du front de déformation vers le Sud et la réactivation des structures internes. La dernière phase de déformation est enregistrée au Plio-Pléistocène et est associée à un partitionnement des contraintes et à une déformation transpressive. Ces observations ont été reliées entre elles en utilisant les données offshore qui permettent une compréhension régionale et les données de terrain qui permettent une bonne compréhension des affleurements et des timings de déformation.

La partie orientale de l'arc de Chypre est finalement marquée par des déformation transformantes tandis que le domaine central est marquée par la collision continent / continent conduisant à des déformations compressives.



***Chapter 1***

***Introduction***

The Eastern Mediterranean region is governed by a complex geological setting depicting different, interactive plate boundaries, which create major tectonic structures (*Figure 1 - 1*). The continuous changes in tectonic regime through the geological periods, have shaped this rather rugged corner of the world in a monumental way. The opening of the Neo-Tethys in Early Mesozoic time in connection with the rifting phase from Triassic to Jurassic times, the continuous convergence of the African and Eurasian plates since Late Cretaceous resulting in the emplacement of the ophiolite bodies in the region and the expulsion of the Anatolian micro-plate towards the West, are considered major geodynamic processes that impacted profoundly the tectonic evolution of the Eastern Mediterranean.

The Cyprus Arc System which is situated just south of the island of Cyprus (*Figure 1 - 1*), is described as a major plate boundary that separates the African and Eurasian plates. It is bordered to the north-east by the Cyprus Basin, which is covered by at least 4-6km of sediments as identified on seismic profiles [Ben-Avraham et al., 1995; Vidal et al., 2000; Hall et al., 2005; Calon et al., 2005; Bowman, 2011; Montadert et al., 2014] and a proposed crustal nature consisting of obducted ophiolites [Calon et al., 2005; Bowman, 2011]. To the south-east, the Cyprus Arc is bordered by the Levant Basin, which is considered as a deep basin infilled by a thick sedimentary cover of around 12-14km [Makris et al., 1983; Vidal et al., 2000a, b; Ben-Avraham et al., 2002; Montadert et al., 2014] and underlain by thin attenuated continental crust [Netzeband et al., 2006; Granot, 2016; Inati et al., 2016]. Directly south it is bordered by the Eratosthenes Seamount, a Mesozoic carbonate platform which is underlain by continental crust [Welford et al., 2015]. Finally, the south-west boundary is the Herodotus Basin, a deep basin filled by ~12km of sediments [Montadert et al., 2014], and floored by oceanic crust [Makris et al., 1983; Vidal et al., 2000a, b; Ben-Avraham et al., 2002; Netzeband et al., 2006; Montadert et al., 2014; Granot, 2016; Inati et al., 2016]. The eastern continuation of the Cyprus Arc system is the Latakia Ridge system which extends onshore Syria and joins up with the Eastern Anatolian Fault [Kempler and Garfunkel, 1991, 1994; Faccenna et al., 2006]. The western continuation of the Arc joins up with the Florence Rise [Baroz et al., 1978; Woodside et al., 2002; Hall et al., 2014] and passes from the offshore Anaximander Mountains [Zitter et al., 2003; Aksu et al., 2005] to Antalya region (southwest Turkey) [Hall et al., 2014].

To this accord a large number of studies have been published in the last fifty years focusing on deciphering the tectonic evolution of the eastern Mediterranean region by establishing models that explain the key geological processes. A sizeable amount of studies focuses on the onshore deformation and the tectonic structures in Cyprus [Lapierre et al., 1975; Cleintuar et al., 1977; Mantis, 1977; Pantazis 1978; Robertson, 1977; Simonian and Gass, 1978; Swarbrick and Naylor, 1980; Swarbrick and Robertson, 1980; Swarbrick, 1993; Eaton and

Robertson, 1993; Payne and Robertson, 1995, 2000; Bailly et al., 2000; Lord et al., 2000; Baill Harrison et al., 2004, 2008, 2012; Geoter, 2005; Kinnaird 2008; Kinnaird et al., 2011, 2013], in Syria [Brew et al., 2001a, b; Kempler and Garfunkel, 1994; Al Abdala et al., 2010], in Lebanon [Ghalayini et al., 2014, 2017; Homberg et al., 2010; Hawie et al., 2013], in Israel [Garfunkel and Derin, 1984], in Egypt [Moustafa et al., 2010], in Turkey [Dilek and Altunkaynak, 2009; Dilek and Sandvol, 2009; Robertson et al., 2012; Faccenna et al., 2006; Kelling et al., 1987] and in Greece in the Aegean region [Jolivet and Facenna, 2000]. Offshore investigations have proved extremely important for the recognition of tectonic structures, and since the last decade they were beneficial for oil-gas companies. Indeed, such investigations led to a number of major hydrocarbon discoveries such as Tamar, Leviathan, Aphrodite-A and Zohr fields [[www.nobleenergyinc.com](http://www.nobleenergyinc.com); Montadert et al., 2010; Esestime et al., 2016], making this a very prospective area for further research. These studies have highlighted structures such as the Cyprus Arc system [Montadert et al., 2014; Reiche et al., 2015], the Latakia Ridge System [Ben-Avraham et al., 1995; Vidal et al., 2000; Hall et al., 2005; Calon et al., 2005; Bowman, 2011; Montadert et al., 2014], and the Eratosthenes Seamount [Kempler, 1998; Robertson, 1998; Montadert et al., 2014; Welford et al., 2015]. They helped in gathering data about the crustal nature that constitutes the different basins offshore via different geophysical techniques [Makris et al., 1983, Ben-Avraham et al., 2002; Ergun et al., 2005; Netzeband et al., 2006; Granot, 2016; Inati et al., 2016]. Nevertheless, questions still remain regarding the tectonic deformation of the Cyprus Arc system through time. What impact does its configuration and longitudinal change in tectonic regime have on the geodynamic context at a plate scale? What are the deformation mechanisms that can explain this plate boundary?

The Levant Basin area is well documented [Gardosh and Druckman, 2006; Roberts and Peace, 2007; Gardosh et al., 2010; Bowman, 2011; Hawie et al., 2013; Montadert et al., 2014; Ghalayini et al., 2014], as is the Latakia Ridge [Vidal et al., 2000; Hall et al., 2005; Calon et al., 2005; Bowman, 2011; Montadert et al., 2014]. Although data exist on the Cyprus Basin it is not well constrained as most studies focus on the Latakia Ridge itself [Vidal et al., 2000; Hall et al., 2005; Calon et al., 2005; Bowman, 2011; Montadert et al., 2014]. In contrast the sedimentary cover of the Herodotus Basin is still debated [Montadert et al., 2014]. Due to the water depth and the lack of drilled wells, it is very difficult to describe the facies of the sediments and thus understand the timing of deformation on the various tectonic structures.

Paleo-geographic, structural reconstruction models focusing on the Eastern Mediterranean [Stampfli and Borel 2002; Garfunkel 1998, 2004; Barrier and Vrielynck, 2008; Gardosh et al., 2010; Frizon de la Motte et al., 2011; Robertson et al., 2012; Montadert et al., 2014] have illustrated that the region was first molded by a rifting phase that commenced in the

Early Mesozoic and halted in Mid-Late Jurassic time [Gardosh and Druckman, 2006]. A compressional regime followed suite from Late Cretaceous until Late Miocene, expressed by the continuous northward convergence of the African continental plate with respect to the Eurasian continental plate and evidenced by the emplacement of the ophiolite suite at Baer-Bassit (Syria), at Troodos (Cyprus) and at Antalya (Turkey) [Montadert et al., 2014]. From Late Miocene onwards, a change in tectonic regime from a compressional to a transpressional regime (Latakia Ridge) is attributed to the westward expulsion of the Anatolian micro-plate [McClusky et al., 2003; Wdowinski et al., 2006; Faccenna et al., 2006; Le Pichon and Kreemer, 2010].

This complexity of the Eastern Mediterranean region is directly connected with the northward movement of the African continental plate with respect to the Eurasian plate and the differential crustal nature that underlays each domain. The results of this displacement are well documented from investigations on tectonic structures such as: a) the Zagros Thrust belt (Figure 1 - 2), which resulted from continent-continent collision [Agard et al., 2011]; b) the Hellenic Arc (Figure 1 - 3), developed under an extensional regime due to the northward subduction of the African plate under the Aegean region which later changed into slab roll back [Dilek and Sandvol, 2009]; and c) the Cyprus Arc system (Figure 1 - 4), with its eastern segment illustrating transpressional regime in response to the collision between a thin attenuated continental crust (Levant Basin) and a suspected ophiolite basement (Cyprus Basin) and its central segment displaying a compressional regime from the collision of Eratosthenes Seamount with the island of Cyprus [Montadert et al., 2014].

Several authors attribute the general tectonic evolution of Cyprus and the particular evolution of the Cyprus Arc system to an advanced collision setting of the African and Eurasian plates. This collision in Eocene time, resulted in the creation of southward verging thrust systems [Sage and Letouzey, 1990; Calon et al., 2005]. By Miocene time, thrusting on the Troodos-Larnaca culmination and the Kyrenia Range results in the creation of the Mesaoria Basin which is considered as a piggy back basin [Calon et al., 2005]. Evidence of activity is indicated by two deep boreholes [Cleintuar et al., 1977], where Eocene deep pelagic carbonates of the Lefkara formation and Miocene hemi pelagic carbonates of the Pakhna Formation are juxtaposed with a thick sequence of Miocene flysch deposits of the Kythrea Formation [Calon et al., 2005]. A second group of authors, associate the tectonic evolution with a transpressive regime as most of the tectonic structures identified onshore from Late Miocene onwards are in accordance with strike slip deformation [Harrison et al., 2004, 2008, 2012]. The Ovgos fault in the Mesaoria Basin is one example as sediments of Miocene and Pliocene age are laterally displaced and juxtaposed [Harrison et al., 2004, 2008]. Thus a restraining bend model is proposed in order to explain the evolution of the region [Harrison et al., 2008]. A third scenario

is proposed invoking subduction and collision in Pliocene to Recent times [Robertson, 1990]. During the Early Neogene the pre-existing subduction zone was reactivated as evidenced by the change in depositional sediments from Paleogene deep pelagic chalks of the Lefkara Formation to the Miocene hemipelagic chalks of the Pakhna Formation [Eaton and Robertson, 1993]. From Early Miocene onwards, slab roll-back is proposed associated with extensional faults in the Polis graben [Payne and Robertson, 1995]. The uplift in Pliocene time is attributed to the collision of the Eratosthenes Seamount with Cyprus, as it is indicated by the deposition of clastic material throughout the island [Robertson, 1998; Kinnaird et al., 2011; Kinnaird and Robertson, 2013].

The differentiation of the crustal nature along strike of the Cyprus Arc system is an integral part of the deformation style with the interaction not fully understood in this compressional/transpressional setting. Question marks still loom large with respect to the deformation mechanisms that explain the mixture of tectonic structures and styles along of the Cyprus Arc system. How does the deformation style evolve along strike at this major plate boundary? How do the different crustal natures of the interacting domains affect the deformation patterns recorded in the sedimentary cover?

Thus the aim of this PhD project is to test the pre-existing theories of tectonic evolution onshore and offshore Cyprus and provide an adequate understanding for the geodynamic processes which are tied with the small scale tectonic structures, by proposing a working conceptual model regarding the role of major plate boundaries such as the Cyprus Arc system, in this complex geodynamic region. This will be achieved by examining the deformation style onshore Cyprus through field work undertaken in the south and south-west areas of the island, in combination with the interpretation of industrial quality reflection seismic profiles (24 profiles, 2D) that cover the Exclusive Economic zone of Cyprus (courtesy of PGS and the Ministry of Energy, Commerce, Industry and Tourism of the Republic of Cyprus).

Onshore field campaigns and acquisition of structural data, enabled the documentation of the tectonic stress prevailing during different time periods. Field investigations also helped in constructing key geological cross sections. The seismic interpretation aided in the documentation of the main tectonic structures in the Eastern Mediterranean basin (offshore Cyprus), thus providing the tools to constrain the timing and deformation mechanisms of the Cyprus Arc system. As a result by combining the onshore and offshore data a regional synthesis is proposed. Through this work it is illustrated that the variation in crustal nature influences the deformation style distinctively in the onshore sedimentary basins (in the west Polis Basin, in

the south Limassol Basin and in the north Mesaoria Basin) and similarly offshore Cyprus as it is portrayed at the eastern and western segment of the Cyprus Arc system.

The PhD Thesis is organized in six chapters, which are presented as follows: the introduction of the thesis indicates the geography of the Eastern Mediterranean region, it portrays the pre-existing studies in the different domains, discusses the scientific questions and the significance of the work undertaken. The second chapter, focusses on the literature review with regard to the major tectonic structures that are documented in the Eastern Mediterranean region, thus aiming to comprehend the tectonic evolution of this region. In chapter 3 the offshore tectonic structures are described as the interpretation of seismic data highlights the deformation timing and mechanism of the investigated structures. This chapter is in the form of an article, which is accepted in the journal of AGU Tectonics with the title: Longitudinal and temporal evolution of the tectonic style along the Cyprus Arc system, assessed through 2D reflection seismic interpretation. The fourth chapter examines the onshore deformation as it was documented from field campaigns and the recorded fault measurements and field observations. Chapter 5 consists of a synthesis of the results obtained throughout this PhD and the assessment of the onshore and offshore data in order to comprehend the regional tectonic evolution. The last chapter exhibits the conclusions derived from this thesis.

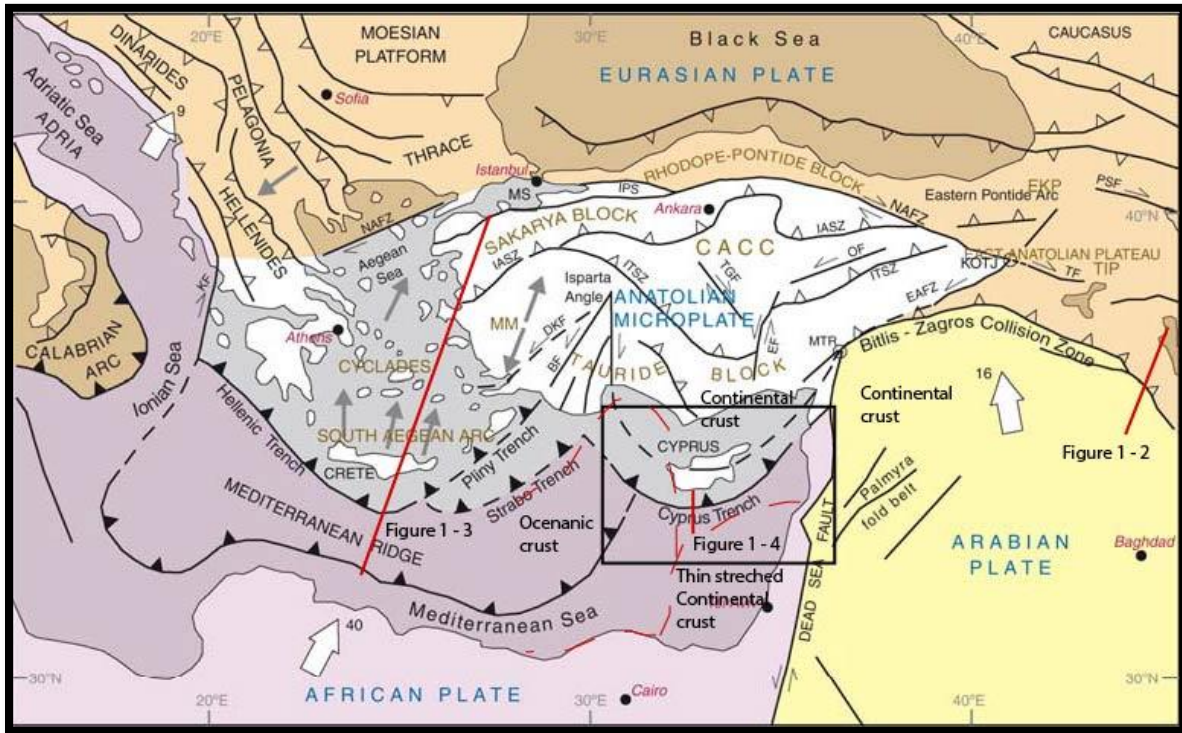


Figure 1 - 1: Tectonic map of the Aegean and eastern Mediterranean region, showing the main plate boundaries, major suture zones, and fault systems. Thick, white arrows depict the direction and magnitude (mm/a) of plate convergence; grey arrows mark the direction of extension (Miocene–Recent) (from Reilinger et al., 2006). Light-grey tone north of the North Anatolian Fault Zone (NAFZ) and west of the Calabrian Arc delineates Eurasian plate affinity, whereas the grey tones south of the Hellenic, Strabo and Cyprus Trenches delineate African plate affinity. BF, Burdur fault; CACC, Central Anatolian Crystalline Complex; DKF, Datca-Kale fault; EAFZ, East Anatolian fault zone; EF, Eceemis fault; EKP, Erzurum-Kars Plateau; IASZ, Izmir-Ankara suture zone; IPS, Intra-Pontide suture zone; ITS, Inner-Tauride suture; KF, Kefalonia fault; KOTJ, Karliova triple junction; MM, Menderes massif; MS, Marmara Sea; MTR, Maras triple junction; NAFZ, North Anatolian fault zone; OF, Ovacik fault; PSF, Pampak-Sevan fault; TF, Tutak fault; TGF, Tuz Golu fault; TIP, Turkish-Iranian plateau [from Dilek and Sandvol, [2009], as it was modified from Dilek [2006]. Red lines indicate the locations of the three figures that follow.

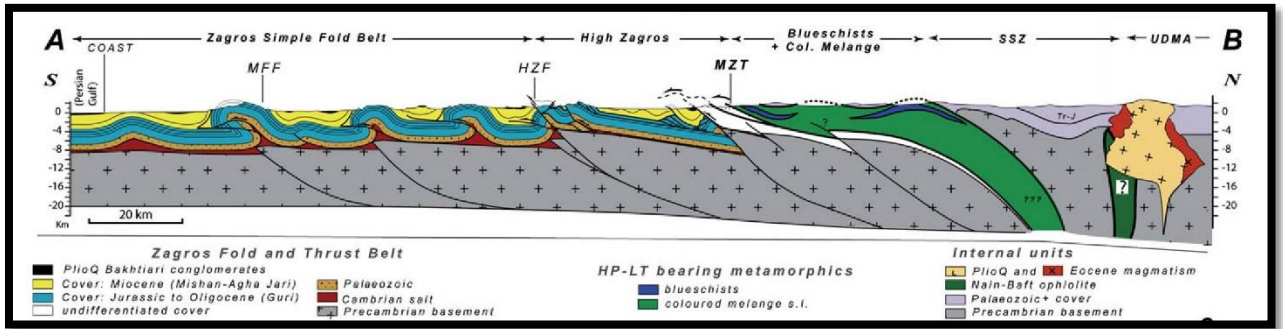


Figure 1 - 2: Geological cross section through the Zagros Fold and Thrust belt, illustrating the tectonic deformation in the Zagros region [Agard et al., 2011].

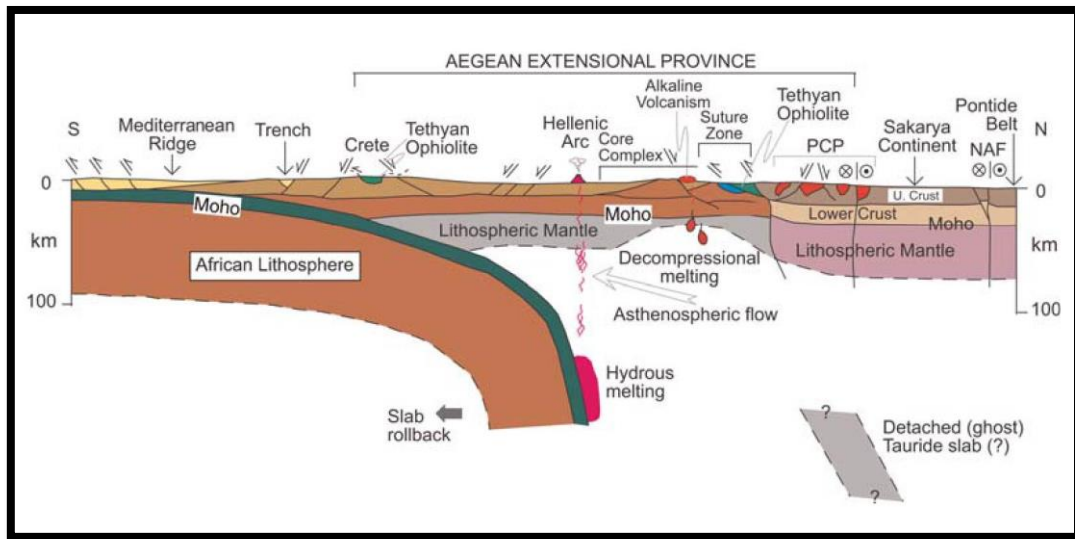


Figure 1 - 3: Geological cross section indicating the subduction of the African plate under the Aegean region and slab roll back [Dilek and Altunkaynak, 2009].

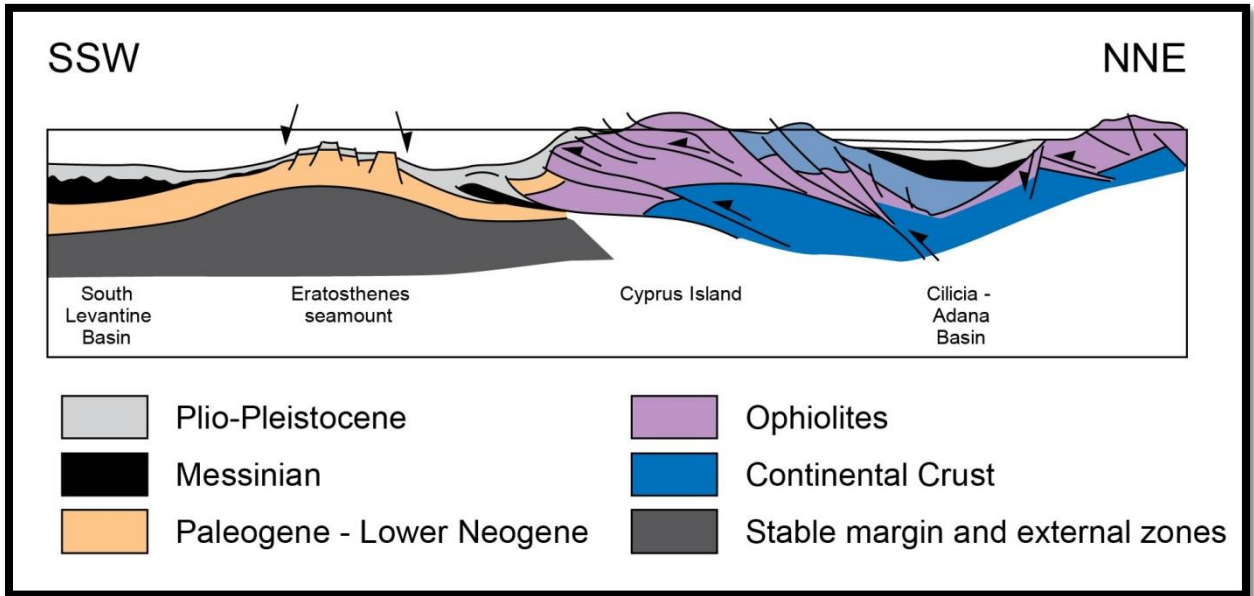


Figure 1 - 4: Geological cross section illustrating the collision of the Eratosthenes Seamount with the island of Cyprus [modified by Kinnaird, 2008 from original Sage and Letouzey, 1990].



**Chapter 2**  
**Geological Setting**

## 2.1 Regional geology

The Eastern Mediterranean domain is considered as a remnant of the Neo-Tethys Ocean [Robertson, 2007; Gardosh et al., 2010; Montadert et al., 2014]. Its present day configuration consists of various lithospheric plates, under a collisional regime. These lithospheric plates are the African continental plate, the Arabian continental plate, the Eurasian continental plate and the Anatolian micro plate.

The African and Arabian continental plates are moving northwards at a rate of ~10mm/yr and ~15-18mm/yr respectively, in correlation with a fixed Eurasian plate. [McClusky et al., 2000]. In comparison, the Anatolian micro plate is moving towards the West at ~15mm/yr (central Turkey), while in the Aegean region the Anatolian plate is moving towards the SW at a rate of ~30mm/yr [McClusky et al., 2000].

The northward movement of the African plate results in a convergence regime as currently it collides with the Eurasian plate with the main plate boundary expressed as the Cyprus Arc system (Figure 2 - 1). The northward movement of the Arabian plate (which results in the creation of the Dead Sea Transform Fault) and the slab pull of the subducting African plate in the Aegean region, result in the westward escape movement of the Anatolian micro plate. This westward escape is evidenced as a transpressional regime at the eastern part of Turkey and at the eastern extent of the Cyprus Arc system.

The Eastern Mediterranean region is divided into different domains with different composition as they correspond to the Late Eocene closing of the Neo-Tethys Ocean [Barrier and Vrielynck, 2008; Frizon de la Motte et al., 2011]. These domains are: a) the Levant Basin which consists of thin attenuated continental crust; b) the Herodotus Basin consisting of oceanic crust; c) the Cyprus Basin, which is poorly constrained but it is proposed that it consists of obducted ophiolite onto continental crust; d) the island of Cyprus underlain by continental crust, characterized by the exposure of the ophiolite sequence on the Troodos Mountains; and e) the Eratosthenes micro continent interpreted as a Mesozoic carbonate platform which is underlain by continental crust (Figure 2 - 2).

The breakup of the supercontinent of Pangea and the formation of the Neo-Tethyan Ocean took place in Late Paleozoic time [Gardosh et al., 2010]. The initial rifting phase in the Eastern Mediterranean region was followed by a convergent phase that resulted in the creation

of tectonic structures (i.e. Cyprus Arc zone, Latakia Ridge), basins (i.e. Levant and Herodotus Basins) and the emplacement of the ophiolitic belt in the region [Garfunkel, 1998; McClusky et al., 2003]. A number of palinspastic maps were proposed in order to constrain the geodynamical context of the Neo-Tethys Ocean, which will be presented below.



Figure 2 - 1: Regional geological map illustrating the main tectonic elements [Ghalayini, 2015].

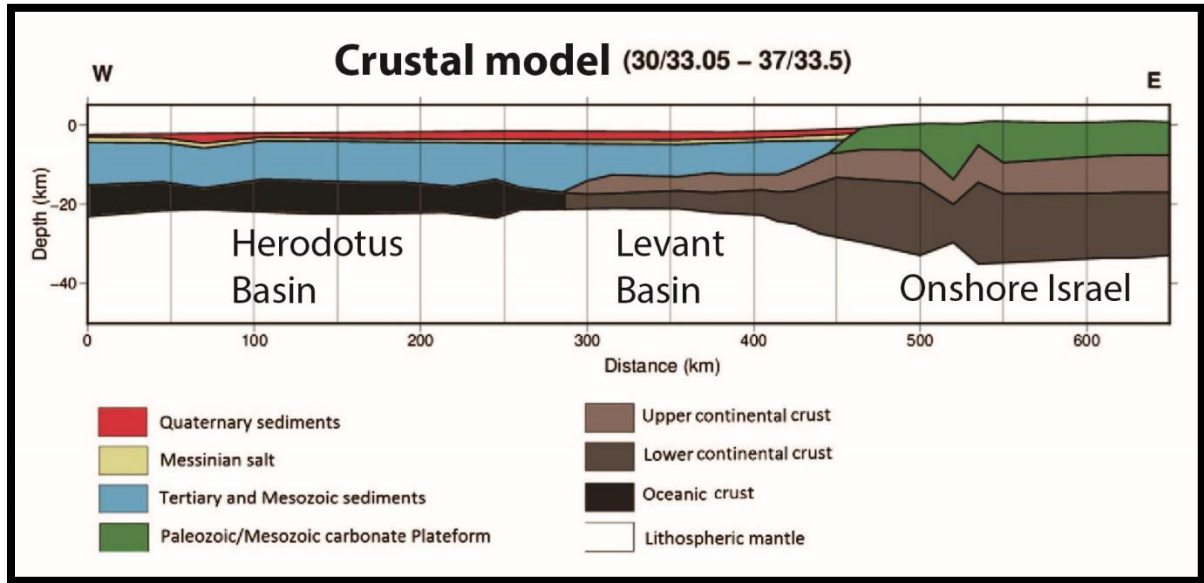


Figure 2 - 2: Schematic cross section across the Levant lithosphere, showing the main units and interfaces used during the isostatic calculation. Position indicated in Figure 2 - 1. [Inati, et al., 2016].

### 2.1.1 Late Permian – Early Jurassic

The Late Paleozoic to Early Mesozoic period is considered to be at the onset of fragmentation of the northern margin of the super-continent of Pangea and Tethyan rifting [Gardosh et al., 2010; Montadert et al., 2014]. The breakup of the Gondwana (southern part of Pangea) resulted in the creation of smaller continental fragments like the Tauride micro-continent (Figure 2 - 6) which rifted from the northern margin of Gondwana and then drifted further north towards the Eurasian continental plate [Garfunkel, 2004; Bowman, 2011]. The breakup led to the opening of the Neo-Tethys Ocean and the gradual creation of smaller oceanic basins, separated by the resulting continental fragments [Robertson, 2007; Robertson et al., 2012]. Garfunkel [2004] suggests that the rifting of the Tauride micro-continent caused the formation of the Eastern Mediterranean (perceived as a relic of the southern Neo-Tethys) and the Levant margin. The southern Tethys Ocean is preserved, although it is fragmented into several pieces including oceanic basins (Herodotus Basin), relic oceanic crust emplaced as ophiolitic belts (Baer Bassit in Syria and Troodos ophiolites in Cyprus) and a hyper extended domain (Levant Basin). The Tethyan rifting in Early Mesozoic, culminated in the creation of the Levant Basin from an extensional regime of NW-SE orientation [Garfunkel, 1998; Gardosh and Druckman, 2006; Gardosh et al., 2010]. The Levant Basin is in-filled by 12-15km of sediments of probably Triassic-Jurassic age until recent [Makris et al., 1983; Vidal et al., 2000a, b; Ben-Avraham et

al., 2002; Montadert et al., 2014]. Its crustal nature is considered as a thin (~8 km) attenuated continental crust [Netzeband et al., 2006; Granot, 2016; Inati et al., 2016]. The Eratosthenes micro-continent is described as a Mesozoic carbonate platform underlain by continental crust [Markris et al., 1983; Welford et al., 2015] which was rifted from the northern margin of the African plate [Garfunkel, 1998]. Towards the west, the Herodotus Basin is constructed by oceanic crust [Granot, 2016] and it is covered by a thick sedimentary sequence of 12-14km [Montadert et al., 2014]. The ophiolitic belt is regarded as a remnant of the southern Tethys Ocean and was obducted during Early Campanian to Late Maastrichtian time. Biostratigraphic dating of foraminifera bearing radiolarian sediments observed at the contact between the Upper and Lower Pillow Lavas, suggested an extrusion age of Cenomanian to Campanian time for the Upper Pillow Lavas [Mantis, 1971]. A later study based on U-Pb dating of the plagiogranites of the Troodos Ophiolites revealed an age of early Late Cretaceous time (Cenomanian, 92-95 Ma) [Mukasa and Ludden, 1987] which is in good accordance with the biostratigraphic data presented by Mantis [1971].

Whereas most of the Tethyan structures were amalgamated in the collision zones, the Levant Basin constitutes a well preserved and moderately deformed domain. Rifting in the Levant Basin started from Middle Triassic (Anisian), and continued through the Late Triassic (Liassic) (Figure 2 - 6) and Early-Mid Jurassic (Bajocian-Bathonian) (Figure 2 - 6, Figure 2 - 8). It finally ended in Mid-Late Jurassic time [Gardosh and Druckman, 2006; Gardosh et al., 2010; Montadert et al., 2010; Bowman, 2011]. The Tauride micro-continent which emanates from the continental breakup and the Tethyan rifting (Figure 2 - 3), is initially placed opposite Egypt due to its Pre-Cambrian basement and the similarity in Paleozoic sediments with the Northern Egypt and Western Sinai regions [Garfunkel and Derin, 1984]. Offshore Israel, continuous rifting during the Anisian-Liassic period [Gardosh and Druckman, 2006], led to the thinning of the crust. Wells drilled onshore show that in Middle Triassic faulting was intense as sediments in the Helez drill hole (Figure 2 - 13) were displaced by 0.5-1km [Garfunkel and Derin, 1984]. In north Sinai, Moustafa [2010] indicates that the divergence of Arabia and Eurasia resulted in the thinning of the continental crust from 32km to 27km and the creation of the extensional basins of Maghara, Yelleg and Halal in Egypt (Figure 2 - 13).

Several geodynamic models were proposed to explain formation of the Levant Basin [e.g. Gardosh et al., 2010, and references therein]. Dewey et al. [1973], Robertson and Dixon [1984], Stampfli and Borel [2002], all suggest that the Levant Basin opened in a NE-SW direction. The Levant margin (now located along the Israeli, Lebanese and Syrian coast) is interpreted by these authors as a N-S directed transform margins as depicted in Figure 2 - 3a.

Garfunkel and Derin [1984], suggested extension and rifting of NW-SE orientation. The separation was accommodated by a transform fault which runs along the Sinai coast and projected a southern transform margin (Figure 2 - 3b). Gardosh et al. [2010] state that the normal faults found in the area have a dominant direction of NE-SW to ENE-WSW (i.e. offshore/onshore Israel or even in northern Sinai). The proposed direction shows that the extension in the area is perpendicular to the strike of the normal faults with a direction of NW-SE and NNW-SSE as it was suggested by Garfunkel [1998] (Figure 2 - 3d). The outcome was the separation of the Tauride micro-continent and the Eratosthenes continental block from the Gondwana plate.

By comparing the models of Dewey et al. [1973], Robertson and Dixon [1984], Stampfli and Borel [2002] in Figure 2 - 3a, Gardosh et al., [2010] realized that this model is not supported by the geological data as the main structural elements and the directions of the faults found in the Levant Basin were not consistent with NE-SE extension along a N-S transform margin [Gardosh et al., 2010]. It is proposed that the main trend of rifting, follows a NW-SE direction of opening as it is illustrated in the proposed models (Figure 2 - 3c and d) and from field observations [Gardosh et al., 2010].

Montadert et al. [2014] suggested the creation of the Levant Basin from Triassic to Middle Jurassic times (Figure 2 - 4), in contrast with the model proposed by Gardosh et al., [2010], who suggested the basin formed from Late Permian to Early Triassic time. Gardosh et al., [2010] propose the creation of a small number of faults during the rifting process. Montadert et al., [2014] suggest segmented structures in the Levant Basin including numerous transform faults, with the rifting occurring in pulses and opening in the western part of the region with the creation of oceanic crust (Figure 2 - 4, orange arrows) under the Herodotus Basin which is attested by the gravity and magnetic anomalies maps [Woodside, 1977].

Ongoing rifting resulted in the separation of the Eratosthenes Continental Block (ECB) from the Arabian continental plate (Figure 2 - 6) [Montadert et al., 2014], with many authors proposing that its current shelf edge fits closely to the present day coastline and therefore it is perceived as a continental block which was detached from the Arabian plate [Garfunkel, 2004; Gardosh et al., 2010].

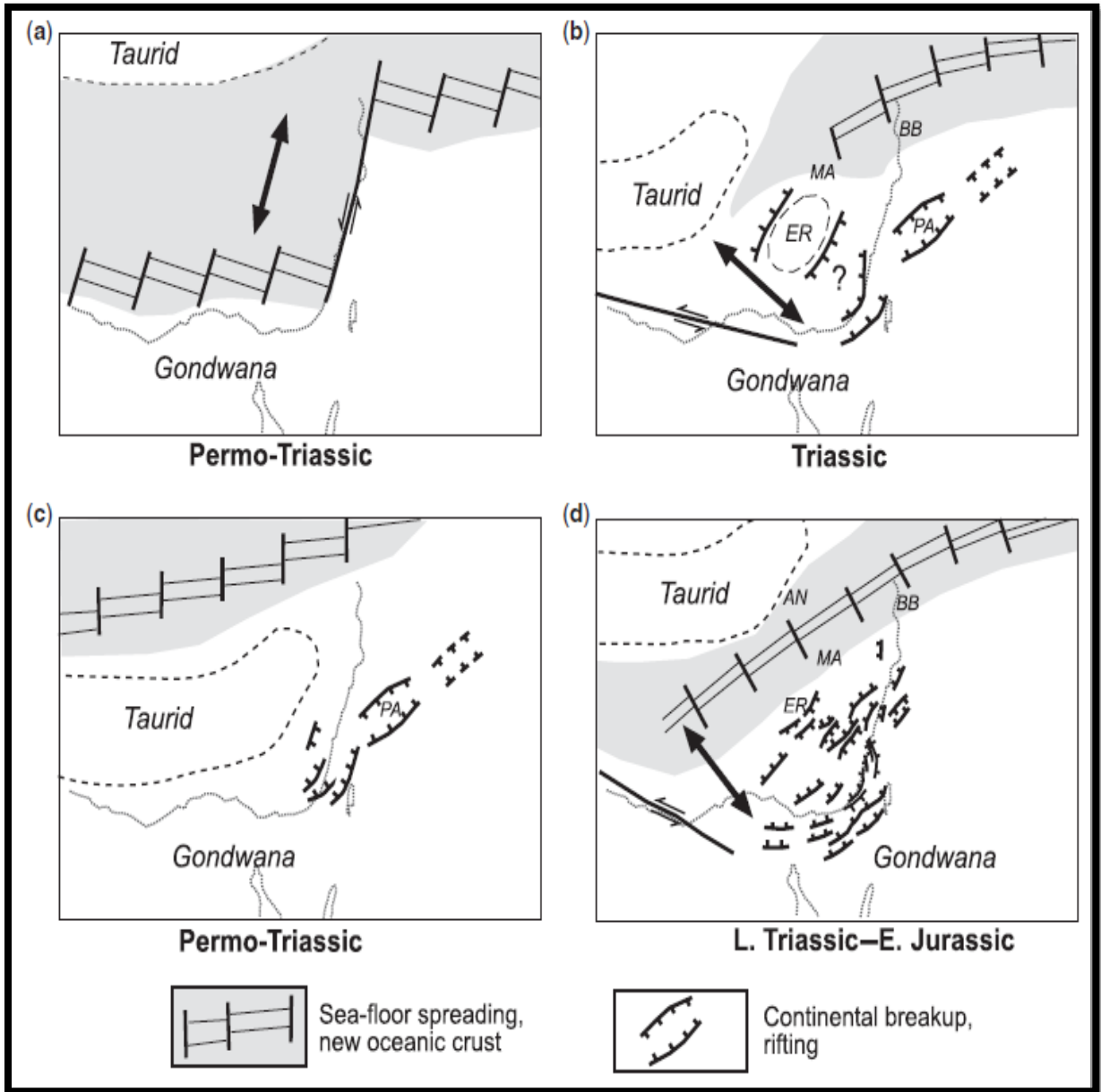


Figure 2 - 3: Several alternative reconstructions of the Tethyan rifting in the Levant region. Two previously proposed models are: (a) After Dewey et al. [1973] and Stampfli and Borel [2002], showing north-south extension with eastern transform margin and (b) after Garfunkel and Derin [1984] and Garfunkel [1998], showing NW-SE extension with southern transform margin. Reconstructions (c) and (d) are based on Gardosh et al., [2010]. Tethyan rifting on the northern margin of Gondwana was pulsed and progressed from the Late Paleozoic (c) to Early Jurassic (d) [from Gardosh et al., 2010].

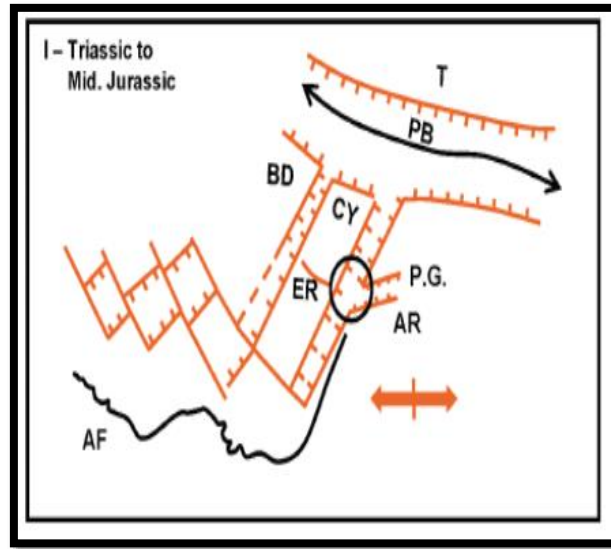


Figure 2 - 4: Paleotectonic sketch maps of the Eastern Mediterranean since the Triassic (ER=Eratosthenes Continental Block, CY=Cyprus, BD= BeyDaglari, HB=Herodotus Basin, PB=Pamphylian Basin, T=Taurus, AR=Arabia, AF=Africa, MR=Mediterranean Ridge). (I) rifting from Triassic to Middle Jurassic. [from Montadert et al., 2014].

The southern branch of Tethys, which is now identified as the Tauride block in south Turkey, is a core complex consisting of Precambrian and Jurassic to Early Cretaceous carbonate rocks intercalated with volcano-sedimentary rocks [Ricou et al., 1975; Dilek and Sandvol, 2009]. Emplacement of the ophiolitic belt onto the Tauride block occurred in Late Cretaceous and is linked with metamorphism in the Anatolide-Tauride block [Dilek and Sandvol, 2009]. The closure of the northern branch of the Neo-Tethys in Early Eocene, resulted in the collision of the Sakarya continent with the Anatolide-Tauride block, which caused regional deformation and metamorphism, observed in the central and southern part of Turkey [Dilek and Sandvol, 2009].

### 2.1.2 Late Jurassic – Early Cretaceous

Rifting ceased by Mid-Late Jurassic time as it is suggested by the transition from volcanics to the deposition of clastic sediments [Gardosh and Druckman, 2006; Gardosh et al., 2010; Bowman, 2011; Montadert et al., 2014].

During Early Cretaceous the Lebanese margin and nearby areas were dominated by the deposition of either shallow marine carbonates or continental sandstones [Homberg et al., 2010]. Measured faults in the Mount Lebanon anticline are characterized by steeply dipping planes implying normal faults of WSW-ENE to WNW-ESE direction, associated with an extensional setting of roughly N-S direction that occurred during Early Cretaceous time, up until the Cenomanian (Upper Cretaceous time) [Homberg et al., 2010]. The field-investigated faults of Mesozoic age were located in the Chouf sandstone (Lebanon). Lenses of Upper Oxfordian to Early Kimmeridgian basaltic formations were also observed in the fluvial deposits of the Chouf sandstone [Homberg et al., 2010]. These deposits attest to an extensional regime and subsequent volcanic activity of Early Cretaceous age in Lebanon [Homberg et al., 2010]. Brew et al., [2001a] are in agreement with this volcanic activity as they suggest Early Cretaceous mantle plume activity underneath Syria, marked by alkaline volcanism and block-faulting.

Montadert et al., [2014], propose that the Eratosthenes Continental Block (ECB) was detached from the African plate during Late Triassic to Early Jurassic times. In contrast with Gardosh et al. [2010], the model of Montadert et al. [2014] proposes that the ECB was moving faster towards the NW as they postulated spreading and extension (Figure 2 - 5, orange arrows) by Upper Jurassic to Lower Cretaceous time (Figure 2 - 5).

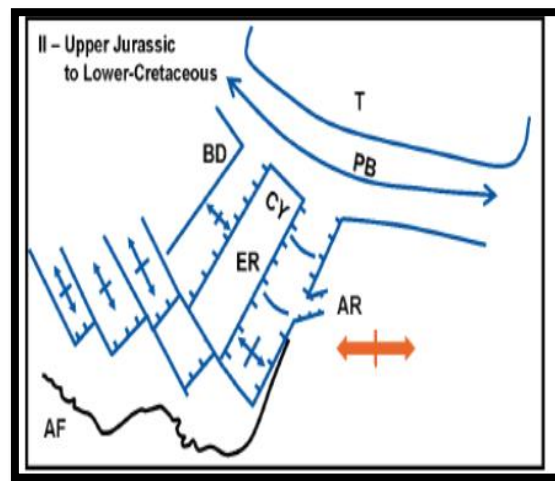


Figure 2 - 5: Paleotectonic sketch maps of the Eastern Mediterranean from Late Jurassic to Early Cretaceous (ER=Eratosthenes Continental Block, CY=Cyprus, BD= BeyDaglari, PB=Pamphylian Basin, T=Taurus, AR=Arabia, AF=Africa). (II) Blue arrows indicate extension and spreading from Upper Jurassic to Lower Cretaceous. [from Montadert et al., 2014].

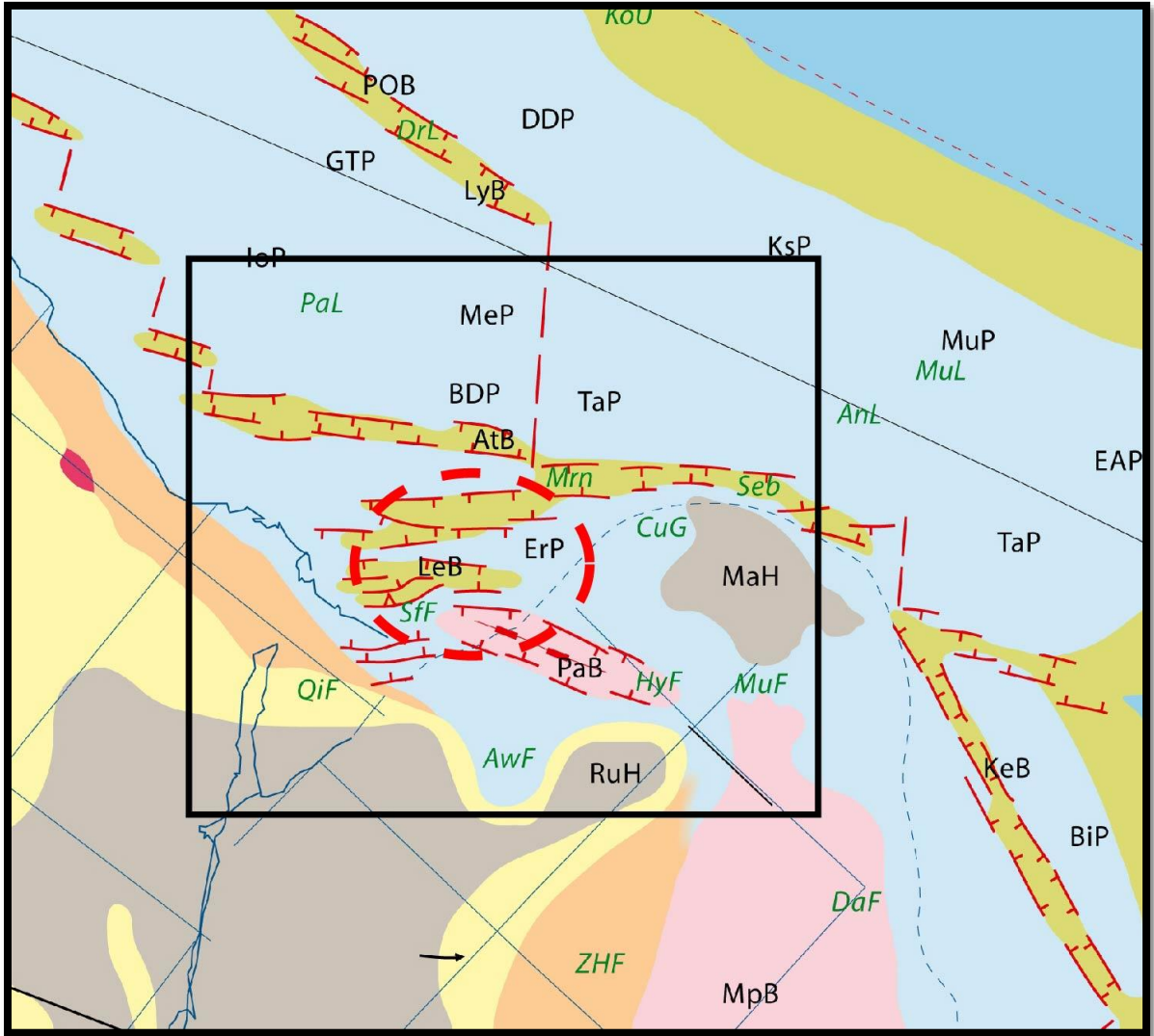


Figure 2 - 6: Palinspastic reconstruction of the Tethys region in Late Triassic times, indicating the main structural elements [Barrier and Vrielynck, 2008]. Black box indicates the study area. Lithology and tectonics elements as in Figure 2 - 7.

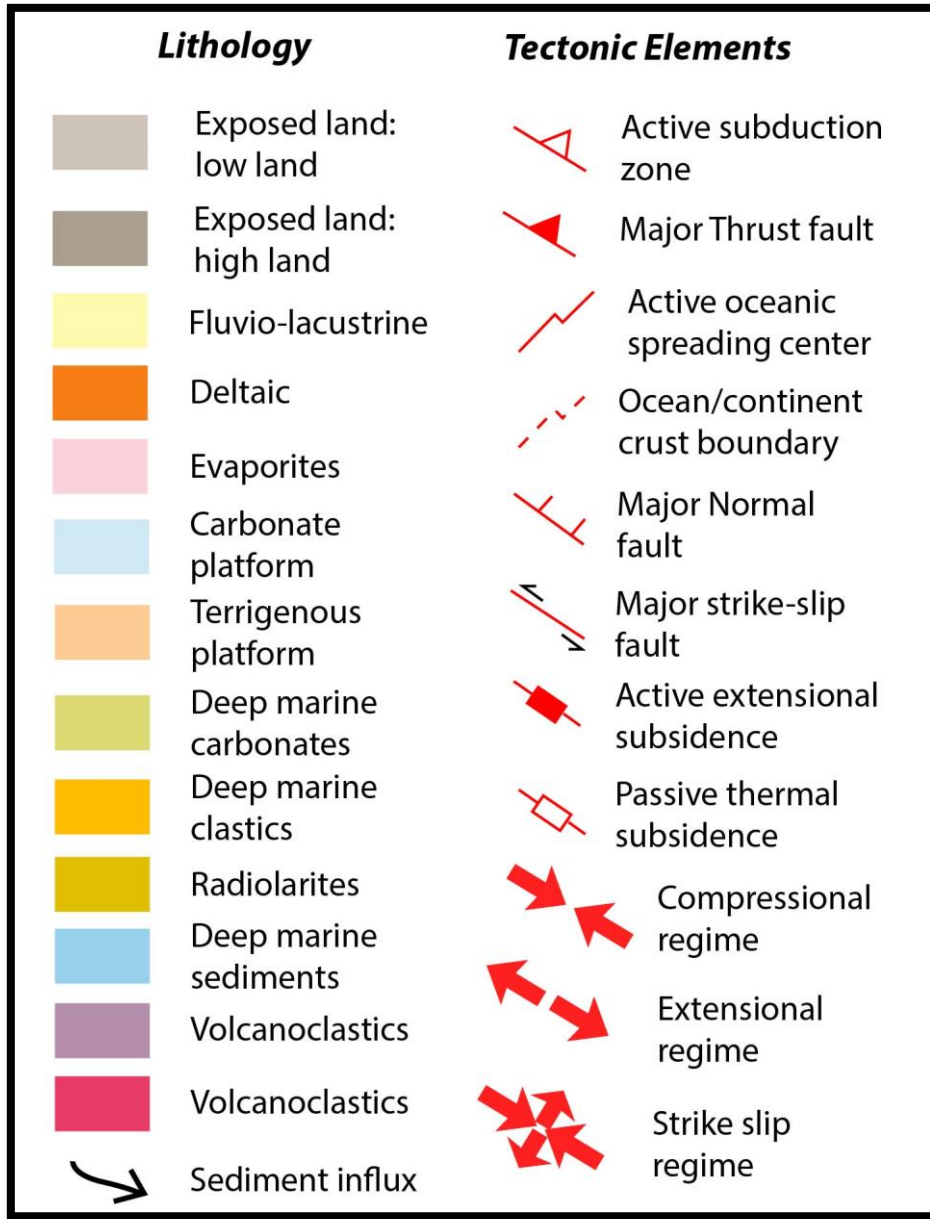


Figure 2 - 7: Description of tectonic elements, lithology, kinematics and palaeogeography for the palinspastic reconstruction models as illustrated in Figure 2 - 6, Figure 2 - 8, Figure 2 - 9, Figure 2 - 10, Figure 2 - 11.

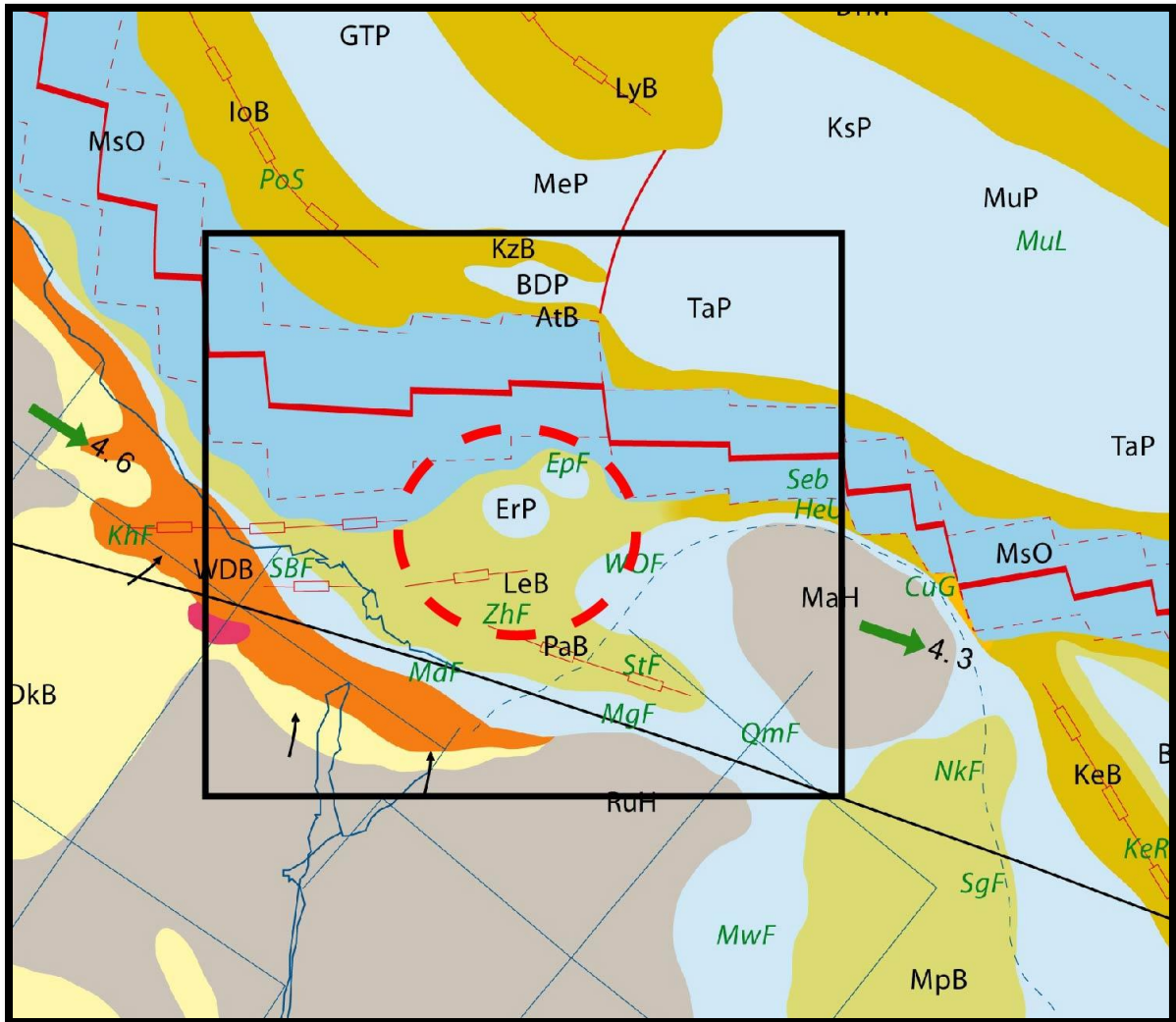


Figure 2 - 8: Palinspastic reconstruction of the Tethys region in Middle to Late Jurassic times, indicating the main structural elements and the NW-SE opening of the Neo-Tethys Ocean [Barrier and Vrielynck, 2008]. Black box indicates the study area. Lithology and tectonics elements as in Figure 2 - 7.

### 2.1.3 Upper Cretaceous – Oligocene

The Upper Cretaceous to Paleogene period (Figure 2 - 9) is considered to be the start of convergence between the African and Eurasian plates [Bowman, 2011; Klimke and Ehrhardt, 2014; Montadert et al., 2014]. It resulted in the formation of the Cyprus Arc belt which is described by Montadert et al. [2014] as a “south-verging fold and thrust belt, still active today”

that runs from the Syrian coast to Turkey through the island of Cyprus. In Late Maastrichtian times, the initial closing stage of the Neo-Tethyan Ocean due to the convergence of the tectonic plates had come to an end and ophiolites were emplaced in Baer-Bassit in Syria, Hatay in Turkey and the Troodos ophiolites of Cyprus [Garfunkel, 2004]. Some authors suggest that the Latakia Ridge system initiated during Late Cretaceous times, as a compressional fold-thrust belt due to the convergent movement between the African and Eurasian plates [Vidal et al., 2000a, b; Bowman, 2011].

The first phase of the Syrian Arc formation (Up. Cretaceous to Early Eocene) emanated from the Upper Cretaceous compressional regime that affects the region, as evidenced in the west Coastal Ranges of Syria where uplifted Jurassic and Upper Triassic sediments are exposed on the surface [Brew et al., 2001b]. In North Sinai, compression and folding of Upper Cretaceous time is evident from the echelon folds of the Mitla Pass area (Figure 2 - 13), where Cenomanian, Turonian and Late Senonian formations are deformed [Moustafa, 2010]. A model for the Upper Cretaceous (Figure 2 - 12) illustrates the change in motion that affected the Eastern Mediterranean region (Figure 2 - 12, orange arrows). The compressional motion creates the subduction of pre-existing oceanic basins (Pamphylian Basin) and the generation of the Cyprus Arc zone that runs from Baer-Bassit in Syria to the Antalya region of southern Turkey through Cyprus [Montadert et al., 2014].

An active subduction zone of Paleogene age (Figure 2 - 10) is proposed south of the Cyprus Arc system from the seismic data recorded in the northern Levant Basin, as it postulated by the contrast in thickness between the older and thicker Late Cretaceous (Senonian)-Eocene sediments with the thinner and younger Oligo-Miocene sediments [Montadert et al., 2014]. In the Eocene period the on-going convergence of the African and Eurasian plates, led to the final closure of the Neo-Tethyan Ocean [Bowman, 2011].

Brew et al., [2001b] argue that the first stage of uplift of the Syrian coastal ranges decelerates by Mid-Eocene. This is indicated from field observations as limestone deposits seal the Paleogene deposits throughout Syria. A second uplift was proposed by Early Eocene to Miocene time as no strata of this age is identified in the Syrian coastal ranges [Brew et al., 2001b]. In north Sinai, Moustafa [2010] postulates folding of Middle to Late Eocene age, as observed from the folded rocks of Falig anticline and El Dirsa (Figure 2 - 13) (Early Eocene and M. Eocene rocks respectively).

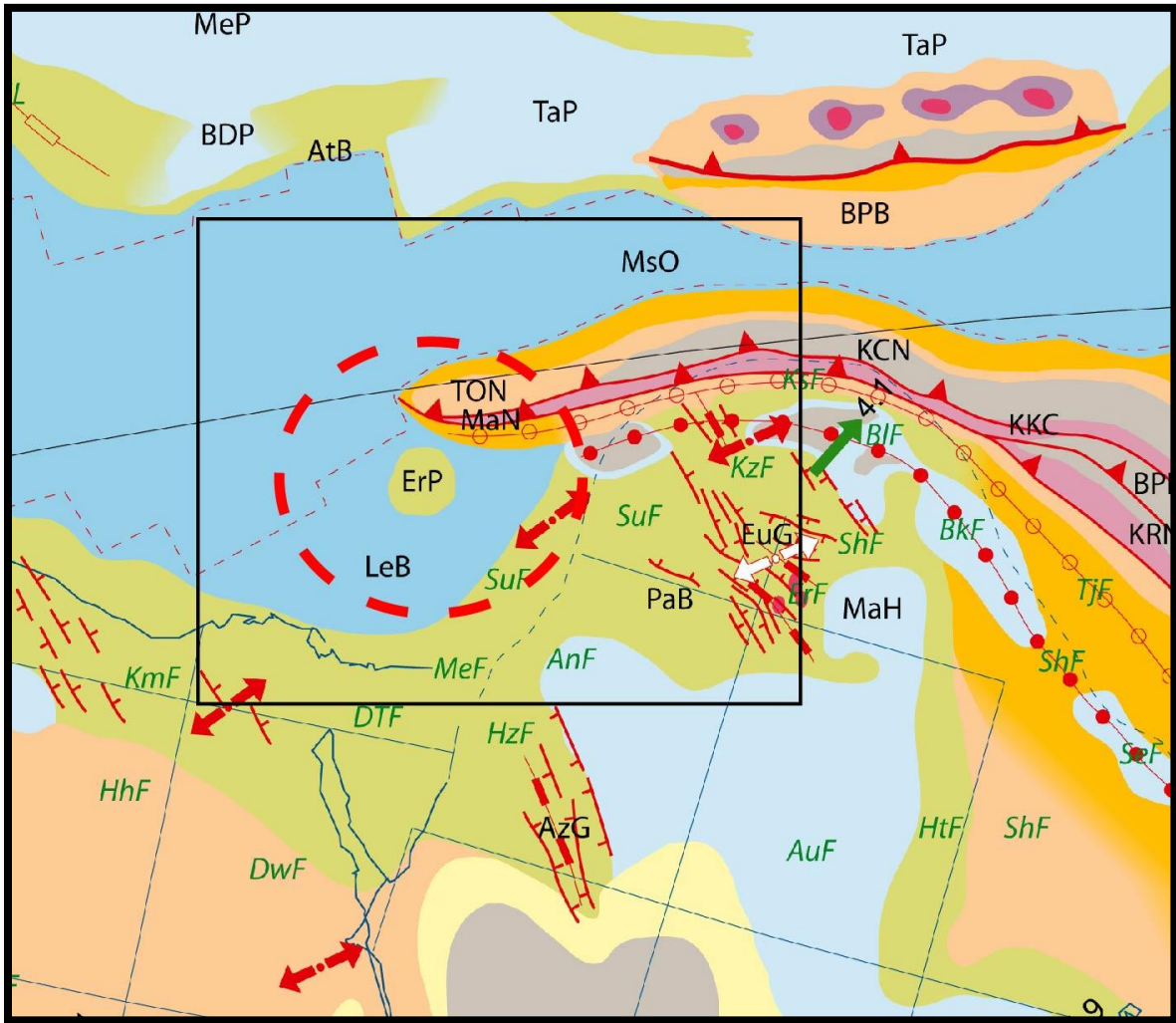


Figure 2 - 9: Palinspastic reconstruction of the Tethys region in Early Campanian times, indicating the main structural elements [Barrier and Vrielynck, 2008]. Black box indicates the study area. Lithology and tectonics elements as in Figure 2 - 7.

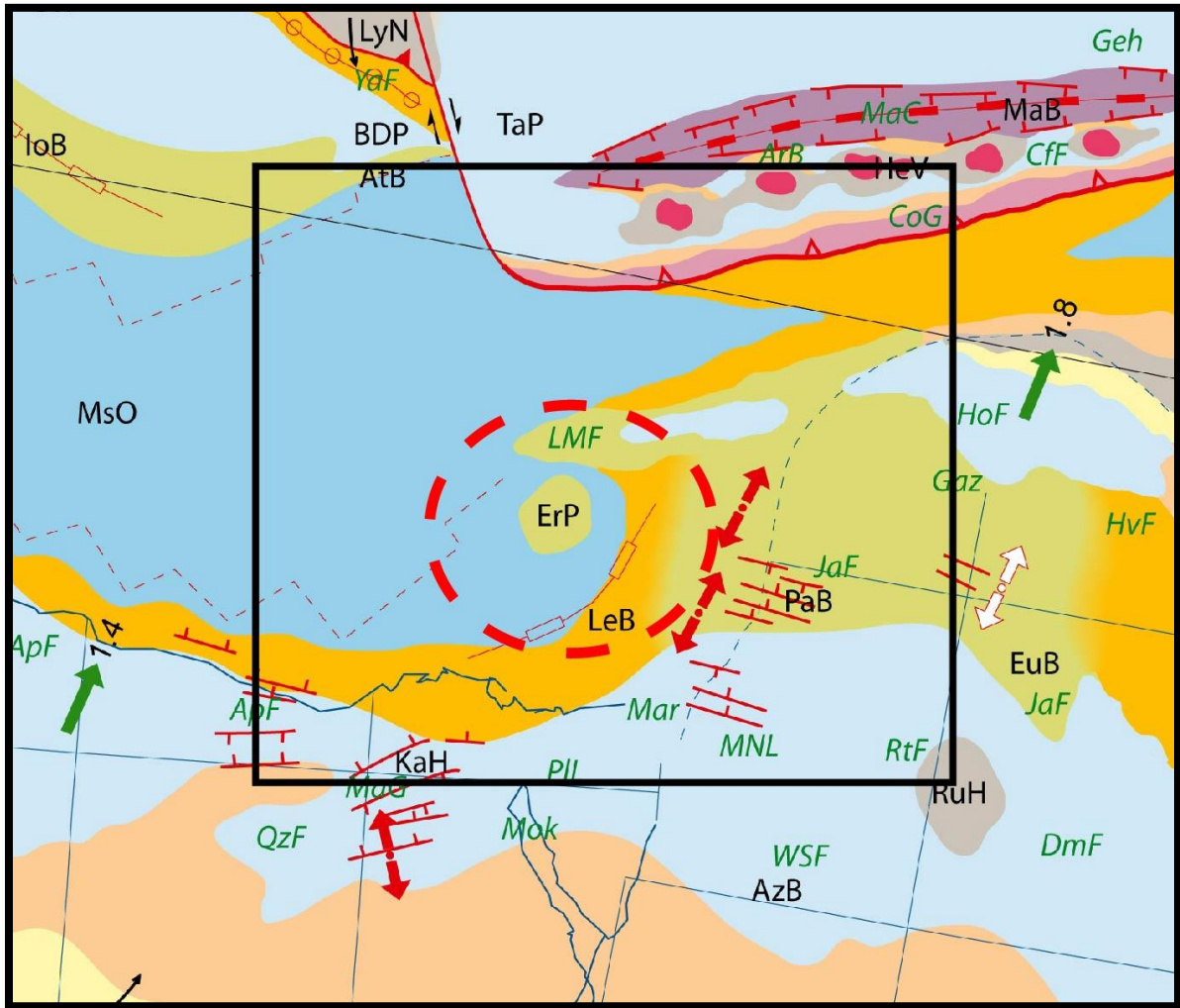


Figure 2 - 10: Palinspastic reconstruction of the Tethys region in Middle Eocene times, indicating the main structural elements [Barrier and Vrielynck, 2008]. Black box indicates the study area. Lithology and tectonics elements as in Figure 2 - 7.

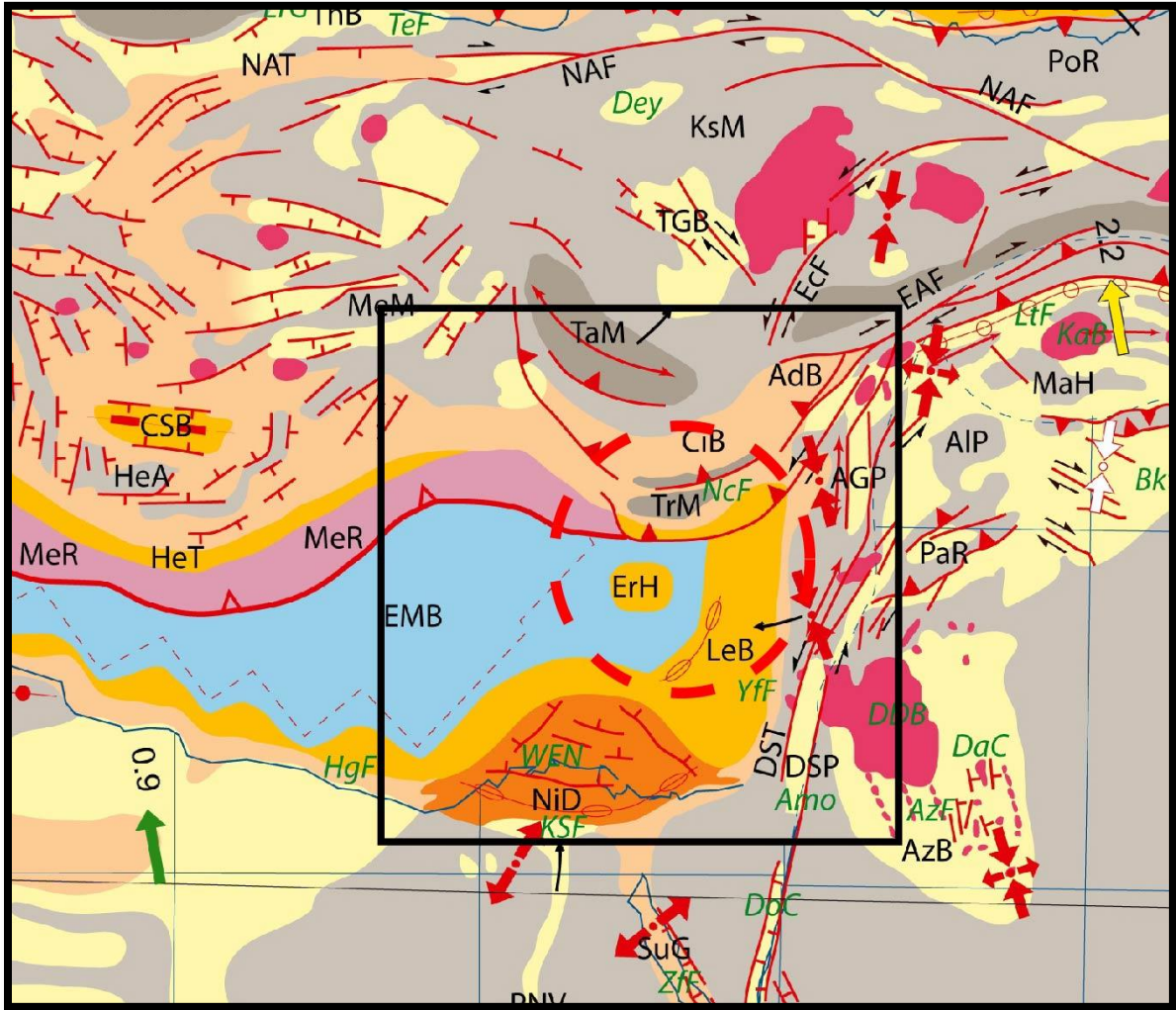


Figure 2 - 11: Palinspastic reconstruction of the Tethys region in Plio-Pleistocene times, indicating the main structural elements [Barrier and Vrielynck, 2008]. Black box indicates the study area. Lithology and tectonics elements as in Figure 2 - 7.

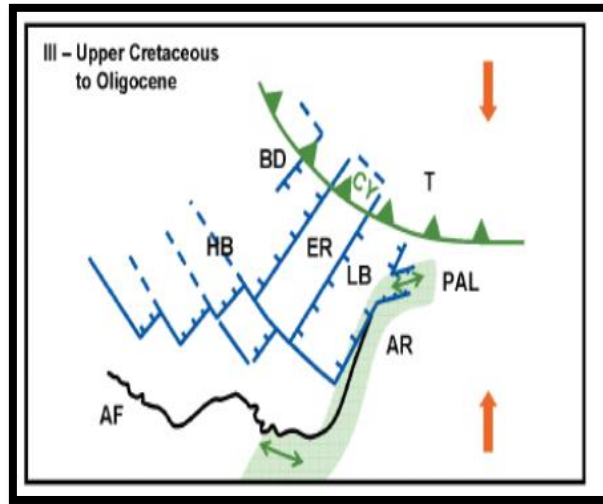


Figure 2 - 12: Paleotectonic sketch maps of the Eastern Mediterranean from Late Cretaceous to Oligocene (ER=Eratosthenes Continental Block, CY=Cyprus, BD= BeyDaglari, HB=Herodotus Basin, PAL=Pamphylian Basin, T=Taurus, AR=Arabia, AF=Africa). (III) Late Cretaceous: Formation of the Cyprus Arc and Ophiolite Belt, subduction continuing during Paleogene [from Montadert et al., 2014].

#### 2.1.4 Miocene – Present

The Miocene is marked by the separation between Arabia and Africa, the initiation of the Dead Sea Transform fault and the movement of the Anatolian micro-plate towards the west [Montadert et al., 2014]. By Middle Miocene the increased northward movement of Arabia (~18-25 mm/yr [McClusky et al., 2000]) with respect to Africa (~10 mm/yr [McClusky et al., 2000]) was accommodated by the Dead Sea Transform fault [Brew et al., 2001b].



Figure 2 - 13: Regional map of the Eastern Mediterranean illustrating the main structural elements in the region. Inset map indicates the area of interest. Abbreviations: EAF=East Anatolian Fault, M=Maghara fold, Y=Yelleg fold, H=Halal fold, G.F=Falig anticline, G.ED=El Dirsa anticline, MP=Mitla Pass. [modified from Bowman, 2011].

The northward movement of the Arabian plate resulted in the westward escape of the Anatolian microplate during latest Miocene to Early Pliocene (Figure 2 - 11) [Le Pichon and Kreemer, 2010; Montadert et al., 2014]. The result of this movement is the creation of a triple junction point, which is comprised of the East Anatolian Fault (sinistral strike-slip fault), the Latakia Ridge (sinistral strike-slip fault) and the Dead Sea Transform fault (sinistral strike-slip fault) (Figure 2 - 13) [Kempfer and Garfunkel, 1994; Aksu et al., 2005]. Westward of the triple

junction the motion changes from slight compression to extension with regard to the strike of the boundaries, while east of the triple junction the motion is characterized by shortening which is transverse to the plate boundary [Kempfer and Garfunkel, 1994]. The result of the movement of the Anatolian micro-plate towards the SW is the creation of strike-slip faulting in the eastern part of the Cyprus Arc system and the initiation of the strike-slip movement of the Latakia Ridge system, which constitutes the offshore continuation of the Eastern Anatolian fault [Kempfer and Garfunkel, 1994; Montadert et al., 2014]. Montadert et al. [2014] evolutionary model (Figure 2 - 14) refers to the progressive but continued separation of Arabia from Africa and the compressional deformation due to the movement of Africa-Eurasia plates (Figure 2 - 14, orange arrows).

Bowman [2011] suggested that the initial compressional nature of the Latakia Ridge system changes to a sinistral strike-slip regime, as is supported by seismic interpretation from data that cover the northern part of the Levant basin [Hall et al., 2005a, b]. This change in motion is associated with the re-organization of tectonic stresses of the major plates by Late-Miocene to Early-Pliocene time [Bowman, 2011]. Analogue modelling experiments indicate that this re-organization of the stress is due to slab break-off under the Bitlis-Zagros suture zone [Faccenna et al., 2006].

The strike slip deformation in the Tartus Ridge (eastern segment of the Latakia Ridge, Figure 2 - 13) is defined by sub-vertical faulting and uplift along its margins, while the deformation at the Latakia and Margat Ridges is defined by the back-thrusts with opposite direction from the earlier SE trending compression thrusts close to the Syrian margin, thus creating pop-up and flower structures [Bowman, 2011].

Kinnaird and Robertson [2013] suggested that the ECB collided with the Cyprus arc during Early Pleistocene times, thus subducting underneath the arc and causing intense uplift [Garfunkel, 1998; Robertson et al., 2012] of the island of Cyprus. The arrival of the ECB at the Cyprus Arc system during this time is portrayed as the point at which a change in plate tectonics occurs passing from subduction to a continent-continent collision [Schattner, 2010]. Plate kinematics and GPS velocities in recent times [McClusky et al., 2000, 2003; Reilinger et al., 2006], suggest that while the Anatolian plate rotates counter-clockwise, Africa continues its N-NW motion, resulting in the sinistral strike-slip movement along the Cyprus Arc system in accordance with the Latakia Ridge [Vidal et al., 2000a, b; Hall et al., 2005a, b; Le Pichon and Kreemer, 2010; Bowman, 2011].

At the foot of the Cyprus arc in the Levant Basin, subduction was still active [Robertson, 1998], and compressional structures were shaped while to the west the creation of the Mediterranean Ridge is perceived [Montadert et al., 2014].

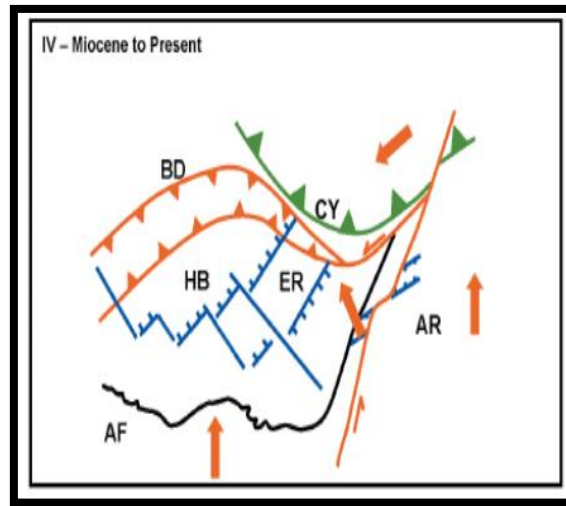


Figure 2 - 14: Paleotectonic sketch maps of the Eastern Mediterranean of Miocene to Present (ER=Eratosthenes Continental Block, CY=Cyprus, BD= BeyDaglari, HB=Herodotus Basin, AR=Arabia, AF=Africa). (IV) Miocene to Plio-Pleistocene geodynamic model [from Montadert et al., 2014].

## 2.2 Gravity and magnetic data

The palinspastic reconstructions of the Eastern Mediterranean indicate the complex tectonic evolution of the region. The different crustal fragments described above are further constrained through gravity and magnetic data. These data give further indication for the nature of the crust thus clarifying the different pieces that make up the Eastern Mediterranean.

### 2.2.1 Gravity data

A positive anomaly that relates to the Late Cretaceous ophiolites of the Cyprus Arc belt is observed, passing from Baer-Bassit in Syria to Antalya in Turkey through Cyprus (Figure 2 - 15), with the values changing along the Arc presumably due to the subduction of Eratosthenes continental block under Cyprus which causes the uplift of the island and can be connected with the high values found onland Cyprus [Woodside, 1977; Montadert et al, 2014].

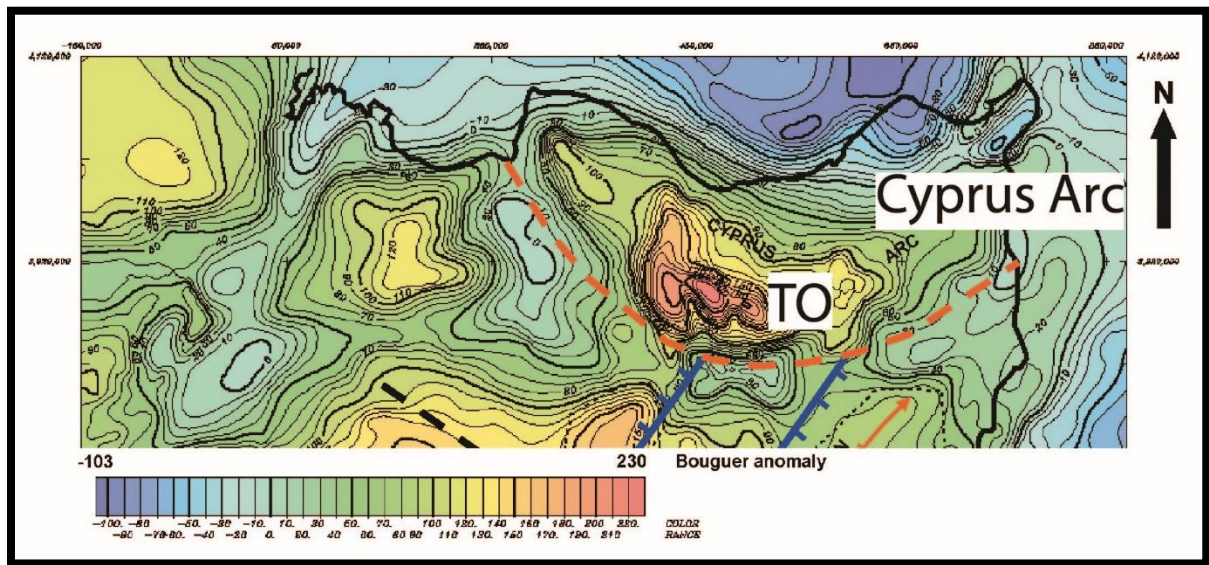


Figure 2 - 15: Bouguer gravity anomalies map, orange arcuate line represents the Cyprus Arc, TO refers to the Troodos ophiolite. High anomalies indicate the ophiolite body [from Woodside, 1977 as modified by Montadert et al, 2014].

The negative anomalies observed south and east of the island bounding the Cyprus Arc may be associated with the combined effect of low-density sediments and the ECB continental crust that subducts below Cyprus [Montadert et al, 2014]. This idea is further enhanced by four gravity profiles and 2D models (Figure 2 - 16, Figure 2 - 17) produced by Ergun et al. [2005].

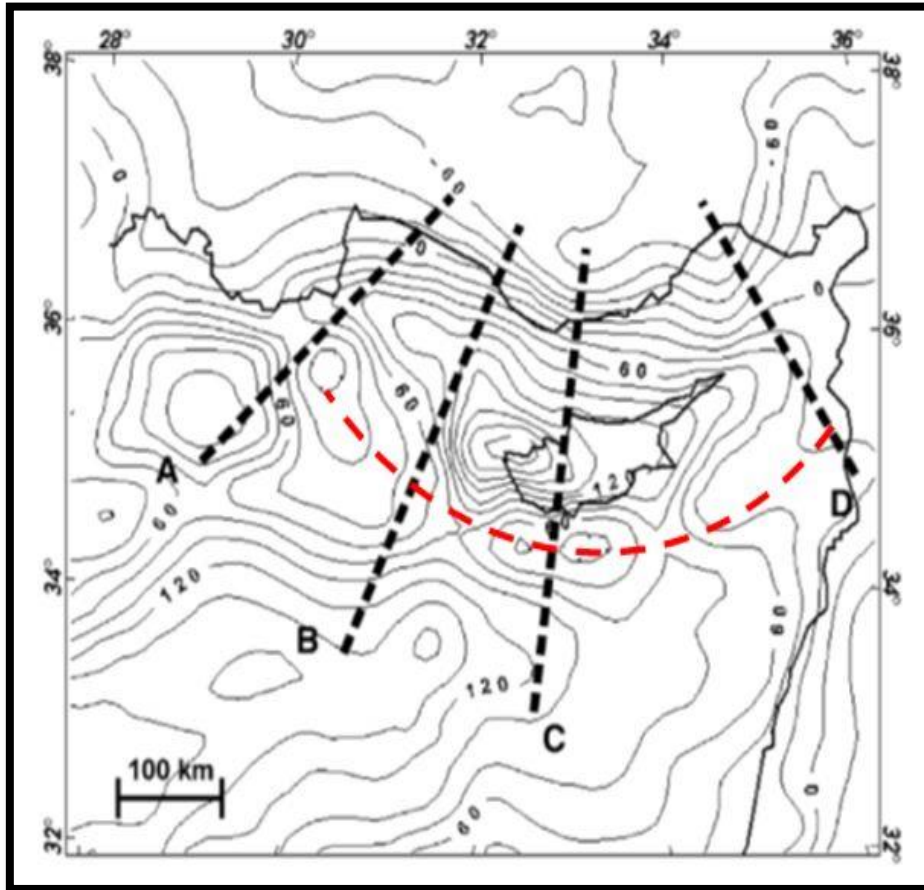


Figure 2 - 16: Bouguer gravity map of the eastern Mediterranean. Location of modelled gravity profiles A–D shown. Red dashed line represents the Cyprus Arc [modified from Ergun et al., 2005].

Profile A runs from SW to NE passing from the Anaximander Mountains towards the west part of the Antalya Basin (Figure 2 - 16, Figure 2 - 17). South of Turkey, around the 220km position a gravity high is observed and is considered as a combination of the thin continental crust moving closer to Turkey, the thin sediments encountered south of it and the possible occurrence of an ophiolitic body at a shallow depth. To the NE, relatively low gravity values can be correlated with the continental crust found under Turkey and the elevated onshore

topography. The high values to the SW of the profile are difficult to evaluate as the section runs obliquely to important structures in the area [Ergun et al., 2005].

Profile B extends from the deep Herodotus Basin across the Florence Rise up to the Antalya Basin (Figure 2 - 16, Figure 2 - 17). The first high observed to the SW is attributed to the oceanic crust of the Herodotus Basin, while the following low (red arrow) is associated with the thick sedimentary cover of almost 14km that covers the Florence Rise. At the 270km mark north of the Florence Rise, the high identified is thought to be an ophiolitic body under the Antalya Basin and the contrasting low at the end of the profile is caused by the thick continental crust in Turkey [Ergun et al., 2005].

Profile C runs from the Eratosthenes seamount, passes through Cyprus and the outer Cilicia Basin and stops at the Taurus Mountains in Turkey (Figure 2 - 16, Figure 2 - 18). A high at the start of the profile is attributed to the Eratosthenes seamount which is considered as a thinned continental block at the north tip of the African plate. South of Cyprus at 120km position on profile C (red arrow), a gravity low is observed between the ECB and Cyprus and it is interpreted as the plate boundary due to the thick sediments that have accumulated here as a result of the accretionary wedge that sits in the pre-existing trench. Further north the next high on the section is connected with the Troodos ophiolite onshore Cyprus and the thin sedimentary succession observed onshore. The ongoing gravity decrease towards the north, passing from the Cilicia Basin to mainland Turkey is attributed to the change in crustal thickness from oceanic to continental [Ergun et al., 2005].

Profile D spanning from the coastline of Syria, across the Cyprus Basin, Latakia and inner Cilicia Basins, ends onland Turkey at the Taurus Mountains (Figure 2 - 16, Figure 2 - 18). The authors model a thin crust under Syria which corresponds to a structural high at the start of the section while the next high is attributed to the continuation of the Troodos ophiolites which plunge to the east [Ergun et al., 2005].

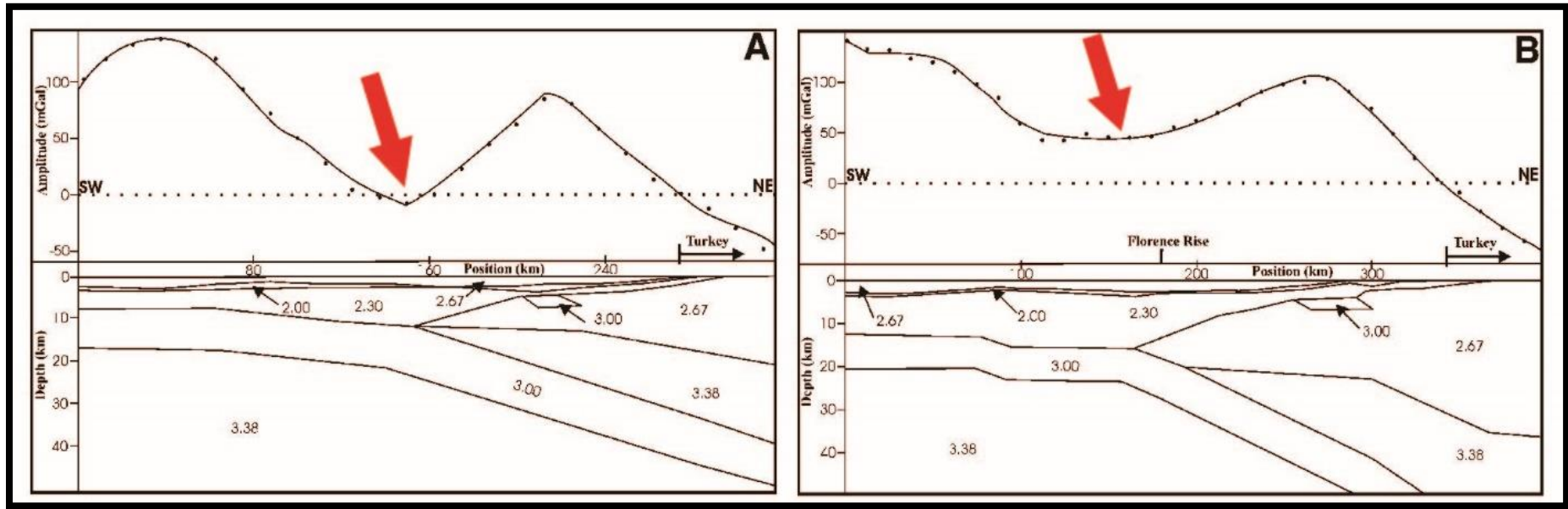


Figure 2 - 17: Bouguer gravity profiles and 2D models. Dots are observed gravity, full line shows model values, red arrows show lows where the Cyprus arc runs. Densities of layers are given in  $\text{mg.m}^{-3}$  [modified from Ergun et al., 2005]. Locations of profiles A and B are indicated in Figure 2 - 16.

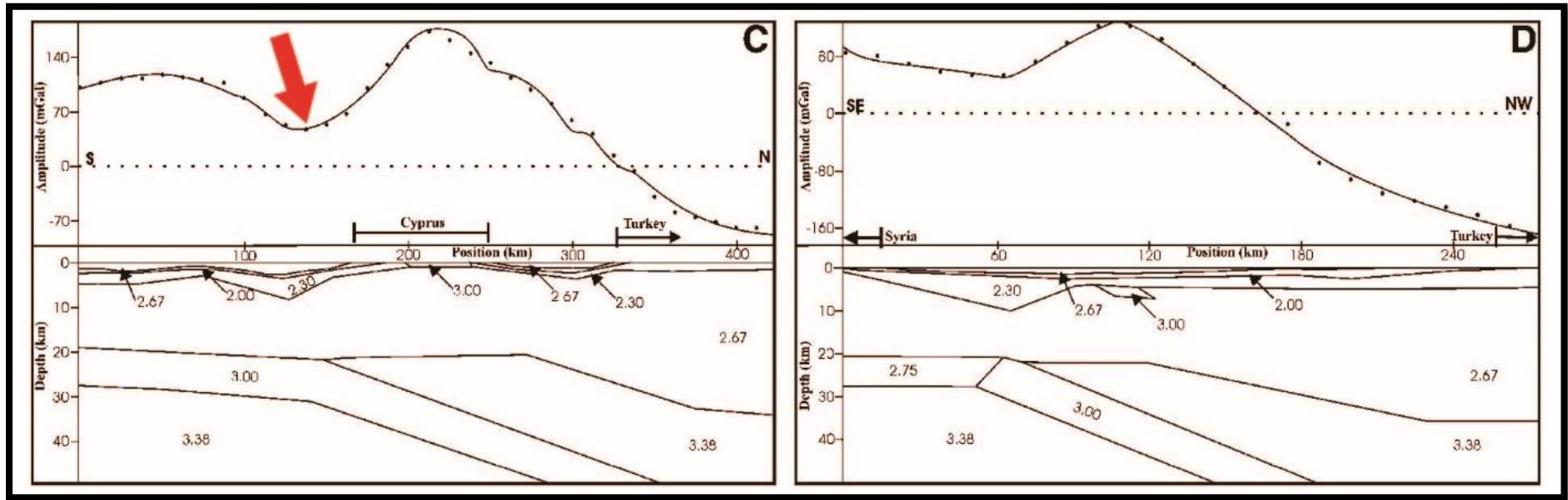


Figure 2 - 18: Bouguer gravity profiles and 2D models. Dots are observed gravity, full line shows model values, red arrows show lows where the Cyprus arc runs. Densities of layers are given in  $\text{mg.m}^{-3}$  [modified from Ergun et al., 2005]. Locations of profiles C and D are indicated in Figure 2 - 16.

### 2.2.2 Magnetic data

From the magnetic map of Woodside [1977], anomalies (Figure 2 - 19) were identified along the Levant margin and can be associated with volcanic rocks of different ages, while a set of positive anomalies can be related to the ophiolite belt of Late Cretaceous time that runs from Syria to Turkey, passing through the Cyprus arc [Montadert et al, 2014]. A positive magnetic anomaly identified east of ECB, can be associated with the continental nature of the crust under the Levant basin [Woodside, 1977].

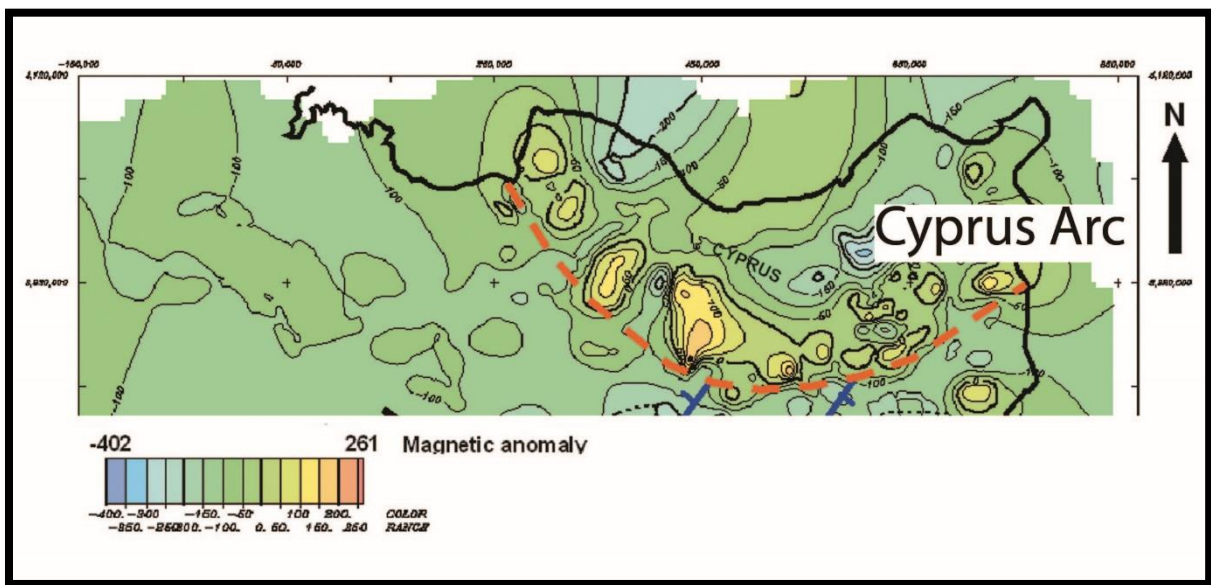


Figure 2 - 19: Magnetic anomalies map, orange arcuate line represents the Cyprus Arc [from Woodside, 1977, as modified by Montadert et al, 2014].

## 2.3 Geology of Cyprus

### 2.3.1 Stratigraphic Units

The Island of Cyprus is situated in the farthest corner of the Eastern Mediterranean Sea. It is 225km long from east to west and 95km wide from north to south. The most prominent features that govern the topography of the island are the Troodos ophiolite complex (highest elevation about 1952m above sea level), the Kyrenia mountain range (highest elevation: 1024m

above sea level) to the north, the Mesaoria valley between these two ranges, the Mamonia Complex to the west and the predominantly marine sedimentary units that cover the southern part and extend from east to west.

The Troodos Ophiolite Complex (Figure 2 - 22), which was emplaced in Early Campanian to Late Maastrichtian (Figure 2 - 20) time, is comprised of the ophiolitic sequence which consists of serpentinite, tectonized harzburgite, dunite, gabbros, diabase and basalts (lower/upper pillow lavas) [Kinnaird, 2008]. Another major geological zone is the Mamonia Complex, comprised of volcanic and sedimentary formations of Mid-Upper Triassic age [Swarbrick and Robertson, 1980; Lapierre et al., 2007]. To the north of the island the Kyrenia range is of Permian to Lower Cretaceous age and it is comprised of massive limestone slivers, re-crystallized limestones, dolomites and flysch [Montadert et al., 2014].

The Mamonia Complex is considered as a tectonized remnant of a Mesozoic continental margin (Figure 2 - 20), which is divided in two groups; each of which is further subdivided into different formations [Swarbrick and Robertson, 1980]. The first group is the Ayios Fotios group and consists of sedimentary deposits that record the Late Triassic to Cretaceous evolution of an inactive continental margin [Swarbrick and Robertson, 1980]. This group is subdivided from older to younger sediments in: a) the Vlambouros Formation which consists of quartzose sandstones, siltstones and mudstones, b) the Episkopi Formation consisting of siltstones, calcilutites and radiolarian mudstones, and c) the Marona Formation which consists of strongly bioturbated calcilutites with considerable stylolites [Swarbrick and Robertson, 1980]. The second group is the Diarizos Group which reflects Triassic alkalic volcanism and the sedimentation in close proximity to a continental margin [Swarbrick and Robertson, 1980]. This group is subdivided from older to younger deposits in: a) Petra tou Romiou Formation comprised of coralline limestone observed as detached blocks, b) the Fasoula Formation consisting of pillow lavas which are intercalated with pink and grey calcilutites, and c) the Loutra tis Aphroditis Formation comprised of lava breccias, volcanoclastic breccias and in a lesser extent by volcanoclastic siltstones and radiolarian mudstones [Swarbrick and Robertson, 1980].

The Circum Troodos sedimentary succession is made up by Upper Cretaceous and Cenozoic sediments affected by the compressional tectonics and the erosion of the Troodos ophiolites. The Perapedi Formation consists of radiolarites and manganese-rich sediments described as umbers which are associated with volcanic activity and hydrothermal vents [Robertson, 1975; 1976; Urquhart and Banner, 1994; Prichard and Maliots, 1998]. The

Campanian Kannaviou Formation [Urquhart and Banner, 1994] is comprised of grey bentonitic clays, radiolarian mudstones, volcanoclastic siltstones and sandstones (Figure 2 - 20) [Swarbrick and Robertson, 1980]. At certain localities it conformably overlies the Perapedi Formation, whereas in areas where the Perapedi Formation was not deposited or it was eroded, the Kannaviou Formation overlies unconformably the pillow lavas of the Troodos ophiolites [Swarbrick and Robertson, 1980]. The Maastrichtian Moni Formation is observed south of the Troodos ophiolites and is made up of siltstones and radiolarian mudstones, in a matrix of bentonitic clays, most probably derived from the older Kannaviou Formation [Swarbrick and Robertson, 1980]. The Kathikas Formation is considered as a sedimentary melange (Figure 2 - 20) of red argillaceous silt riddled by angular clasts derived from the Mamonia Complex and rarely by clasts of the Kannaviou Formation [Swarbrick and Robertson, 1980]. The Kathikas Formation is of Maastrichtian age, it is encountered predominantly at the western edge of the island and it generally passes upwards into the Lefkara Formation [Swarbrick and Robertson, 1980].

In the Paleogene period a change in sedimentation is observed passing to the deep marine biogenic deposits of the Lefkara Formation which span for approximately 50Ma (Figure 2 - 20) and are composed of calcareous nannofossils and planktonic foraminifera [Lord et al., 2000]. It is subdivided in three members: a) the Lower Lefkara marl member which is sparsely deposited throughout Cyprus and is of Mid-Maastrichtian to Late Paleocene age, according to bio-stratigraphic dating at the southern flank of the Troodos Mountain; [Lord et al., 2000]; b) the Middle Lefkara Formation characterized by the deposition of chert and massive chalk beds—its age is most probably Late Paleocene to Late Eocene [Lord et al., 2000]; and c) the Upper Lefkara marl member which is not widely exposed (or even deposited in the first place) where an Oligocene to early Mid Miocene age has been determined [Lord et al., 2000].

The change from deep pelagic Lefkara Formation to the sedimentation of the hemipelagic deposits of Pakhna Formation (16Ma), is an indication of an uplift of the Troodos ophiolite due to collision of the leading edge of Africa with Cyprus [Robertson 1977, 1990]. This uplift is evidenced in the Pakhna Formation, as terrigenous fragments are identified in its beds [Lord et al., 2000].

The Miocene time is characterized by the deposition of the Pakhna Formation (Figure 2 - 20). In Early Miocene time, shallow water bio clastic carbonate is deposited which is named the Tera Member of the Pakhna Formation. This formation is encountered mainly on the eastern and western shores of Cyprus (i.e. Androlykou quarry; Figure 2 - 22) and by dating benthic

forams a Late Oligocene-Early Miocene (Aquitanean-Burdigalian) age is proposed [Lord et al., 2000]. In Middle Miocene time most of south and west Cyprus is covered from the deposition of chalks, marls and chalky marls of the Pakhna Formation. It is difficult to distinguish the upper and lower boundary of this formation at each outcrop, however bio-stratigraphic dating has given a range of late Early Miocene to Late Miocene (Burdigalian to Tortonian) age [Lord et al., 2000]. The Late Miocene deposits are associated with the Koronia Member and are dominated by the growth of coral reef limestones. These limestones grew on palaeohighs situated on the flanks south, southwest and north of the Troodos ophiolites and on the Akamas peninsula. Micro paleontological dating of these reef limestones suggest a Tortonian age [Follows et al., 1992; 1996; Lord et al., 2000].

The uppermost Miocene age deposits are called the Kalavassos Formation (Figure 2 - 20) and are characterized by the gypsum deposits alternating with chalky marls and marly chalks. These deposits are consistent with the widespread Messinian Salinity Crisis that affected the Mediterranean Sea during this time [Lord et al., 2000]. Ongoing uplift in Plio-Pleistocene times [Kinnaird et al., 2011] is characterized by the deposition of the Nicosia Formation (Figure 2 - 20) calcarenites and sandstones (Pliocene age), while the Apalos Formations (fluvial sands and gravels) and the Fanglomerate (gravels, sands, silts) are considered to be of Pleistocene age [Geological Survey Department of Cyprus].

### 2.3.2 *Sedimentary basins*

Well preserved tectonic elements recognized onshore Cyprus include several Neogene basins and faults of various extend. These sedimentary basins (Figure 2 - 22) are: a) the Late Miocene/Plio-Pleistocene Polis Graben to the west of the island formed by an extensional regime due to slab roll back of the African plate [Robertson, 1990; Payne and Robertson, 1995, 2000]; b) the Late Miocene/Plio-Pleistocene Pegeia half-Graben created from extension [Payne and Robertson, 1995, 2000]; c) the Early-Middle Miocene Pissouri and Limassol Basin situated south-centrally of the island formed from an extensional due to slab roll back of the southward subducting African plate [Payne and Robertson, 1995]; d) the Maroni-Psematismenos Basin to the south-east, perceived as an Early to Middle Miocene basin [Robertson, 1990; Eaton and Robertson, 1993; Kinnaird, 2008]; and e) the Mesaoria plain in the center of the island, perceived as a Late Miocene to Early Pliocene basin [Harrison et al., 2004, 2008].

## Chapter 2: Geological Setting

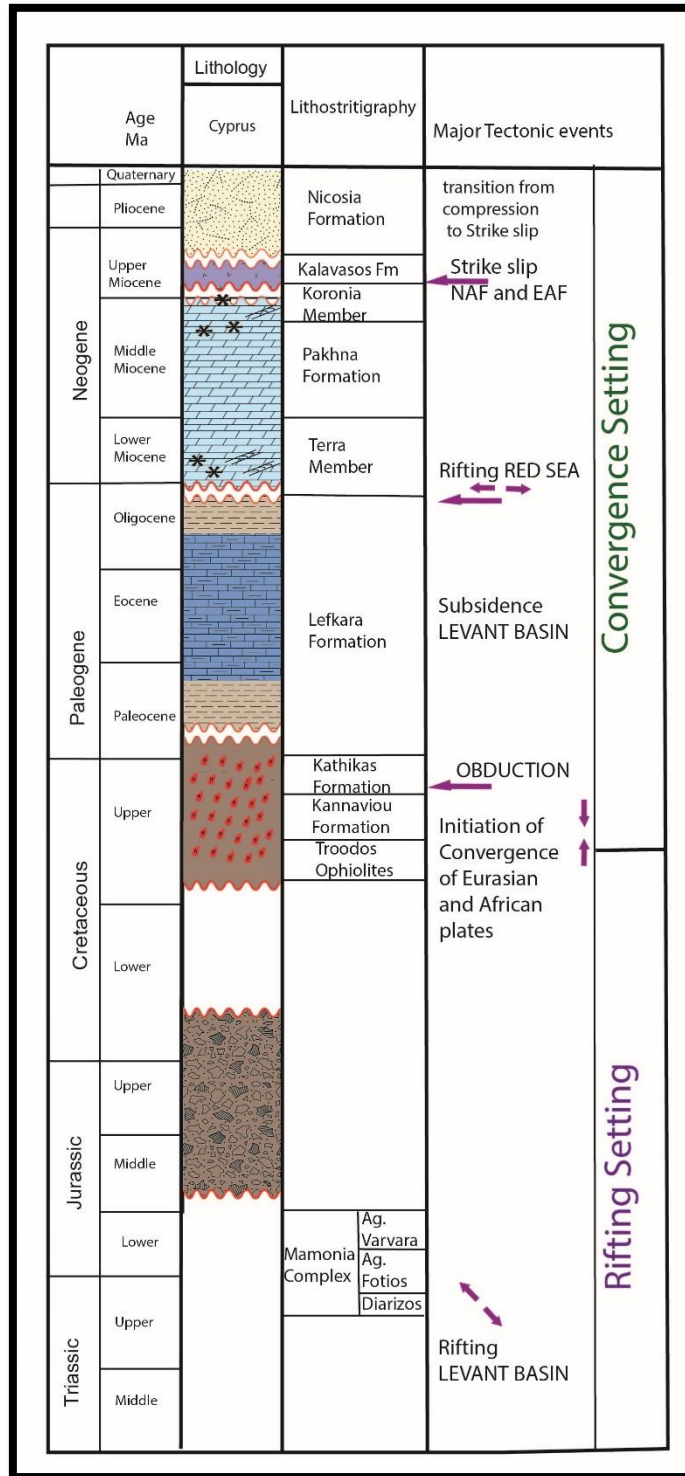


Figure 2 - 20: Stratigraphic chart illustrating the main lithological units identified onshore Cyprus, correlated with the major tectonic events in the Eastern Mediterranean region.

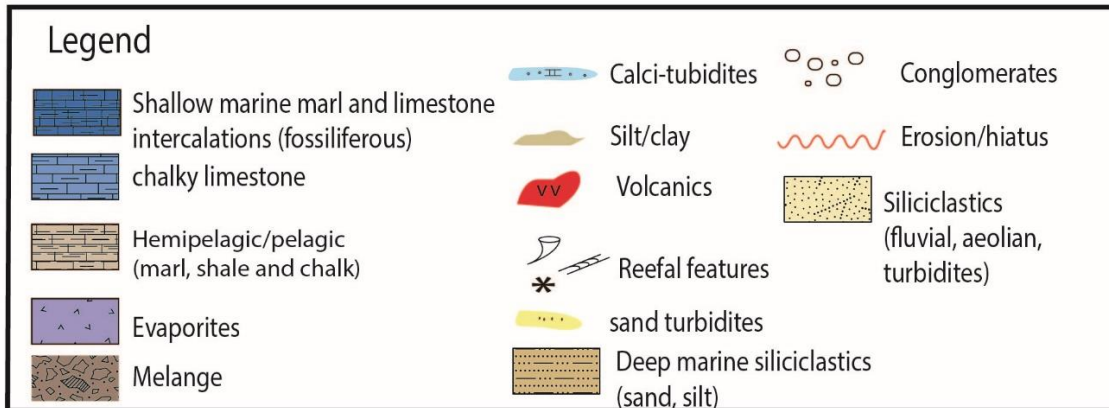


Figure 2 - 21: Legend of Figure 2 - 20, describing the lithological units of the chart.

In the Paphos region, the Polis and the adjacent Pegeia Basins trend in a NW-SE direction and are infilled by Neogene, Paleogene and Cretaceous sediments. Payne and Robertson [1995; 2000] interpreted these basins as a graben and a half graben respectively, which were produced by a rifting episode associated with roll back of the slab of the African plate, on the western end of the Cyprus Arc. Payne and Robertson [1995; 2000] postulate the existence of major NNW-SSE faults and further propose that the normal faults created local highs (horst structures) on which Tortonian reef carbonates grow. Kinnaird [2008], describes three deformational events: a) a Late Miocene extensional event (Figure 2 - 23) which gives rise to NNW-SSE or N-S striking faults; b) a second extensional event in Pliocene time, responsible for the formation of WNW-ESE normal faults; and c) a compressional/transpressional episode of Pleistocene/Holocene time (Figure 2 - 24), which reactivated structures of the two previous events.

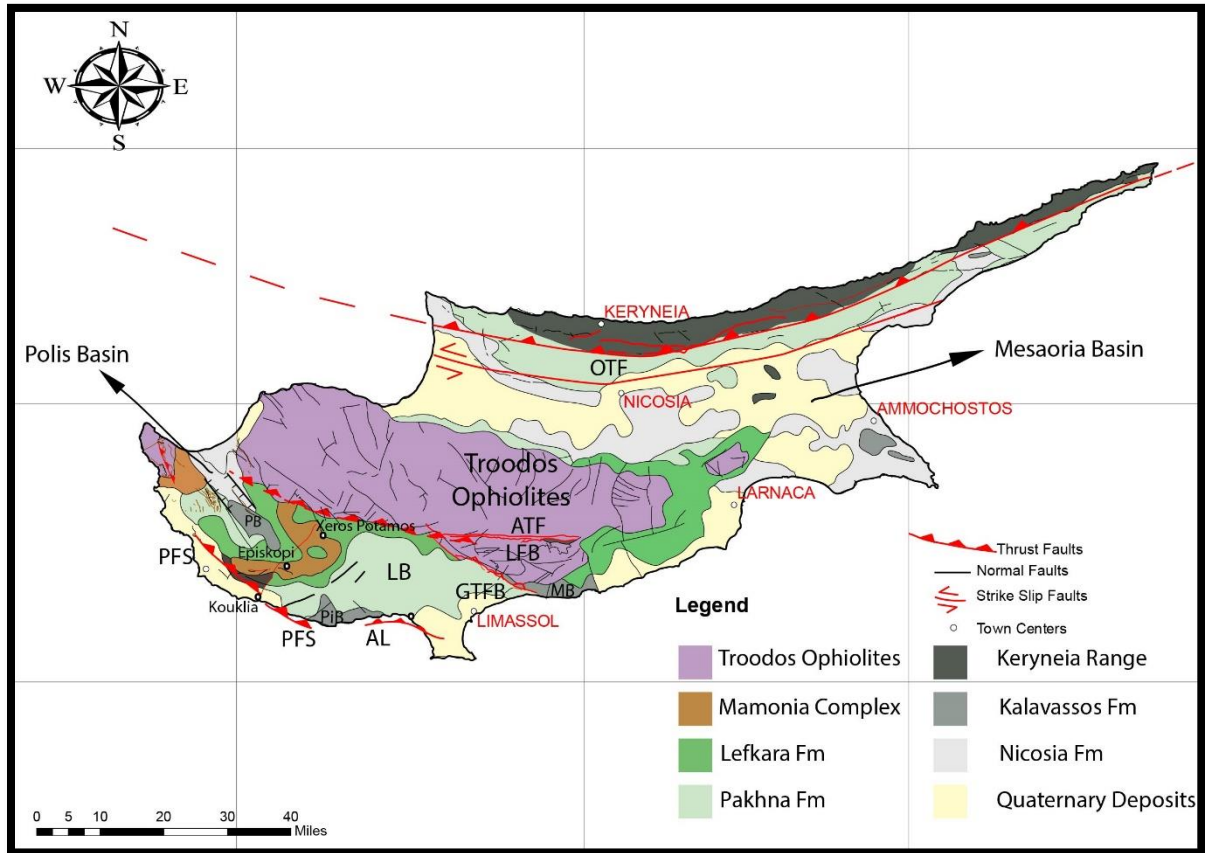


Figure 2 - 22: Outline geological map of Cyprus illustrating the main tectonic structures and sedimentological formations. AL=Akrotiri Lineament; ATFS=Arakapas Transform Fault system; AQ=Androlykou Quarry; GTFB=Gerasa Thrust and Fold Belt; LB=Limassol Basin; LFB=Limassol Forest Block; MB=Maroni Basin; OTF=Ovgos Transform Fault; PB=Polis Basin; PFS=Paphos Fault system; PiB=Pissouri Basin [modified after Kinnaird et al., 2011].

A similar origin is proposed for the Pegeia half graben but its structure is still debated. The first assumption by Payne and Robertson [1995, 2000] was the creation of the so called Pegeia half-graben by WNW-ESE normal faults that were dipping to the south. In his study, Kinnaird [2008] observed NNW-SSE normal faults, WNW-ESE normal faults and sinistral faults striking from NNE-SSW. Kinnaird's [2008] most important observation was that WNW-ESE striking faults dipping to the NNE were more widespread than the expected WNW-ESE faults dipping to the SSW and concluded that the half graben configuration proposed by Payne and Robertson [1995, 2000] does not fit the puzzle. Thus, the existence of NW-SE and WNW-

ESE normal faults in the Paphos region may suggest that both areas were affected by the same tectonic regime [Kinnaird, 2008].

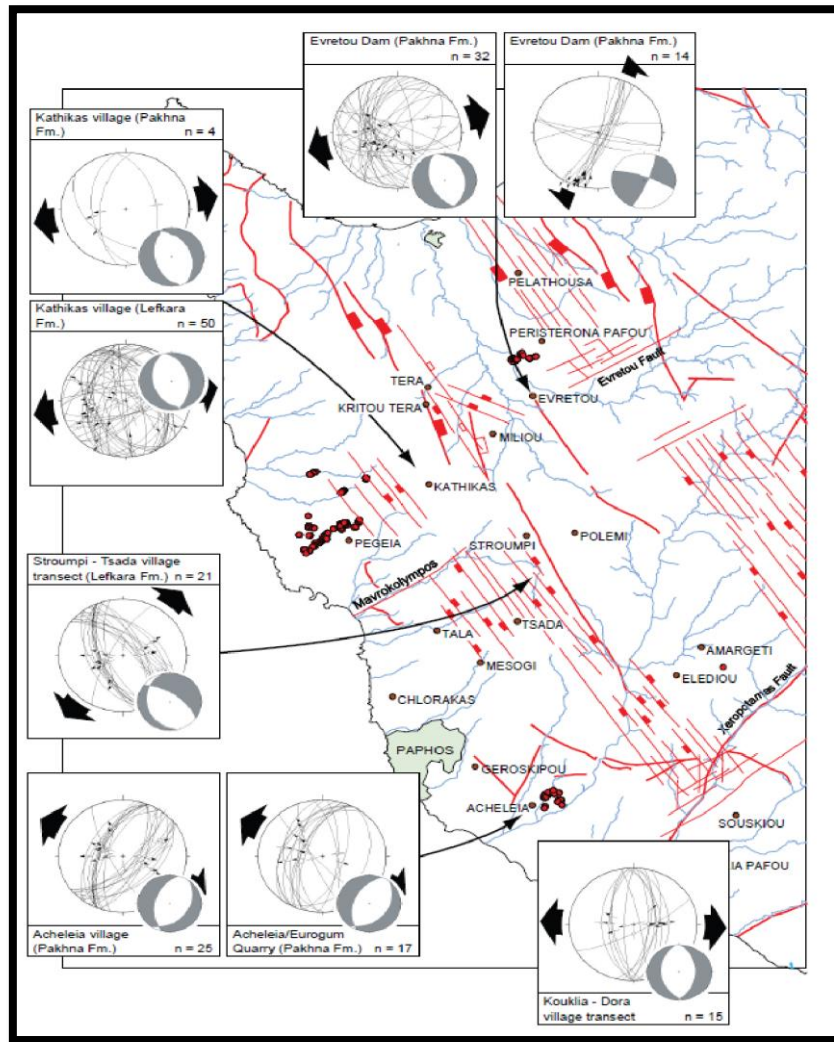


Figure 2 - 23: Late Miocene extension in the Polis Graben from structural data collected by Kinnaird. The faults shown in the figure are as mapped by Payne and Robertson [1995], [from Kinnaird, 2008].

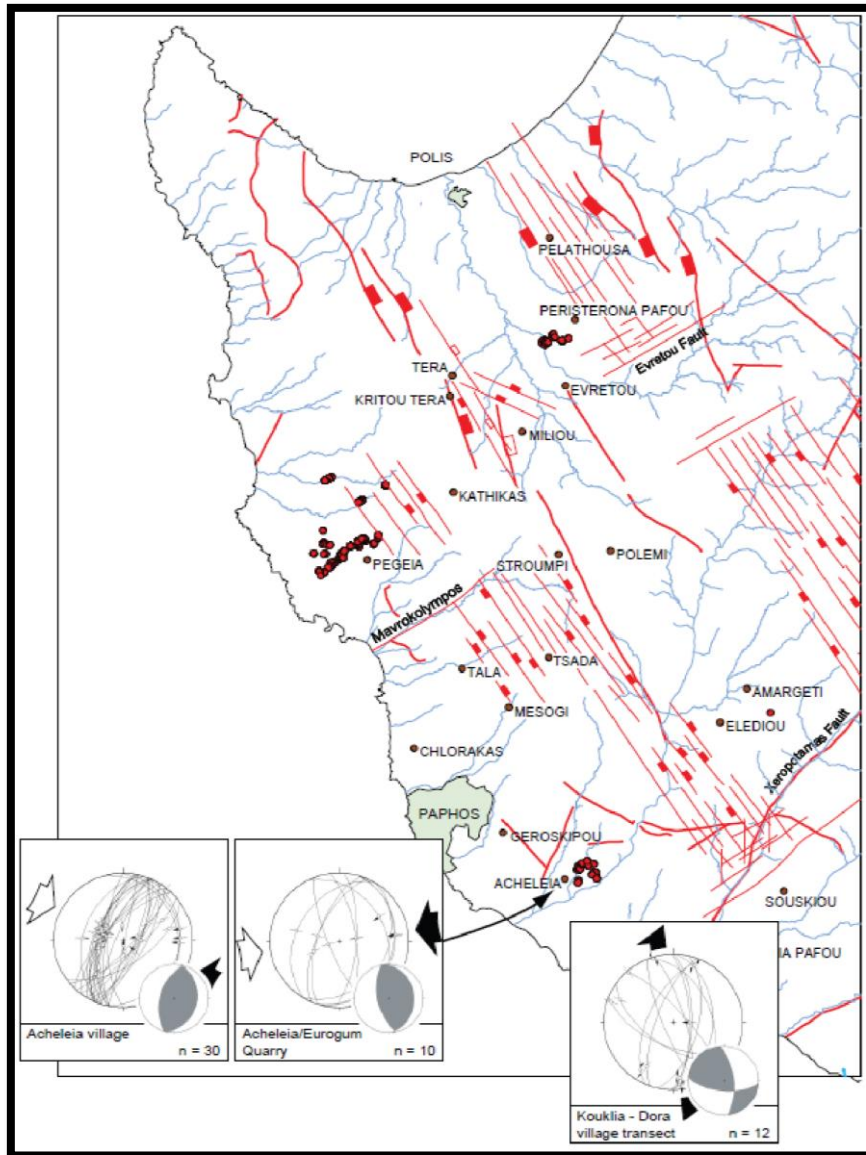


Figure 2 - 24: Post Miocene compression expressed from structural data collected by Kinnaird from the Polis Graben. This event is constrained to Pleistocene/Recent times. The faults shown in the figure are as mapped by Payne and Robertson [1995] [from Kinnaird, 2008].

The Pissouri Basin (south Cyprus, Figure 2 - 22), is considered as an extensional basin of Burdigalian to Mid-Miocene age associated either with slab roll back of the African plate [Payne and Robertson, 1995, 2000] or with a transpressional regime [Harrison et al., 2004]. Kinnaird [2008] identified four deformation events (Figure 2 - 25): a) a Late Miocene extension

trending east-west controlled by N-S and NW-SE oriented normal faults; b) an extensional episode in the Messinian associated with NNW-SSE, NNE-SSE and NE-SE normal faults; c) a compressional/transpressional event of Early to Mid-Pleistocene age responsible for the re-activation of the N-S striking faults of Late Miocene age; and d) a Late Pleistocene/Holocene extension due to dissolution of Messinian salt and the collapse of the overlying Fanglomerate group and Terra Rosa soils.

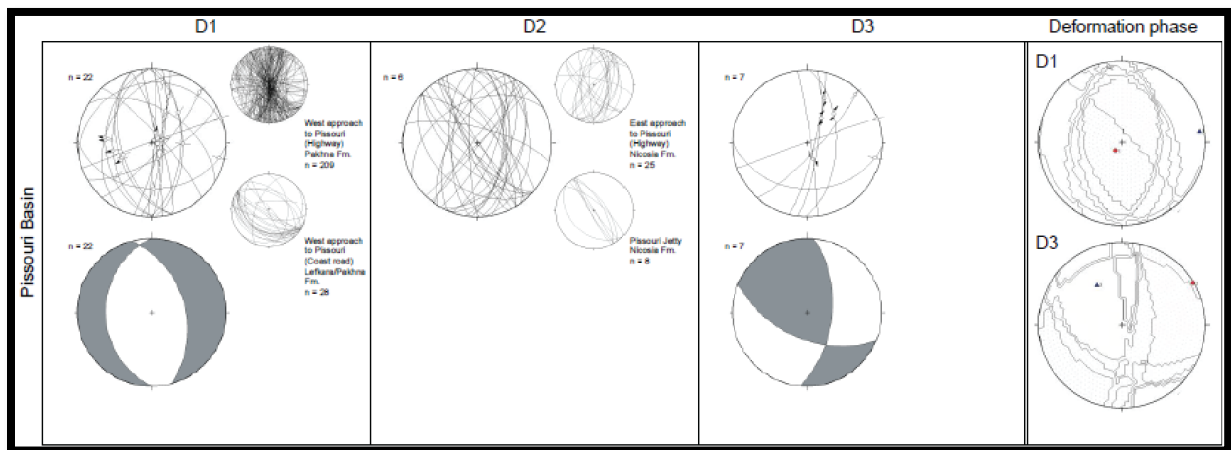


Figure 2 - 25: Deformation phases in the Pissouri Basin from structural data collected by Kinnaird: D1:- ~ N-S orientated faults formed during Tortonian E-W extension; D2:- ~ NE-SW orientated faults formed due to dissolution and collapse of gypsum; and, D3:- reactivation of D1/D2 structures in a dextral sense [from Kinnaird, 2008].

The Maroni-Psematismenos Basin (Figure 2 - 22), is considered of Early to Mid-Miocene age, created during the beginning of the uplift of Cyprus [Kinnaird, 2008]. Near the village of Choirokoitia a submarine channel containing poorly sorted chalk of Lefkara and Pakhna Formation, reworked corals of the Koronia member and igneous clasts of the Troodos massif are evidence of the first uplift and erosion of the Troodos Massif. This channel was dated to be of Middle to Late Miocene age, by tetrapod assemblages [Kinnaird, 2008; Geological Survey Department of Cyprus]. Data gathered by Kinnaird [2008] in this area attest to three deformational events: a) a Late Miocene extension (Figure 2 - 26) governed by NE-SW trending faults; b) an extension due to normal faults of ENE-WSW orientation in the Messinian; and c) a compressional/transpressional episode of Pleistocene age which was responsible for the reactivation of the of the NE-SW oriented faults of the previously described events (Figure 2 - 27).

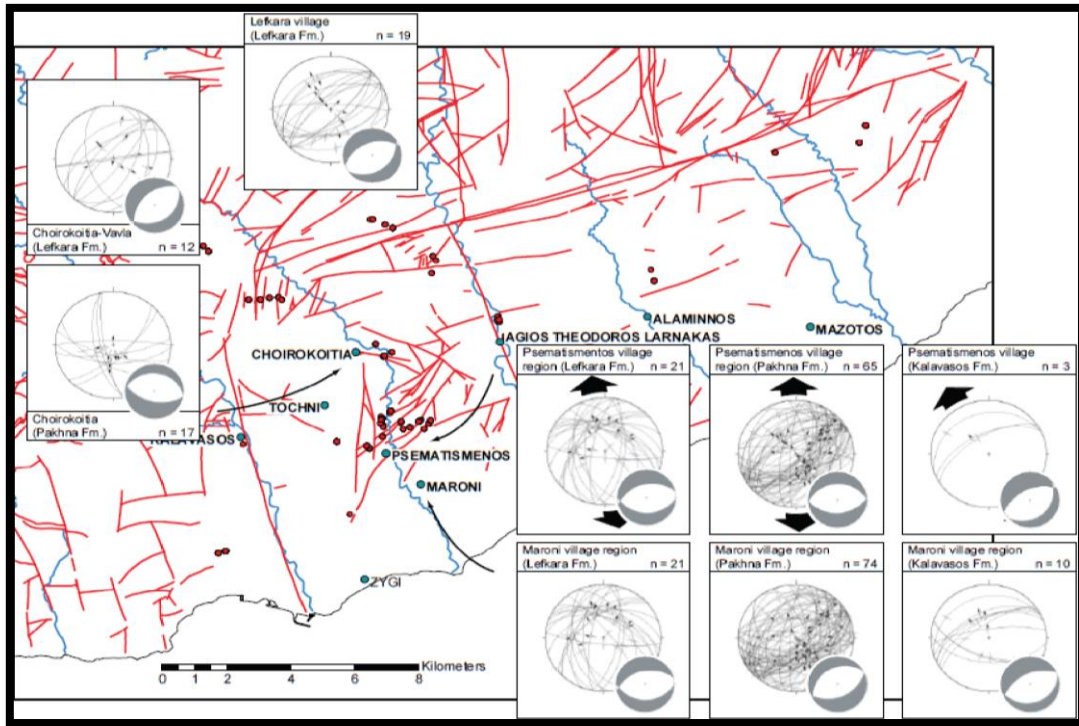


Figure 2 - 26: Structural data collected by Kinnaird from the Maroni-Psematismenos Basin showing extension in the area during Late Miocene time. Faults shown are as mapped by the Geological Survey Department of Cyprus [from Kinnaird, 2008].

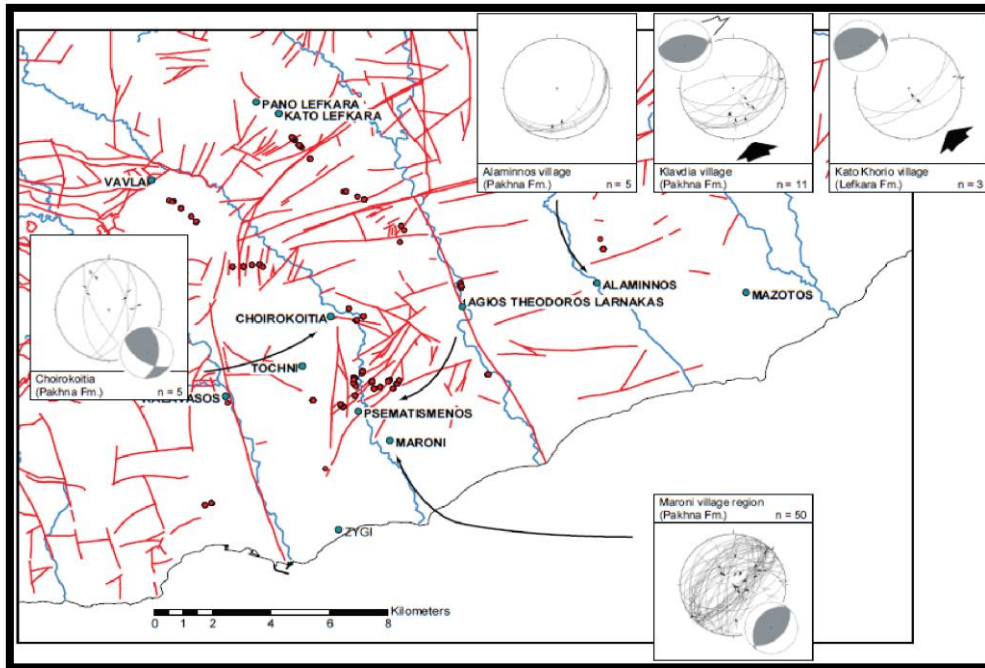


Figure 2 - 27: Structural data collected by Kinnaird from the Maroni-Psematismenos Basin showing compression in the area during Pleistocene time. Faults shown are as mapped by the Geological Survey Department of Cyprus [from Kinnaird, 2008].

The Mesaoria plain (Figure 2 - 22), is an east-west oriented basin that is situated between the northern extremity of the Troodos Massif and the southern limit of the Kyrenia range. Three scenarios are proposed for the creation of the Mesaoria Basin. Robertson [1998] suggests that the basin formed as a half-graben from fore-arc extension that was active from Oligocene until Middle Pliocene time (Figure 2 - 28a). Calon et al. [2005a, b] infer an evolution as a large piggy back Basin during Eocene-Oligocene until Recent times in the middle of the active Troodos-Larnaca culmination and the Kyrenia Thrust belt (Figure 2 - 28b). A third hypothesis from Harrison et al. [2004] proposes the development of the basin as a fore-deep in front of the Ovgos Fault (Figure 2 - 28c).

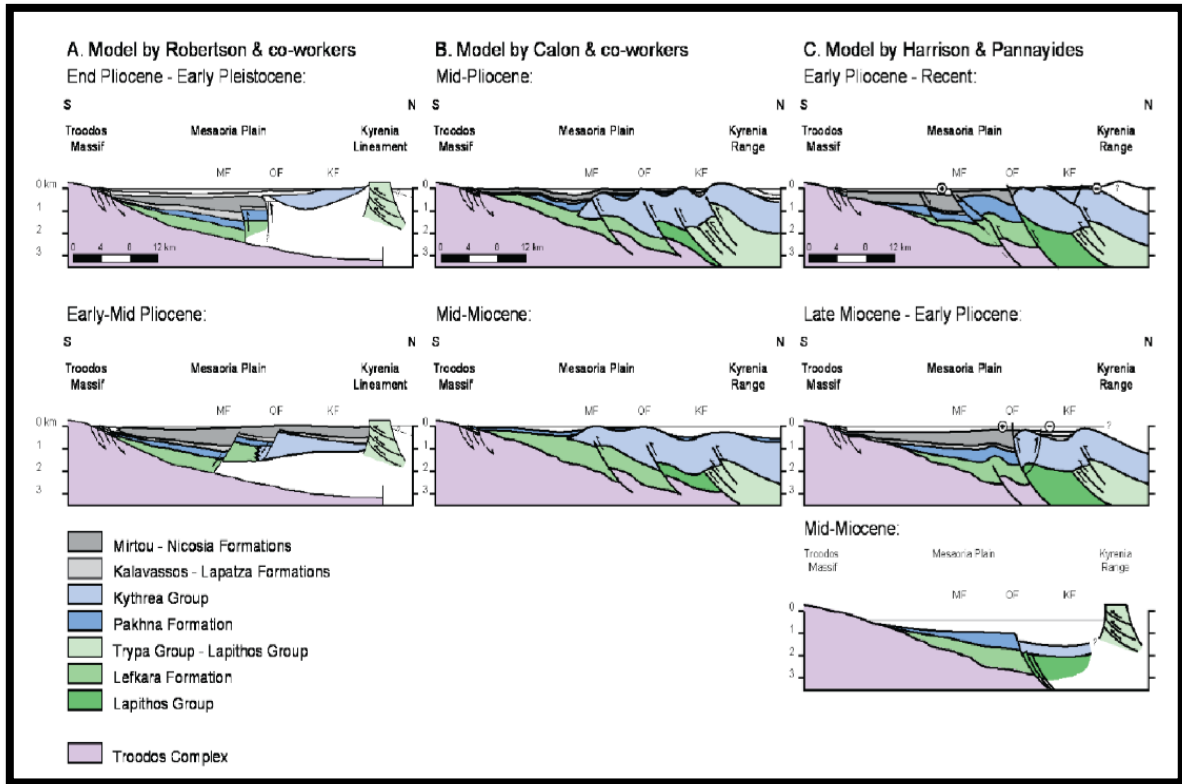


Figure 2 - 28: Models for the tectonic evolution of the Mesaoria Basin and Kyrenia range as proposed by different authors (seen in text), MF = Mesaoria fault, OF = Ovgos fault, KF = Kyrenia fault [from Kinnaird, 2008].

### 2.3.3 Main faults

The Arakapas transform fault zone (Figure 2 - 22) is identified as a large structure that runs from east to west and consists of oceanic crust which is intensely brecciated [Simonian and Gass, 1978]. It is considered as a Late Cretaceous structure characterized by right lateral strike slip movement [Kinnaird, 2008]. The study undertaken by Geoter [2005] on the active seismic hazards onshore Cyprus, proposes that the northern part of the Arakapas transform fault was re-activated as a left-lateral strike slip fault in Quaternary time from geomorphological observations in the field.

The Gerasa Lineament (Figure 2 - 22) is a WNW-ESE trending zone of left lateral movement, considered to be of Early to Middle Miocene age and corresponds with the southward thrusting and folding of the ophiolites of the Limassol Forest Block over the chalks

and cherts of the Lefkara Formation observed to the south [Kinnaird, 2008]. Eaton and Robertson [1993] suggested that the activity on this lineament ceased by Late Miocene connecting it with the deposition of Tortonian reefs (Koronia Member) on top of the pillow lavas of the Troodos ophiolite in several locations (i.e. Parekkklisia, Moni Formation, Armenochori). The neo-tectonic study of Geoter [2005] proposes the reactivation of the Gerasa lineament in a right-lateral sense in Quaternary time from field geomorphological observations.

As described in the previous section, the large normal faults (Mid/Late Miocene time) that bound the Polis Graben (Figure 2 - 22), are trending NNW-SSE and it is perceived that these faults formed by slab-roll back during the subduction in the western part of Cyprus and are associated with extension [Payne and Robertson, 1995, 2000].

Bailey et al. [2000], identified three deformational events that shaped western Cyprus and they further divided this area into the northern and southern regions (Figure 2 - 29). The first event is associated with dextral strike-slip with its activity calculated from 83-90Ma, while evidence of dextral shear and the parallelism of the orientation of the foliated Ayia Varvara Formation indicate a dextral strike slip system [Bailey et al., 2000]. The second event is associated with dextral transtension and it covers almost the same time span as the first event (73-90Ma). In the southern region the coeval timing of dextral and extensional faults indicates a dextral transtensional regime, while field observations are suggestive of serpentinite protrusions along these faults [Bailey et al., 2000]. In the Northern Region tectonic structures are dominantly thrusts and folds [Bailey et al., 2000], while Malpas et al. [1993] report that the Kannaviou Formation was deposited within hollows which are bounded by faults, indicative of the extensional regime during Campanian time and further justified by the observations of serpentinites adjacent to extensional contacts [Bailey et al., 2000]. The close proximity or the initial juxtaposition of the Mamonia Complex onto the Troodos Ophiolite complex is perceived as the Campanian to Early Maastrichtian time [Bailey et al., 2000]. This is suggested by field observations where in both terranes extensional and dextral strike slip structures are evident [Bailey et al., 2000]. Another indication is the deposition of the Moni Formation on top of both terranes in South Cyprus (Limassol area), with the Moni Formation (Figure 2 - 29) described as an olistostrom derived from the Mamonia Complex and deposited on a north verging slope [Robertson, 1977]. The third event is associated with transpression (sinistral strike slip in the Southern region, whereas in the Northern region SW directed thrusting prevails) and the final collision between the Mamonia Complex and the Troodos Ophiolites [Bailey et al., 2000]. The timing of the final juxtaposition is believed to be between late Campanian and early Maastrichtian as it is defined by the deformation of the Kannaviou Formation and the deposition of the overlying Kathikas and Lefkara Formations [Swarbrick and Naylor, 1980; Urquhart and

Banner, 1994; Bailey et al., 2000]. Furthermore, Swarbrick and Naylor [1980] argue that the emplacement of the serpentinites is restricted to Early Maastrichtian due to the small amount of serpentinite clasts identified in the Kathikas debris flows. Field observations from SW Cyprus, suggest that displacements are small with the maximum offset of the serpentinite thrusts ranging from 1 to 2 km in the Northern region and roughly 500m in the Southern region [Bailey, 1997]. The Southern region is connected with shortening oriented towards N-S to NE-SW (Figure 2 - 29) [Bailey, 1997; Bailey et al., 2000]. In the Northern region, SW, West or NW thrusting was observed with the shortening oriented E-W (Figure 2 - 29) [Bailey, 1997; Bailey et al., 2000].

Swarbrick [1993] proposed a general scheme to interpret SW Cyprus (Figure 2 - 30), stating that from the juxtaposition of the Mamonia Complex and the Troodos ophiolite a suture zone was created which originated from sinistral restraining bend. This conclusion was based on the anastomosing pattern of the high angle faults, the contacts between unrelated basement types, the tectonic setting and the interweaving nature of the tectonic slivers of metamorphosed lavas and sediments are all consistent with strike slip displacement. Thus Swarbrick [1993] suggested that the southern extend of the Polis Basin (Figure 2 - 29, southern region) was a result of pull apart at a releasing bend. In the northern region (Figure 2 - 29, current western flank of the Polis Basin) the Diarizos basement was uplifted due to push up at a restraining bend thus giving rise to submarine slopes from which the Kathikas Formation was derived due to debris flows.

The Ovgos fault system (Figure 2 - 22) is an E-W trending, left lateral strike slip fault that separates the Mesaoria plain and the Kyrenia range. This fault zone is characterized by faults and folds and was active since Miocene time [Harrison et al., 2004, 2008]. By that time the Mesaoria Basin was a shallow open marine platform with deposits of the Pahnka Formation, while further north the Kyrenia range was a deep ocean basin with deposits of turbidites (Kythrea Formation) [Harrison et al., 2004]. A continuous change of facies across the Ovgos fault zone led Geoter [2005] to suggest that the deposition of sediments was transported along the fault in a strike-slip manner since Late Miocene time. Indeed Harrison et al., [2008] agree with this notion and proposed that the change in convergence between Africa and Eurasia in Tortonian time (9My), correlates with the movement observed on the Ovgos fault zone, where the left lateral strike slip nature of the fault preserved the Kalavastos Formation of Messinian age in pull-apart basins.

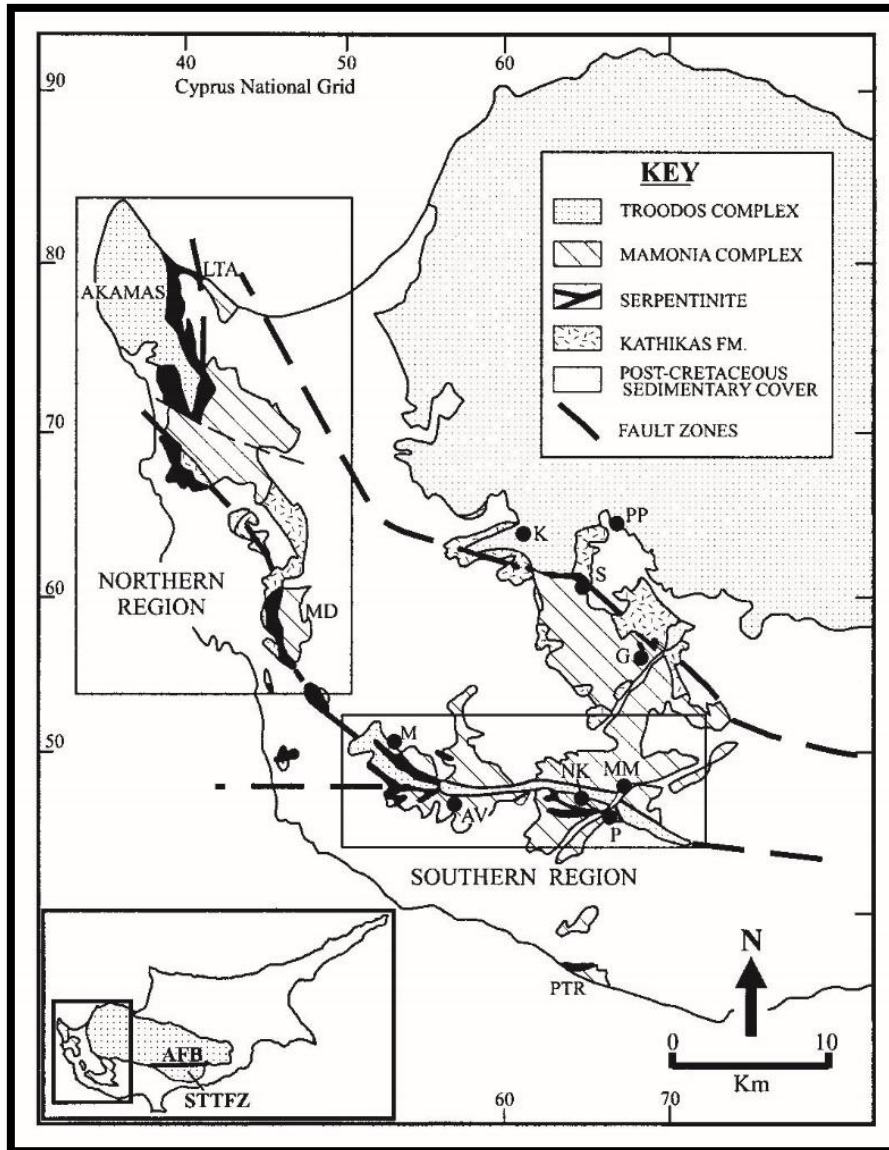


Figure 2 - 29: Geological map of southwest Cyprus, showing the outcrop patterns of Diarizos oceanic basement (part of the Mamonia Complex) and the Troodos oceanic basement (Troodos Complex), serpentinite (marking the location of basement faults) and the Kathikas Formation. The main outcrops of metamorphic rocks are at: 1, Loutra tis Aphroditis; 2, Galataria; 3, Ayia Varvara. Place names referred to in the text: Kt, Kathikas; K, Kannaviou; S, Statos; MD, Mavrokolymbos Dam; N, Nata; PTR, Petra tou Romiou. A Cyprus Geological Survey borehole BH, near Neokhorion, indicates Troodos oceanic basement beneath the Tertiary chalks [Bailey et al., 2000].

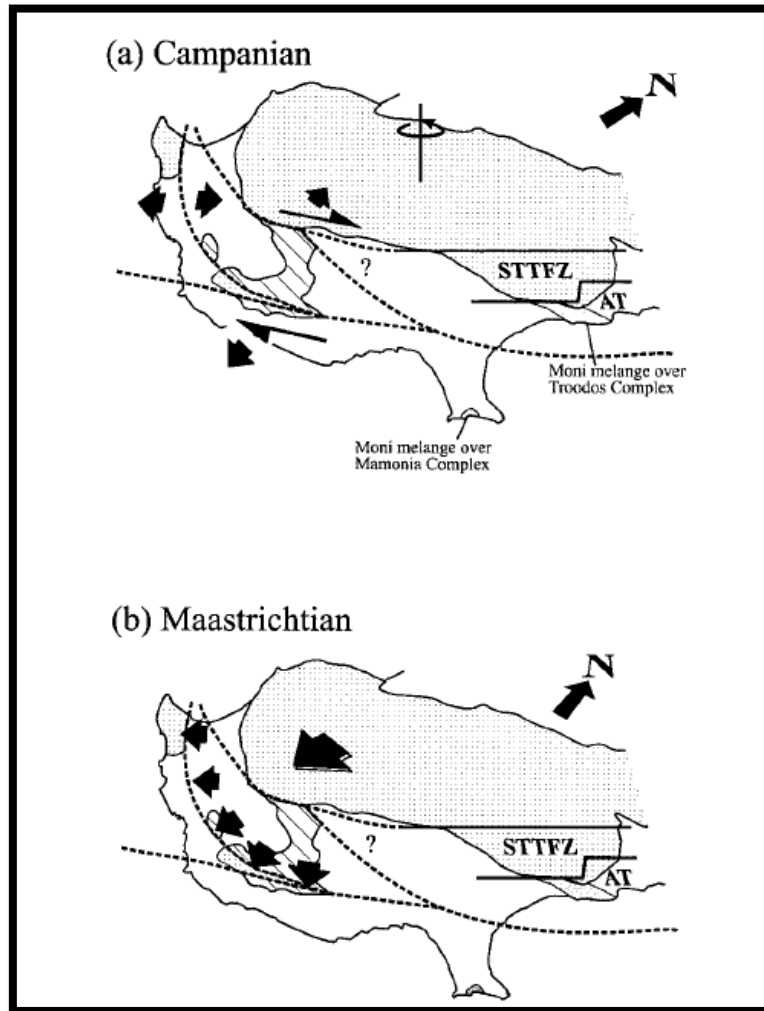


Figure 2 - 30: Campanian to Maastrichtian deformation along the Mamonia Complex suture zone. A) Dextral transtension along the suture zone during the anti-clockwise rotation of the Troodos microplate in Campanian, with fragments of the Troodos ophiolites detached and locally juxtaposed against the Mamonia Complex. The Moni Formation is deposited above the Troodos ophiolites indicative of the close proximity of the two terranes. B) SW directed impingement of Troodos ophiolites into the Mamonia Complex. Black arrows illustrate the radial pattern of shortening [Bailey et al., 2000].

The Paphos Thrust system (Figure 2 - 31) was described by Geoter [2005] from fieldwork in Cyprus. It comprises of a serpentinite belt, the Agia Marinouda and Kouklia fold,

the Cape Aspro fault and the Mavrokolymbos river-Theletra transverse fault zone. The Kouklia fold is a NW-SE trending anticline which deforms Paleocene/Miocene strata and marine sediments of Pleistocene age [Geoter, 2005]. It is suggested that the compression in Pleistocene to Recent times that is the result of the subduction of the Eratosthenes seamount under Cyprus [Robertson, 1998], was responsible for the creation of the Agia Marinouda and Kouklia fold belt [Kinnaird, 2008].

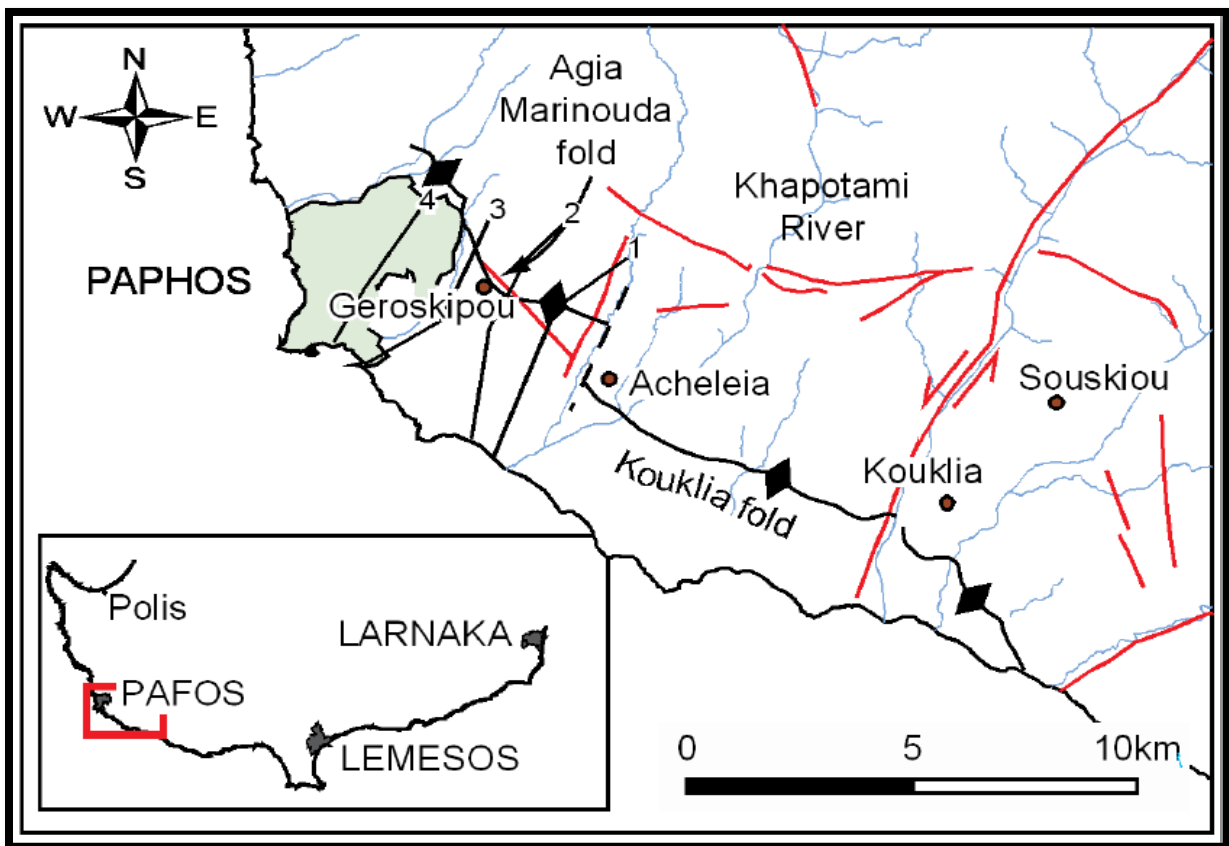


Figure 2 - 31: The location of the Agia Marinouda and Kouklia folds in the Paphos area [from Kinnaird, 2008].

### 2.3.4 Offshore Structures

Offshore Cyprus the sea bottom topography (Figure 2 - 13) is dominated by the Cyprus Arc system and the Eratosthenes Seamount to the south, the Hecataeus Rise, the Cyprus Basin and the Latakia Ridge to the east, with the Anaximander Mountains and the Florence Rise

located to the west [Papazachos and Papaioannou, 1999; Vidal et al., 2000a, b; Zitter et al., 2000; Zitter et al., 2003; Hall et al., 2005a, b; Wdowinski et al., 2006; Bowman, 2011; Reiche and Hubscher, 2015; Welford et al., 2015].

The Cyprus Arc system can be divided in three segments. The western segment which was identified from focal mechanisms, portrays a compressional element with NW striking planes that could be linked with the Florence Rise thus indicating the continuation of the Arc towards the northwest. The central part is situated south of Cyprus where the Eratosthenes Seamount is subducting under Cyprus and is considered as the plate boundary between the African and the Eurasian plates [Kempfer and Garfunkel, 1994; Robertson, 1998; Vidal et al., 2000a, b; Bowman, 2011]. The final part is located to the south east where the strike slip component is more notable on the Latakia Ridge system and it is associated with the change in movement between the Arabian and African plates by Late Miocene time [Kempfer and Garfunkel, 1994; Robertson, 1998; Vidal et al., 2000a, b; Hall et al., 2005b; Bowman, 2011].

The Latakia Ridge system (Figure 2 - 1) is considered as the boundary between the Levant Basin and the Cyprus Basin [Kempfer and Garfunkel, 1994; Vidal et al., 2000a, b; Hall et al., 2005b; Bowman, 2011; Montadert et al., 2014]. It consists of structural lineaments that trend towards the NE from the Hecataeus rise to offshore Syria and it is characterized by sinistral strike slip movement [Hall et al., 2005b]. It is perceived that the Latakia Ridge system started off as a compressional thrust belt by Mid-Late Cretaceous time and it is associated with the convergence between the African and Eurasian plates due to the closure of the Neotethys [Bowman, 2011].

The Cyprus Basin extends from the coastline of Cyprus to offshore Syria as an elongated E-W trending basin, which is bound by the Hecataeus Rise offshore Cyprus, the Latakia Ridge system to the south and the Larnaca Ridge to the north (Figure 2 - 1). The creation of the Cyprus Basin is linked with the first convergent movement between the African and Eurasian plate around late Maastrichtian time [Garfunkel, 2004; Bowman, 2011].

The Florence Rise (Figure 2 - 1) constitutes the western segment of the Cyprus arc. It is identified as a zone with long folds, which are earmarked by NE-SW and NW-SE sub-vertical faults and it is considered as a transpressive trench zone responsible for the creation of flower structures [Zitter et al., 2000, 2003]. Its continuation to the north runs through the Anaximander Mountains, a rifted block from the Taurus Mountains of southwestern Turkey [Zitter et al.,

2000, 2003]. The Anaximander Mountains is cut by faults trending NNW-SSE [Zitter et al., 2000, 2003].

### *2.3.5 Present-day tectonics*

Papazachos and Papaioannou [1999] focused their work on available seismological data and the fault plane solutions of earthquakes that shook the area, in order to define the lithospheric boundaries and the plate motion around Cyprus. The results that arose from the earthquake epicenters are assembled in three main zones of which the two are arcuate while the other is a linear seismic zone termed as the Paphos Transform Fault (PTF) to the southwest of Cyprus (Figure 2 - 32) with a strike orientation of NNE and is considered as a dextral fault [Papazachos and Papaioannou, 1999]. They also observed that strong seismic phenomena of intermediate depth are confined mainly to the west of the island in contrast with the east side, which prompted them to suggest that subduction is not active in the east due to ECB's collision which leads to the creation of a deformation zone [Papazachos and Papaioannou, 1999]. Papadimitriou and Karakostas [2006] also agree that a deformation zone is created and affects the trench and the trench slope and not the fore-arc region, due to the fact that this collisional event is created by a rather small seamount, the Eratosthenes Seamount. By analyzing the fault plane solutions they have concluded that the dextral PTF is governed by "strike-slip faulting with a thrust component" with a direction parallel to the alignment of the epicenters (Figure 2 - 33) which implies that southern Cyprus moves southwestwards, while the Larnaca set of earthquakes indicates a thrust component also showing a southwestward movement with Cyprus overriding the African plate in the eastern Mediterranean [Papazachos and Papaioannou, 1999].

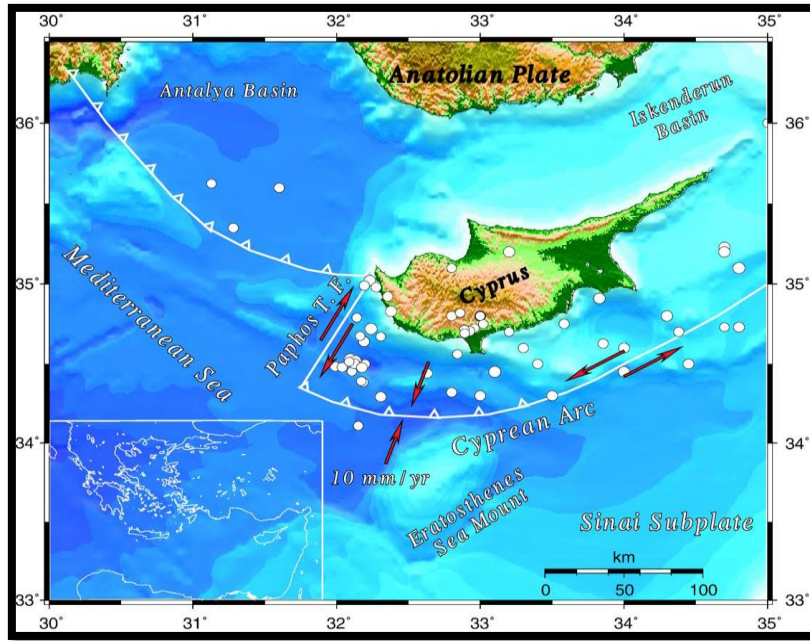


Figure 2 - 32: Geomorphological map of Cyprus with plate boundaries and relative motion [from Papadimitriou and Karakostas, 2006].

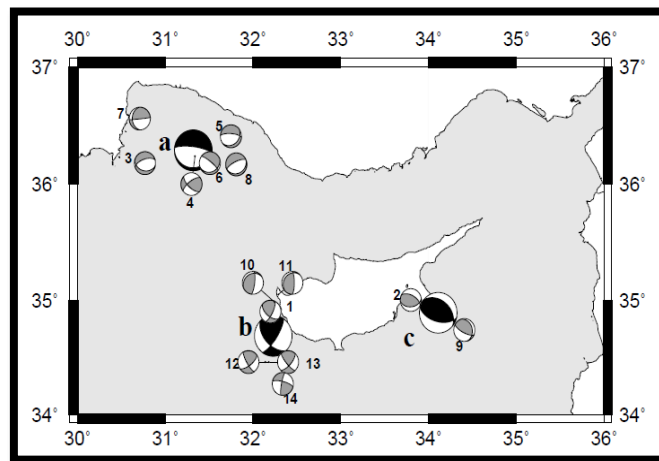


Figure 2 - 33: Graphical representations of the fault plane solutions of earthquakes in the area. The typical solutions of the three clusters (a, b, c) are denoted by larger symbols [from Papazachos and Papaioannou, 1999].

Seismic models (Figure 2 - 34) illustrating the crustal architecture and evolution of the plate boundary at the vicinity of the Cyprus Arc, indicate that the geometry of the slab is better presented as a slab-breakoff which dips deeper in the Antalya Basin, while under Cyprus the slab is not rolling-back but is rather buoyant due to asthenospheric upwelling [Dilek and Altunkaynak, 2009; Dilek and Sandvol, 2009]. This model is consistent with the existence of oceanic crust in the Herodotus basin [Granot, 2016] and a continental crust underneath Cyprus and the Eratosthenes Seamount [Gass and Masson-Smith, 1963; Makris et al., 1983; Ben-Avraham et al., 2002].

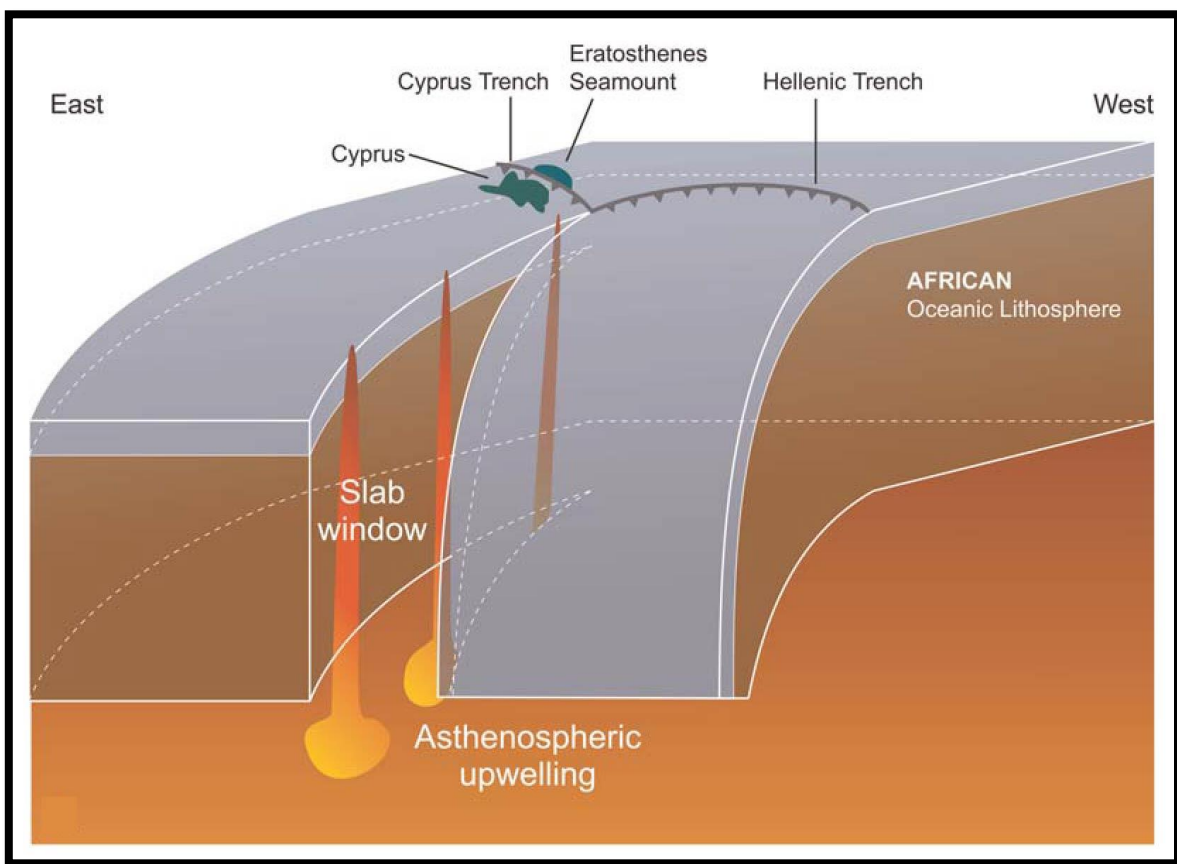


Figure 2 - 34: Interpretive geodynamic model of the evolution of the north-south trending field in the western Anatolia along a subduction-transform edge propagator (STEP) fault zone, developed in a tear within the northward subducting African lithosphere [Dilek and Altunkaynak, 2009].



**Chapter 3**

**Offshore tectonic structure  
investigation**

This chapter is divided in two parts. The first part discusses the methodology that was utilized for the interpretation of the seismic profiles. The second part is presented in the form of an article that is to be published in *AGU – Tectonics* journal [Symeou et al., in print]. The article is entitled “*Longitudinal and temporal evolution of the tectonic style along the Cyprus Arc system, assessed through 2D reflection seismic interpretation*”. It focuses on the identification, mapping, constraining the timing and the deformation mechanisms of key tectonic structures offshore Cyprus. Thereafter, the impact of such structures on the local and regional geodynamics in the Eastern Mediterranean is inferred. Industrial quality 2D reflection seismic profiles that cover the Exclusive Economic Zone of Cyprus were used to investigate for the first time the longitudinal evolution of the Cyprus Arc System. A number of structures were identified and described, such as south verging thrusts, flexural basins and an array of extensional faults. These structures are closely connected to the prevailing regional geodynamic setting as a result of the convergence of the African and Eurasian plates and the expulsion of the Anatolian micro-plate (discussed above, Chapter 2). The main objective of this chapter and the attached article is to illustrate the change in tectonic style along strike of the Cyprus Arc system, which is best described by the migration of the deformation front towards the south.

### 3.1 Methodology

The area of interest covers the length of the Cyprus Arc system and the different domains that border it, between the latitudes 34°N-32°N and longitudes 34°E-30°E (Figure 3 - 1). For the purposes of this study, 24 profiles of 2D reflection seismic lines are available, courtesy of Petroleum Geo-Services (PGS) and the Ministry of Energy, Commerce, Industry and Tourism of Cyprus. Details on the acquisition of the data are provided in the article. The seismic interpretation was performed on the 2D interpretation software GeoFrame Charisma (v4.4), which was available at IFP Energies nouvelles (Rueil-Malmaison).

#### 3.1.1 Data

2D seismic data were acquired from two surveys undertaken by PGS in collaboration with the Cypriot Government. The 2D surveys that were designed, cover the 13 exploration blocks in the Exclusive Economic Zone of Cyprus. These seismic data provide a regional overview of prospective oil and gas leads that interest oil companies.

During the two surveys, a large number of seismic profiles were acquired, namely 6770km of 2D profiles in 2006 and 12200km of 2D profiles in 2008, covering the EEZ of Cyprus. The distance between the profiles of the first survey was 10 x 25 km. For the second a different approach was taken, as it was deemed more important to adequately image the eastern segment of the EEZ, where the distance between the profiles was designed to be 5 x 5 km, whereas in the western extend the coverage was 20 x 20 km.

The striking difference between the two surveys is the method applied for the imaging. The 2006 survey was undertaken with the use of a conventional hydrophone streamer which resulted in profiles lacking clear images under the thick Messinian salt deposits identified throughout the Levant Basin. This problem was dealt with in the second survey in 2008, where the GeoStreamer® technology was introduced, a dual sensor hydrophone which resulted in better clarity of the seismic profiles under the Messinian salt. For both surveys the specifications of the seismic profiles were similar, as a shot interval of 25m was used and the length of the profiles extended up to 8100m.

### *3.1.2 Stratigraphic picking and time determinations*

The identification of the seismic horizons and seismic packages was based on previous studies that correlated the offshore Levant Basin with offshore wells in Israel and onshore rock exposures in Lebanon [Gardosh et al., 2010; Hawie et al., 2013], as well as the Cyprus Basin with onshore wells in Syria [Bowman, 2011]. This approach was deemed necessary due to the lack of access to the existing wells offshore Cyprus (Aphrodite well drilled by Noble Energy, Amathusa and Onasagoras wells drilled by Eni/Kogas, Onisiforos well drilled by Total/Eni). Thus the ages proposed for the litho-stratigraphic units offshore Cyprus, follow the description of the main markers as they are identified in previous studies. For example the Base Messinian horizon has a characteristic clear signature due to the presence of a thick layer of salt which makes it easily recognizable. In similar fashion the Base Pliocene horizon is easily identified due to the sharp contrast between the clastics and the salt layer seismic signals.

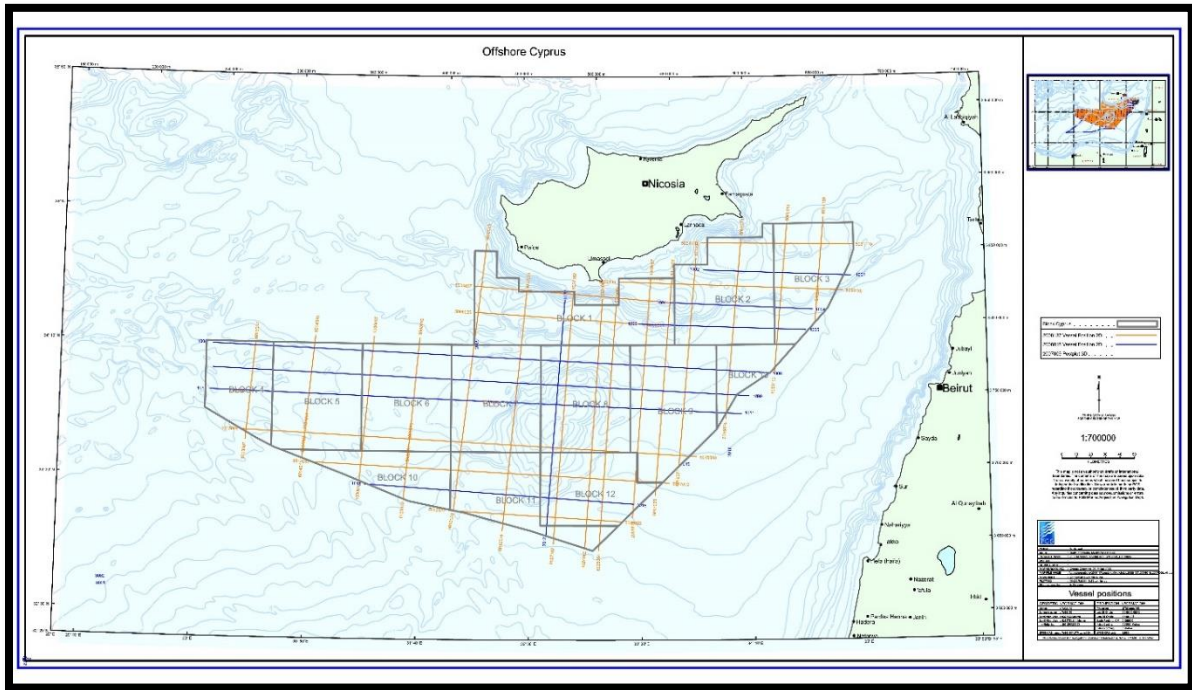


Figure 3 - 1: Location map of the 2D seismic profiles available for this study. Grey line depicts some of the blocks in the Exclusive Economic Zone of Cyprus. Blue lines represent the seismic profiles available from the MC2D-CYP2006 survey and orange lines represent seismic profiles from the MC2D-CYP2008 survey (courtesy of PGS).

Advancements in geophysical methods such as the new dual sensor GeoStreamer® technology used by PGS have managed to enhance the imaging of the sediments underlying the Messinian salt package. Hence, the seismic profile imagery and the confidence for the resulting interpretation are improved. The seismic units identified in this study include eight seismic packages which are believed to correspond to (from base to top): Late Jurassic, Early Cretaceous, Eocene/Senonian, Oligocene/Eocene, Lower Miocene, Middle-Upper Miocene, Messinian and Pliocene (Figure 3 - 2). These seismo-stratigraphic assumptions are based on the best practice and correlations with available studies in the East-Mediterranean region [e.g., Gardosh et al., 2010; Bowman, 2011; Hawie et al., 2013; Montadert et al., 2014; Nader, 2014, Ghalayini et al., 2014; 2016].

### 3.1.3 Structural interpretation on seismic profiles

Following the picking of the seismic horizons, various tectonic structures were identified, through the displacement of the sedimentary cover. Each structure was investigated

to deduce the timing of deformation and the likely involved mechanisms. This led to mapping of the main tectonic elements along strike of the Cyprus Arc system. Besides, the mapped tectonic elements could be organized in various domains – such as the Levant Basin, the Cyprus Basin and the Eratosthenes domains. This was important in order to understand and further constrain the tectonic regime through different time periods and to propose a working model that best explains the mapped tectonic elements and their history of deformation.

Depth (m)	Proposed Age	Seismic Units Horizons
1000		
2000	Pliocene Pleistocene	SP8 R9 R8
3000	Messinian	SP7 R7
4000	Middle - Upper Miocene	SP6 R6
5000	Lower Miocene	SP5 R5
6000	Oligocene / Eocene	SP4 R4
7000	Eocene / Senonian	SP3 R3
8000	Early Cretaceous	SP2 R2
9000	Late Jurassic	SP1 R1
10000		

Figure 3 - 2: Different seismic units and horizons utilized in this study. Ages and seismic units are in accordance with previous studies [Gardosh et al., 2010; Hawie et al., 2013].

### 3.1.4 Time to Depth conversion

Dix Formula (Figure 3 - 3) was used to achieve time to depth conversion models for each interpreted seismic horizon. This was done based on the stack velocities that PGS provided. Thus the artifacts created in certain domains, due to the large difference between the seismic wave velocities of the salt layers compared to the overlying clastic deposits, were accordingly corrected, while the thickness of the sediments was used to deduce the timing of movement of the faults.

$$V_{\text{int}} = [(t_2 V_{\text{RMS}2}^2 - t_1 V_{\text{RMS}1}^2) / (t_2 - t_1)]^{1/2},$$

where

$V_{\text{int}}$  = interval velocity

$t_1$  = travelttime to the first reflector

$t_2$  = travelttime to the second reflector

$V_{\text{RMS}1}$  = root-mean-square velocity to the first reflector

$V_{\text{RMS}2}$  = root-mean-square velocity to the second reflector.

Figure 3 - 3: Dix Formula, an equation used to calculate the interval velocities of flat or parallel layers [Dix, 1955].

## Start of Article

### **Longitudinal and temporal evolution of the tectonic style along the Cyprus Arc system, assessed through 2D reflection seismic interpretation**

**Vasilis Symeou<sup>1,2</sup>, Catherine Homberg<sup>1</sup>, Fadi H. Nader<sup>2</sup>, Romain Darnault<sup>2</sup>, Jean-Claude Lecomte<sup>2</sup>, Nikolaos Papadimitriou<sup>1,2</sup>**

<sup>1</sup>Universite Pierre et Marie Curie, ISTEP, 4 place Jussieu, 75005, Paris, France

<sup>2</sup>IFP Energies nouvelles, Geosciences Division, 1-4 Avenue du Bois-Preau, 92852, Rueil-Malmaison, France

#### **Key points:**

- Lateral changes from a compressional to a strike-slip regime along the Cyprus Arc.
- Different crustal nature in the Eastern Mediterranean.
- Forward propagation of thrusting towards the south.
- Shortening observed towards the West of the Cyprus Arc.

## **3.2 Abstract**

The Cyprus Arc system constitutes a major active plate boundary in the Eastern Mediterranean region. This structure is directly linked with the northward convergence of the African and Eurasian plates since the Late Cretaceous. 2D reflection seismic data were utilized, that image the main plate structures and their lateral evolution within the 150km-250km Exclusive Economic Zone of Cyprus. Interpretation of these data allowed the identification of nine tectono-sedimentary packages in three different crustal domains south of the Cyprus Arc system: (1) The Levant Basin (attenuated continental crust), (2) The Eratosthenes micro-continent (continental crust) and (3) The Herodotus Basin (oceanic crust). Within these domains, numerous tectonic structures were documented and analyzed in order to understand the mechanism and timing of deformation. In the north, south verging thrusting commenced in Early Miocene along the Larnaca and Margat ridges, whereas no activity was identified before Middle Miocene along the Latakia Ridge. Thus, the deformation front migrated southwards and was accompanied by the development of flexural basins and stratigraphic onlaps as in the Cyprus Basin. The acme of deformation occurred in Mid-Late Miocene. A regional unconformity of Pliocene age marks the end of the first deformation sequence. In Plio-Pleistocene time, the westward escape of the Anatolian micro-plate resulted in the reactivation of existing structures. The evolution of deformation along the plate boundary is identified from the creation of positive flower structures revealing transpressive movements along the Larnaca and Latakia Ridges (eastern domains) whereas in the Eratosthenes domain a flexural basin highlights a compressive regime.

### 3.3 Introduction

The geological evolution of the Eastern Mediterranean, which is directly linked with the opening and closing of the Neo-Tethys ocean [Garfunkel, 1998, 2004; Stampfli and Borel, 2002; Gardosh *et al.*, 2010], has attracted great interest and is still debated. The Cyprus Arc system, which includes the Cyprus Island, is located in the central part of the Eastern Mediterranean region and constitutes the present-day boundary of the African and Anatolian plates (Figure 3 - 4).

Different scenarios attempting to describe the tectonic evolution of the region exist. The three main scenarios are the following: a) long-lived collision scenario: depicting continuous thrusting and folding onshore and offshore Cyprus from Eocene until recent as a result of the continent-continent collision between the African and Eurasian plates. This scenario is suggested by the change in facies of the juxtaposed Paleogene-Oligocene deep pelagic carbonates with the Miocene flysch deposits in the Mesaoria basin, a basin considered as a piggy back basin which developed between the Troodos-Larnaca culmination and the Kyrenia thrust belt [Sage and Letouzey, 1990; Calon *et al.*, 2005 a, b]; b) strike-slip scenario, supported by the absence of a volcanic arc and a Benioff zone offshore Cyprus, in addition to the recognition of strike-slip structures onshore, which suggests that the emplacement of the ophiolites and the creation of the Cenozoic basins and Recent structures are associated with a left-lateral strike-slip regime since Late Cretaceous [Harrison, 2008; Harrison *et al.*, 2012]; and c) Pliocene collision scenario: where the Pliocene compressional tectonics followed a succession of compressional (from Late Cretaceous to Paleogene) and extensional regimes (Miocene time due to slab roll-back of the northward subducting African plate). This last scenario rests on the recent uplift of Cyprus and the change in sedimentation from Miocene hemi-pelagic carbonates to Pliocene clastics as a result of the continent-continent collision between the Eratosthenes micro-continent and the Eurasian plate in Pliocene [Robertson *et al.*, 2012; Kempler, 1998; Kinnaird *et al.*, 2011].

These different models/scenarios highlight the main plate-scale driving mechanisms responsible for the Cenozoic deformations in the Eastern Mediterranean region. The deformation commenced with the northward convergence of the Afro-Arabian plates with respect to Eurasia and is later accompanied by the westward extrusion of the Anatolian microplate relative to the African plate through time. Only a limited amount of published work on the Cyprus Arc system focuses on the lateral evolution of the structural style along this major

boundary. Even less emphasis is given on the integration of the tectonic structures of the Cyprus Arc system within the frame of the complex nature of the Eastern Mediterranean Basin.

Recent magnetic and gravity studies [Granot, 2016], indicate the boundary between the thinned stretched continental crust of the Levant Basin [Netzeband *et al.*, 2006; Montadert *et al.*, 2014; Granot, 2016; Inati *et al.*, 2016] and the oceanic crust of the Herodotus Basin [Montadert *et al.*, 2014; Granot, 2016] (Figure 3 - 4, red dashed line). This entices us to investigate the following scientific interrogations: How is the convergent movement of the plates and the deformation along the Cyprus Arc accommodated in this type of setting? Does the variation of the crustal nature affect the deformation style?

The main objective of this paper consists in investigating the aforementioned questions related to the structural style of deformation and the crustal variation between the Eastern, Central and Western domains. In the Eastern domain thin continental crust (Levant Basin) and obducted ophiolite (Cyprus Basin) are in contact. In the Central domain the continental crust underneath the Eratosthenes micro-continent is colliding with the continental crust under Cyprus. Finally in the Western domain, the oceanic crust of the Herodotus Basin is subducting northwards under the continental crust of the Antalya Basin (Southern margin of Turkey). Interpretation of industrial quality 2D (TwT) seismic reflection data which cover the Exclusive Economic Zone offshore Cyprus (Figure 3 - 4, Figure 3 - 6) were the key tool utilized in order to materialize this objective. These seismic data cover the E-W extension of the Cyprus Arc system which allows for comparison with previous data in order to observe along strike the lateral evolution of the Arc system, by mapping the various tectonic structures in order to deduce the mechanism and timing of the observed deformations.

### 3.4 Geological Setting

The tectonic evolution of the Eastern Mediterranean starts with the break-up of the supercontinent of Pangea and the creation of the Neo-Tethys Ocean [Gardosh *et al.*, 2010; Frizon de Lamotte *et al.*, 2011]. Rifting was followed by a convergent phase, resulting in the creation of tectonic structures (i.e. Cyprus Arc system), and the emplacement of the ophiolitic belt [Garfunkel, 1998] from East in Baer-Bassit in Syria, through Troodos Mountains in Cyprus to the West in the Antalya region in Turkey.

### 3.4.1 Early Triassic – Early Cretaceous

The Early Mesozoic period is considered as the onset of fragmentation of the northern margin of the super-continent of Pangea and the beginning of Tethys rifting [Gardosh *et al.*, 2010; Montadert *et al.*, 2014]. This break-up resulted in the creation of smaller continental fragments, such as the Tauride micro-continent which drifted northwards from the northern margin of Gondwana towards the Eurasian plate [Garfunkel, 2004; Bowman, 2011]. The outcome was the opening of the Neo-Tethys Ocean in late Middle Jurassic time (Calloviaian time) [Barrier and Vrielynck, 2008; Frizon de Lamotte *et al.*, 2011] and the gradual creation of smaller oceanic basins, separated by the resulting continental fragments [Robertson, 2007; Robertson *et al.*, 2012]. Rifting commenced in Mid-Triassic (Anisian) and halted in Mid-Late Jurassic time [Gardosh and Druckman, 2006; Gardosh *et al.*, 2010; Bowman, 2011; Montadert *et al.*, 2014]. Tethys rifting (Figure 3 - 5, box A), culminated in the creation of the Levant Basin from an extensional regime oriented in a NW-SE direction, with NE-SW trending normal faults [Garfunkel, 1998; Gardosh and Druckman, 2006; Gardosh *et al.*, 2010]. The Levant Basin is regarded as a basin overlain by ~12-14 km of sediments of probably Triassic-Jurassic age until recent [Makris *et al.*, 1983; Vidal *et al.*, 2000a, b; Ben-Avraham *et al.*, 2002; Montadert *et al.*, 2014], with its crustal nature considered as a thin attenuated continental crust of ~8 km [Netzeband *et al.*, 2006; Segev *et al.*, 2011; Granot, 2016; Inati *et al.*, 2016]. In contrast the Herodotus Basin, is constructed of oceanic crust [Makris *et al.*, 1983; Granot, 2016] and is covered by a thick sedimentary sequence of ~14-16 km [Montadert *et al.*, 2014]. Ongoing rifting [Gardosh and Druckman, 2006] resulted in the ‘‘separation’’ of the Eratosthenes micro-continent from the Arabian continental plate [Montadert *et al.*, 2014]. Faulting ceased by Mid-Late Jurassic time in the southern Levant, whereas tectonic activity continued during Early Cretaceous onshore Lebanon [Homberg *et al.*, 2010].

### 3.4.2 Upper Cretaceous – Oligocene

The Upper Cretaceous period is regarded as the start of the convergence regime between the African and Eurasian plates [Gardosh *et al.*, 2010; Bowman, 2011; Klimke and Ehrhardt, 2014; Montadert *et al.*, 2014] and the inversion of the East Mediterranean basins. In Late Maastrichtian, the initial closing stage of the Neo-Tethys Ocean results in the obduction of ophiolites in Baer-Bassit - Syria, in Antalya - Turkey and in Troodos - Cyprus [Garfunkel, 2004] (Figure 3 - 5, box B) described as the peri-Arabian ophiolitic crescent that extends from Turkey and Cyprus to the Oman ophiolites [Ricou, 1971]. Some authors suggest that the Latakia Ridge system initiated during Late Cretaceous time, as a compressional fold-thrust belt due to

the convergent movement between the African and Eurasian plates [Vidal *et al.*, 2000a, b; Bowman, 2011]. In Late Eocene to Early Oligocene time the on-going convergence of the African and Eurasian plates, led to the closure of the eastern strand of the Neo-Tethys Ocean [Barrier and Vrienlynck, 2008; Frizon de Lamotte *et al.*, 2011; Bowman, 2011].

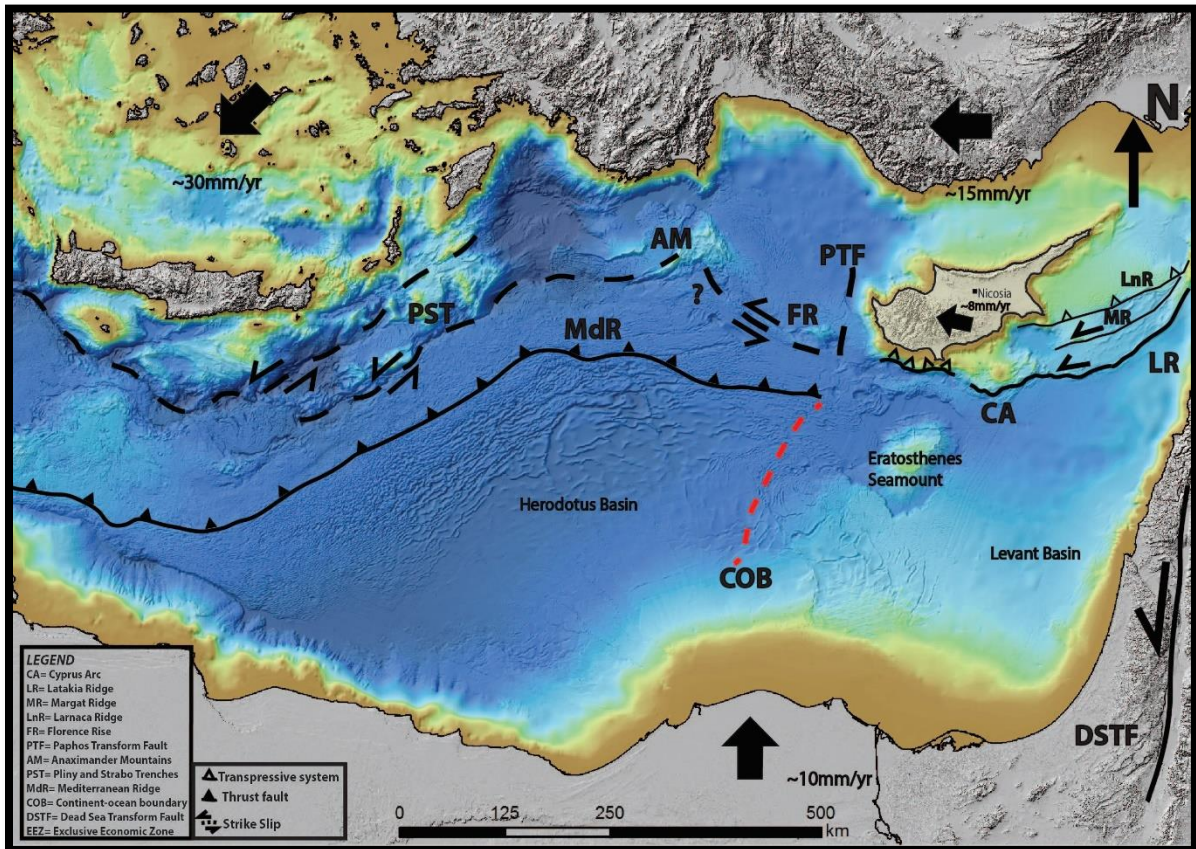


Figure 3 - 4: Regional bathymetric map [EMODnet], with the main tectonic structures. Red dashed line delineates the boundary between the thin continental crust (Levant Basin) and the oceanic crust (Herodotus Basin) as it was identified by Granot [2016]. Black arrows indicate the relative motion and average slip rate for the African and Anatolian plates [McClusky *et al.*, 2000]. Abbreviations: AM=Anaximander Mountain, CA=Cyprus Arc, COB=Continent-ocean boundary, DSTF=Dead Sea Transform Fault, FR=Florence Rise, HA=Hellenic Arc, LR=Latakia Ridge, MdR=Mediterranean Ridge, PTF=Paphos Transform Fault, PST=Pliny and Strabo Trenches.

### 3.4.3 Miocene – Present

By Miocene time, the “separation” between Arabia and Africa resulted in the initiation of the Dead Sea Transform fault [Montadert *et al.*, 2014]. This event was largely due to the difference in motion between the two plates. The increased northward movement of Arabia relative to Eurasia (~18-25 mm/yr [McClusky *et al.*, 2000]), in comparison with the smaller movement of the African plate relative to Eurasia (~10 mm/yr [McClusky *et al.*, 2000]), was accommodated by the opening of the Red Sea and the propagation of the Dead Sea Transform Fault [Brew *et al.*, 2001].

The westward escape of the Anatolian plate is associated with the slab pull of the northward subducting Hellenic Arc system and the asthenospheric flow [Le Pichon and Kreemer, 2010] in the Aegean region. This slab pull effect is created due to the slab roll back of the subducting Hellenic Arc resulting in an extensional regime and arc volcanism which is observed in the south Aegean [Dilek and Altunkaynak, 2009; Dilek and Sandvol, 2009] and is correlated quoted as the main mechanism for the escape of the Anatolian plate [Le Pichon and Kreemer, 2010]. A second scenario proposes that the western movement of the Anatolian plate is related with the northward movement of the Arabian plate during Latest Miocene to Early Pliocene time [McClusky, *et al.*, 2000, 2003; Hall *et al.*, 2005b; Montadert *et al.*, 2014].

A consequence of the westward movement of the Anatolian microplate, was the creation of a triple junction point, where the East Anatolian fault (left-lateral strike-slip fault), the North Anatolian fault (right-lateral strike-slip fault) and the Dead Sea Transform fault (left-lateral strike-slip fault) meet [Kempler and Garfunkel, 1994; Aksu *et al.*, 2005]. In addition, strike-slip faulting in the eastern part of the Cyprus Arc system and the initiation of the strike-slip movement along the Latakia Ridge system occurred at the same time and facilitated Anatolia’s escape tectonics [Kempler and Garfunkel, 1994; Montadert *et al.*, 2014].

Bowman [2011], proposes that the initial compressional nature of the Latakia Ridge system changes to a left-lateral strike-slip regime during Pliocene to Recent times, as it is supported by positive flower structures identified from the interpretation of seismic data that cover the Northern part of the Levant Basin and the Cyprus Basin [Hall *et al.*, 2005a, b; Bowman, 2011]. This change in motion is associated with the re-organization of tectonic stresses of the major plates in the region by Late-Miocene to Early-Pliocene time [Bowman, 2011], which is in accordance with analogue modelling experiments indicating slab break-off under the Bitlis-Zagros suture zone [Faccenna *et al.*, 2006].

*Kinnaird and Robertson* [2013] suggest that the ECB collided with the Cyprus Arc during Early Pliocene times, thus subducting underneath the arc and causing uplift of the island of Cyprus [*Garfunkel*, 1998; *Robertson et al.*, 2012]. Analysis of plate kinematics and GPS velocities [*McClusky et al.*, 2000, 2003; *Reilinger et al.*, 2006], suggests that the African plate moves towards the N-NW, while the Anatolian plate is experiencing a counter-clockwise rotation. These two movements are in accordance with the left-lateral strike-slip movement proposed for the Latakia Ridge [*Vidal et al.*, 2000a, b; *Hall et al.*, 2005a, b; *Le Pichon and Kreemer*, 2010; *Bowman*, 2011].

### 3.5 Data and Methodology

A multi-client seismic reflection data library courtesy of Petroleum Geo-Services (PGS) exists offshore Cyprus. This data base includes 12,200 km of 2D seismic data shot with the dual sensor GeoStreamer® technology, 6,770 km of conventional 2D seismic and 5,000 km<sup>2</sup> of 3D data covering part of the Exclusive Economic Zone (EEZ) of Cyprus (Figure 3 - 4) (<https://www.pgs.com/data-library/europe/mediterranean/>). For the purposes of this study and under the authorization of PGS and the Ministry of Energy, Commerce, Industry and Tourism of Cyprus, access to 24 lines of 2D seismic data was granted (Figure 3 - 6).

The conventional 2D seismic lines were acquired during the MC2D-CYP2006 survey and cover 6,770 km of the EEZ. One conventional hydrophone streamer was used extending 8100 m, with a shot interval of 25 m, a sample rate of 2 ms and a recorder two-way travel time (TwT) of 9216 ms in water depths of 1000 to 2500 m. The chosen seismic grid (seismic profile spacing) for this first survey was 10 x 20 km. Ten conventional 2D seismic lines, reprocessed by PGS in 2011 are available for this project.

With the use of the dual sensor GeoStreamer® technology a second survey, MC2D-CYP2008 that covers 12,200 km of the EEZ was acquired in 2008, with the processing completed in 2009. The dual sensor was utilized with a cable length of 8100 m, a shot interval of 25 m, a sample rate of 2 ms and a recorder two-way travel time (TwT) of 9216 ms in water depths extending from 1000 to 2500 m. The gridding for the second survey was 20 x 20 km in the western side while a denser grid of 5 x 5 km was drawn in the eastern side. Fourteen lines of the second survey are utilized in this project.

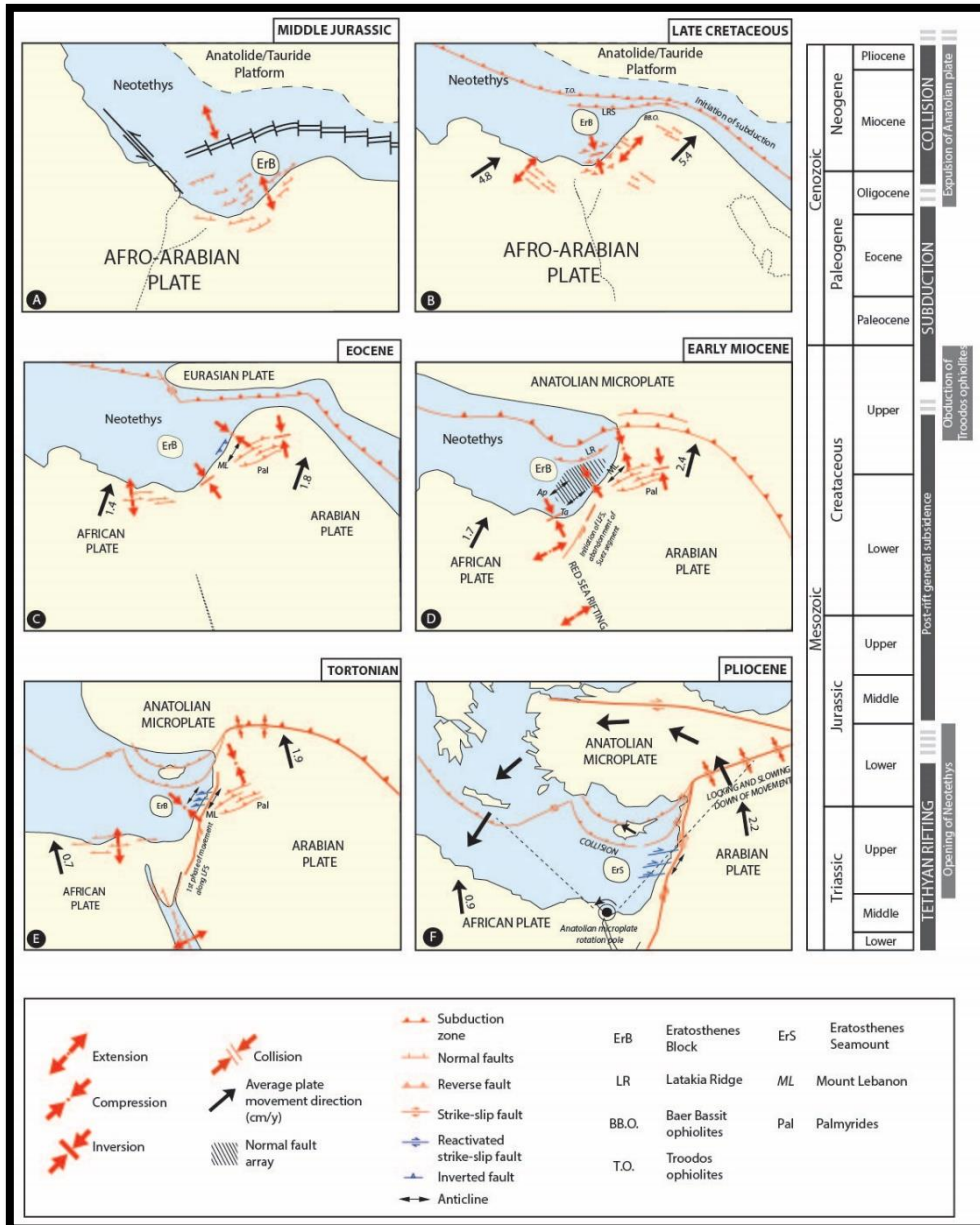


Figure 3 - 5: Paleo-geographic maps of the Levant region illustrating the tectonic evolution: (A) Mesozoic rifting phase, normal fault activity ceases by Middle Jurassic time; (B,C) initial closure of the Neo-Tethys due to convergence; (D) initial folding along the Levant margin; (E) westward expulsion of the Anatolian microplate; and (F) current tectonic regime [modified from Ghalayini et al., 2017].

The use of the dual sensor technology ensured an improved signal to noise ratio and better seismic imaging in geological areas with complex structures and a thick salt deposition of 1,5-2 km [Hsu et al., 1977], as sub-salt imaging with the conventional methods didn't herald

good results. Towed at a deeper depth, it ensured a quieter environment and less noise providing a better image [Montadert *et al.*, 2010].

Both data sets were processed by PGS as 'conventional marine data including SRME, noise removal in common depth point (cdp) domain, Kirchhoff pre-stack time migration, residual move-out correction, radon de-multiple, and post-stack processing' (see also Montadert *et al.*, [2010]).

The seismic data were loaded in GeoFrame Charisma (v. 4.4) a 2D interpretation software available at IFP Energies nouvelles (Rueil-Malmaison). The identification of different seismic packages and the picking of fault planes from the offset horizons was undertaken through this software. A velocity model provided by PGS was loaded in the GeoFrame Charisma database in order to convert the picked horizons from two-way travel time to depth, allowing for the creation of depth grids.

### 3.6 Results

#### 3.6.1 Seismo-stratigraphy and structural domains

Description and interpretation of seismic horizons and seismic packages was composed in accordance with previous studies [Roberts and Peace, 2007; Gardosh *et al.*, 2010; Bowman, 2011; Hawie *et al.*, 2013; Ghalayini *et al.*, 2014] as there is a lack of physical evidence (no access to borehole data) in the investigated area. Eight major seismic packages were identified from the interpretation of the reflection seismic data at our disposal (Figure 3 - 6) (courtesy of PGS and the Ministry of Energy, Commerce, Industry and Tourism of the Republic of Cyprus). These packages are constrained by nine key, regional horizons (Figure 3 - 7; [Roberts and Peace, 2007; Gardosh *et al.*, 2010; Bowman, 2011; Hawie *et al.*, 2013]): R9-Seabed, R8-Base Pliocene, R7-Base Messinian, R6-Base Mid-Miocene, R5-Top Oligocene, R4-Eocene unconformity, R3-Senonian unconformity, R2-Top Jurassic and R1-Middle Jurassic.

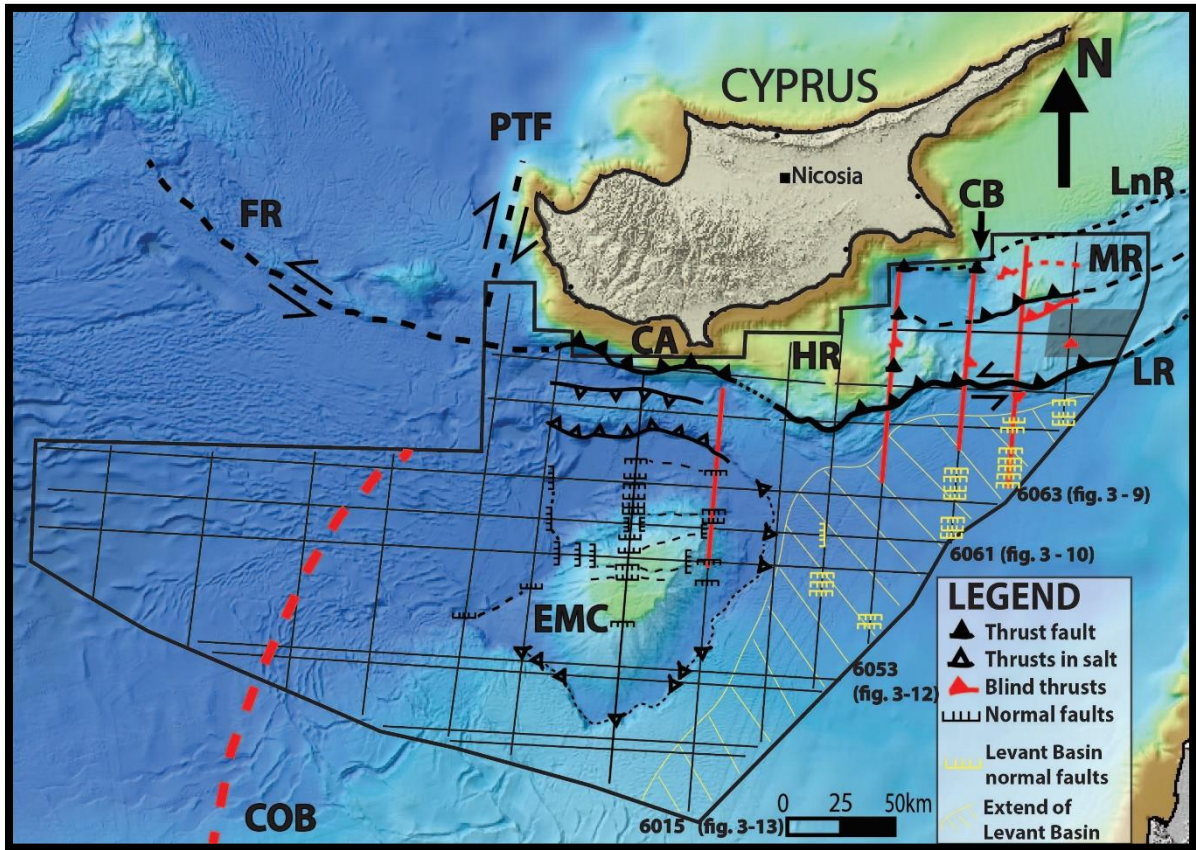


Figure 3 - 6: Map of offshore Cyprus. Main structural elements identified after seismic interpretation. Red dotted line delineates the transition boundary between continental and oceanic crust [Granot, 2016]. Black thin lines delineate the available seismic data, while the red thick lines delineate the seismic profiles illustrated in this paper. Abbreviations: CA=Cyprus Arc, CB=Cyprus Basin, COB=Continent-ocean boundary, EMC=Eratosthenes micro-continent, FR=Florence Rise, HR=Hecataeus Rise, Lnr=Larnaca Ridge, LR=Latakia Ridge, MR=Margat Ridge, PTF=Paphos Transform Fault.

The R1 is a high amplitude horizon which delimits the deepest chaotic seismic package identified on the data from a seismic package with more continuous reflectors. Horizon R2 is a high amplitude continuous horizon which delimits the Upper Jurassic from the overlying Lower Cretaceous seismic unit. The R3 horizon corresponds to a regional unconformity described as the Senonian unconformity and correlates with a major subsidence of the Levant Basin. Horizon R4 represents the Eocene unconformity where low-stand siliciclastic sediments (deposited from the uplift and tilting of the eastern Levant margin), are overlaid by deep marine Oligocene sediments (mixed system of carbonates, shales and marls) which indicate the continuous subsidence of the Levant Basin. Horizon R5 is the lower boundary of the Early Miocene sediments which are characterized as deep water clastic deposits. The R6 horizon, of Mid

Miocene age, is a high amplitude reflector identifiable throughout the Levant Basin [*Gardosh et al.*, 2010; *Hawie et al.*, 2013]. The R7 horizon is considered as the Base Messinian horizon overlain by the evaporitic sequence, mixed with some low stand clastics derived from the Nile Delta. Horizon R8 relates to the inundation of the Mediterranean Sea during Pliocene time and the deposition of hemi-pelagic sediments [*Hawie et al.*, 2013]. Finally, R9 horizon represents the seabed.

The study area can be sub-divided in four different domains, based on the seismic interpretation and the identification of the different horizons and seismic packages (Figure 3 - 8). The first domain relates to the Levant Basin (Figure 3 - 8A) and it is located south-east of Cyprus (Figure 3 - 8, box 8A). The Levant Basin which is floored by a thin attenuated continental crust [*Inati et al.*, 2016], is infilled by a thick sedimentary sequence of ~12-14 km. This deepening of the basin is directly linked with the continuous subsidence of the Levant Basin and the uplift of the eastern passive margin [*Hawie et al.*, 2013].

The second domain is the Cyprus Basin (Figure 3 - 8B) just east of Cyprus (Figure 3 - 8, box 8B). It is proposed that this basin is floored by obducted ophiolites and constitutes the continuation of the Troodos ophiolites towards the East where it connects with the Baer-Bassit ophiolites of Syria [*Calon et al.*, 2005 a, b; *Bowman*, 2011]. The uplifted position of the Cyprus Basin due to the compressional events in the region, played an important role in the infilling of this basin as sediments of approximately 5 km thick were deposited, considerably less compared to the thickness of the Levant Basin sediments. The continuous uplift of this basin is also attested by the thin lenses of Messinian salt or the total absence of the salt in this domain.

The third domain is dominated by the Eratosthenes micro-continent (Figure 3 - 8C), south of Cyprus (Figure 3 - 8, box 8C). This is a carbonate platform constructed by carbonate build-ups of Cretaceous and presumably Miocene age, overlain by a thin Pliocene cover ~100 m. Seismic interpretation of the Eratosthenes micro-continent suggests that the Eocene/Oligocene sediments are either absent or extremely thin. The basement of the Eratosthenes micro-continent is considered to be of thin continental crust [*Welford et al.*, 2015].

The Herodotus basin is the fourth domain (Figure 3 - 8D) situated south-west of Cyprus (Figure 3 - 8, box 8D). It is filled by an estimated 14 km of sediments. Due to the lack of wells and data to tie the horizons, the older horizons are not identified. The thick Pliocene sediments (~2.5 km) and the very thick Messinian salt deposition (~2.5-3.8 km) are an indication of the

continuous subsidence of the basin and the drastic infill from the Nile Delta. The challenges of sub-salt imaging renders it very difficult to identify any deep structures in this area.

### *3.6.2 Tectonic structures and timing of deformation*

A major sub-vertical fault described as the Latakia Ridge is identified on the seismic data and corresponds to a major boundary that separates the deeper Levant Basin to the south from the shallower Cyprus Basin to the north (i.e. the two first domains, presented above). This fault trends NE-SW to E-W and offsets the R8-Base Pliocene, R7-Base Messinian, R6-Base Mid-Miocene, R5-Top Oligocene and R3-Senonian unconformity horizons.

A comparison of the deposition of sediments north and south of the Latakia Ridge and from east to west, is important in order to understand the spatial displacement of this structure. North and South of the Latakia Ridge the thickness differentiation of the deposited sediments is more evident. South of the Latakia Ridge in the Levant Basin (Figure 3 - 9, position A), Mid-Miocene deposits are ~1600-1800 m, the Messinian salt is ~1500 m and the Pliocene sediments are ~500-600 m. North of the Ridge, in the Cyprus Basin (Figure 3 - 9, position B), the Mid-Miocene sediments are ~1300-1500 m, the Messinian salt is ~450 m, while the Pliocene deposits are ~400-500 m, indicative that the sedimentary sequence is thinner in the Cyprus Basin in comparison with the Levant Basin.

This thickness differentiation north and south of the Latakia Ridge provides evidence of the offset nature of the different seismic packages (SP), in particular SP6 (Mid-Miocene ~1400-1600 m in the north compared to ~1600-1800 m in the south) and SP7 (Messinian ~450 m in the north and ~1500 m in the south), an indication of the active thrusting nature of the Ridge from Middle Miocene until Messinian time. The rather constant thickness of the SP8 package north and south of the Latakia Ridge provides difficulties in order to precisely determine the timing of the later deformation. However, it provides evidence of minor vertical movement since Pliocene time in the eastern area (Figure 3 - 9).

Comparing the Latakia Ridge from East to West, more information is collected in order to describe the lateral evolution of the Latakia Ridge. Just north of the Ridge, at the eastern extend of the Cyprus Basin the Mid-Miocene sediments (SP6) are ~1300-1500 m, the Messinian salt (SP7) is ~450 m, while the Pliocene deposits (SP8) are ~400-500 m (Figure 3 - 9, position B). In comparison in the western extend of the Cyprus Basin, deposition of Mid-Miocene

sediments (SP6) ranges from 500-800 m, Messinian salt (SP7) is restricted to ~250 m or it is not deposited and the Pliocene sediments (SP8) are ~300-400 m (Figure 3 - 10, position D, Figure 3 - 11). Deposition of sequences SP6 and SP7 is observed to be thinning towards the west, indicative of the increasing vertical displacement along the Latakia Ridge and towards the west during Mid-Late Miocene time. For the depositions of SP8 in Pliocene time the thickness across the Latakia Ridge is rather constant. In the west (Figure 3 - 12), the SP8 is thicker in the Levant Basin in comparison with the Hecataeus Rise (Figure 3 - 6) situated north of the Latakia Ridge, which reflects an activity of Plio-Pleistocene time. This observation is in agreement with the pronounced bathymetric morphology associated with the Latakia Ridge. Notably the relief observed on profile 6063 (Figure 3 - 9) is smaller than that on profile 6053 (Figure 3 - 12) marked by the Hecataeus Rise. This westward increase of vertical movement along the Latakia Ridge during Pliocene time, is further attested by the deformation in the western domain of the Eratosthenes micro-continent. In the eastern domains, additional evidence for the active nature of the Ridge during Pliocene time is the transpressive flower structures identified north of the Latakia Ridge (Figure 3 - 9) which offset the SP6 and SP8 sediments.

Numerous extensional faults exist in the Levant Basin, which offset the Miocene and Oligocene sediments (Figure 3 - 9, position A). The offset of these normal faults is estimated to range between 150-450 m. The majority of the faults are dipping towards the South while occasionally normal faults dipping to the north are observed. In positions where antithetic faults are observed small horst structures are identified. The direction of the faults is E-W, although it's not well constrained from one profile to another, due to the sparse 2D seismic data available (distance between lines ~20-30 km apart). These south dipping normal faults identified in the Levant Basin portray a deformation of Middle to Late Miocene age as they offset Oligocene - Miocene sediments and are confined in the R4 Eocene unconformity horizon at the base and the R7 Base Messinian horizon at the upper end.

The Cyprus Basin is an elongated structure that runs from East to West, with the Latakia and Larnaca Ridges constituting its southern and northern borders respectively (Figure 3 - 4). It is filled with sediments of Pre-Tertiary time (age undefined), SP5-Early Miocene, SP6-Middle/Late Miocene, SP7-Messinian and SP8-Pliocene/Pleistocene age. A regional unconformity marked by the R8 reflector is followed along all profiles and indicates a discontinuity in the deformation process. Folds in the Miocene units are sealed by the Pliocene package, indicating temporary interruption of the shortening. The convergence between the African and Eurasian plates, results in the division of the Cyprus Basin into two smaller basins from the prominent Margat Ridge that trends almost E-W (Figure 3 - 9, position C). This

structure is active during or in late Early Miocene time, as evidenced by the thickness variations of SP5 in seismic profile 6063 (Figure 3 - 9, position C), where SP5 north of the Margat Ridge is thinner in contrast to the south of the Ridge.

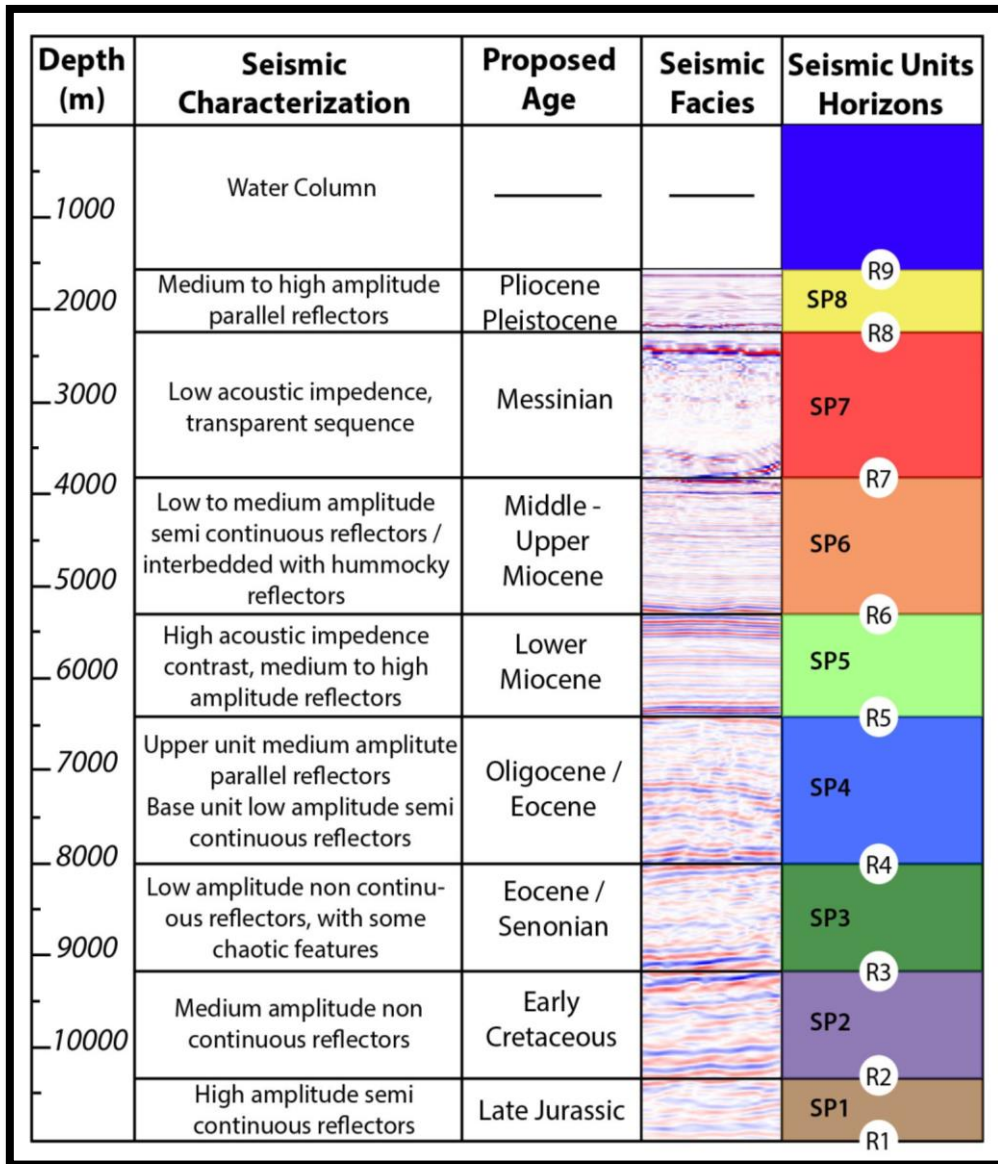


Figure 3 - 7: Chrono-stratigraphic chart depicting the horizons identified during seismic interpretation with the proposed ages, seismic facies and thicknesses.

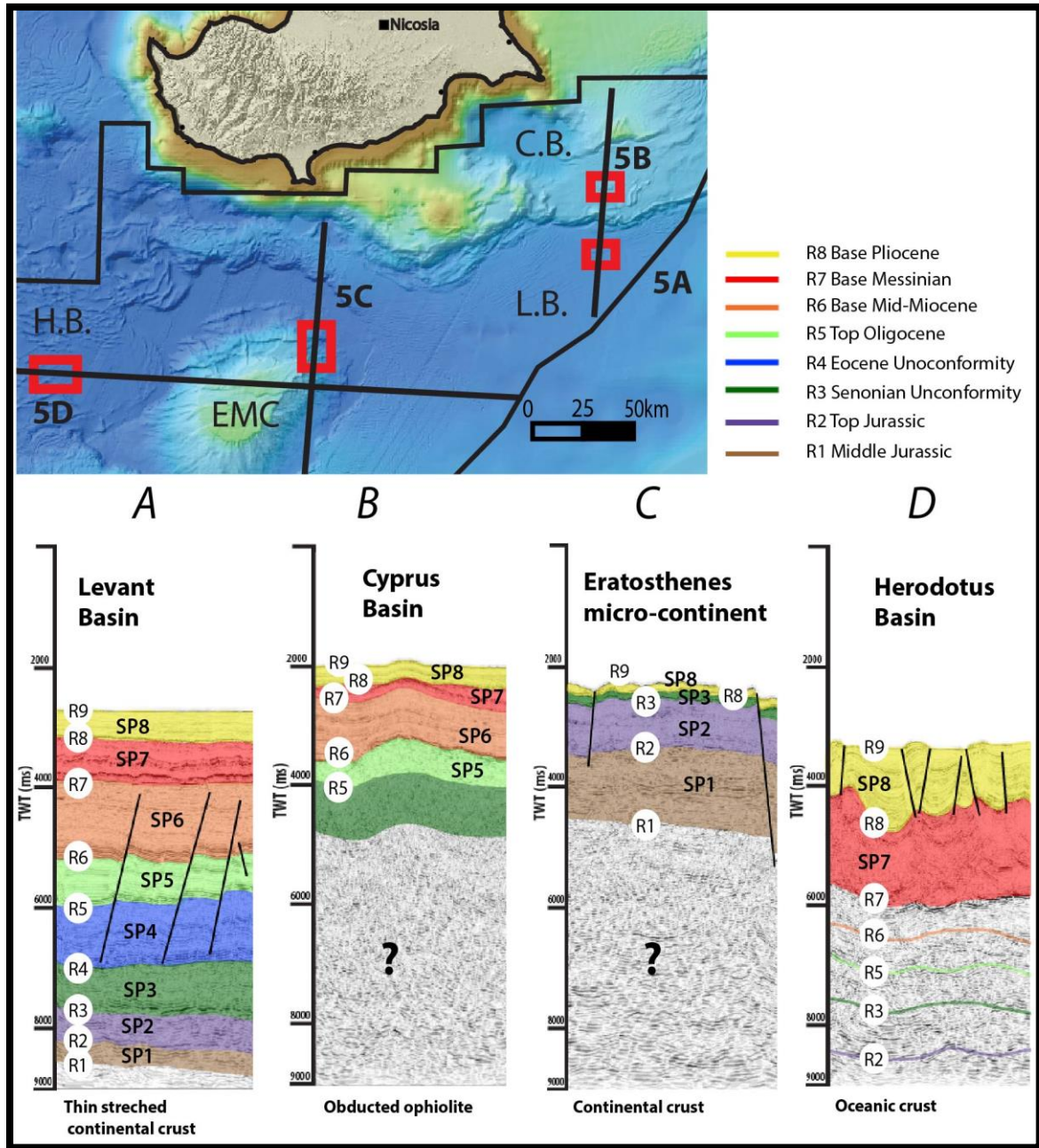


Figure 3 - 8: Stratigraphic columns illustrating the sedimentary filling of the four different domains, which are examined. Red boxes indicate the location of each column. Sequences as described in Figure 3 - 7. A) Levant Basin domain: Thick sedimentary infill above a thin stretched continental crust, B) Cyprus Basin domain: Thin sedimentary sequence, lacking in deposition of several seismic packages, perceived to be floored by obducted ophiolite, C) Eratosthenes micro-continent domain: carbonate platform of Mesozoic age covered by Pliocene sediments, believed to be floored by continental crust, D) Herodotus Basin domain: Infilled by a very thick layer of Pliocene and Messinian deposits and floored by an oceanic crust. Abbreviations: L.B.= Levant Basin, C.B.=Cyprus Basin, E.S.=Eratosthenes micro-continent, H.B.=Herodotus Basin.

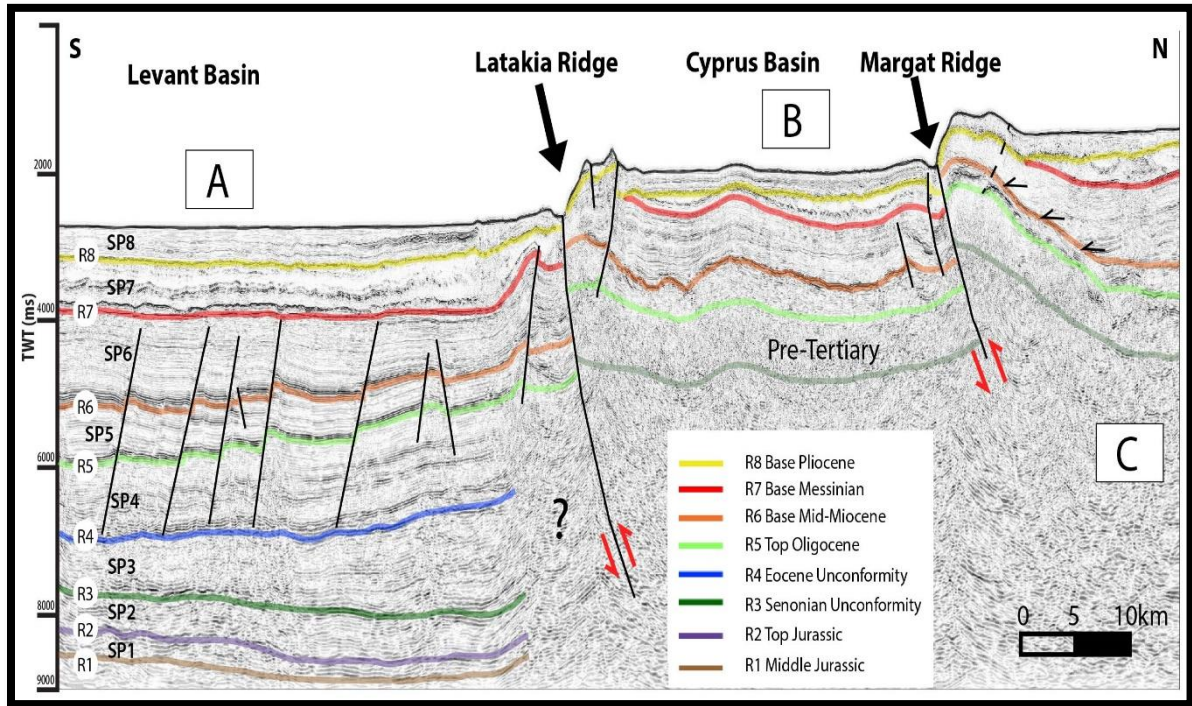


Figure 3 - 9: Seismic line 6063 trending South-North. Letters in squares are used to refer to a specific zone in the text. Position of this profile found in Figure 3 - 6. Position A: Normal faults offsetting the Early to Middle Miocene sediments, commencing at the Eocene Unconformity horizon (R4) and dying out at the base of the Messinian horizon (R7). Position B: Structurally higher position of the Cyprus Basin, infilled by a thin sedimentary sequence in comparison with the Levant Basin. Change in thickness of the Messinian salt between the Levant and Cyprus Basins implies the active nature of the Latakia Ridge. Position C: Small basin of Middle Miocene age as the Early Miocene sediments are inclined towards the north with the Mid Miocene sediments onlapping on the slope of the basin. A3 size Interpreted and un-interpreted profiles in Appendix.

In Mid Miocene, thickness variations are observed at the northern side of the Margat Ridge (Figure 3 - 9, position C) where the Middle Miocene sediments are onlapping on northerly dipping Early Miocene deposits. The thicker SP6 sequence south of the Ridge compared with the thinner SP6 deposition north of the Ridge (Figure 3 - 9, position C), indicate the thrusting activity of the Margat Ridge during Middle Miocene time. In Late Miocene time the Margat Ridge was active, as it is displayed by the absence of the Messinian salt on the anticline north of the Margat Ridge (Figure 3 - 9, position C), while a salt body was deposited in the depression further north, which is directly linked with this thrusting activity. In line 6061 (Figure 3 - 10, position D) the piggy back basins express the active nature of the Ridge as the Mid-Miocene strata are folded and the Messinian salt is not deposited.

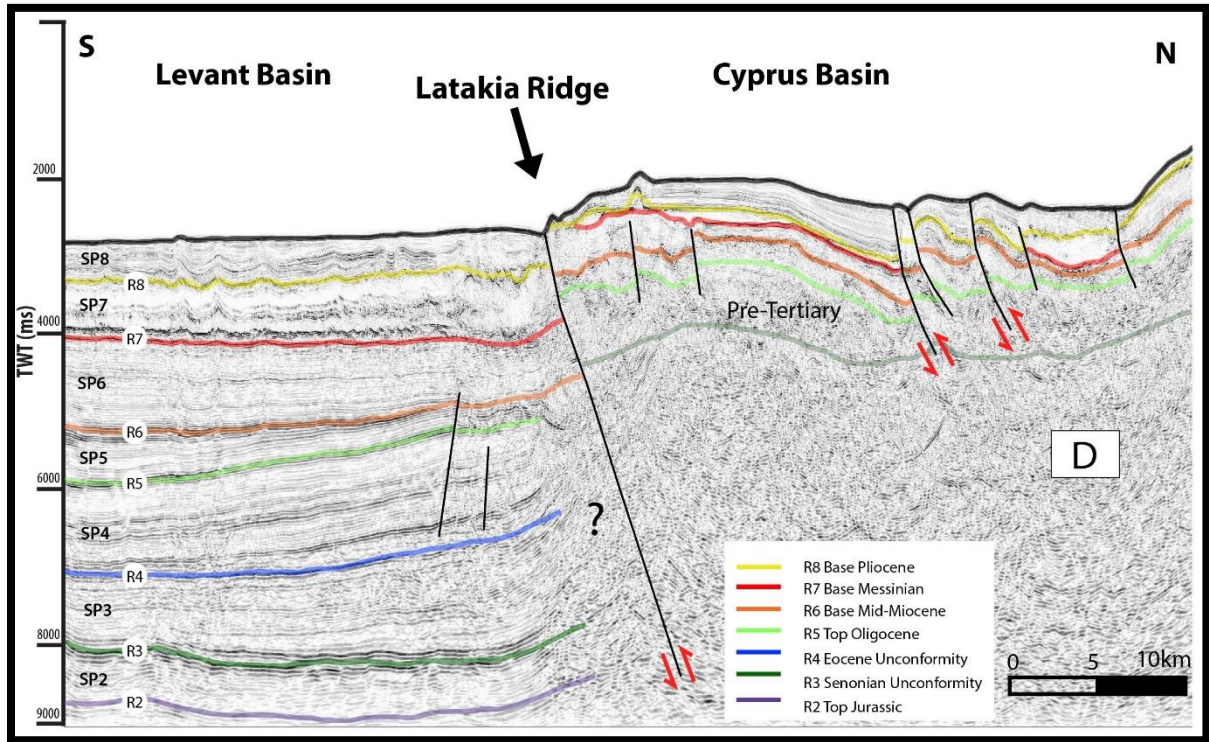


Figure 3 - 10: Seismic line 6061 trending South-North. The Letter in square is used to refer to a specific zone in the text. Position of this profile found in Figure 3 - 6. Position D: Piggy back basins created due to continuous convergence of the African plate with respect to the Eurasian plate. A3 size Interpreted and un-interpreted profiles in Appendix.

Towards the west in-line 6053 (Figure 3 - 12), no substantial thickness differentiation of SP5 and SP6 is observed north and south of the Margat Ridge, which illustrates its limited or non-existent activity during Early to Middle Miocene time at this locality. The difference in depositional thickness of SP7 north and south of the Ridge points towards the renewed vertical movement along the Margat Ridge in Messinian time. Deformation during Pliocene to Recent time is identified through the seabed elevation. The higher bathymetric relief in the east (Figure 3 - 9, position C) compared to the west (Figure 3 - 11) may indicate that seismic line 6053 profile cuts the western tip of the Margat Ridge. Another feature illustrating Pliocene activity is the perceived transpressive flower structure observed north of the Margat Ridge (Figure 3 - 9, position B) offsetting SP6 and SP8 packages.

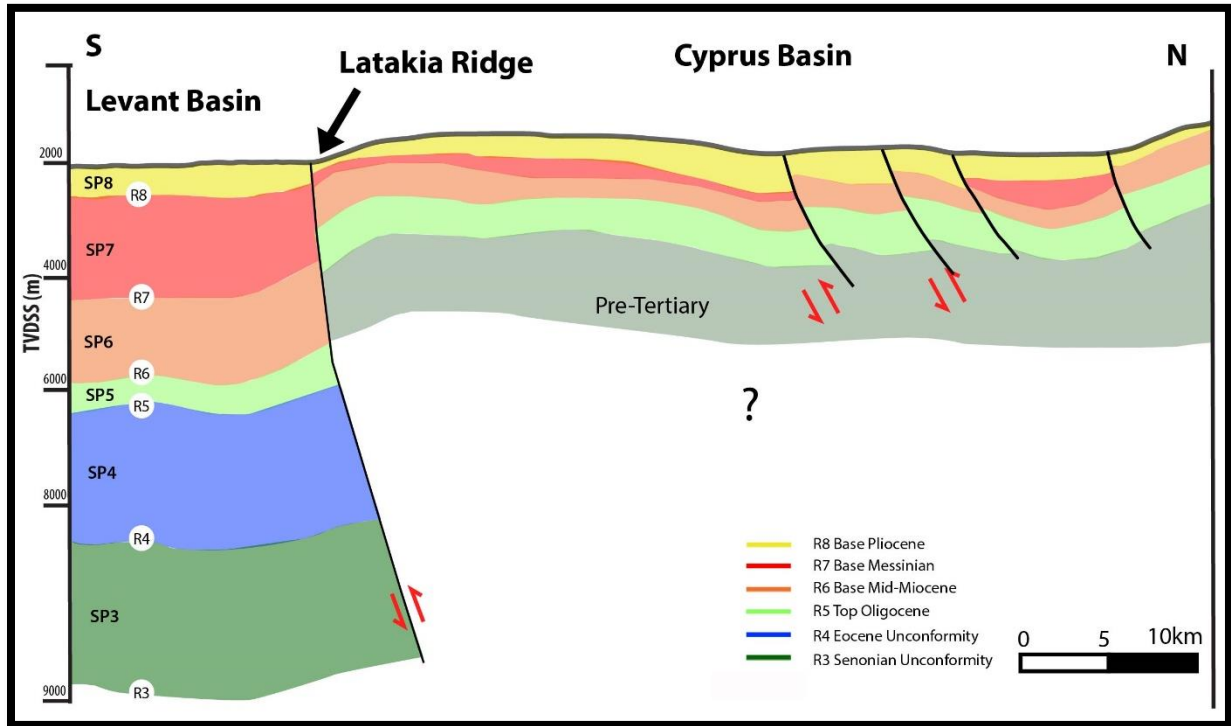


Figure 3 - 11: Schematic illustration of depth converted seismic reflectors, illustrating the depth converted packages as they were obtained by using the Dix formula and the stacked velocities.

Although the Larnaca Ridge is observed only on a few of the available seismic lines for this study, evidence of its activity is observed from structures south of its position. A good example is seismic profile 6063 (Figure 3 - 9, position C) where the progressively thickening sequence of the Middle Miocene sediments towards the north is connected with the thrusting activity of the Larnaca Ridge at this time.

During Late Miocene time it is difficult to identify whether the Larnaca Ridge was active, as the Messinian salt deposition (Figure 3 - 9, position C) is of constant thickness and its continuation towards the north is not observed. In contrast the active nature of the Larnaca Ridge during the Pliocene is illustrated in profile 6053 (Figure 3 - 12), where the seabed elevation changes abruptly in Pliocene time and a big flexural basin (fig. 9, position F) is created in filled by Plio-Pleistocene sediments of ~1500 m. Detailed analysis of the flexural basin (Figure 3 - 12, inset image) illustrates the thrusting activity of the Larnaca Ridge in Pliocene time, as it is evident from the thinning Pliocene sediments towards the south and the

onlaps depicted by the black arrows. These observations illustrate the syn-sedimentary thrusting activity of the Larnaca Ridge in Plio-Pleistocene time.

Further west in the Eratosthenes domain, thrusts and flexural basins are identified south and south-east of the Cyprus Island (Figure 3 - 13). On the northern dipping flank of the Eratosthenes micro-continent a flexural basin (Figure 3 - 13, position G), is observed in filled by Pliocene-Pleistocene sediments (~1300 m) which are onlapping on the Cretaceous carbonate deposits. This flexural basin is a result of the thrusting of the Cyprus Arc (the arc is not observed on this profile, for position refer to inset image of Figure 3 - 14) due to the ongoing northward movement of the African plate and the collision of Eratosthenes micro-continent with Cyprus. The south verging thrust fault (Figure 3 - 13, position G) with a decollement level in the Messinian salt, is indicative of shortening and could be the latest collision front between Eratosthenes micro-continent and Cyprus. The geometry of this thrust as it is observed on the seismic profile, is connected with a pull-up effect due to the thick salt layer at this position and the big difference in velocities between the salt deposition of SP7 and the clastics of SP8.

On the bathymetry map the geometry is indicative of salt advancement and salt flow, evidenced by the southward verging lobes (Figure 3 - 6) (e.g. Sigsbee escarpment, [*Hudec and Jackson, 2009*]). The salt is perceived as allochthonous as it rests on top of Pliocene sediments [*Reiche et al., 2015*]. Similarly the normal fault just below the salt which is illustrated with the dashed line in Figure 3 - 13, could be an inherited structure or it could be related to a pull-up effect as explained above.

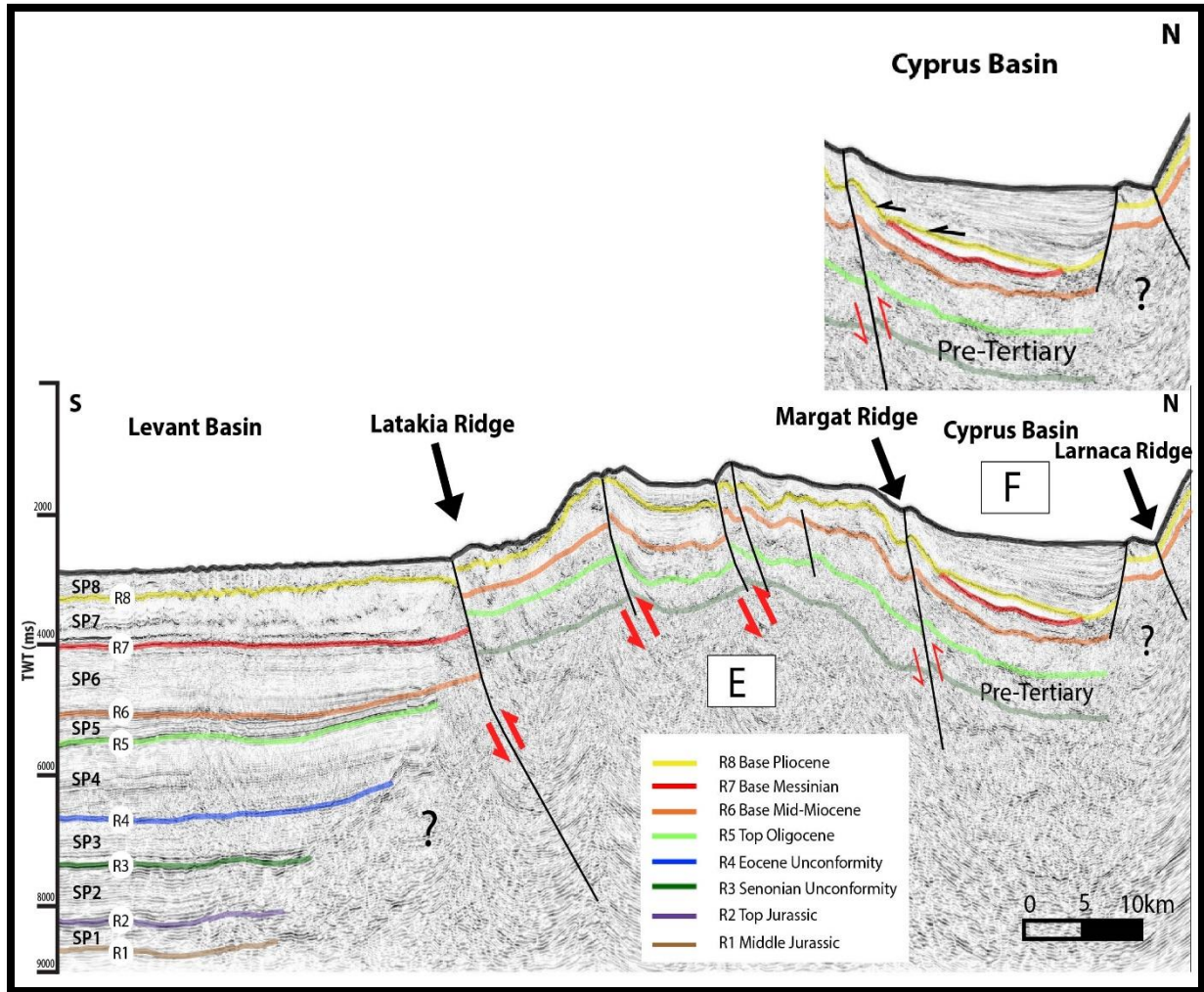


Figure 3 - 12: Seismic line 6053 trending South-North. The Letter in square is used to refer to a specific zone in the text. Position of this profile found in Figure 3 - 6. Position E: Thinning of the sedimentary sequence as we move towards the west, in comparison with the Middle Miocene depositions of profile 6063. Position F: Flexural basin created from the uplift of the Larnaca Ridge north of this seismic profile (as identified by Calon et al., [2005]). Inset is a zoomed image of the Cyprus Basin, illustrating thinning of the Pliocene sediments towards the south and onlaps on the Messinian and Miocene sediments. A3 size Interpreted and un-interpreted profiles in Appendix.

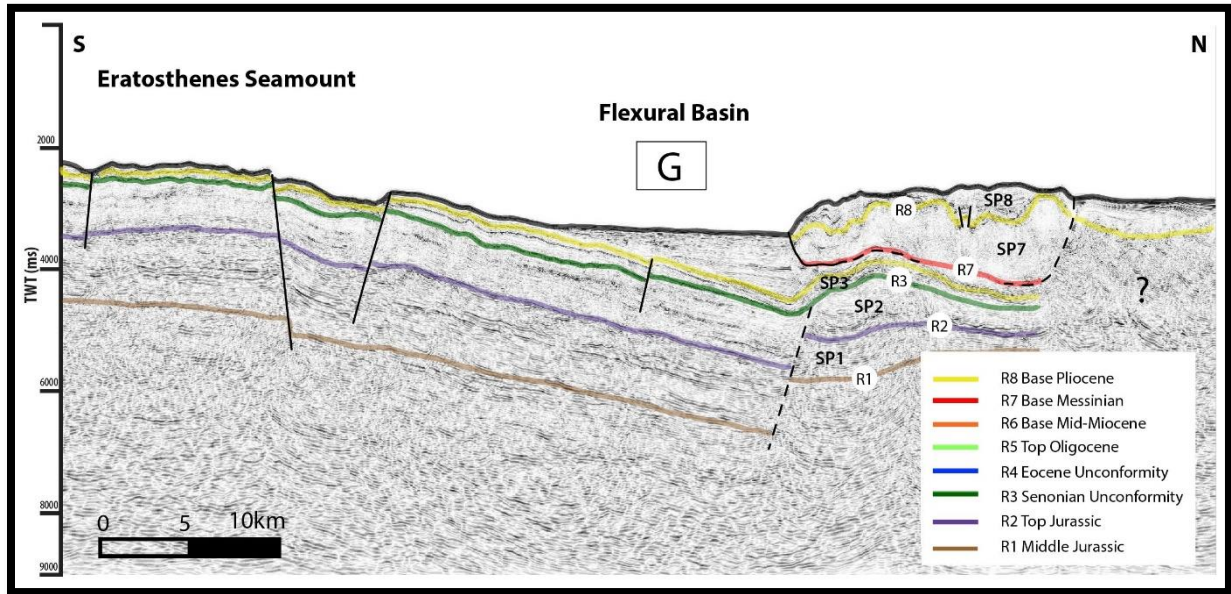


Figure 3 - 13: Seismic line 6015 trending South-North. The Letter in square is used to refer to a specific zone in the text. Position of this profile found in Figure 3 - 6. Position G: Flexural basin created from the convergence of Eratosthenes micro-continent with Cyprus and infilled by Plio-Pleistocene sediments. A thin skinned thrust with a decollement level north of the basin portrays the shortening. A3 size Interpreted and un-interpreted profiles in Appendix.

A schematic illustration of depth converted seismic profiles is proposed (Figure 3 - 14) that portrays the elimination of the pull-up effect due to the big velocity contrast discussed above. By applying the standard Dix formula, a time to depth conversion model was built for each seismic horizon, by utilizing the stack velocities provided by PGS for every 2D seismic profile. It is believed that the SP3 package (Figure 3 - 13) will not bend so steeply upwards but will rather have a similar continuation as observed on the slope of Eratosthenes micro-continent. By accepting this scenario, the geometry of the fault becomes flat, with a decollement level in the salt, which could probably extend and connect at depth with the Cyprus Arc (Figure 3 - 6, Figure 3 - 13).

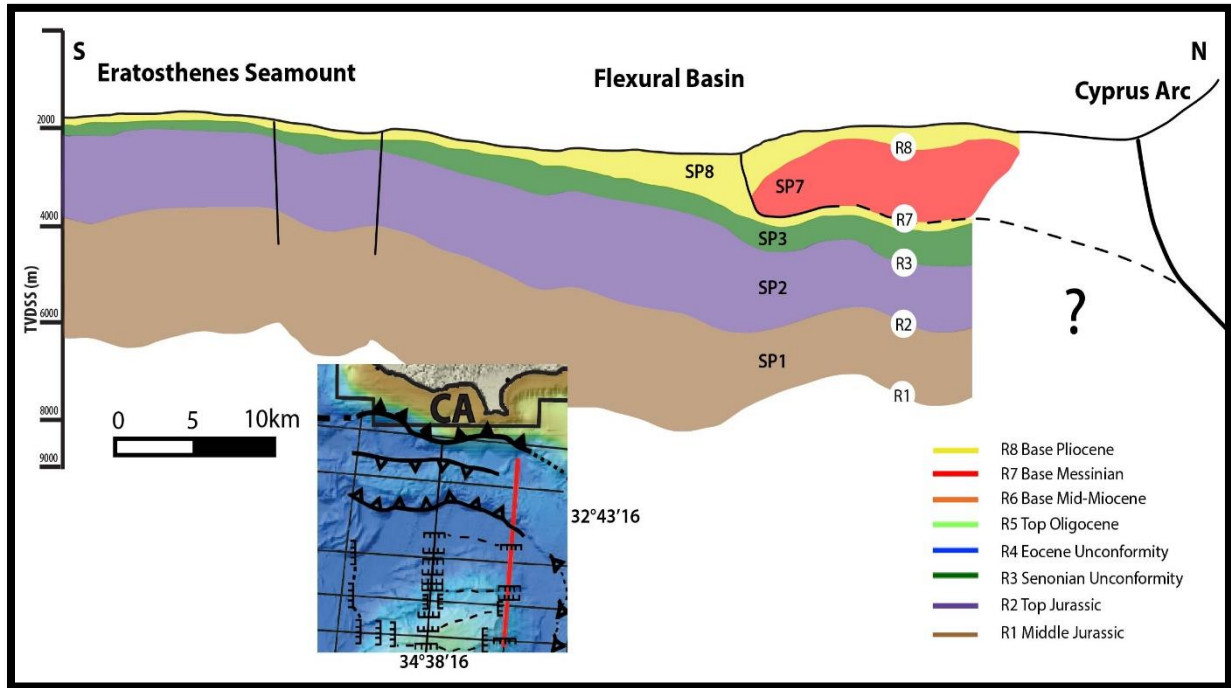


Figure 3 - 14: Schematic illustration of depth converted seismic reflectors that eliminates the large velocity contrast between SP8 (clastics) and SP7 (salt) which results in a pull-up effect as observed in Figure 3 - 13. SP3 is not steeply bending upwards and thus a thrust fault is illustrated with a decollement level in the salt. The continuation towards the north is complex due to the limited and poor imaging. The seismic profile does not cross the Cyprus Arc, although the thrust fault (dashed line) is expected to connect with the Cyprus Arc. In-set bathymetry map with the location of the seismic profile displayed in red.

Several normal faults are identified on the crest of the Eratosthenes micro-continent (Figure 3 - 13). The main direction of these faults is E-W to WNW-ESE and they offset Cretaceous and Pliocene sediments. The normal faults observed on the crest and northern flank of the Eratosthenes are of Pliocene age as they offset almost the whole sedimentary sequence. This feature could be associated with the flexure of the Eratosthenes micro-continent and the releasing of stress, due to the shortening that prevails in front of Eratosthenes as it collides with Cyprus.

### 3.7 Discussion

A variety of tectonic structures were identified and mapped offshore Cyprus. The main deformation mechanisms are related with thrust faults and later transpressive structures. As a result of the compressional regime flexural basins of various sizes are created. Other notable

features are the array of normal faults described in the Levant Basin and on the Eratosthenes micro-continent. Fault activity is evident at least since Early Miocene time and extends until the Present time, expressed through the continuous deformation identified along the Cyprus Arc system. The observed structures occur within a mosaic of juxtaposed domains, with each domain characterized by a distinctive crustal nature. Passing from East to West, these domains are: (1) the Levant Basin domain which is comprised by a thick sedimentary sequence of ~12 km and floored by a thin attenuated continental crust, (2) the Cyprus Basin domain infilled by a thin sequence of ~5 km of sediments (Pre-Tertiary and Neogene age) and presumably underlain by obducted ophiolites, (3) the Eratosthenes micro-continent domain which constitutes a carbonate platform (~4 km) on top of a continental crust and (4) the Herodotus Basin domain floored by an oceanic crust covered by a thick sedimentary sequence of ~14 km (Figure 3 - 4). Observations from the interpreted 2D seismic profiles, indicate that fault activity was more or less intense since Early Miocene. Based on these results and by integrating data from previous onshore and offshore studies, a two stage model of the deformation along the Cyprus Arc system from Neogene until Present time is proposed (Figure 3 - 15). This model takes into account the basic information observed from the seismic interpretation and illustrates the longitudinal change in deformation style along the Cyprus Arc system from East to West and through time.

### 3.7.1 Miocene

Deformation during Miocene is dominated by a compressive regime which is expressed through a number of thrust faults. This thrusting activity results in the development of flexural basins and controls the geometry of the deposited sediments by shifting the positions of depocenters. Structures identified on the seismic profiles, such as the Latakia and Margat Ridges, illustrate a thrusting displacement at least since Mid-Miocene and time until Late Miocene as it is observed from the thickness variation of the sediments, north and south of these structures (Figure 3 - 15A, B, C).

Observations in this paper with regards to the deformation of the structures are in agreement with previous seismic reflection studies. *Hall et al.*, [2005b] place the timing of uplift of the Latakia Ridge from Mid-Miocene to Late Miocene time as SP6 and SP7 are thickening towards the NNW. Similarly, *Bowman* [2011] connects the uplift of the Latakia Ridge with the deposition of a thinner sequence of SP6 and SP7 in the Cyprus Basin in comparison to the Levant Basin.

In order to counter data coverage limitations north of the Cyprus Basin, existing studies were taken in account. *Calon et al.*, [2005b] identified that the Larnaca Ridge is uplifted in Middle to Late Miocene time as the sediments are thick towards the north (away from the Ridge) but thin rapidly towards the Ridge. Mid-Miocene thrusting activity is also identified onshore in the Mesaoria Basin [*Cleintuar et al.*, 1977; *Harrison et al.*, 2008] as the Ovgos Fault zone is thrusting the deeper Kythrea Formation flysch next to the shallower pelagic marls and chalks of the Pakhna Formation [*Cleintuar et al.*, 1977].

A new model is proposed regarding the thrusting activity of the structures and the propagation of deformation (Figure 3 - 15A, B, C). A moderate activity is described for the Margat Ridge commencing in Early Miocene time (Figure 3 - 15A). Although concrete evidence is missing from the available data for this study, moderate activity on the Larnaca Ridge is proposed in Early Miocene time. A good indication of Early Miocene activity of the Larnaca Ridge are the Oligo-Miocene highs identified onshore at the Cape Greco locality (eastern extend of Cyprus), which correspond to carbonate build-ups of the Terra Formation [*Cleintuar et al.*, 1977]. The prominent activity of the Margat Ridge is evident in Mid-Miocene time with the onlapping Mid-Miocene sediments on the inclined Early Miocene sediments, while the southward Latakia Ridge is less active during this time (Figure 3 - 15B). Late Miocene activity on both structures is roughly equivalent, (Figure 3 - 15C). All together these data indicate that thrusting activity migrates southwards through time, thus following an in sequence development of the structures and a forward propagation of the deformation. The eventual end of this compressional event in Pliocene time resulted in a regional unconformity.

Continuous Neogene deformation along the Cyprus Arc system as it is described in this study, commences in Early Miocene time with an acme in Late Miocene time can be correlated with the convergent regime between the Afro-Arabian and Eurasian plates. To the east, shortening in Syria is evidenced by the second phase of Syrian Arc folding which initiated in Early Miocene time in response to plate collision [*Brew et al.*, 2001; *Al Abdala et al.*, 2010]. In comparison to this prominent tectonic event in Syria, observations in this study indicate that deformation is limited in the west and more precisely on the Margat and Larnaca Ridges, while onshore Cyprus local uplift is suggested during the same time interval [*Cleintuar et al.*, 1977]. In conjunction with previous observations and evidence illustrated in this study, it is herein proposed that the westward attenuation of the deformation from Syria to Cyprus, is related with the diversification of the crustal nature as in the vicinity of the Levant Basin continental crust and thin attenuated continental crust interact.

Despite the prominent compressional regime dictating the deformation style since the Late Cretaceous, normal faults of Oligo-Miocene age are identified in the Levant Basin. A clear deformation mechanism to connect the compressional regime and the normal faults is difficult to envisage. *Ghalayini et al.*, [2014; 2016] identified these NW-SE trending normal faults offshore Lebanon, suggesting that the faults are of non-tectonic origin and are connected with the sedimentary nature of the Miocene deposits.

These normal faults are also identified on the seismic profiles (Figure 3 - 9A) that cover the Levant Basin offshore Cyprus (Figure 3 - 6). In this study, data limitations lead to a cautious approach as to the origin of these structures. Either the normal faults originate from non-tectonic processes aided by the clay content in the host units, similar to what *Ghalayini et al.*, [2014; 2016] proposed in Lebanon, or they are connected with the flexure of the upper crust and the creation of the normal faults in the sedimentary infill, in response to the continuous convergence of the African and Eurasian plates. These normal faults extend up to the Late Miocene deposition of a thick layer of salt (~ 1.5-2 km) in the Levant Basin, which acts as the upper boundary that constrains the deformation in the Miocene deposits. The root of the normal faults terminates on the Eocene unconformity (horizon R4) and this could be related with the deposition of siliciclastic sediments that act as a barrier to the propagation of the deformation in older sediments. A solution for the origin of the normal faults could be attained through the interpretation of additional 2D and 3D data. This could provide the detailed direction of these structures, thus enabling the correlation of the faults with the prevailing tectonic regime.

### 3.7.2 Pliocene to Recent

Pliocene deformation along the Cyprus Arc evolved within a tectonic regime of thrust faulting and strike slip structures, thus reflecting partitioning of deformation. This tectonic regime is described by a detailed description of transpressive flower structures, back thrusts and more specifically by the comparison of the thickness of the Neogene sediments in the Cyprus Basin as they identified in this study, from observations across the Latakia and Margat Ridges (Figure 3 - 9 and 12D). Interpretations in this study illustrate that the Larnaca Ridge is reactivated by a thrusting mechanism with the creation of a Pliocene flexural basin in the footwall of the thrust (Figure 3 - 12F and Figure 3 - 15D). These conclusions are in accordance with previous studies which recognized positive flower structures along the Latakia and Margat Ridges [*Hall et al.*, 2005b; *Bowman*, 2011] and further enhanced by the comparison of the thickness of the Neogene sediments as identified herein. In contrast the Pliocene sediments

which are thickening northwards away from the Larnaca Ridge [*Calon et al.*, 2005b], correlate well with the thrusting activity and the creation of the flexural basin described in this paper.

By combining the onshore and offshore data from previous publications and this research, it is evidenced herein that during the Pliocene, the tectonic regime at the plate boundary changes into a transpressive regime. This deformation style is connected with the fragmentation of the Eurasian continental plate and the westward expulsion of the Anatolian microplate, which is considered as the driving mechanism of the strike-slip motion. Deformation associated with the new tectonic regime was accommodated by the re-activation of previous structures, such as the steeply vertical Latakia Ridge which is located at a pre-existing zone of weakness which separates different crustal domains (Levant and Cyprus Basins).

As identified by the interpretation of different seismic profiles in this study, the longitudinal evolution of deformation along the Cyprus Arc system changes along strike. In the eastern domain the Latakia Ridge is mainly described by strike slip motion, whereas in the western domain directly south of Cyprus a thrusting regime is evidenced from the creation of a big flexural basin (Figure 3 - 13G and Figure 3 - 15D). This shortening, is connected with the collision of the Eratosthenes micro-continent with Cyprus, and it is considered as the most intense phase of uplift on Cyprus [*Harrison et al.*, 2012; *Kinnaird et al.*, 2013]. The intense uplift at that period is also supported inland, by the change in sedimentation, with the deposition of carbonates ceasing (chalks and marls of Pakhna Formation) and the deposition of clastics initiating in Early Pliocene (sandstones and biocalcarenes of Nicosia Formation). The Mesozoic structuration of the Levant Basin which juxtaposed different crustal blocks, is therefore regarded as a major cause for the East-West evolution of the deformation along the plate structures of the Cyprus Arc.

### 3.8 Conclusions

Based on the interpretation of the 24 regional 2D reflection seismic profiles traversing the Cyprus Arc system and the regional structural settings, the following conclusions can be drawn:

1. Mapped tectonic structures with a pronounced bathymetric expression, include thrust faults and strike-slip faults active from Miocene to Present and the creation of flexural basins of the same age. A number of layer bound normal faults were recognized within the Eocene-Miocene package.
2. Generally, shortening dominated during the interpreted Neogene time interval, whereas strain partitioning, with both thrusting and strike-slip movements, characterizes the Plio-Pleistocene deformations as the result of the westward movement of Anatolia.
3. The temporal and longitudinal evolution of the deformation style along the investigated Cyprus Arc system, is a consequence of the composite nature of the Eastern Mediterranean crust and the individualization of the Anatolia microplate.
4. The documented Plio-Pleistocene tectonic structures (positive flower structures in the east and flexural basin in the west) suggest a westward increase of shortening, in relation with the lateral change in nature of the crust, passing from a thinned continental crust in the Levant Basin (eastern domain) to the continental crust that underlays the Eratosthenes micro-continent domain.

Acknowledgement: The first author would like to acknowledge the Ministry of Energy, Commerce, Industry and Tourism of the Republic of Cyprus for funding this project. Petroleum Geo-Services (PGS) is acknowledged for providing the seismic data. A very warm thank you to Jean Letouzey for his insights and the constructive discussions on the geological structures in the Eastern Mediterranean. Dominique Frizon de Lamotte, an associate editor, an anonymous reviewer and Editor John Geissman are thanked for their valuable reviews which aided in improving this manuscript. Data presented in this study could be accessed at <https://www.pgs.com/data-library/europe/mediterranean/> by contacting PGS.

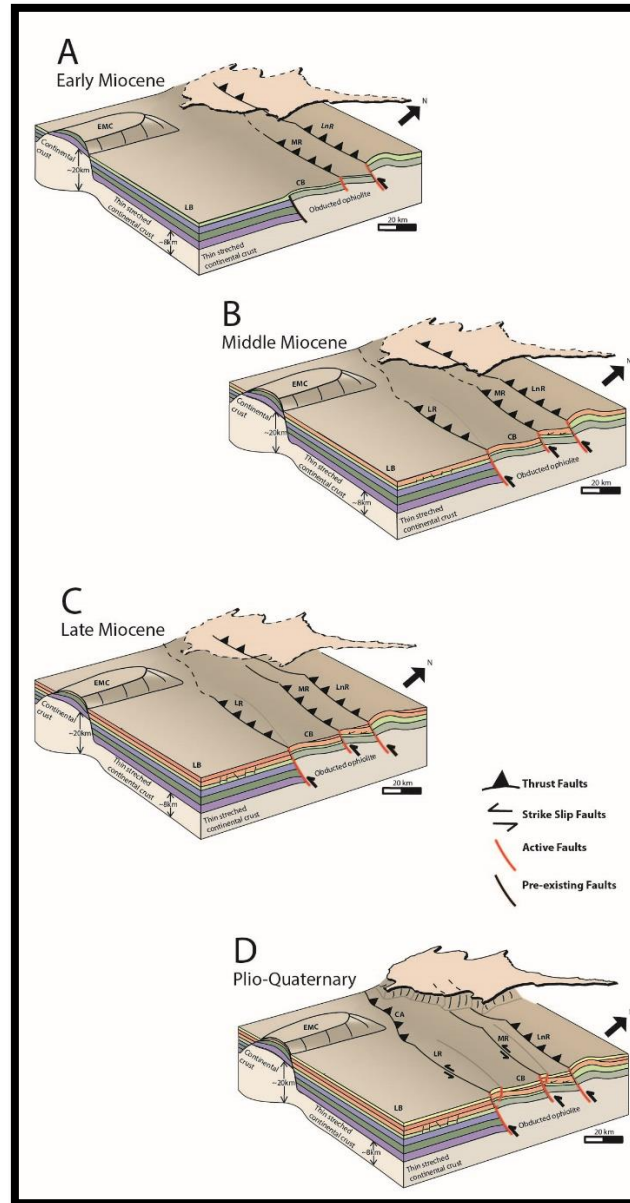


Figure 3 - 15: Tectonostratigraphic evolution offshore Cyprus in accordance with seismic interpretations in this paper and in connection with previous seismic studies from Calon et al., 2005a; Hall et al., 2005; Bowman, 2011; Montadert et al., 2014. A: Oligocene-Early Miocene: The Larnaca and Margat Ridges are active as the Early Miocene sediments are thinning north of the Margat Ridge, while the Latakia Ridge is covered by a thin sequence of Early Miocene sediments. B: Middle Miocene: Latakia and Margat Ridges are active, with Mid Miocene sediments onlapping on the inclined Early Miocene sediments. Normal faults are initiating in the Levant Basin. C: Late Miocene: Continuous activity of the Latakia, Margat and Larnaca Ridges as Messinian salt is deposited into small depressions. Normal faults in the Levant Basin reach full growth restricted between the Eocene unconformity and base Messinian horizons. D: Pliocene-Recent: Active Latakia and Margat Ridges give rise to positive flower structures that indicate a transpressive strike slip nature. Abbreviations as in Figure 3 - 6. Each period is illustrated in A3 size in the Appendix.



**Chapter 4**

**Onshore tectonic structure  
investigations**

A first phase of field work was undertaken in Cyprus from the 22<sup>nd</sup> of March until the 30<sup>th</sup> of April 2015, with a second survey following suite in September 2016. The goal of these field campaigns was to build a conceptual model which depicts the tectonic evolution of Cyprus from Late Cretaceous to Present. For this purpose, three basins were investigated (Figure 4 - 1) and a number of sites were identified onshore Cyprus in order to study the tectonic structures that shape the circum Troodos sedimentary succession which covers most of Cyprus. The sedimentary sequences range from Late Cretaceous to Plio-Pleistocene time.

It is acknowledged herein that the nomenclature for the basins in this study was used as it was described in the studies of Payne and Robertson [1995; 2000] and Kinnaird and Robertson [2012], for simplicity of comparison in the discussion chapter of this thesis. It is further noted that the Limassol Basin is also known as Pakhna Basin and Alassa sub-Basin as it was described by Eaton and Robertson [1993].

Onshore investigations were deemed necessary as they provide a better constrain on the timing of deformation of tectonic structures and the outcropping Cenozoic sediments can be investigated outright. The two field campaigns were conducted in order to observe and record the tectonic structures and the sedimentary contacts in Polis, Polemi and Limassol basins, in order to construct two cross sections in West Cyprus and one cross section in Southern Cyprus (Figure 4 - 1), using field observations and published information. A SW-NE cross-section intersecting the Polis Basin (passing from the coastline (Pegeia village) and reaching the foothill of the Troodos Mountain (Lysos village)) was built from the measurements acquired. A second cross section in a WSW-ENE direction in the same vicinity is proposed, passing from the Akamas peninsula to the foothills of Troodos Mountain (Pelathousa village) in order to incorporate and understand the role of the Troodos pillow lavas and the serpentinites that are outcropping in the Akamas peninsula. The third cross section is at the eastern limit of the Limassol Basin, trending from SW-NE and intersects the Gerasa fold and thrust belt (GTFB) at the village of Armenochori (Figure 4 - 1).

The observations documented during fieldwork provided the necessary structural data and arguments to constrain the age and style of the deformations of major faults that shaped onshore Cyprus. Additional data were gathered from the measurements of meso-scale fault planes that contribute to determine the stress regime driving the related deformations. In total ~245 measurements of fault planes, striations, fractures and beddings were obtained from the survey of the Polis and Limassol Basins. At various localities a number of samples were collected for

dating purposes, which were used to identify the age of the sedimentological units and to delineate the timing of displacement of the main tectonic structures.

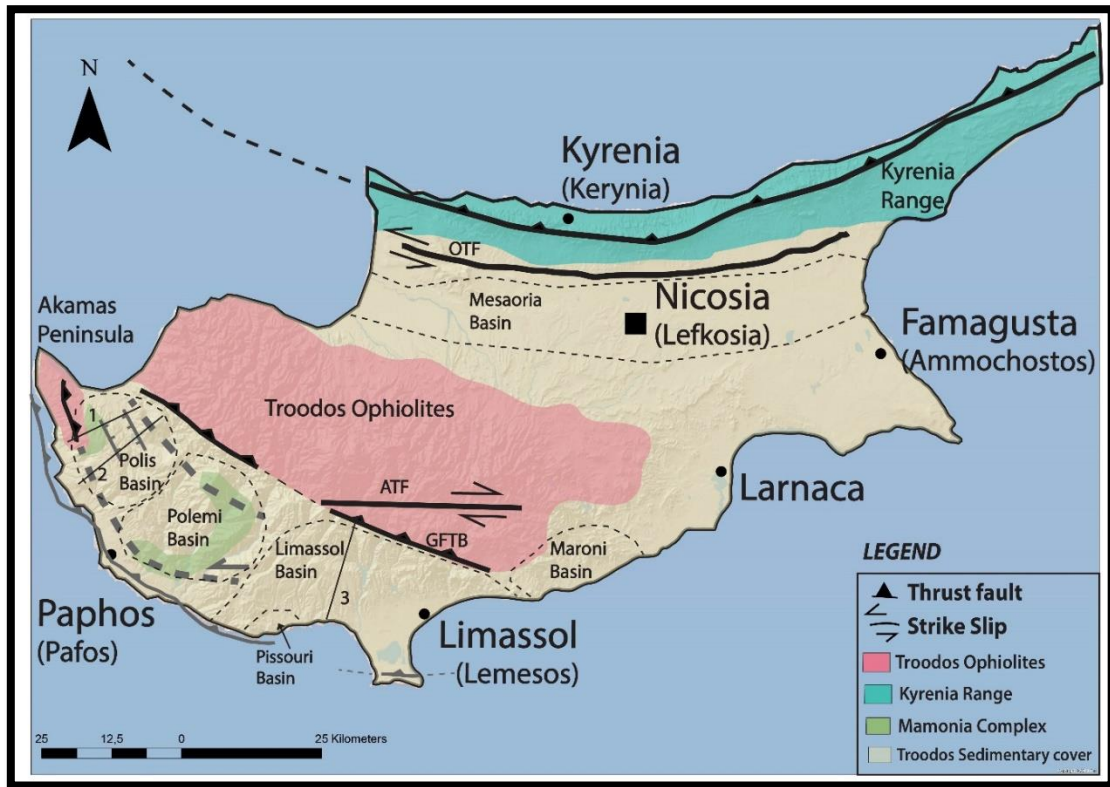


Figure 4 - 1: Geological map of Cyprus illustrating the main structural elements, the geological sedimentary cover of the investigated basins and the locations of the cross sections. Black lines indicate the tectonic structures which are generally accepted, while gray lines indicate structures proposed in different studies [Payne and Robertson, 1995; Bailey et al., 2000; Geoter, 2005]. The investigated basins south of Troodos ophiolites are indicated, Polis, Polemi, Pissouri, Limassol and Maroni/Psematismenos Basins. Abbreviations: 1) Akamas cross section, 2) Polis cross section, 3) Limassol cross section. Abbreviations: ATF: Arakapas Transform Fault; GFTB: Gerasa Fold and Thrust Belt; PTF: Paphos Transform Fault; OTF: Ovgos Transform Fault.

## 4.1 Surface and sub-surface data analysis

### 4.1.1 Borehole data analysis and sedimentary units

Onshore Cyprus, hydrogeological, exploration and geotechnical boreholes are drilled by the Geological Survey Department of Cyprus (GSD) which provide subsurface data based

on borehole chips or boreholes cores. These drillings resulted in borehole data ranging up to 300m that are used here in order to document the basement of the Polis/Polemi Basins and a section of the Limassol Basin (Figure 4 - 2). Out of the provided data (courtesy of GSD), 19 boreholes were chosen and analysed for the purposes of this study (Figure 4 - 3 and Figure 4 - 4).

In the Polis Basin 8 boreholes were utilized in accordance with the locations of the two cross sections that will be described later (Figure 4 - 2). In borehole 1, the first 50 m consist of calcarenite deposits, the underlying unit is made up of ~70m of chalky limestone, which rests on ~100m of grey-marly chalk/whitish chalk which is silicified at places, while the base of the borehole is poorly described. The succession in borehole 2 starts with ~100m of whitish chalky marls, passes downwards into ~100m of grey chalk with silica identified in places, with the last ~20m described as Mamonia clays. In borehole 3 (top of the western flank of the Polis Basin, Figure 4 - 2), the upper ~80m are described as chalks and limestones, rest on ~50m of chalks and cherts, while in deeper part of the borehole ~10m of melange clays was drilled. In borehole number 4 the first ~70m are described as marly chalk which overly ~100m of whitish limestone and ~10m of Mamonia clay. Borehole 5 was drilled in the center of the Polis Basin and the sedimentary succession is comprised of ~25m of yellowish marl, ~75m of grey marly chalk and ~70m of marly chalk with chert. Borehole number 6, also drilled in the center of the Polis Basin, consists of ~50m of calcarenites, ~50m of white chalky marl and ~60m of white to grey chalky marl with cherts bands in some places. Borehole 7 is close to the eastern flank of the Polis Basin and is made up of ~75m of white limestone and greyish marly chalk, which passes deeper to ~30m of white chalks with chert. Drilled in the center of Polis Basin, borehole 8 consists of ~40m of yellowish marl, ~50m of white chalky marl and ~60m of white to grey marly chalk with chert bands.

In the Polemi Basin close to the city of Paphos (Figure 4 - 2, Figure 4 - 4) 7 boreholes were utilized by Geoter [2005] to construct 4 cross sections near the main highway leading to the city. Borehole 9 consists of ~25m of calcarenite and ~20m of white chalk. In borehole 10 ~20m of calcarenite overlie ~30m of white chalk. The succession in borehole 11 consists of ~20m of calcarenite, a 25m thick unit of limestone and chalk and ~100m of chalk and chert. In borehole 12 the first unit consists of ~120m of limestone and chalk which overlay ~40m of chalk and chert. In borehole 13, ~15m of calcarenite and a thick layer of ~170m of chalk and chert was described. The succession in borehole 14 starts with a unit of calcarenite with a thickness of ~110m and passes deeper to a unit of chalk and chert ~90m thick. In borehole 15 three units are described which are from top to bottom, a ~10m thick unit of calcarenite, a ~110m thick unit of chalks and cherts, with the deeper unit consisting of ~20m of pillow lavas.

## Chapter 4: Onshore Investigations

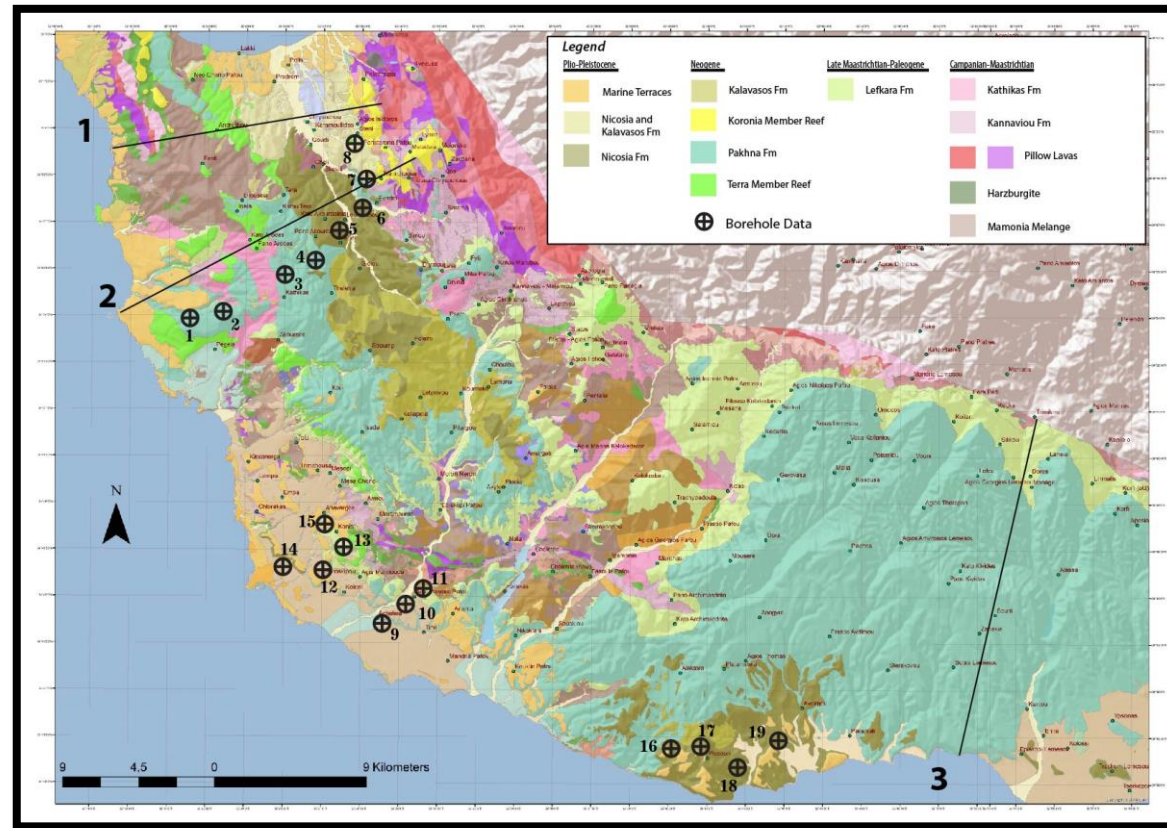


Figure 4 - 2: Geological map of southern and western Cyprus with the available borehole data (courtesy of GSD Cyprus). Black lines represent the locations of the cross sections. Maps are from the GSD database based on previous maps of Lapierre [1971], Turner [1992], Zomeni and Tsiolakis [2008], Zomeni and Georgiadou [2015].

In the south of the Limassol Basin (Figure 4 - 2, Figure 4 - 4), four boreholes were described. Borehole 16 consists of a thick unit of calcarenite of ~140m. In borehole 17 the succession consists of ~40m of calcarenite that overlies ~70m of limestone and chalk. The sequence in borehole 18 starts with a unit of calcarenite of ~65m, which is underlain by ~40m of limestone and chalk. The units in borehole 19 pass from ~10m of calcarenites to ~130m of limestone and chalk.

According to the descriptions from the GSD, field observations during the two surveys and descriptions of the formations from previous studies [Lord et al., 2000], a universal interpretation was applied on the different units of the borehole data. The yellowish marls and the calcarenites are interpreted as Plio-Pleistocene sediments deposited in a shallow restricted marine environment and correspond with the Nicosia Formation. In boreholes where the sediments are described as chalky limestone, whitish chalky marls, chalks and limestones, grey marly chalk, white limestone, greyish marly chalk and white chalky marl, these units are interpreted as Middle Miocene sediments deposited in an open shelf environment and are associated with the Pakhna Formation. Descriptions such as marly chalks, whitish chalk which is silicified at places, grey chalk with silica identified in places, chalks and cherts, whitish limestone and white to grey marly chalks with cherts bands in some places, are interpreted as sediments Paleogene age which are deposited in a basinal setting and correspond with the Lefkara Formation. Units described as Mamonia clays and Melange clays are interpreted as continental margin sediments of Triassic age which are derived from the Mamonia Complex, while units described as pillow lavas refer to Upper Cretaceous deposits of the Troodos ophiolites.

Considering the 30 boreholes studied in the Polis Basin, 8 were chosen in close proximity to the cross sections in order to better constrain the thicknesses and the geometries applied for the creation of the cross sections (Figure 4 - 2). The formations encountered in each well are the Pakhna and Lefkara Formation with the thickness changing with regard to the position of each well. The Nicosia Formation is observed mainly in the center of Polis Basin and in the Pegeia area, while the Mamonia Complex is only described in a few wells and extrapolated for the others.

The Lefkara Formation in the Pegeia area illustrates a change in thickness passing from ~150m (minimum thickness) in well 1, ~80m in well 2 and ~40m in well 3 (Figure 4 - 3). This northward thinning pattern could reflect an uplift of the Kathikas area and subsidence to the east during Oligocene to Early Miocene time. In the center of the Polis Basin, the Lefkara

sediments are ~100m thick in well 4. Unfortunately, boreholes 5 to 8 do not penetrate the base of the Lefkara Formation, so the eventual thickness variation through the Polis Basin cannot be documented. The large thickness variation between boreholes 3 (~40m) and 4 (~100m) could represent the movement of the Kathikas thrust and the subsidence of the center of the Polis area. Throughout the Polis basin, the thickness of the chalks and marls of the Pakhna Formation does not vary as it records ~70-100m (boreholes 4-5-6, Figure 4 - 3). This probably indicates that no major tectonic structures were active during Middle Miocene time. In the Pegeia area, the calcarenites and sandstones unit of the Nicosia Formation is ~50m while no equivalent deposition was described in boreholes 2 and 3 (Figure 4 - 3). This indicates the uplifted location of boreholes 2 and 3 during the Pliocene time. Accordingly, in the center of the basin wells 4 and 7 at both flank of the Polis Basin are lacking the Nicosia Formation which illustrates that either a thin layer was deposited and then eroded or it was never deposited due to the high position of the flanks. In the center of the Polis Basin, a thin layer of ~30-50m was deposited as identified from wells 5 and 6. The absence of the Nicosia Formation in boreholes 2, 3, 4 coincides with the eastern flank of the Polis Basin which was probably a high during the Plio-Pleistocene time, as is borehole 7 which corresponds to the western flank of the basin.

In the Polemi Basin, Geoter [2005] used approximately 40 boreholes to construct four cross sections, out of which 7 characteristic boreholes are presented here. The Lefkara Formation in boreholes 9 and 10 was not drilled whereas in borehole 11 the thickness of the unit is ~90m. Boreholes 12, 13, 14 and 15 illustrate a northward thickening of the Lefkara Formation, thus further enhancing the idea of a thrust fault, which was probably active in Oligocene to Early Miocene time. The Pakhna Formation is identified in boreholes 9, 10 and 11 (ranging from ~25-30m) and ~110m thick in borehole 12, however it is missing in boreholes 13, 14 and 15 where the Nicosia Formation is directly overlying the Lefkara Formation. This indicates a local uplift during Middle to Late Miocene time which could be related to the Paphos thrust fault proposed by Geoter [2005]. In boreholes 9, 10, 11 the thickness of the Nicosia Formation ranges from ~20m to ~30m. The sedimentary succession in boreholes 12, 13, 14 and 15 varies significantly, with the thickness of the Nicosia Formation firstly increasing passing from borehole 13 (~20m) to 14 (~100m) and then decreasing towards the north in borehole 15 (~20m). The large thickness in well 14 compared with the reduced thicknesses recorded in the other boreholes (12, 13, 15) shows an increase in subsidence towards the south during the Plio-Pleistocene time [Geoter, 2005].

## Chapter 4: Onshore Investigations

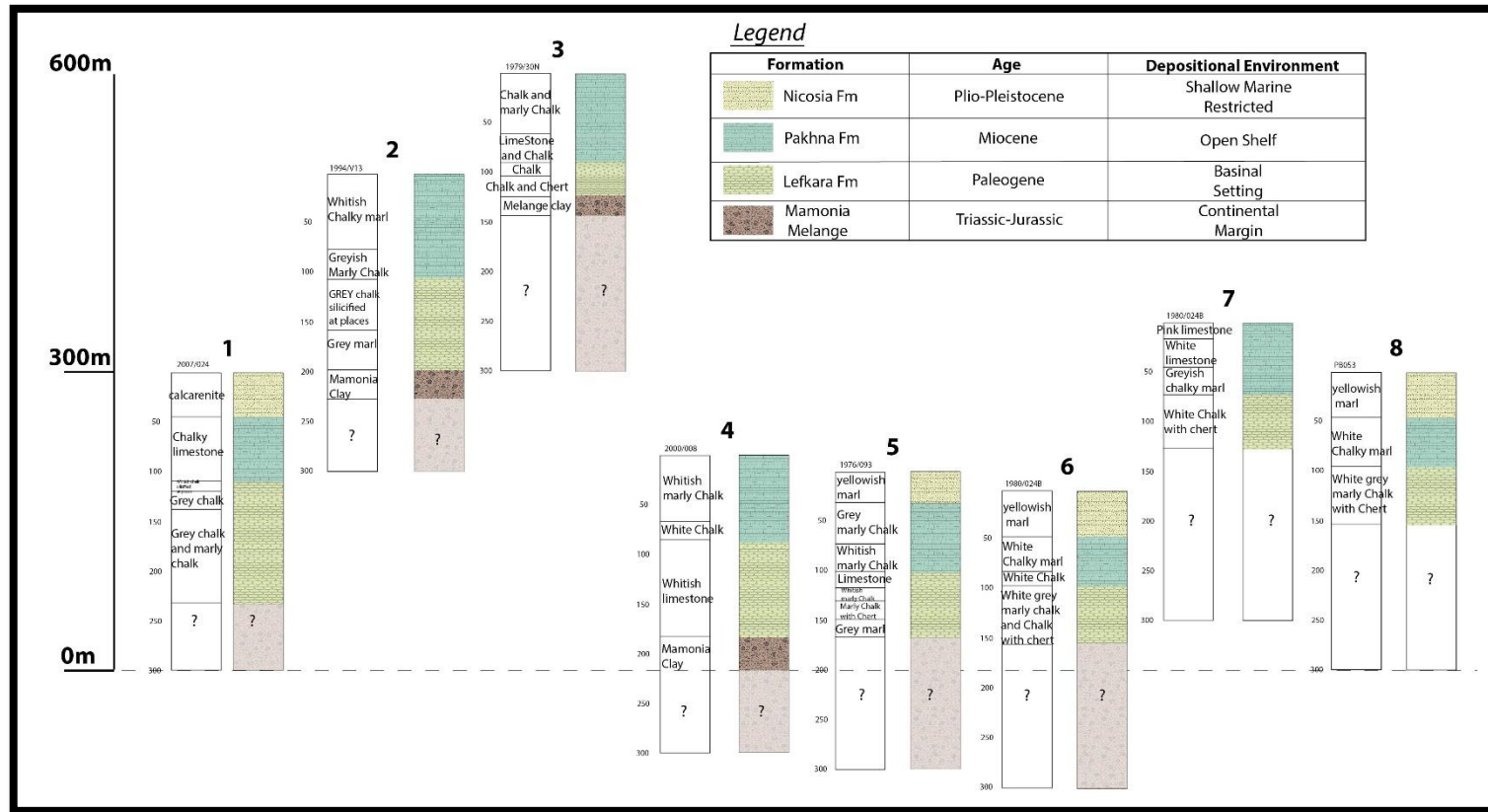


Figure 4 - 3: Borehole data in the Polis Basin courtesy of the Geological Survey Department of Cyprus (locations in Figure 4 - 2). The description of each borehole is presented along with the corresponding formation and age as interpreted herein.

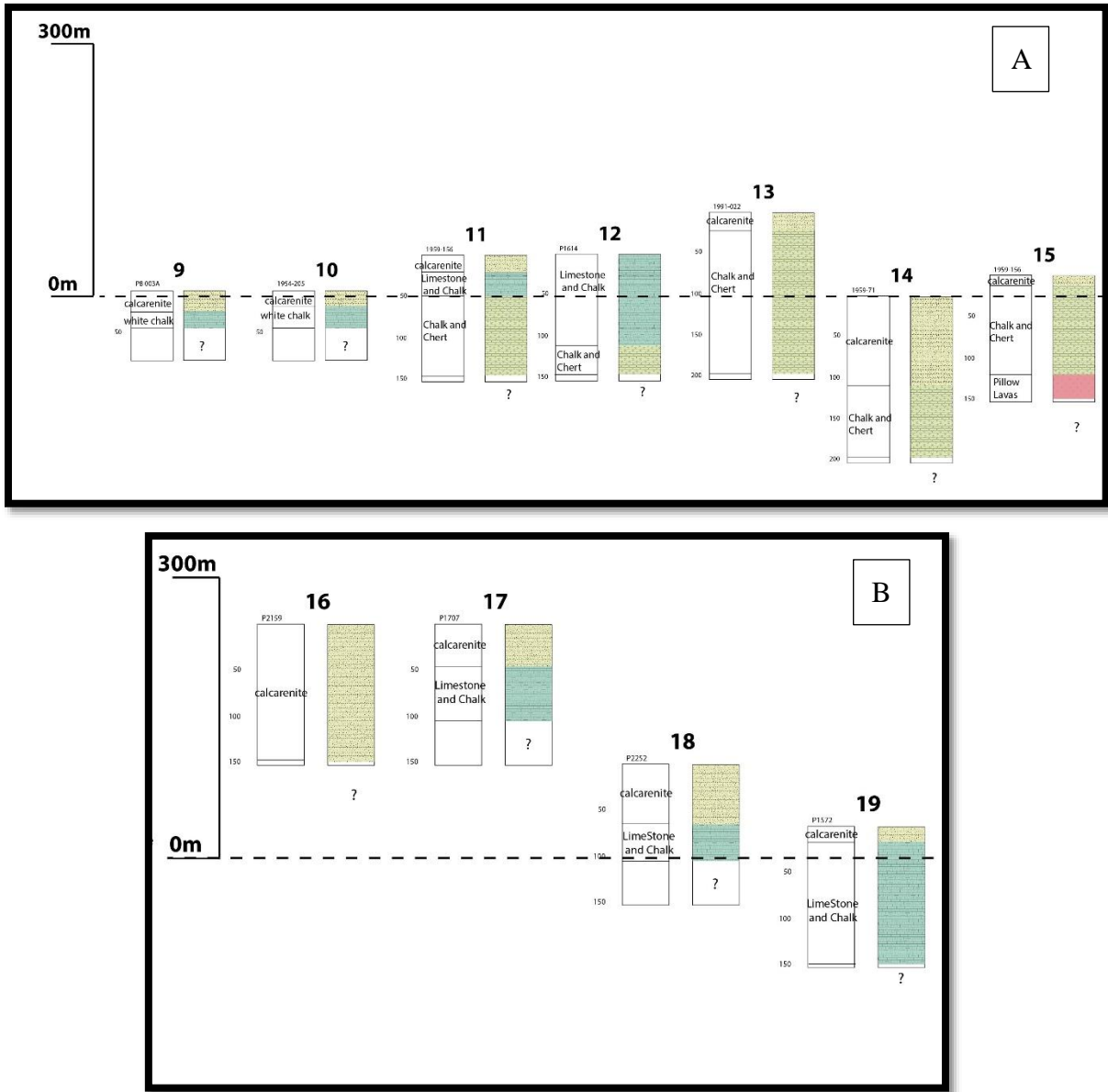


Figure 4 - 4: Borehole data: (A) in the Polemi Basin (9-15) as they are interpreted by Geoter [2005] and (B) in Limassol Basin (16-19) as interpreted by Kinnaird [2008] (locations in Figure 4 - 2).

### *4.1.2 Surface data and map revisions*

The geological map of Cyprus at a scale of 1:250.000, displays the main sedimentary units (see also Chapter 2, Figure 2 - 20) and according to the map the main tectonic structures are the Arakapas Transform Fault, the Gerasa Fold and Thrust Belt, the Ovgos Transform Fault, the Akamas Thrust Fault Zone and normal faults in the Polis Basin. During our two field surveys, four geological maps of south/southwest Cyprus were generated covering the Polis, Polemi and Limassol Basins (Figure 4 - 1) at a scale of 1:35.000, by utilizing an ArcGis database courtesy of the GSD, which was compiled by previous studies that mapped the area [Lapierre, 1971; Turner, 1992; Zomeni and Tsiolakis 2008; Zomeni and Georgiadou, 2015]. A lack of dip data on the main geological map of Cyprus (scale of 1:250.000), prompted the use of these detailed maps. A large number of sedimentary bed dips were measured in order to constrain the geometry of the beds (Figure 4 - 5, Figure 4 - 17, Figure 4 - 22, Figure 4 - 27). Through field observations the contacts between the sedimentary formations were investigated, as the juxtaposition of different units can be an indication of tectonic structures. Measurements near major faults were used to define the nature of the faults and the geometry of the units. In all the aforementioned basins, meso-scale faults and striation data were recorded at a number of sites, with the specific aim of determining the stress regime of certain key areas. These faults were encountered mainly in Cenozoic sediments such as the Middle Eocene Lefkara Formation, the Middle Miocene Pakhna Formation and in the Plio-Pleistocene Nicosia Formation.

## **4.2 Polis Basin**

The Polis Basin is located at the westernmost region of the island of Cyprus (Figure 4 - 1). A large number of studies undertaken in this basin, describe it as an extensional basin bounded by large scale normal faults [Payne and Robertson, 1995, 2000; Kinnaird, 2008]. Previous authors evoked a deformation mechanism connected with the slab roll back of the northward subducting African plate [Payne and Robertson, 1995, 2000].

New offshore studies west of the Polis Basin, based on seismographic recordings and fault plane solution indicate a strike slip structure termed the Paphos Transform Fault (see chapter 2) [Papazachos and Papaioannou, 1999]. These results were further enhanced by the work of Dilek and Sandvol [2009], who proposed a STEP fault geometry (subduction-transform edge propagator) proposing that the northward subducting African plate is not retreating under Cyprus. These results are in sharp contrast with the proposed models by Payne and Robertson

[1995, 2000], thus prompting a re-evaluation and the proposal of a new conceptual model that explains the structures and the deformation encountered during the field campaigns in Cyprus.

Throughout the duration of the field surveys in the Polis Basin, four sectors were investigated resulting in the proposition of geological maps for the Polis area with minor revisions. On the main geological map (Figure 4 - 5, scale of 1:35.000) which is based on the work of Lapierre [1971], Turner [1992] and Zomeni and Georgiadou [2015] new tectonic structures were mapped and the bed dips of the units were added in agreement with the field observations.

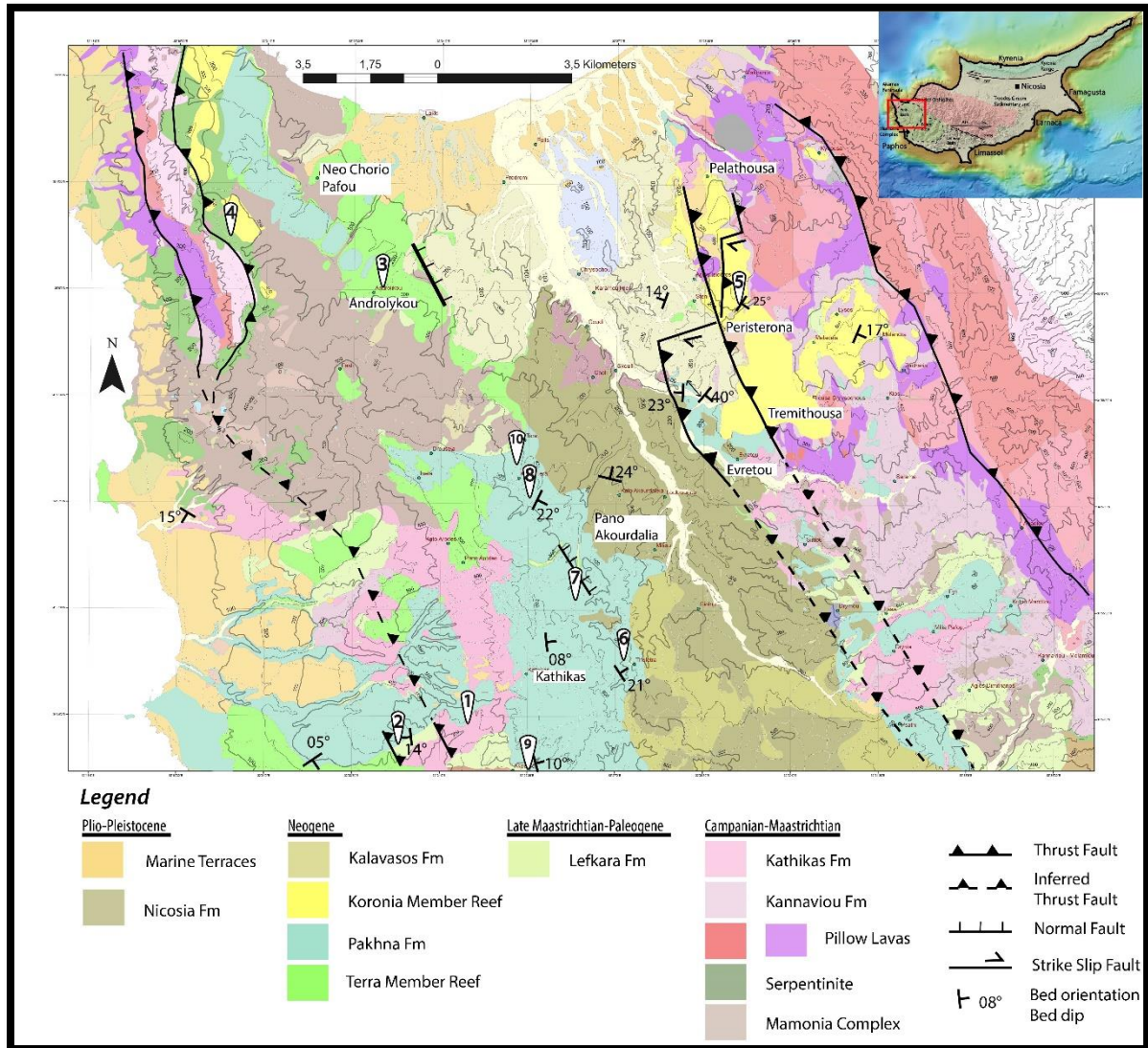


Figure 4 - 5: Geological map of Cyprus (from GSD, compiled by the maps of Lapierre, 1971; Turner, 1992; Zomeni and Tsiolakis 2008; Zomeni and Georgiadou, 2015) in the Polis Basin. The red square in the inset map depicts the position of the Polis Basin on the Island of Cyprus. The points indicate the locations of each outcrop discussed in this manuscript. 1) Figure 4 - 6: Kathikas Panorama view. 2) Figure 4 - 7 and Figure 4 - 8: Panorama unconformity. 3) Figure 4 - 9: Androlykou quarry. 4) Figure 4 - 10: Contact between ophiolites and reefs near Neo Chorio Paphou. 5) Figure 4 - 11: Koronia Member reefs near Peristerona village. 6) Figure 4 - 12: Gravitational scarp in Pakhna Formation or the folding level of the chalks. 7) Figure 4 - 13: Normal faults in Pakhna Formation near Pano Akourdalia village. 8) Figure 4 - 14: Small scale normal faults in Pakhna Formation near Kritou Tera village. 9) Figure 4 - 15: Horst and graben structures in Pakhna Formation near Akoursos village. 10) Figure 4 - 16: Striations in Pakhna Formation indicative of strike-slip displacement near Kritou Tera village. Fault structures at locations 1, 2, 3, 5 are proposed for the first time in this study, as are the inferred thrust faults. Fault structures at location 4 are after Swarbrick [1993] and Bailey et al., [2000]. Structure at location 7 is after Payne and Robertson, [1995]. Faults, bed orientation and dips are from this study.

### 4.2.1 *Compressional structures*

Multiple sites indicative of a compressional regime are identified on both flanks of the Polis Basin (Figure 4 - 1). Near the village of Kathikas at a panorama view on the western flank of the Polis Basin (Figure 4 - 5, point 1), two observations were made: a) south of the village of Kathikas (contact location indicated in Figure 4 - 5) the flat lying Middle Miocene Pakhna rests directly above the Upper Maastrichtian Kathikas Formation (Figure 4 - 6); and b) north of the village of Pegeia (contact location illustrated in Figure 4 - 5) the Middle Miocene Pakhna Formation overlies the Burdigalian chalks and Late Maastrichtian chalks of the Lefkara Formation (Figure 4 - 7). The sedimentary gap observed at both localities, indicates a tectonic contact between the formations. Due to the nature of the Kathikas Formation (debris flows of red argillaceous silt and angular clasts) the fault zone could not be observed. It is proposed herein, that this structure corresponds to a SW verging thrust fault, with an approximate strike of NW-SE direction. As seen in Figure 4 - 6 the Middle Miocene Pakhna Formation seals this thrust fault. This thrust, termed here as the Kathikas Thrust, was probably active during Oligocene to Early Miocene time and its activity ceased before the deposition of the Pakhna units.

In the Panorama sector, north of the village of Pegeia (Figure 4 - 5, point 2), several observations and measurements were recorded which provided the groundwork for revision of the existing geological maps. By examining the Cenozoic sequences different types of sedimentary contacts were revealed. At Panorama, an outcrop of chalks and marls shows a major stratigraphic contact of two formations. The upper layers are characterized by shallow water deposits of creamy buff colored marls and chalks, while the lower layers are characterized by white colored chalks and marls (Figure 4 - 7). Fractures identified in the lower layers are infilled by sub-rounded clasts of green to red color (Figure 4 - 8). Samples collected at this locality were bio-stratigraphically dated using nanno fossils and have provided the necessary information to clarify the timing of deposition and the relationship between these two formations. The lower part of the outcrop consists of marls and chalks of Late Maastrichtian age [nanno fossil zone CC26-CC25 N. Papadimitriou, 2017, pers. comm.] which could correspond to the basal unit of the Lefkara Formation (Lower Lefkara Member of Lord et al., [2000]). This layer is overlain unconformably by carbonates of Burdigalian age [nanno fossil zone NN4, N. Papadimitriou, 2017, pers. comm.] which correlate with the Early Miocene Tera reef member and is proposed herein as the proximal facies of this formation. Field observations of the contact between the two dated layers, indicate an unconformable surface which is associated with the dissolution of limestone beds and is therefore proposed as a karstified/erosive stratigraphic horizon. At the level of the identified karstified surface the

documented dissolution discontinuities are infilled by small round pebbles inferred as eroded material from the Mamonia Complex (Figure 4 - 8). A few meters below this section an outcrop of the Middle Lefkara Member was identified (chalks and cherts) which indicates a Middle Eocene age (Figure 4 - 5). A second thrust is thus proposed although it was not observed (Figure 4 - 5). The absence of the Oligocene Upper Lefkara marl Member (as described by Lord et al., [2000]) in addition with the upward sequence of Late Maastrichtian chalks and the Burdigalian Tera Member limestone, indicates a hiatus which could be the result of thrust activity of the Kathikas fault and associated erosion and weathering.

According to these observations and the ages obtained from the bio-stratigraphic dating, a revised map of the area is proposed (Figure 4 - 5). The NW-SE trending thrust fault which is verging towards the SW (Figure 4 - 6), results in a major thrusting movement near the village of Kathikas (Figure 4 - 5) after the deposition of the Lefkara Formation. From the Kathikas to Pegeia villages (north and south of the area respectively), the Maastrichtian Kathikas Formation and the Maastrichtian lower member of the Lefkara Formation, thrust onto the Middle Eocene, middle member of the Lefkara Formation. The two faults proposed in the revised map (Figure 4 - 5), probably represent two branches of the same SW verging Kathikas thrust, identified in this study, offsetting the pre Pakhna sediments (Figure 4 - 6, Figure 4 - 7) The karstified surface identified (black dotted line) at this outcrop (Figure 4 - 7), supports a thrusting displacement in Oligocene to Early Miocene time associated with a local emersion of the area, which is followed by local subsidence of the basin as evidenced by the deposition of the Burdigalian chalks of the Tera Member (creamy color).

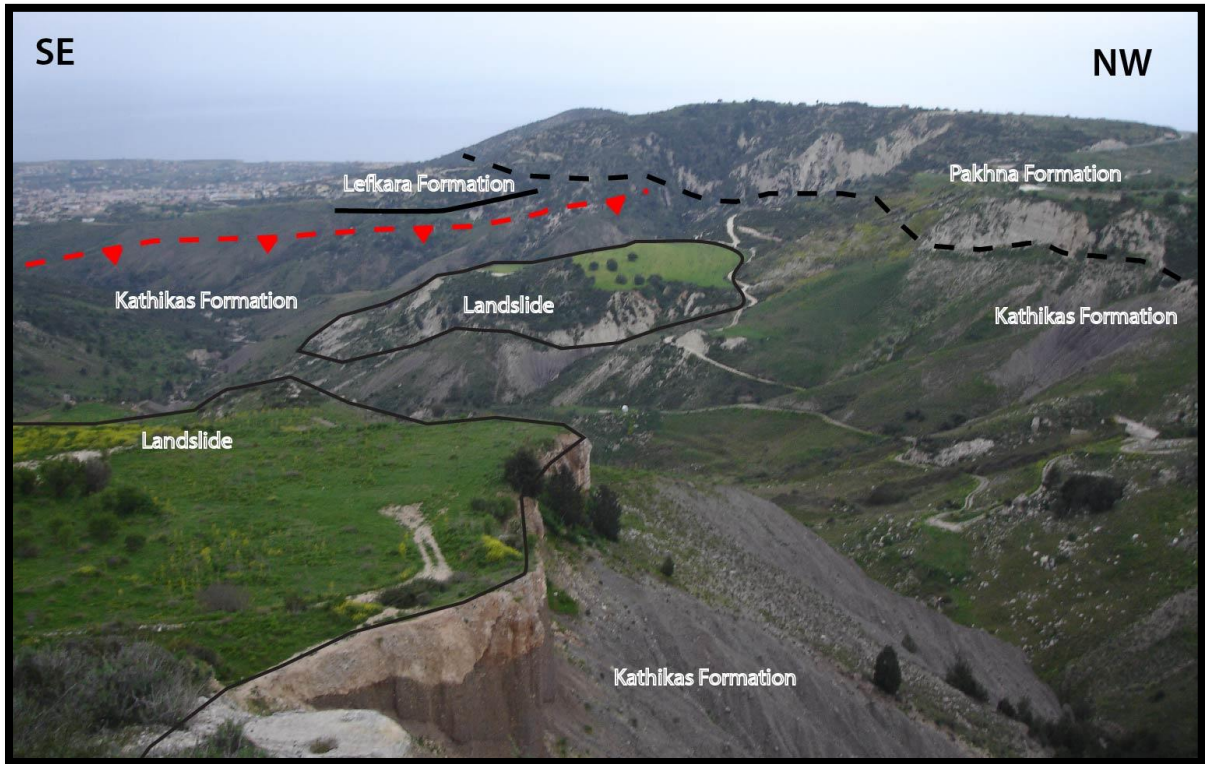


Figure 4 - 6: Panoramic photograph showing the contact between the Kathikas Formation (Maastrichtian age) and Lefkara Formation (Maastrichtian to Middle Eocene age) to the south, which are unconformably overlain by the Pakhna Formation (Middle Miocene age), near the village of Kathikas. The juxtaposition of the Kathikas Fm and Lefkara Fm is connected with the activity of a thrust fault, commencing in Oligocene to Early Miocene time. The thrust fault is verging roughly towards the SW. Field location in Figure 4 - 5, point 1.

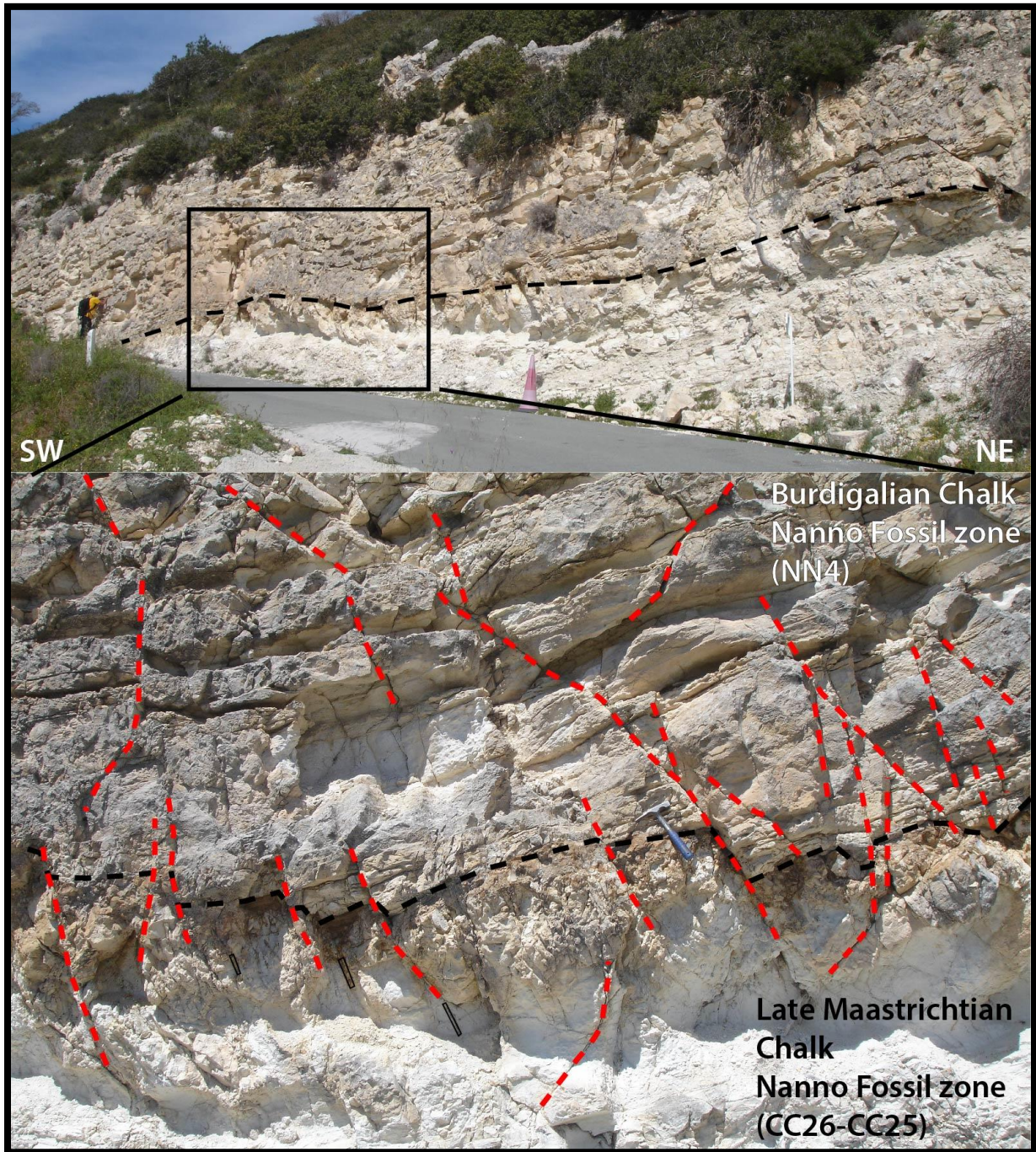
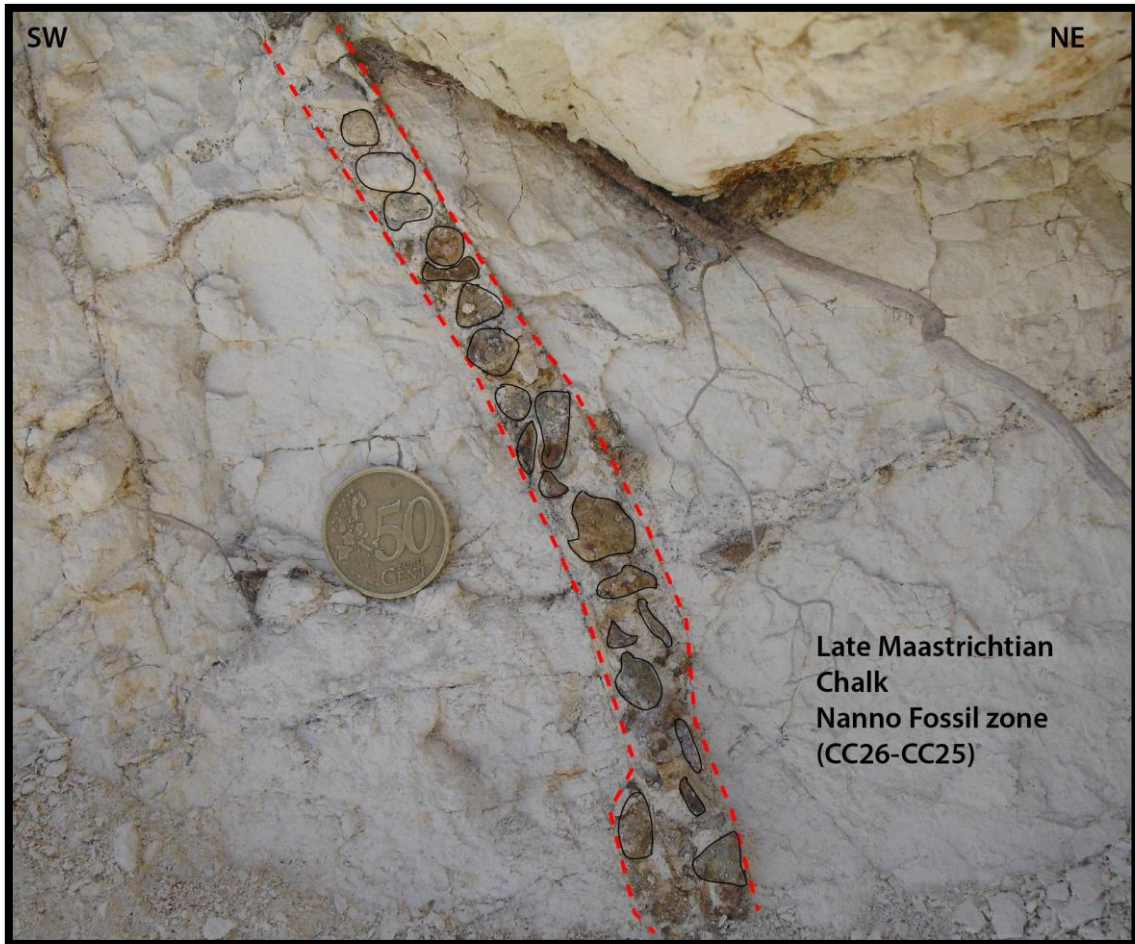


Figure 4 - 7: Photograph showing the contact between the overlying Tera Member Burdigalian chalk and the underlying Maastrichtian chalk presumably of the Lower Lefkara Member, north of the village of Pegeia. The ages were obtained by bio stratigraphic dating [N. Papadimitriou, pers. comm., 2017]. Black dotted line illustrates a karstified surface indicative of the limit between the two formations and the close proximity to the sea level. Red lines illustrate faults or cracks between the two formations. Outcrop location indicated in Figure 4 - 5 point 2.



*Figure 4 - 8: Zoomed in photograph of Figure 4 - 7 illustrating the discontinuities in the Late Maastrichtian chalk filled with fragments from surrounding formations, presumably from the Mamonia Complex. Outcrop position indicated in Figure 4 - 5, point 2 and Figure 4 - 7.*

Near the Androlykou quarry (Figure 4 - 5, point 3), reef limestone deposits are identified from the observation of red algae (Figure 4 - 9). A shearing lens was documented in the quarry as it was identified from its characteristic geometry of thin edges and thicker middle part (Figure 4 - 9). The age of these formations is dated as Aquitanian to Burdigalian [C. Blanpied, pers. comm., 2017] which corresponds with the Tera Member shallow reef limestones. This observation is linked with the uplift of the area followed by the deposition of the Burdigalian reef limestone presumably on the top and next to the Triassic/Jurassic deposits of the Mamonia Complex (Figure 4 - 5, as illustrated in the cross section, Figure 4 - 38). This conclusion is indicative of an Oligocene to Early Miocene tectonic activity, which could be related with the thrusting movement identified in the Kathikas area. A result of this movement is the uplift of

the Pillow lavas and the subsequent folding of the Mamonia Complex which places the western flank of the Polis Basin in close proximity to sea level, ensuring the best environment in order to deposit reef limestones in Early Miocene. Observations of meso-scale thrusts in the Tera reef deposits in the quarry, point towards a later deformation event, identified by the shearing lens (Figure 4 - 9) on the walls of the quarry which may indicate a thrusting activity towards the SSW.



*Figure 4 - 9: Photograph showing Early Miocene Tera Member reef deposits in the Androlykou quarry, depicting Late Miocene or Pliocene compression. Shearing observed by the lenses illustrated, indicative of thrusting-compression towards the S-SSW. Outcrop location indicated in Figure 4 - 5, point 3. Field book used as scale.*

In the Akamas Peninsula (Figure 4 - 5, position 4), serpentinites and Upper Pillow lavas of Upper Cretaceous age and the Mamonia Complex of Triassic age are well exposed (Figure 4 - 10). Patch reef units were identified by the GSD [Zomeni and Tsiolakis, 2008; Zomeni and Georgiadou, 2015] (Figure 4 - 5, NW part of the Polis Basin) and were also observed in this study, as reefal limestones are overlying dark coloured deposits identified as serpentinites (Figure 4 - 10). Dating of reef limestone samples in Akamas (Figure 4 - 10), point towards a Tortonian age [C. Blanpied, pers. comm., 2017], with these brecciated reef limestone perceived as Koronia member reef limestones, unconformably overlying the pillow lavas and the serpentinites (Figure 4 - 10). This contact indicates a large time gap marked by the erosional

surface between the Tortonian Koronia reefs and the Campanian Upper Pillow lavas (Figure 4 - 10) pointing that the Akamas Peninsula was a high at the time. The nearby elongated, NNW-SSE serpentinite bodies are an indication of faulting, however the initial timing of the emplacement of the serpentinites is unclear as currently there is no dating. A Neogene tectonic movement is suggested by the uplift of the Akamas Peninsula, as described above, which continued at least until early Late Miocene resulting in the deposition of the Tortonian Koronia reefs on top of the Upper Pillow lavas (Figure 4 - 10). Bailey et al., [2000] propose that the thrust faults at the Akama Peninsula are verging roughly towards the west, which is in accordance with the observations in this study.

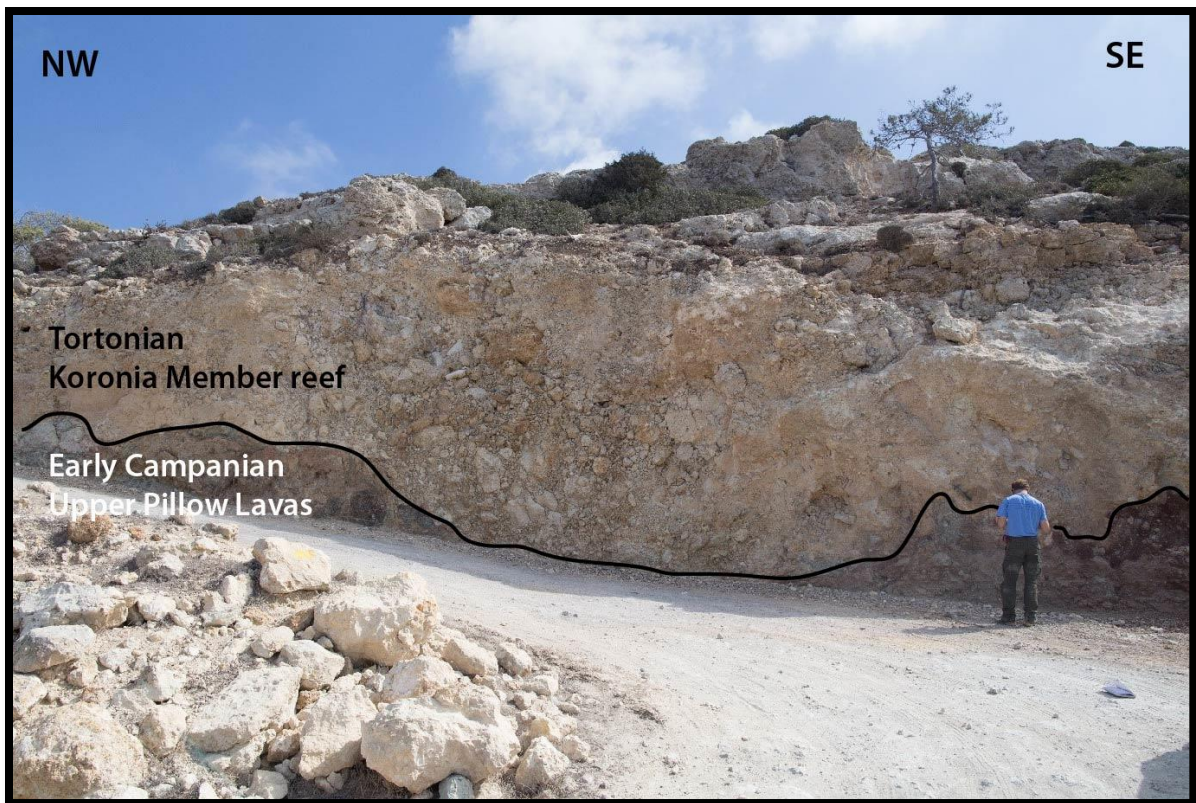


Figure 4 - 10: Photograph depicting the contact between brecciated reefs probably of Koronia Member (Tortonian age), with ophiolites (Upper Pillow lavas) near the village of Neo Chorio Paphou, in the Akamas peninsula. Outcrop location indicated in Figure 4 - 5, point 4.

The eastern flank of the Polis Basin is generally steeper as indicated by the large bed dips observed in the field (bed dip is  $25^{\circ}$  towards the SE, Figure 4 - 11). Bio-stratigraphic dating and Sr-analysis on reefal limestones in the Pelathousa and Peristerona area (Figure 4 - 5, point 5), indicate a Tortonian age [C. Blanpied, pers. comm., 2017] which corresponds with the Koronia Member reef limestones. West of the reef deposits in the center of the Polis Basin, shallow deposits of the Plio-Pleistocene Nicosia Formation (Figure 4 - 5) (calcarenites and sandstones) are overlying the deeper facies of the Middle Miocene Pakhna Formation (hemipelagic chalks and marls) as it is identified from borehole data in the Polis Basin (borehole 8, Figure 4 - 2, Figure 4 - 3). To the west the Tortonian Koronia Member reefs, are in direct contact with Campanian Pillow lavas, while to the east the reefs are in the contact with Campanian sediments of the Kannaviou Formation and no Pakhna Formation sediments were deposited, as illustrated in the revised geological map (Figure 4 - 5). These sedimentary contacts and the tilted Tortonian reefs, are an indication of a tectonic contact and it is proposed herein that an early Late Miocene deformation took place.



Figure 4 - 11: Photograph depicting Late Miocene Koronia member reefs near the village of Peristerona Paphou. Black lines indicate the eastward dip of the Koronia reefs. The tilting of the reef deposits is connected with a westward verging thrust fault (not observed in this figure) Outcrop location indicated in Figure 4 - 5, position 5.

4.2.2 Extensional structures

Investigations in the central part of the Polis Basin were undertaken in order to identify the sedimentary infill of the basin, understand the deformation style and the plausible tectonic mechanisms. Normal faults in the Polis Basin are mainly observed at the western flank of the basin. Near the village of Pano Akourdalia (Figure 4 - 5, position 7) a normal fault displaces the chalk of the Pakhna Formation (Figure 4 - 12). The direction of the fault is NW-SE, dipping towards the center of the basin at approximately 45-50°. The throw of this fault is calculated around 50-60m and can be followed on the topographic map for approximately 1-2km.

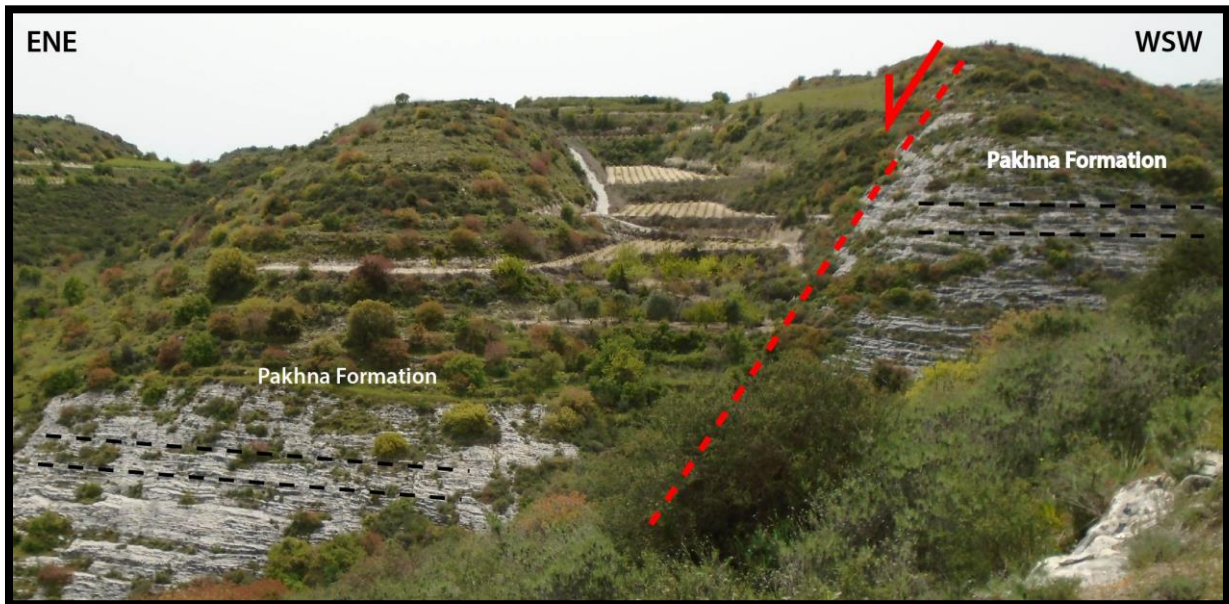
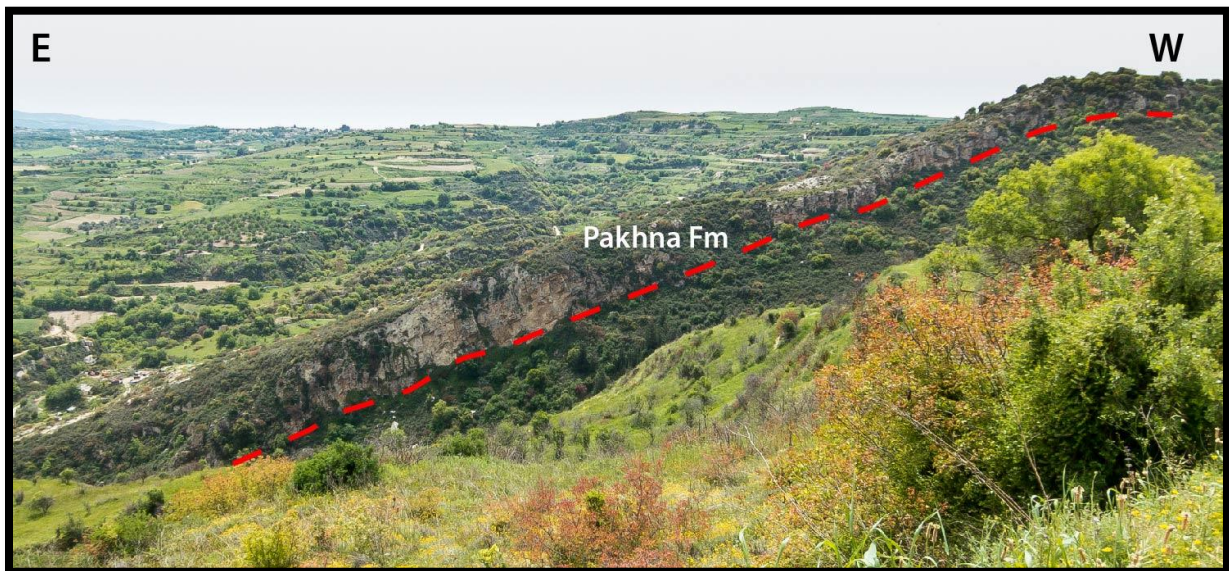


Figure 4 - 12: Photograph depicting a normal fault in the Pakhna Formation near the village of Pano Akourdalia. The fault displaces chalks of the Pakhna Formation, it is trending NW-SE and is dipping eastward at ~45-50°. Outcrop location indicated in Figure 4 - 5, position 7.

At the village of Theletra a sequence of Pakhna chalks is dipping towards the center of the Polis basin (fig. 4-2, position 6). The regional dip is small close to the village of Kathikas (~8°), with the dip of the units constantly dipping towards the east, while moving closer to the center of the Polis Basin the dip is larger (~20°) (Figure 4 - 5). Considering its actual dip is ~30-40° towards the east, it is proposed that the current geometry is due to gravitational processes associated with the uplift of the western flank and the instability of the sediments (Figure 4 -

13). A similar scenario is proposed by Geoter [2005], as they invoke slickenside measurements with a normal displacement.

Meso-scale normal faults were identified near the village of Kritou-Tera (fig. 4-2, position 8). Bedding measurements undertaken at this locality indicate that the sediments are dipping towards the east, towards the center of the Polis Basin. The normal faults trend NW-SE and cut Middle Miocene sediments of the Pakhna Formation with displacements ranging from a few centimeters to one or two meters (Figure 4 - 14). These faults are perceived as gravitational faults created due to the uplift of the Kathikas Thrust and illustrate an extension of NE-SW direction (Figure 4 - 2, position 1).



*Figure 4 - 13: Panoramic photograph showing a sequence of Pakhna cherts dipping towards the East. The red dotted line illustrates either the gravitational surface that displaces the cherts, or the level at which the cherts are folding. Outcrop location indicated in Figure 4 - 5 position 6.*

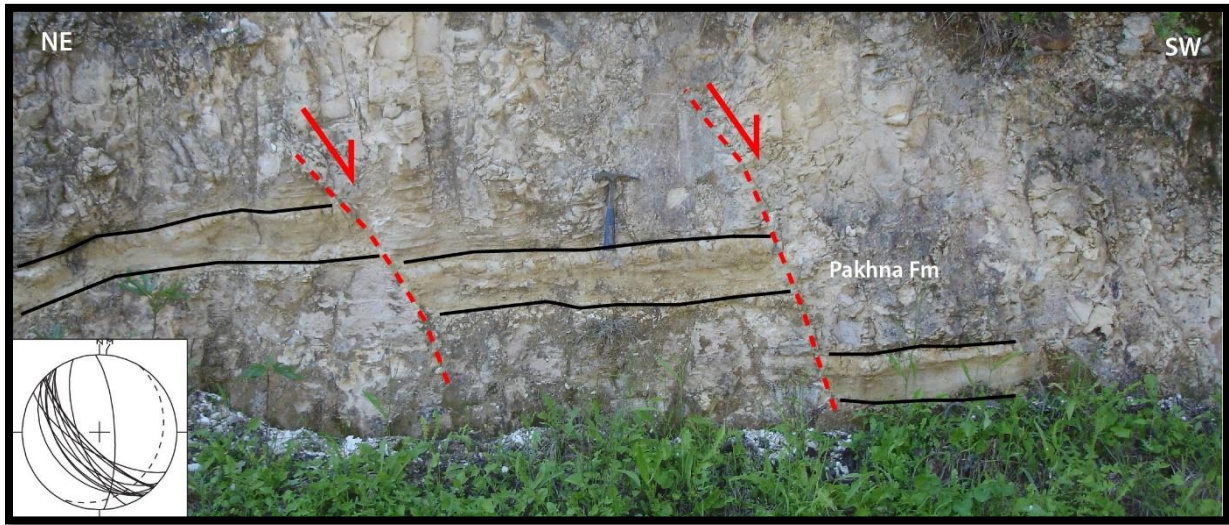


Figure 4 - 14: Photograph depicting normal faults displacing the Pakhna Formation, near Kritou Tera. Direction of faults SSE-NNW. Inset image indicates the stereographic projection of the measured fault planes. Outcrop location indicated in Figure 4 - 5, position 8.

At Akoursos village (Figure 4 - 2, position 9), normal faults trending predominantly NW-SE were identified. These normal faults offset the chinks of the Pakhna Formation, creating a horst and graben pattern (Figure 4 - 15). The offset of these faults is limited to a few tens of centimeters thus indicating a local extensional regime in a NE-SW direction.

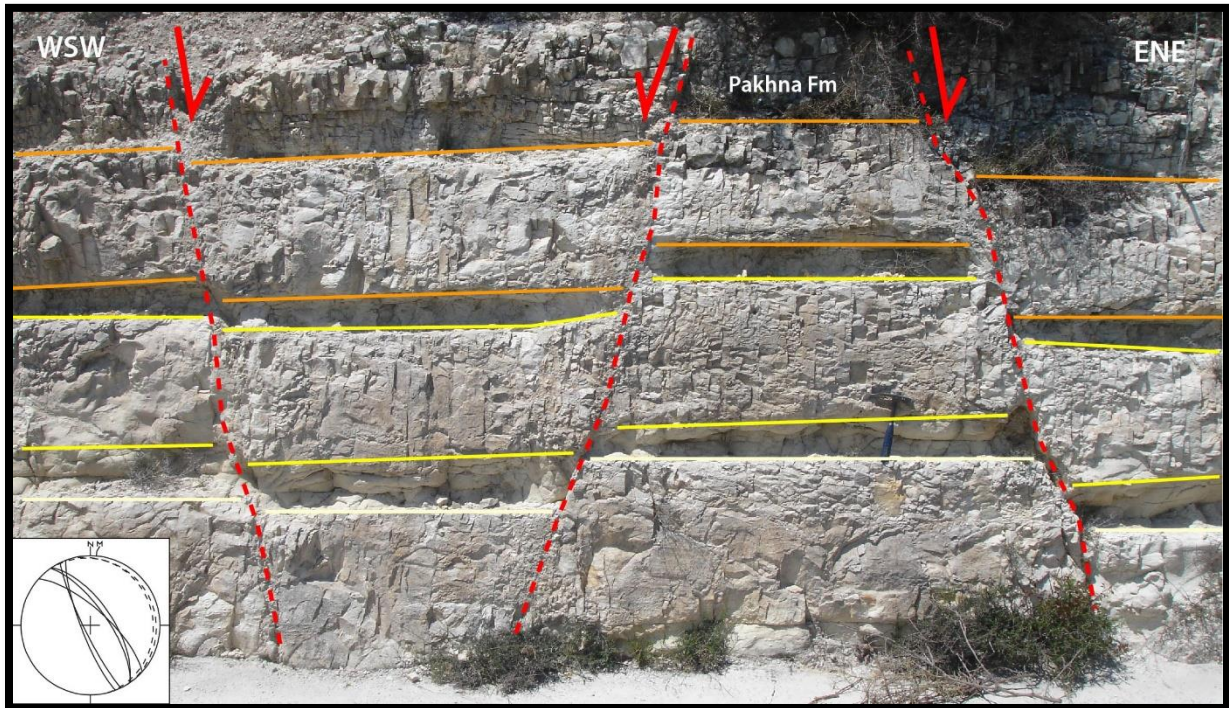


Figure 4 - 15: Photograph of normal faults in the Pakhna Formation, near the village of Akoursos. Fault activity is of Middle to Late Miocene illustrating a NE-SW extension. The fault movements result in the creation of horst and graben structures which is characteristic of an extensional environment. The small offset measured from these faults indicates a rather local displacement. Outcrop location indicated in Figure 4 - 5, position 9.

#### 4.2.3 Transpressional structures

Evidence of a large scale strike slip fault were found near the village of Kritou Tera, on the western flank of the Polis Basin (Figure 4 - 2, position 10, Figure 4 - 16). The fault is marked by a 3m thick brecciated zone, with clast of large sub-rounded and small rounded chinks of the Pakhna Formation. It trends NE-SW, with numerous fault surfaces which show horizontal striae which indicate a strike slip fault. A sinistral sense of movement was deduced from Riedel shear fractures (risers cut solid in the rock units [Petit, 1987]). A stress inversion was performed by using the measured faults in the Tensor software [Angelier, 1990], which computes the stress regime. The obtained stress tensors correspond to a strike slip regime with the maximal principal stress  $\sigma_1$  axis oriented in a NNW-SSE direction, while the minimal principal stress  $\sigma_3$  trends in an ENE-WSW direction. This fault zone denotes a post Middle Miocene movement as it deforms the chinks of the Pakhna Formation.



Figure 4 - 16: Panoramic photograph depicting a large sinistral strike slip fault striking SW-NE, in the Pakhna Formation near the village of Kritou Tera. Inset figures illustrate the Riedel striations measured at this outcrop and the stereo net projections indicate compression (compressional-transpressional stress) in a NNW-SSE direction and an extension (extensional-transensional stress) in an ENE-WSW direction. Outcrop location indicated in Figure 4 - 5, position 10.

### **4.3 Polemi Basin**

The Polemi Basin is located in SW Cyprus (Figure 4 - 17) and illustrates a deformation pattern spanning from Middle Miocene to Messinian time. This basin was associated with the subduction and slab roll back processes proposed by Payne and Robertson [1995]. Evidence on compressional and extensional deformation as observed in the field, are presented below.

#### *4.3.1 Compressional structures*

Reverse faults were identified near Asprokremmos dam at the abandoned village of Foinikas (Figure 4 - 17, position 11) displacing chalks and marls. Observations, indicate reverse faulting as the chalks are displaced and folded as illustrated in Figure 4 - 18. Bio-stratigraphic dating has indicated a Priabonian age (Late Eocene, nanno fossil zone NP 20/19, [N. Papadimitriou, pers. comm., 2017]) for the chalks observed in the field, which is equivalent with the upper Middle Lefkara Member deposits. This implies that shortening occurred in the area.

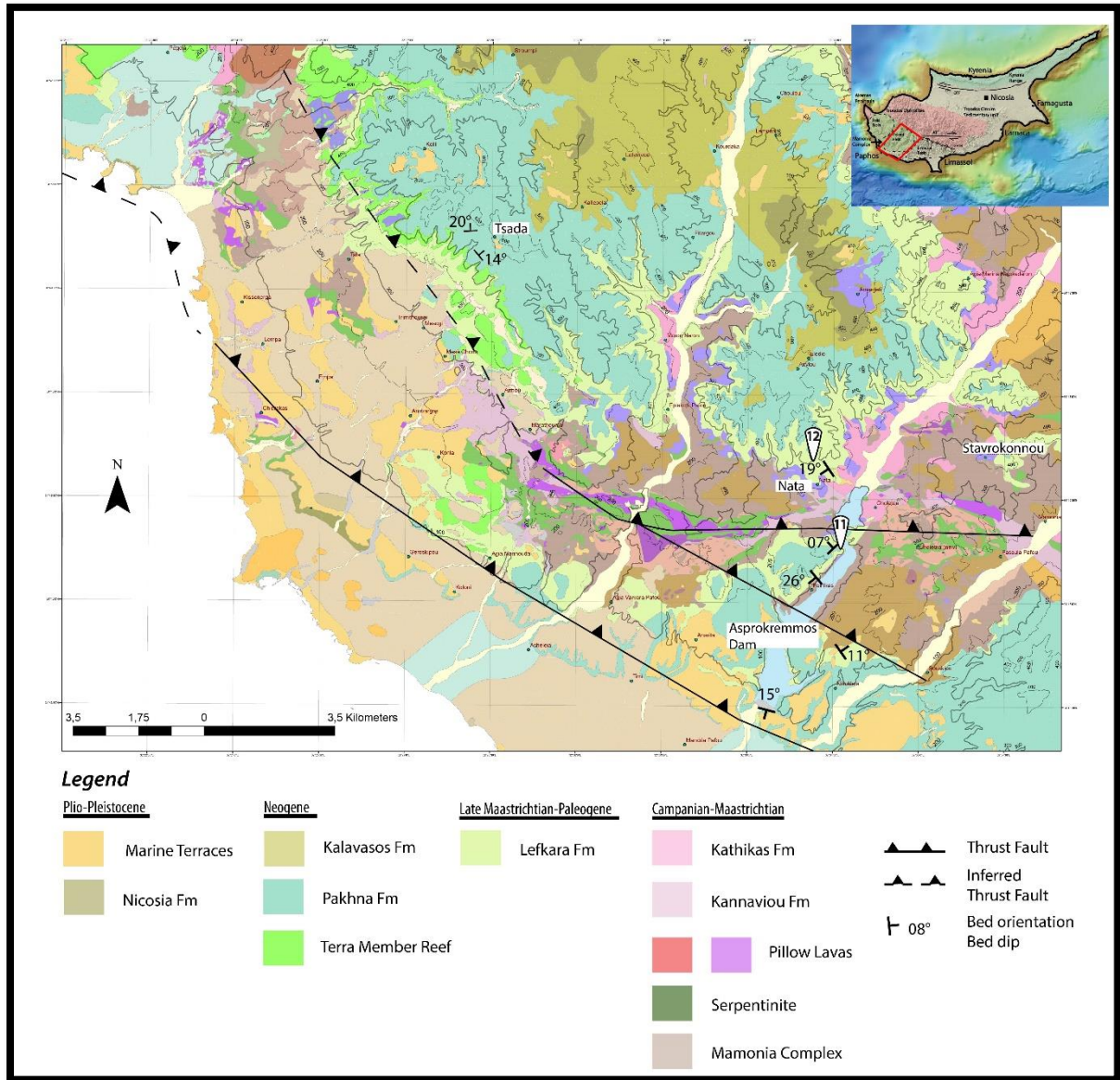
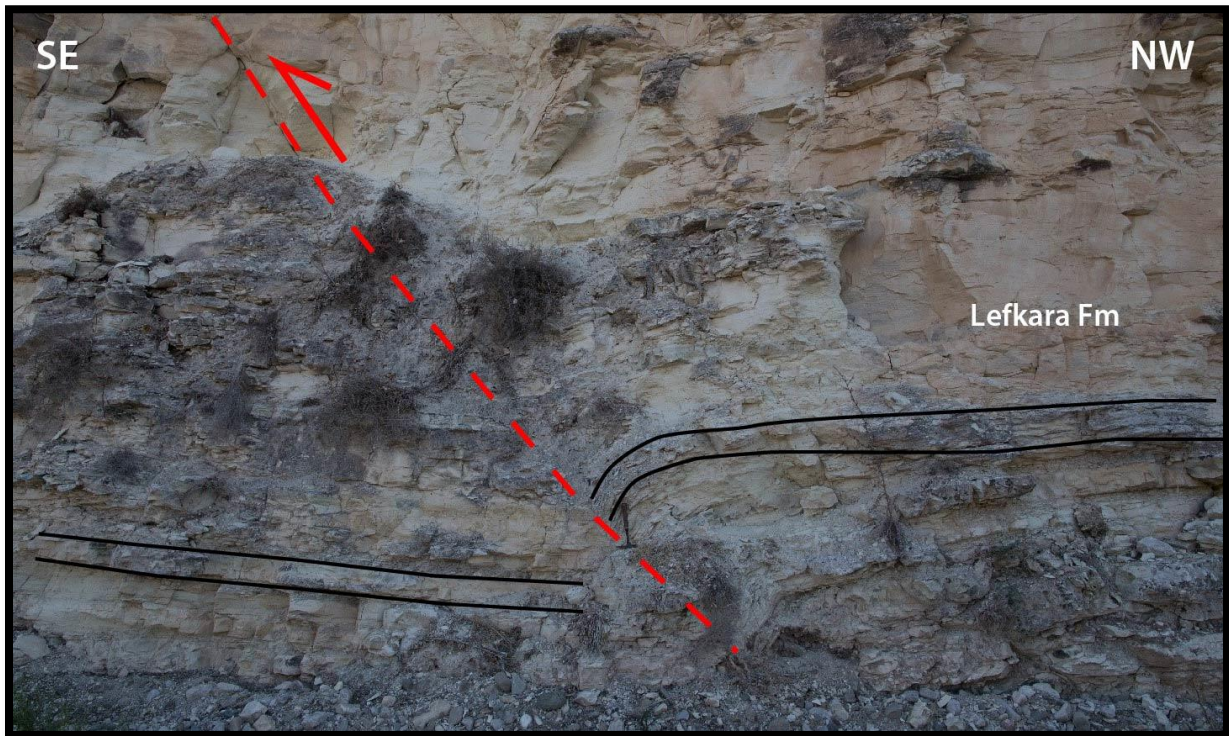


Figure 4 - 17: Geological map of Cyprus (from GSD compiled by the maps of Lapierre, 1971; Zomeni and Tsiolakis 2008) in the Polemi Basin. The red square in the inset map depicts the position of the Polemi Basin. The points indicate the locations of each outcrop displayed in this manuscript. 11) Figure 4 - 18: Reverse fault in Lefkara Formation. 12) Figure 4 - 19 indicates reverse faults in the Lefkara Formation and Figure 4 - 20 illustrates normal syn-sedimentary faults in Lefkara Formation. Northern fault structure is after Swarbrick [1993] and Bailey et al., [2000]. Southern fault structure is after Geoter, [2005]. Bed orientation and dips are from this study.

A few reverse faults were documented near the village of Nata, displacing the chinks and cherts of the Lefkara Formation (Figure 4 - 17, position 12). These reverse faults trend mainly NE-SW and exhibit dips ranging from 40° to 60° (Figure 4 - 19). The large dip measurements suggest that the reverse faults were probably re-activated normal faults but the timing is difficult to precise.



*Figure 4 - 18: Photograph depicting folded Lefkara Formation chinks near the village of Foinikas (Figure 4 - 17, position 11). Bio-stratigraphy dating indicated a Priabonian age (Late Eocene, nanno fossil zone NP 20/19), which is associated with the Upper Lefkara member chinks.*

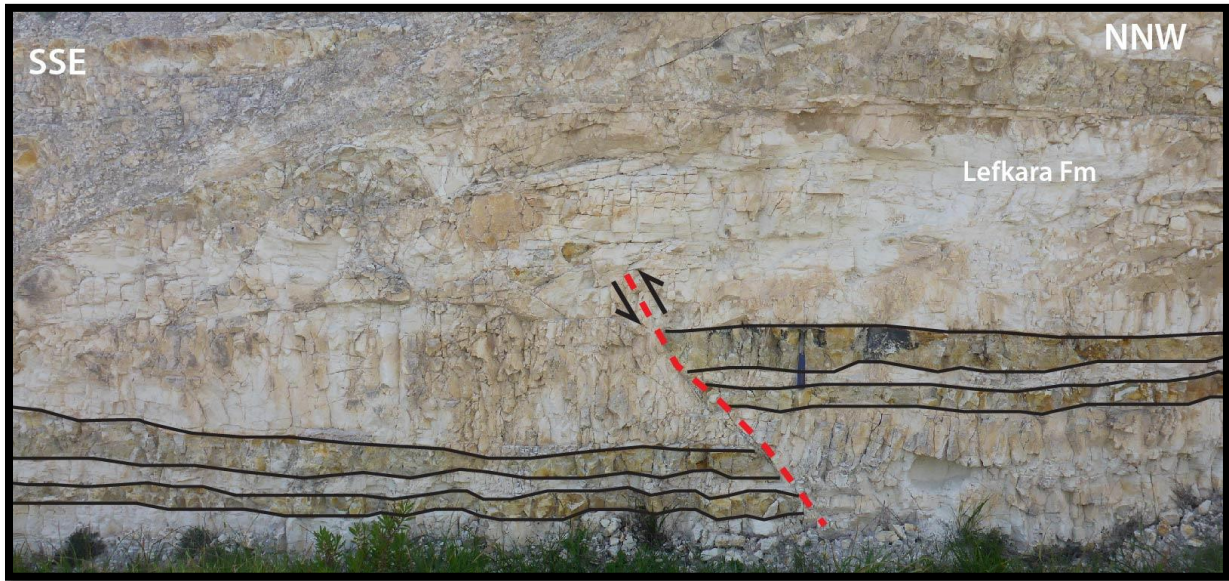


Figure 4 - 19: Photograph depicting a reverse fault displacing the chalks and cherts of the Lefkara Formation near the village of Nata (Figure 4 - 17, position 12). The dip of the measured faults is large between 40 to 60°.

#### 4.3.2 Extensional structures

Numerous normal faults were observed offsetting the chalk and cherts of the Eocene Middle Lefkara member (Figure 4 - 20, Figure 4 - 21) close to the village of Nata (Figure 4 - 17, position 12). The displacement of these normal faults is constrained to a few meters. A syn-sedimentary normal fault was recognized as the middle layer of chert is displaced downwards, while the top layer is also cut but the blocks are not rotated. The thickness variation of the beds left and right of the structure indicative of the continuous activity during the sedimentation. Notably the stereographic projections of the fault planes, from the three studied outcrops near the village of Nata, indicate a significant dispersion in the fault strike. Two main trends are identified, one towards the NW-SE (Figure 4 - 20) and the other towards the NE-SW (Figure 4 - 21), while many faults span between these. This indicates that the area was subjected to extension in all directions, which leads to the assumption that this area was governed by an isotropic horizontal stresses. This implies that a compressive stress did not build up during the Middle Eocene at this locality. It is thus speculated, that the normal faults could be due to extensional processes connected with compaction or other local sedimentary processes.

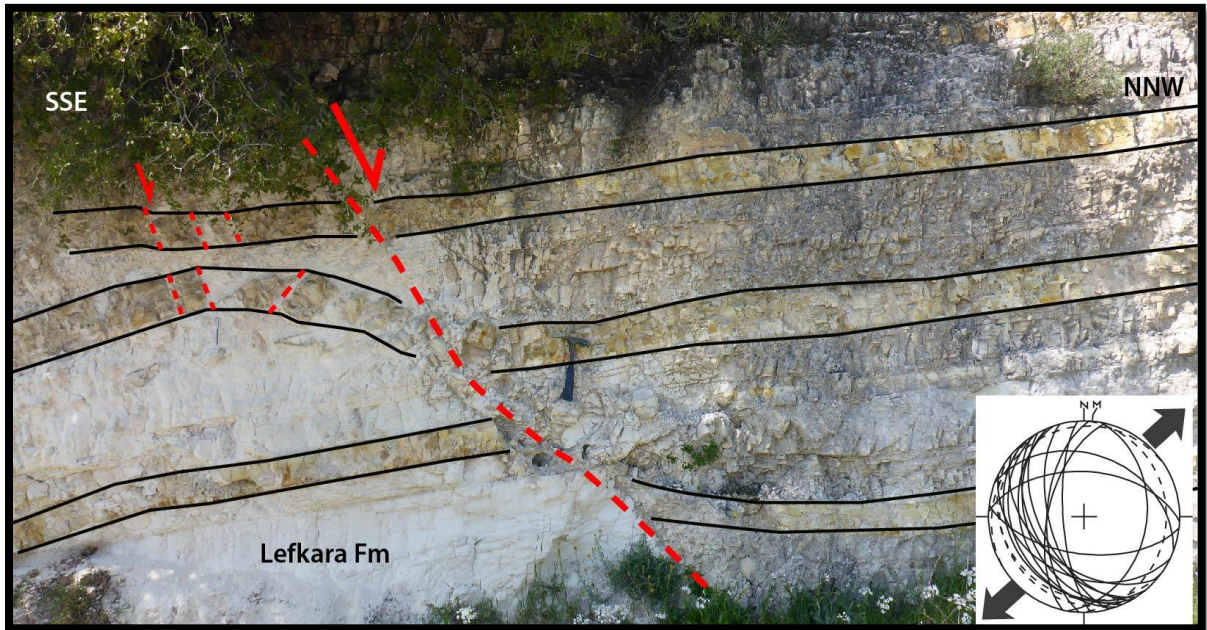


Figure 4 - 20: Photograph depicting normal faults displacing Lefkara Formation chalk and cherts layers (Mid Eocene age), near the village of Nata. Syn-sedimentary fault activity is identified from the change in thickness of the chinks on either side of the depicted fault. The inset stereographic projection illustrates a NE-SW extension. Outcrop location indicated in in (Figure 4 - 17, position 12).

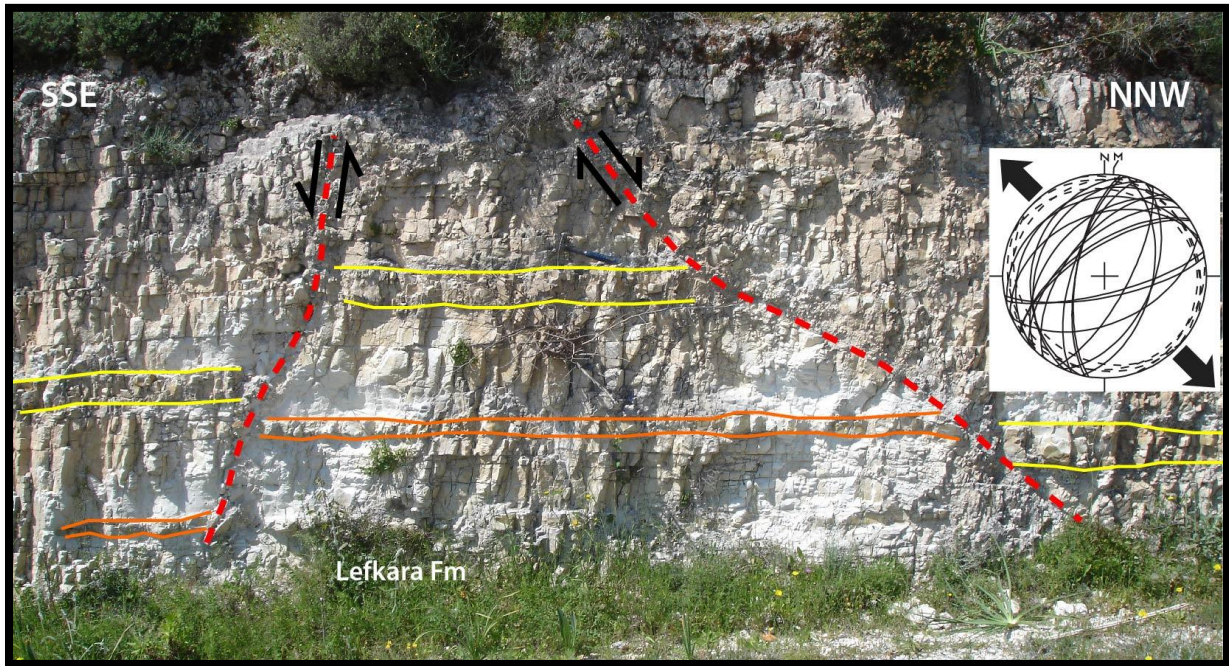


Figure 4 - 21: Photograph showing normal faults in the chalk and chert member of the Lefkara formation (Middle Eocene age), near the village of Nata. A horst geometry is identified at this outcrop. The inset stereographic projection indicates a NW-SE extension (Figure 4 - 17, position 12).

#### 4.4 Limassol Basin

The Limassol Basin (Figure 4 - 22 and Figure 4 - 27), is also known as the Pakhna Basin and Alassa sub-Basin of Eaton and Robertson [1993]. It is located directly south of the Troodos ophiolite range and consists of a thick outcropping layer of Miocene Pakhna Formation with a thickness of ~650m in the south which thins to ~250m in the north [N. Papadimitriou, pers. comm., 2017]. The underlying Paleogene Lefkara Formation mostly outcrops at the northern part of the basin and its total thickness is unknown. A lack of Messinian deposits in the center of the basin is an indication of the deep position of the center of the basin during Late Miocene time. Three sectors were defined for this basin, the western part which consists the border with the Polemi Basin and the northern and eastern parts which are bordered by the Gerasa Fold and Thrust belt.

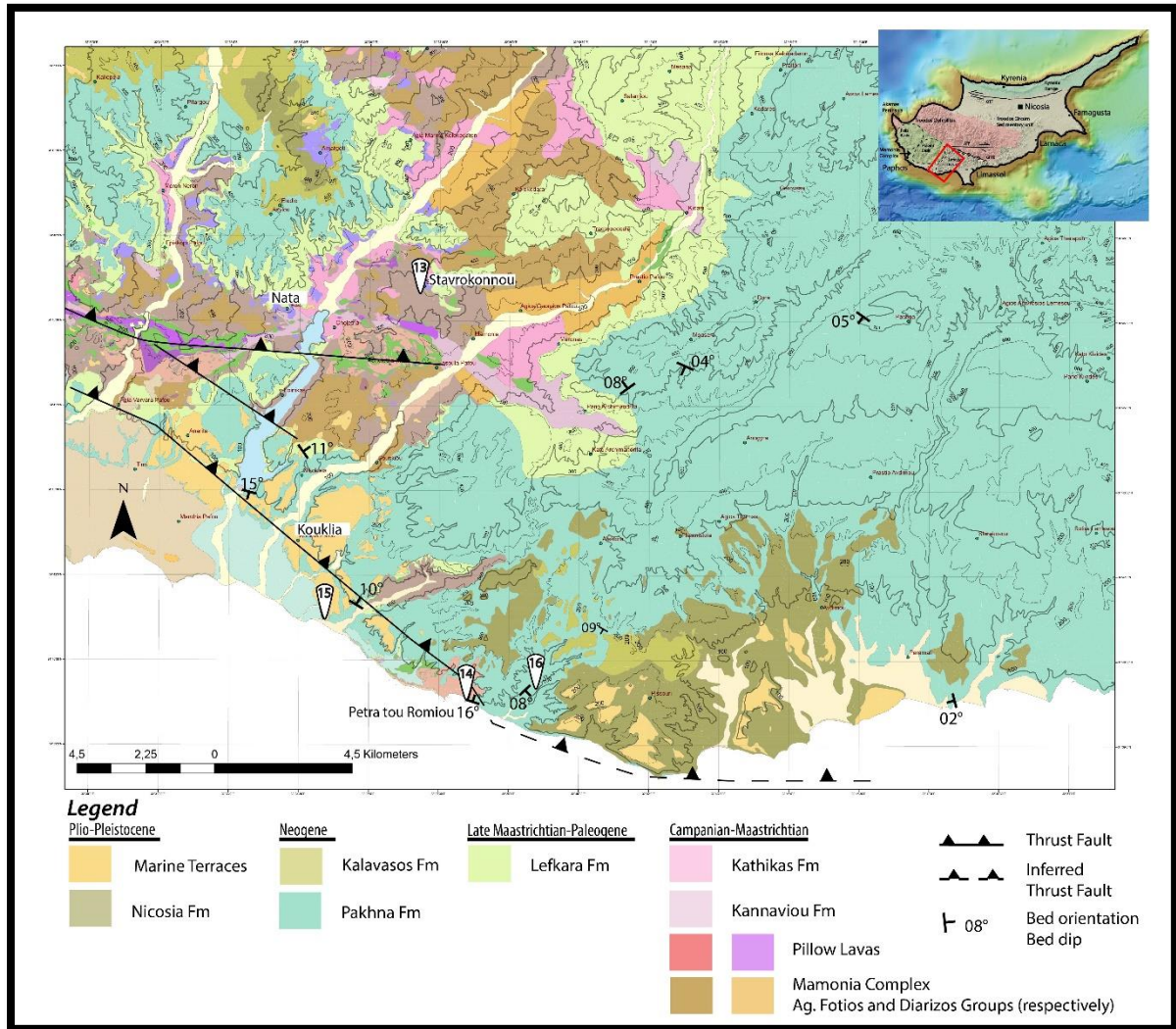


Figure 4 - 22: Geological map of Cyprus (from GSD compiled by the maps of Lapierre, 1971; Zomeni and Tsiolakis 2008) at the western flank of the Limassol Basin. The red square in the inset map depicts the position of the Limassol Basin. The points indicate the locations of each outcrop displayed in this manuscript. 13) Figure 4 - 23: Folding in Mamonia Complex. 14) Figure 4 - 24: Contact between Lefkara and Mamonia Complex. 15) Figure 4 - 25: Folding in the Pakhna Formation indicating Late Miocene thrusting. 16) Figure 4 - 26: S-type shearing in Pakhna Formation. Northern fault structure is after Swarbrick [1993] and Bailey et al., [2000]. Southern fault structure is after Geoter, [2005]. Bed orientation and dips are from this study.

4.4.1 Compressional regime

Shortening is observed on both flanks of the Limassol Basin. At the village of Stavrokonnou (Figure 4 - 22, position 13), radiolarian cherts of the Agios Fotios Group of the Mamonnia Complex are folded due to thrusting activity towards the SW (Figure 4 - 23). The exact timing of deformation of this outcrop is difficult to precise due to the lack of indications as no sedimentary cover is observed on top of this Triassic age formation.



Figure 4 - 23: Photograph depicting the folding of Mamonnia Complex radiolarian chert layers, near the village of Stavrokonnou. Fault thrusting movement is towards the SW, with a Fold Axis of  $155^{\circ}, 04^{\circ} E$ . Exact age of deformation is difficult to determine due to the lack of sedimentary cover. Outcrop location indicated in Figure 4 - 22, position 13.

At the coastline near the Petra tou Romiou (Figure 4 - 22, position 14) a sharp contrast between the white chalks of the Lefkara Formation overlying the brown-red sediments of the Mamonía Complex was observed. This stratigraphic contact between the Triassic age Mamonía Complex and the Lower Member of the Lefkara Formation (Figure 4 - 24), in connection with the lack of Troodos ophiolites and pillow lavas at this locality could be an indication of Late Cretaceous movement, or that this area was a high during the Campanian time where the ophiolites were deposited and then eroded.



*Figure 4 - 24: Panoramic photograph showing the stratigraphic contact between the Triassic Mamonía Complex and the overlying Lefkara Formation (Middle Eocene age) at the Petra tou Romiou (western Limassol Basin). Outcrop location indicated in Figure 4 - 22, position 14.*

Near the village of Koukليا (Figure 4 - 22, position 15) at the western flank of the Limassol Basin, a fold with a steep northern limb was documented in the Pakhna Formation, verging towards the SW with a fold axis of  $125^{\circ}, 04^{\circ}\text{N}$  (Figure 4 - 25). In close proximity at the exit of the old road of Limassol to Paphos, an S-type shearing zone was identified (Figure 4 - 22, position 16), which indicates a thrust fault verging towards the SW (Figure 4 - 26, figure A). In similar fashion, folding of the Pakhna Formation chalk beds are documented outcropping a few kilometres to the east, with the creation of kinks of  $\sim 90^{\circ}$  (Figure 4 - 26, figure B). These three outcrops present evidence of thrusting deformation from Late Miocene onwards, however it is difficult to propose the exact timing of movement due to the lack of sedimentary cover. The study by Geoter [2005], identified folded marine terraces at the Koukليا fold (Figure 4 - 25) which is an indication of quaternary activity on this fault structure.



*Figure 4 - 25: Photograph showing folded Pakhna Formation chalks (Middle Miocene age) near the village of Koukليا. Thrusting movement is of Quaternary time as folded terraces were identified in a trench excavation [results of Geoter, 2005], with the fold verging towards the SW. Fold axis  $125^{\circ}, 04^{\circ}\text{N}$ . Outcrop location indicated in Figure 4 - 22, position 15.*

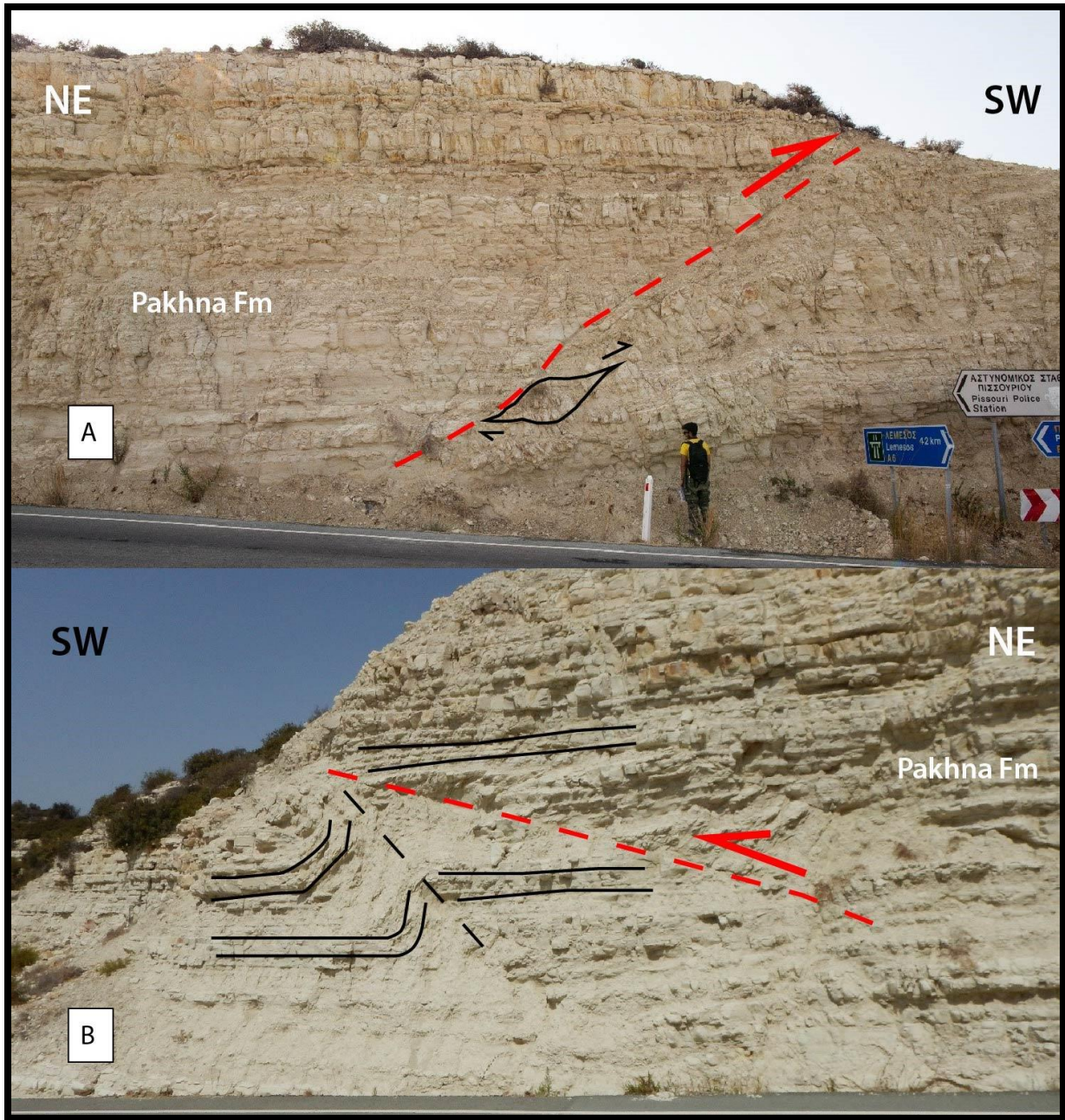


Figure 4 - 26: Photograph depicting folding of the Pakhna Formation (Mid Miocene age) near the Petra tou Romiou. Reverse fault displacement is envisaged in Middle-Late Miocene, with a thrusting direction towards the SW. A) Thrusting and shearing of the sediments B) Folding of chalks creating kinks of approximately 90°. Both outcrops are in the same vicinity. Outcrop location in Figure 4 - 22 position 16.

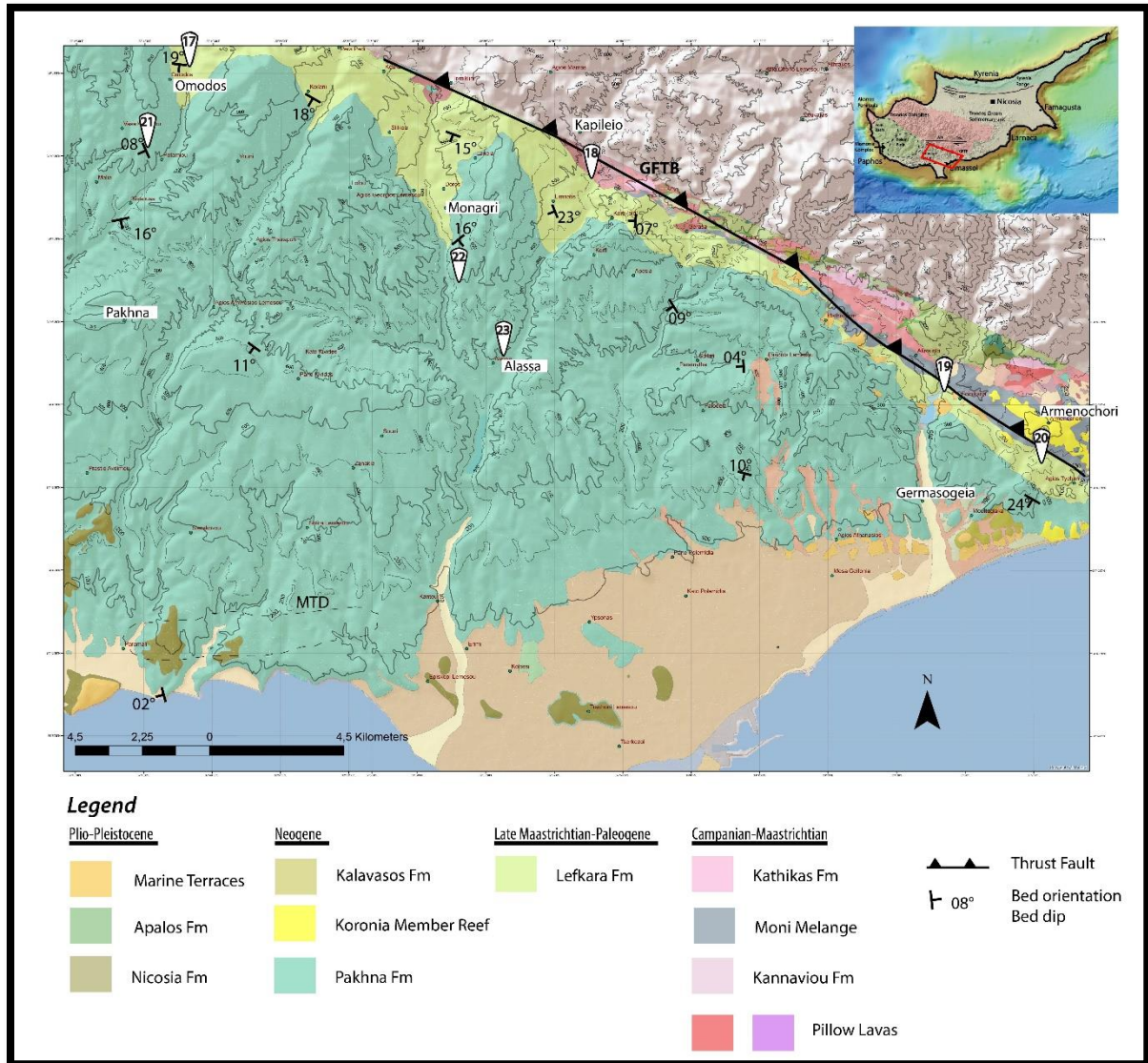


Figure 4 - 27: Geological map of Cyprus (GSD compiled by the maps of Lapierre, 1971; Turner, 1992; Zomeni and Tsiolakis 2008; Zomeni and Georgiadou, 2015) with the main tectonic structures in the eastern flank of the Limassol Basin. The red square in the inset map depicts the position of the Limassol Basin. The points indicate the locations of each outcrop displayed in this manuscript. 17) Figure 4 - 28: Folding in the Lefkara Formation, 18) Figure 4 - 29: Juxtaposed vertical beds of Lefkara Formation with Troodos Ophiolites, 19) Figure 4 - 30: Folding of the Lefkara Formation at the Germasogia Dam, Figure 4 - 31: S-type deformation in the Lefkara Formation indicating thrusting activity towards the SW, near the Germasogia Dam, 20) Figure 4 - 32: Deformation zone in the Lefkara Formation near the village of Armenochori, where s-type geometries are observed indicating SW thrusting activity, 21) Figure 4 - 33: Normal faults in the Pakhna Formation indicating extension in an East –West direction, 22) Figure 4 - 34: Dextral strike fault in the Pakhna Formation identified from measurements of calcite steps and Rieddle striations, 23) Figure 4 - 35: Conjugate strike slip system identified in the Pakhna Formation. Abbreviations: GFTB=Gerasa fold and thrust belt; MTD=Mass Transport Deposits. Fault structure after Eaton and Robertson, [1993]. Bed orientation and dips are from this study.

At the northern flank of the Limassol Basin, Middle Eocene chalk and chert layers of the Lefkara Formation are folded, between the villages of Omodos and Mandria at the southern slope of the Troodos Range (Figure 4 - 27, position 17). Detailed analysis of the measured fold planes at this outcrop (Figure 4 - 28), the stereographic projection of the planes and the poles of the planes, indicate a compressional regime trending SW-NE, implying thrust activity verging towards the SW. It is therefore proposed that the current geometry is a result of erosion due to the uplift of the Troodos Range and the true geometry is indicated by the white dashed lines which illustrate the initial geometry of the folded layers (Figure 4 - 28).

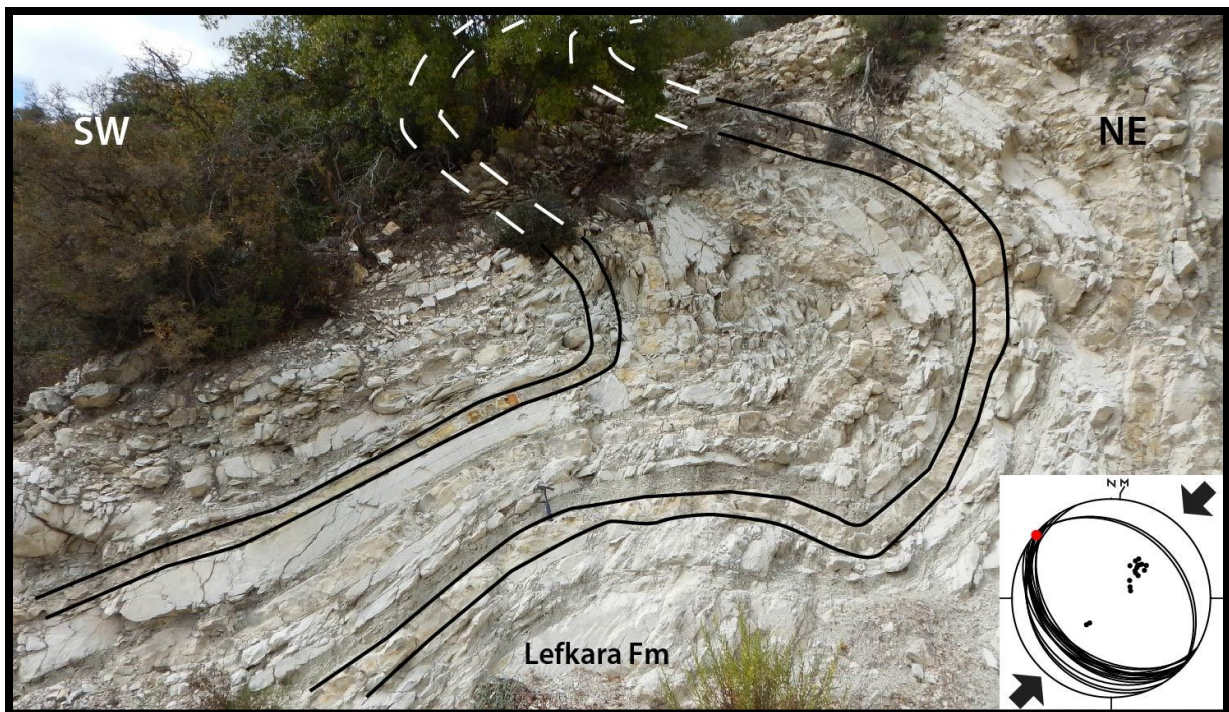


Figure 4 - 28: Photograph showing a typical folding sequence in the Lefkara Formation between the villages of Mandria and Omodos. Bands of cherts and thick beds of chalk are deformed. Thrusting pulse of Oligocene to Early Miocene. Inset stereographic projection illustrates the measured planes (black lines), the poles of the planes (black dots), the constructed fold axis is  $310^{\circ}, 02^{\circ}\text{N}$  (red dot) which matches with the axis measured in the field  $120^{\circ}, 05^{\circ}\text{S}$ . The linear direction of the poles indicates the direction of compression in a SW-NE direction (black arrows). Thus this fold is interpreted as verging towards the south with its upper limbs probably eroded (white dashed lines). Outcrop location in Figure 4 - 27 position 17.

At the eastern flank of the Limassol Basin near the village of Kapilio (Figure 4 - 27, position 18), a thrust verging towards the SW juxtaposes the Campanian ophiolites of the Troodos Range with the northerly steeply dipping Eocene chinks and cherts of the Lefkara Formation. The timing of the thrust movement is envisaged to be during the Neogene (Figure 4 - 27). This thrust is considered as a segment of the Gerasa Thrust.

Additional evidence of the reverse activity of the Gerasa Thrust, is found 15km SE of Kapilio, from the intense deformation within the Lefkara sediments just south of the Gerasa Thrust (Figure 4 - 27, positions 19 and 20). Near the Germasogia Dam (Figure 4 - 27, position 19), the sediments of the Lefkara Formation are folded within a N120-130° axis (Figure 4 - 30). On the road towards the village of Foinikaria, s-type shearing was identified in the Lefkara Formation (Figure 4 - 31), which indicates a thrust fault verging towards the SW. Similarly, near the village of Armenochori, (Figure 4 - 27, position 20), chinks and cherts of the Lefkara Formation are deformed within a possible zone of deformation (Figure 4 - 32). North of the village of Armenochori, Koronia Member reef limestones rest directly on Troodos ophiolites (Figure 4 - 27, position 20).



*Figure 4 - 29: Panoramic photograph showing the juxtaposition of the Troodos melange (Late Cretaceous age, brown area) with the younger Lefkara formation (Paleogene age) with this formation being tilted almost to a vertical limit (white dashed lines) near the village of Kapilio. The fault thrust (dashed red line) is verging towards the SW and the movement is perceived to be from Oligocene onwards. Outcrop location indicated in Figure 4 - 27, position 18.*



Figure 4 - 30: Panoramic photograph of illustrating the folded geometry of the Lefkara Formation near the Germasogia Dam. A thrusting movement of Oligocene to Miocene time is envisaged verging towards the SW. The fold axis is calculated around 120-130°. Outcrop location indicated in Figure 4 - 27, position 19.



Figure 4 - 31: Photograph showing a shearing zone with s-type lenses deformation within the Lefkara Formation near the Germasogia Dam. The thrusting is verging towards the SW which is in accordance with previous observations. Timing of deformation is between Oligocene to Miocene time. Outcrop location indicated in Figure 4 - 27, position 19.

The age thrusting along the Gerasa Thrust described above, postdates the deposition of the Lefkara Formation. This is an indication of the Gerasa thrust movement in Early-Middle Miocene time and a later pulse in Late Miocene time (Figure 4 - 27). This uplift is documented from the deformation zone in the Lefkara sediments, the deposition of the Tortonian reefs on top of the Troodos ophiolites and from the change in sedimentation in the center of the Limassol Basin, where hemipelagic chalks and marls of the Pakhna Formation are deposited. Further evidence for Late Miocene movement of the Gerasa Thrust, are the large MTDs (Mass Transport Deposits) identified near the village of Episkopi (Figure 4 - 27) with a direction of transport from east to west and an age of transport of Late Miocene time [Lord et al., 2009; N. Papadimitriou, pers. comm., 2017].



Figure 4 - 32: Photograph showing the deformation in the Lefkara Formation near the village of Armenochori. Shearing zone with the creation of s-type lenses illustrating thrusting activity towards the SW. Black dotted line is used to envisage the folding of the layers. Outcrop indicated in Figure 4 - 27, position 20.

4.4.2 Extensional structures

During the investigation on the northern part of the Limassol Basin, between the villages of Vasa and Omodos (Figure 4 - 27, position 21) an outcrop was identified in the Pakhna Formation with multiple normal faults. By measuring these extensional faults, a stereonet diagram was produced, illustrating that the extension is in an E-W direction (Figure 4 - 33). As the predominant stress during the Miocene is compressional in a N-S direction, the direction of extension is rather unlikely, leading to the conclusion that the process is probably due to gravitational pull as the sediments are stacked on top of each other.

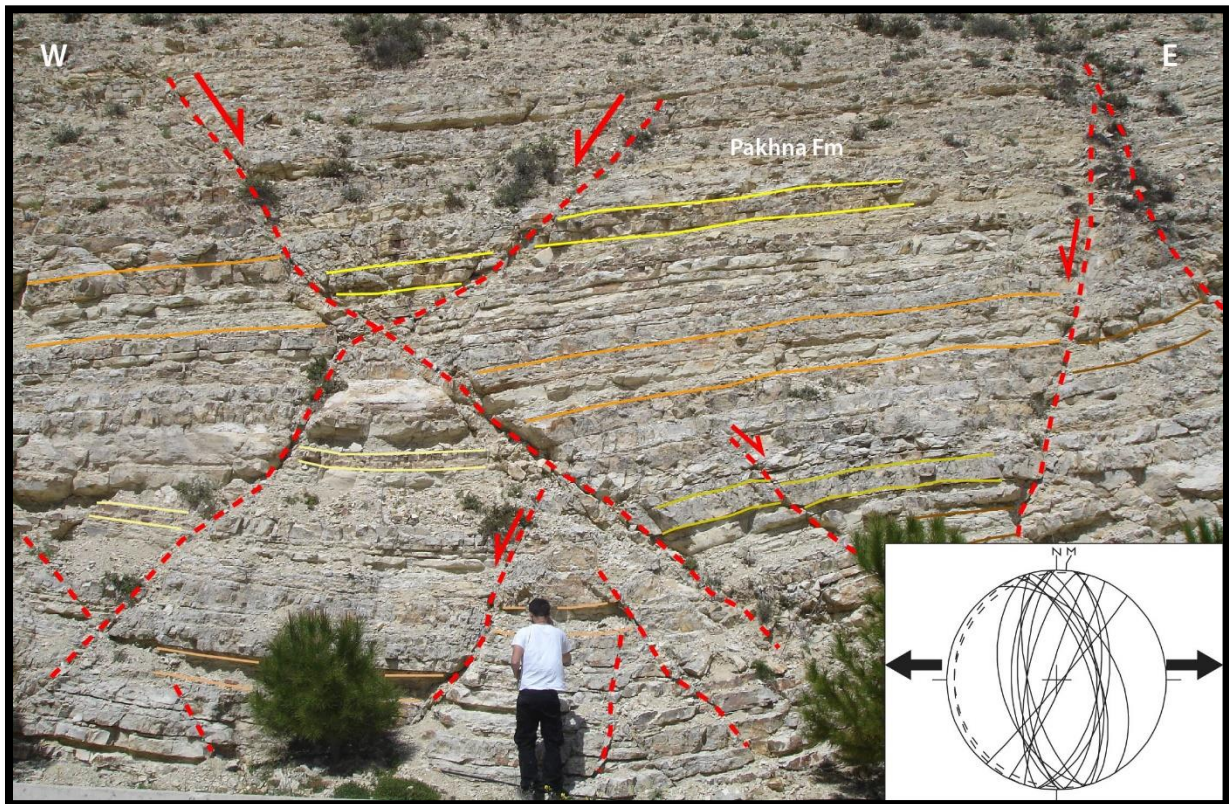


Figure 4 - 33: Photograph depicting normal faults in the Pakhna formation, near the village of Omodos, indicating extension in an E-W direction. Outcrop location shown in Figure 4 - 27, position 21.

4.4.3 Transpressional regime

At the center of the Limassol Basin at two localities meso-scale faults bearing Riedel shear fractures were identified. At Monagri (Figure 4 - 27, position 22), the faults measured in the chalks of the Pakhna Formation illustrate a sinistral and dextral strike slip deformation, with the dextral one being more numerous. Fault inversion indicates a strike slip regime with a maximal principal stress  $\sigma_1$  axis oriented in a NNE-SSW direction (Figure 4 - 34). At Alassa (Figure 4 - 27, position 23) a conjugate strike slip system was observed with a maximal principal stress  $\sigma_1$  axis oriented in in a NNE-SSW direction and indicates a compressional regime (Figure 4 - 35). Considering the continuous uplift of Cyprus and the similarities between the two outcrops, the stress state characterized here may point towards a Late Miocene to Pliocene transpressional regime, which could be associated with the westward escape of the Anatolian micro plate.



Figure 4 - 34: Panoramic photograph showing strike slip deformation in the Pakhna Formation near the village of Monagri. Strike slip faulting observed from Riedel steps and calcite deposition illustrating a transpressional regime in a NNE-SSW which could be connected with the change in deformation style in Late Miocene to Pliocene time to a strike slip regime. Outcrop location shown in Figure 4 - 27, position 22.

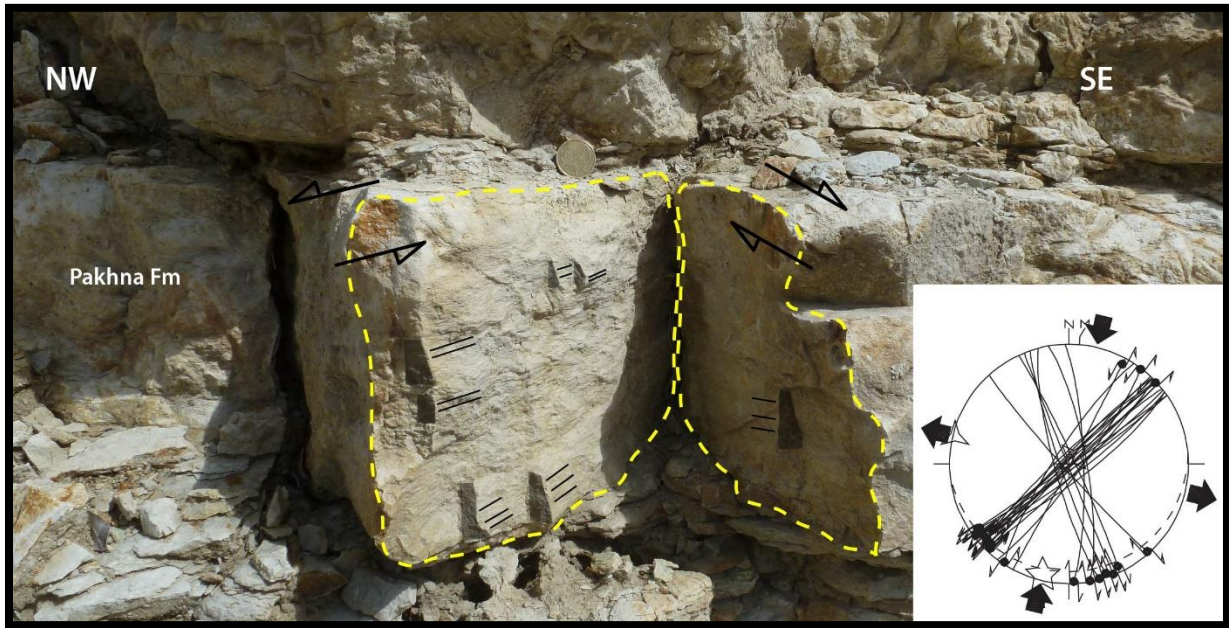


Figure 4 - 35: Photograph showing strike slip movement in the Pakhna Formation near the village of Alassa. A conjugate strike slip system is observed illustrating a transpressional regime in a NNE-SSW which could be connected with the change in deformation style in Late Miocene to Pliocene time to a strike slip regime. Outcrop location indicated in Figure 4 - 27, position 23.

#### 4.5 Synthetic Cross sections

In order to better comprehend the tectonic evolution and compare both the Polis and Limassol Basins, three cross sections were constructed (Figure 4 - 2 and Figure 4 - 36). In the Polis Basin, one cross section covers the northern part of the basin (A-B) passing through the Akamas Peninsula (A) towards the Troodos Ophiolites (B) (Figure 4 - 36 and Figure 4 - 38). The second cross sections passes through the centre of the Polis Basin (C-D), from the Pegeia area (C) and stops at the Troodos Ophiolites (D) (Figure 4 - 36 and Figure 4 - 42 ). In the Limassol Basin one cross section cross cutting the center of the basin was constructed (Figure 4 - 46). The positioning of the cross sections was carefully picked in order to underline the different tectonic and sedimentary contacts in the basin. As described above, various field observations, dip measurements, bio-stratigraphic dating and borehole data were used to construct the cross sections and constrain the timing of deformation.

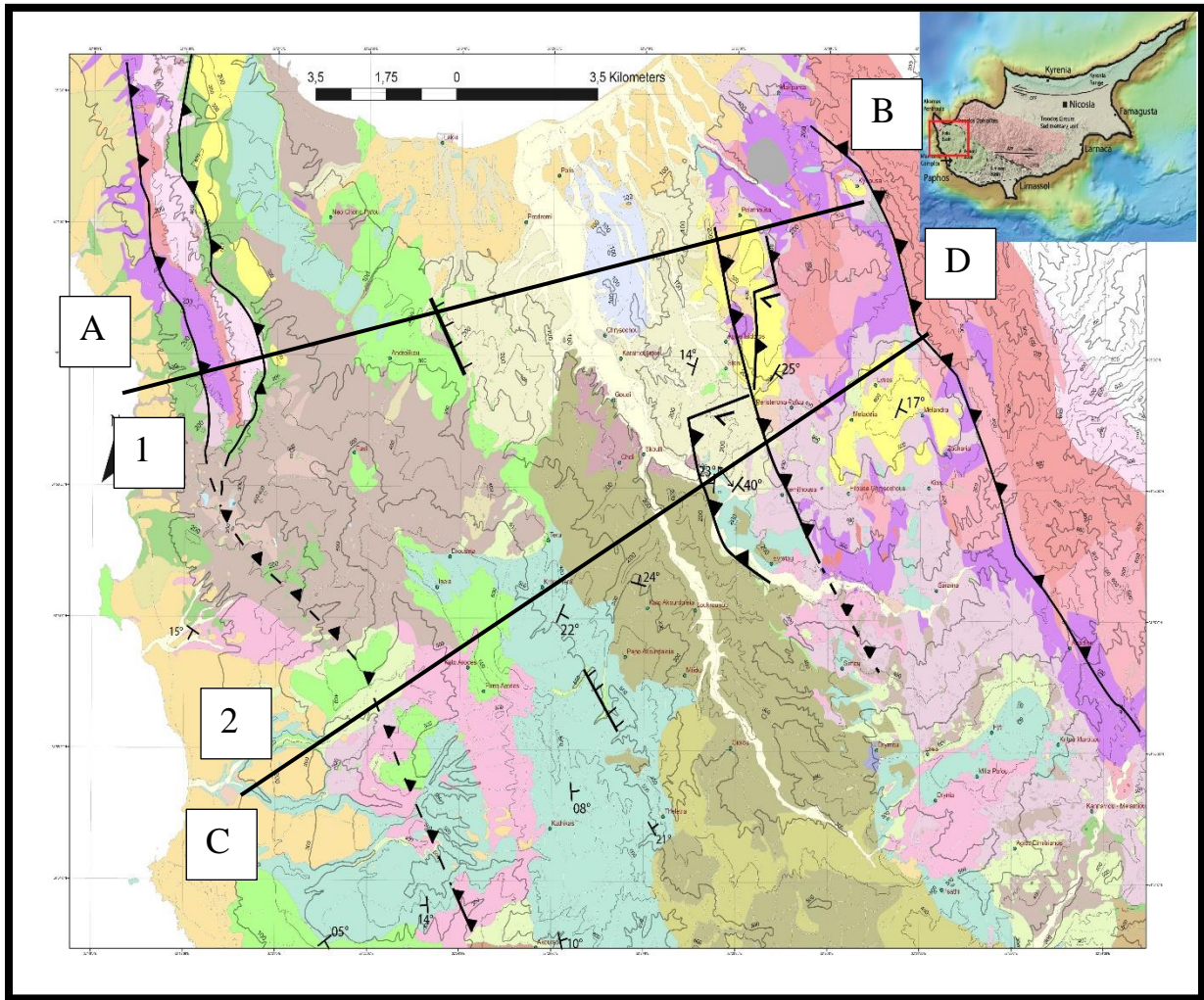


Figure 4 - 36: Geological map of west Cyprus (from GSD, compiled by the maps of Lapierre, 1971; Turner, 1992; Zomeni and Tsiolakis 2008; Zomeni and Georgiadou, 2015) illustrating the locations of the two cross sections. Cross section A-B cuts the Akamas Peninsula (A) in the West and passes through the Polis Basin and ends at the western flank of the Troodos Mountain (B). Cross section C-D starts from the coastline close to the village of Pegeia (C) and cross cuts the Polis Basin through to the village of Lysos (D), close to the foothills of the Troodos Mountain.

#### 4.5.1 Cross sections in Polis Basin

Previous studies have connected the creation of the Polis Basin by extensional processes such as thick skinned normal faults which deform the whole sedimentary sequence [Payne and Robertson, 1995]. The mechanism described for the extensional processes (Figure 4 - 37) was

connected with the continuous northward movement of the African plate and later slab roll-back of this plate. This resulted in the creation of major normal faults of Middle to Late Miocene age, trending in a NW-SE direction which border the east and west flanks of the Polis basin [Payne and Robertson, 1995].

During the two surveys, convincing evidence of major normal faults was elusive. Normal faults recognized on the western flank of the Polis Basin appear to cut the Middle Miocene sediments and are dipping towards the NE. These faults appear to stretch for a few kilometres only and are very local. In contrast, areas where Upper Cretaceous sediments are in contact with Cenozoic sediments have been identified, indicative of compressional structures.

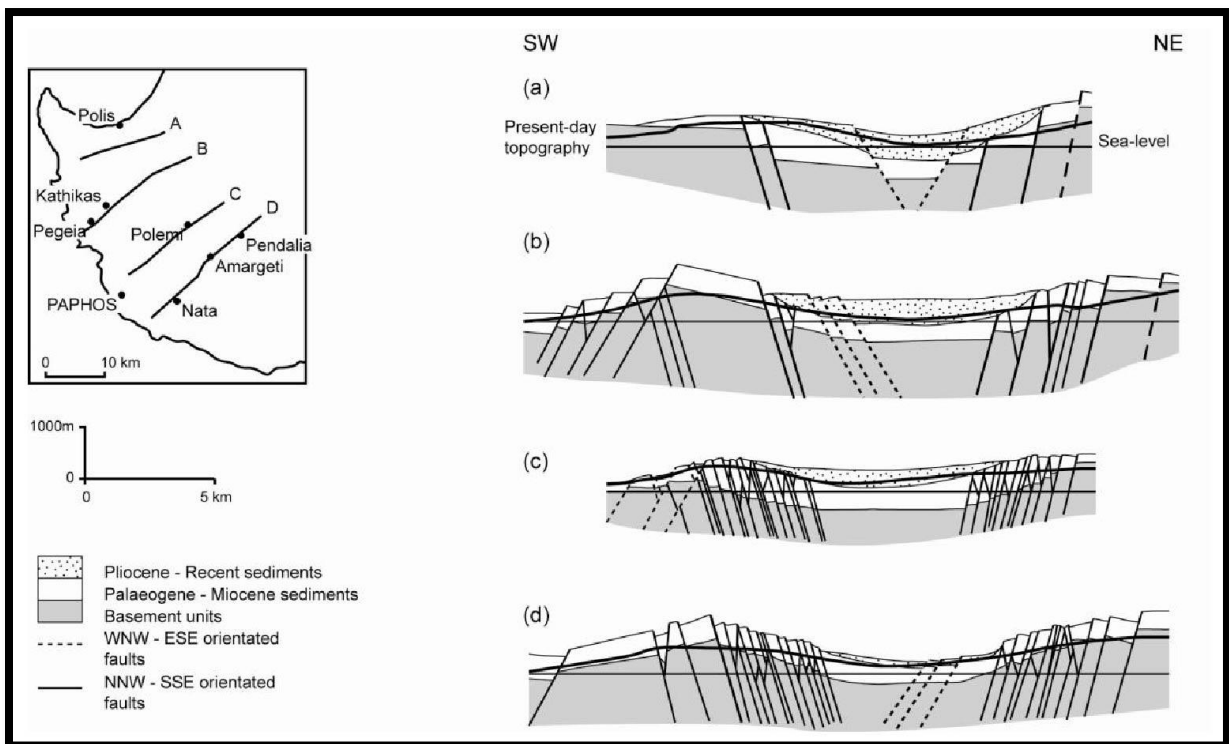


Figure 4 - 37: Structural cross-sections through the Polis Basin (Payne and Robertson, 1995; 2000). Thick lines denote first-order faults (dashed = inferred) and thin lines denote second-order faults. Inset shows the location of the Polis Basin, the locations of the cross-sections and several villages discussed in the text below.

In order to compare these contrasting observations, two cross sections are proposed which are composed from field observations such as tectonic structures and sedimentological records, as they were documented during two field campaigns in NW Cyprus.

The cross sections of the Akamas Peninsula-Pelathousa (Figure 4 - 36, Figure 4 - 38) and Pegeia-Lysos (Figure 4 - 36, Figure 4 - 42) cross cut the Polis Basin on the northern and central part of the structure. The thickness of the formations is a combination of previous descriptions of the sedimentary formations [Swarbrick and Robertson, 1980; Greensmith, 1994] and the borehole data described above (see section 4.1.1).

The meso-scale and large scale tectonic structures recognized during the two field surveys indicate a displacement towards the SW on the eastern and western flank of the Polis Basin, with an exception in the Akamas Peninsula where the displacement is towards the west. For this reason, the cross sections were built in a NE-SW direction perpendicular to the main fault direction. The sedimentary units used for the creation of the cross sections are based on the outcropping Cenozoic (Nicosia, Koronia member, Pakhna, Tera Member, Lefkara Formations), Cretaceous (Kathikas, Kannaviou, hartzburgite/serpentinites, pillow lavas) and Triassic (Mamonia Complex) formations. The thickness of the sediments was constrained through field observations (i.e. Androlykou quarry) and via the available borehole data (see section 4.1.1). The depth of the formations is arbitrary as no deep borehole data are available in the vicinity and it is based on previous studies [Swarbrick and Robertson, 1980]. The fault geometry at depth follows the scenario of thick skinned deformation.

The first cross section (A-B, Figure 4 - 38) that passes through the Akamas Peninsula-Polis Basin consists of 6 thrust faults starting from the T1 belt which corresponds to structures at the southwest foothill of the Troodos Mountain. The T1 thrust is the main structure that bounds the Neogene Polis Basin to the NE. Thrusts T2, 3 are deforming the stratigraphic sequence of the Akamas peninsula, effectively folding the pillow lavas and the Mamonia Complex and through hydrothermal fluid circulation they result in the deformation of the hartzburgite into serpentinite. Thrust T4 is envisaged as a thrust cutting through the Neogene units and constituting today's eastern flank of the Polis Basin. This thrust uplifts and tilts the Koronia Member reefs towards the east. In the center of the Polis Basin, the Tera Member reefs observed in the Androlykou quarry, pass directly to Pliocene deposits of the Nicosia Formation. Thus a normal fault which flattens at depth, with a decollement level in the Mamonia Complex is proposed to explain the juxtaposition of the two formations.

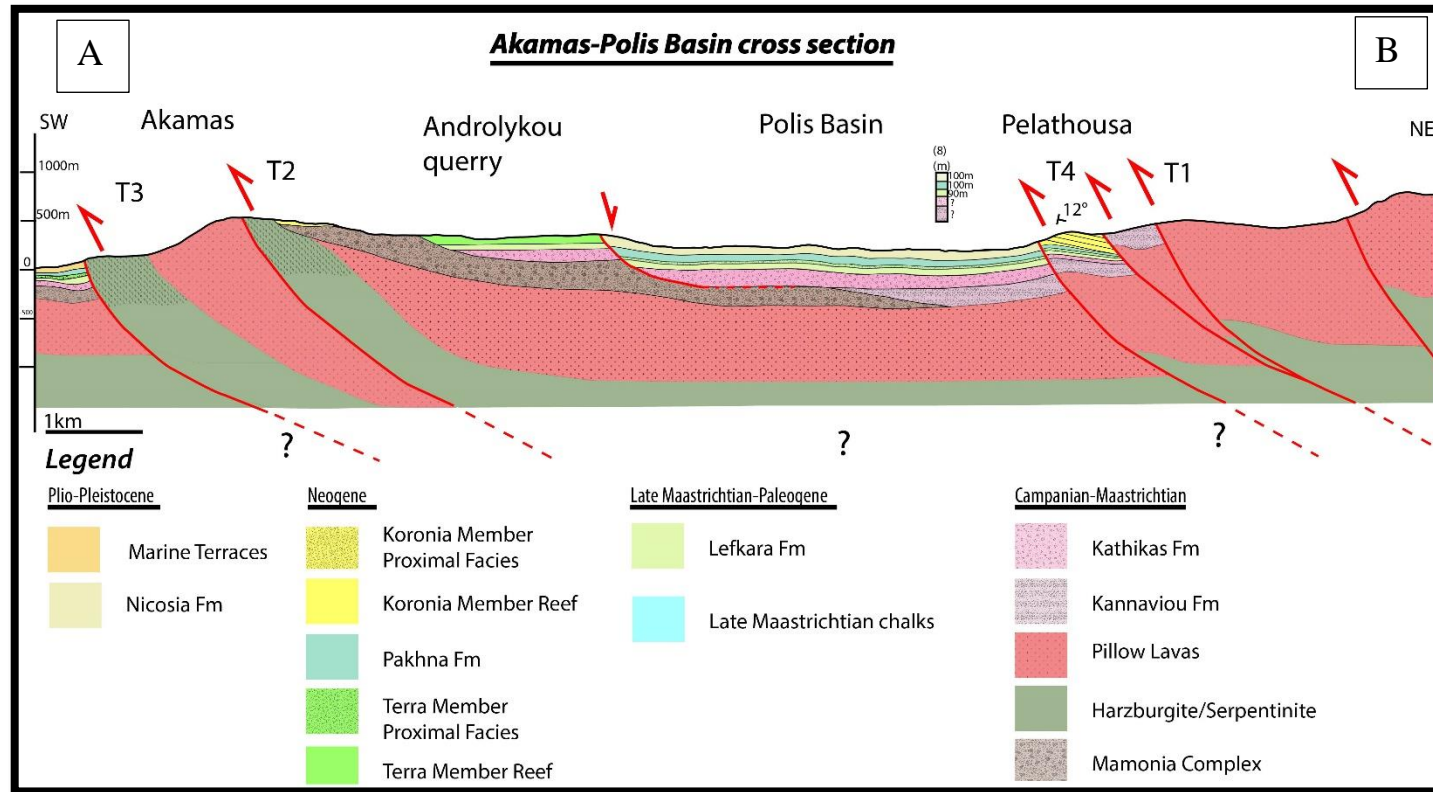


Figure 4 - 38: Cross section passing from the Akamas Peninsula to the Troodos ophiolites illustrating the contacts and the tectonic structures in the Polis Basin. Location of cross section illustrated in Figure 4 - 36 (profile A-B). Location and description of borehole data indicated in Figure 4 - 2 and Figure 4 - 3 (borehole 8). Note: Basement level is arbitrary.

A schematic re-construction of the basin through time is presented in various geological time frames. This step was utilized in order to constrain the deformation, to evaluate the depth of the outcropping and the deeper sedimentary units and to assess the development of the tectonic structures. Unfortunately no slip rates are recorded in the area and thus the shortening rate is not proposed as it is difficult to constrain, indicating that although the proposed model for the deformation in western Paphos works, uncertainties still exist.

Considering the following constraints, a schematic reconstruction commencing from Late Cretaceous until Plio-Pleistocene times is proposed. In Campanian time the Mamonia Complex is juxtaposed on the western flank of the Troodos ophiolite and it is perceived that Mamonia Complex are underlain by the Troodos ophiolites in the Polis Basin. Previous studies [Swarbrick and Robertson, 1980] propose that the Kannaviou Formation (composed of grey marls and bentonitic clays) was deposited in hollows which resulted from the uplift (displacement from T1) and the emplacement of the ophiolites of the Troodos Mountain. In accordance it is proposed here that the first thrust, T1 which trends NW-SE, was active during the Campanian (Figure 4 - 39). The product of this uplift was the Kannaviou Formation that infilled the center of the existing basin.

During the Maastrichtian, three thrust faults are proposed, T1 in the Troodos Mountain and T2/T3 in the Akamas Peninsula (Figure 4 - 39). The center of the basin is covered by the deposition of the Kathikas Formation. At the west flank of the basin, the Mamonia Complex is folded and at the top of the Akamas Peninsula, serpentinites are outcropping. West of T3 a small flexural basin is envisaged due to the activity of the fault. Thrusting activity is envisaged at the Akamas Peninsula as it is expressed by the exposure of pillow lavas and serpentinites. It is inferred that this uplift is responsible for the exposure and subsequent erosion of the Mamonia Complex which results in the deposition of the red bentonitic clays of the Kathikas Formation [Swarbrick and Robertson, 1980] further south (Figure 4 - 39) connected with the convergence between the African and Eurasian continental plates.

In Paleogene time the deep pelagic chalks, cherts and marls of the Lefkara Formation [Lord et al., 2000] are deposited on top of the existing sedimentary sequence. A deep open basin developed and no fault activity is envisaged in the area at that time, leading to the suggestion that the Lefkara Formation deposits cover the whole area (Figure 4 - 40), with thin layers on top of the Troodos ophiolite and the Akamas Peninsula, with a thicker sequence deposited in the center of the Polis Basin.

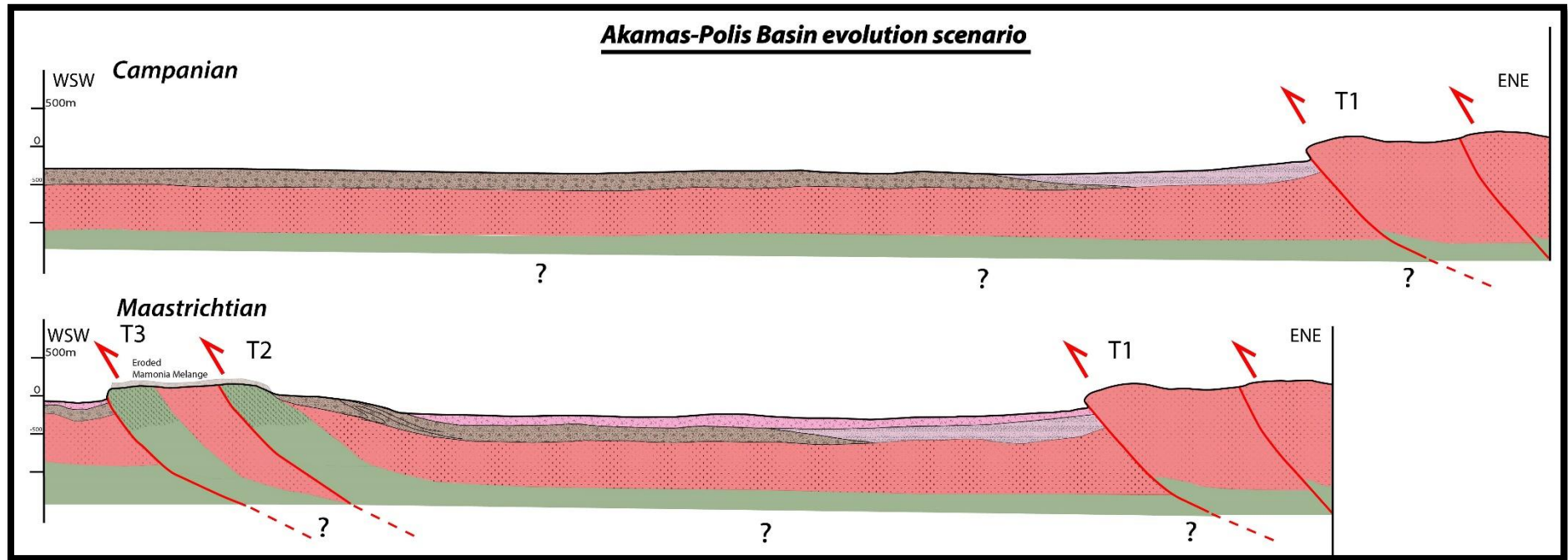


Figure 4 - 39: Reconstruction model illustrating the tectonic activity of the northern part of the Polis Basin (Campanian-Maastrichtian). Red lines indicate active thrusting, while black lines indicate inactivity. Location of cross section illustrated in Figure 4 - 36 (profile A-B). Note: Basement level and shortening rates are arbitrary. Legend as in Figure 4 - 38.

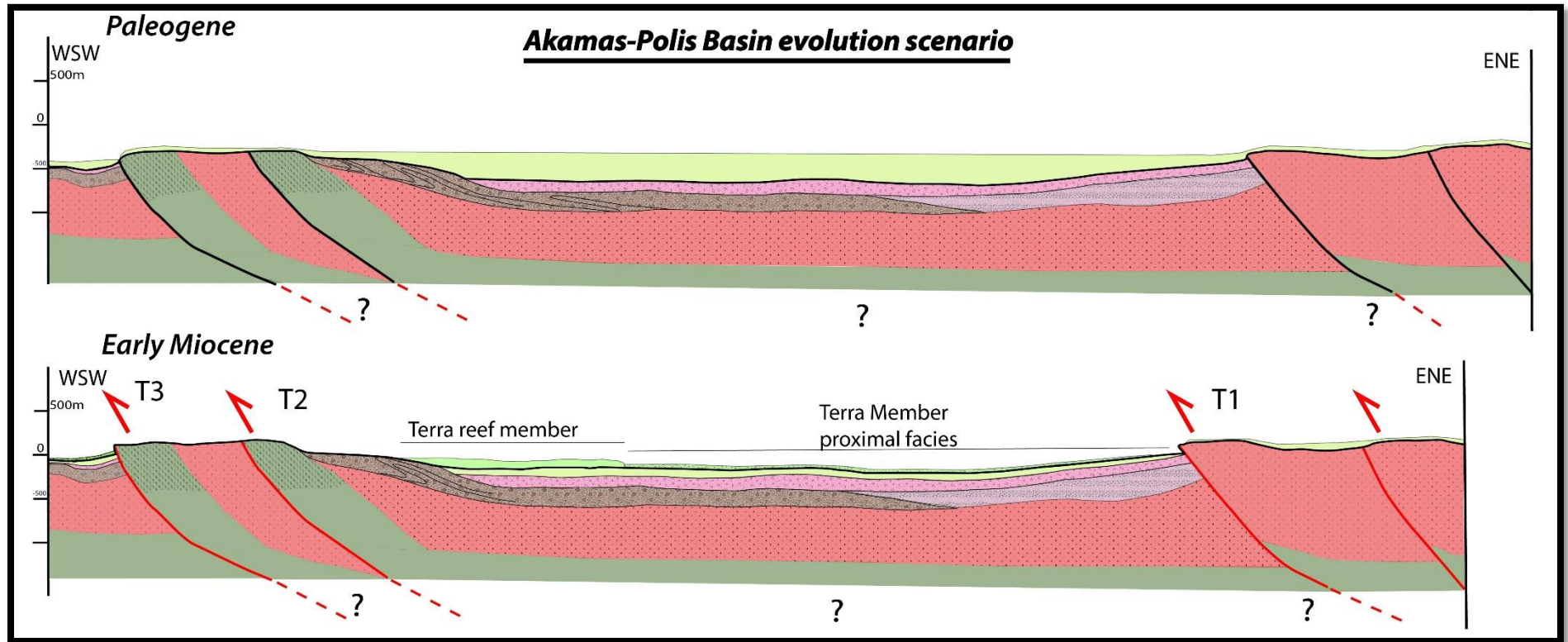


Figure 4 - 40: Reconstruction model illustrating the tectonic activity of the northern part of the Polis Basin (Paleocene-Early Miocene). Red lines indicate active thrusting, while black lines indicate inactivity. Location of cross section illustrated in Figure 4 - 36 (profile A-B). Note: Basement level and shortening rates are arbitrary. Legend as in Figure 4 - 38.

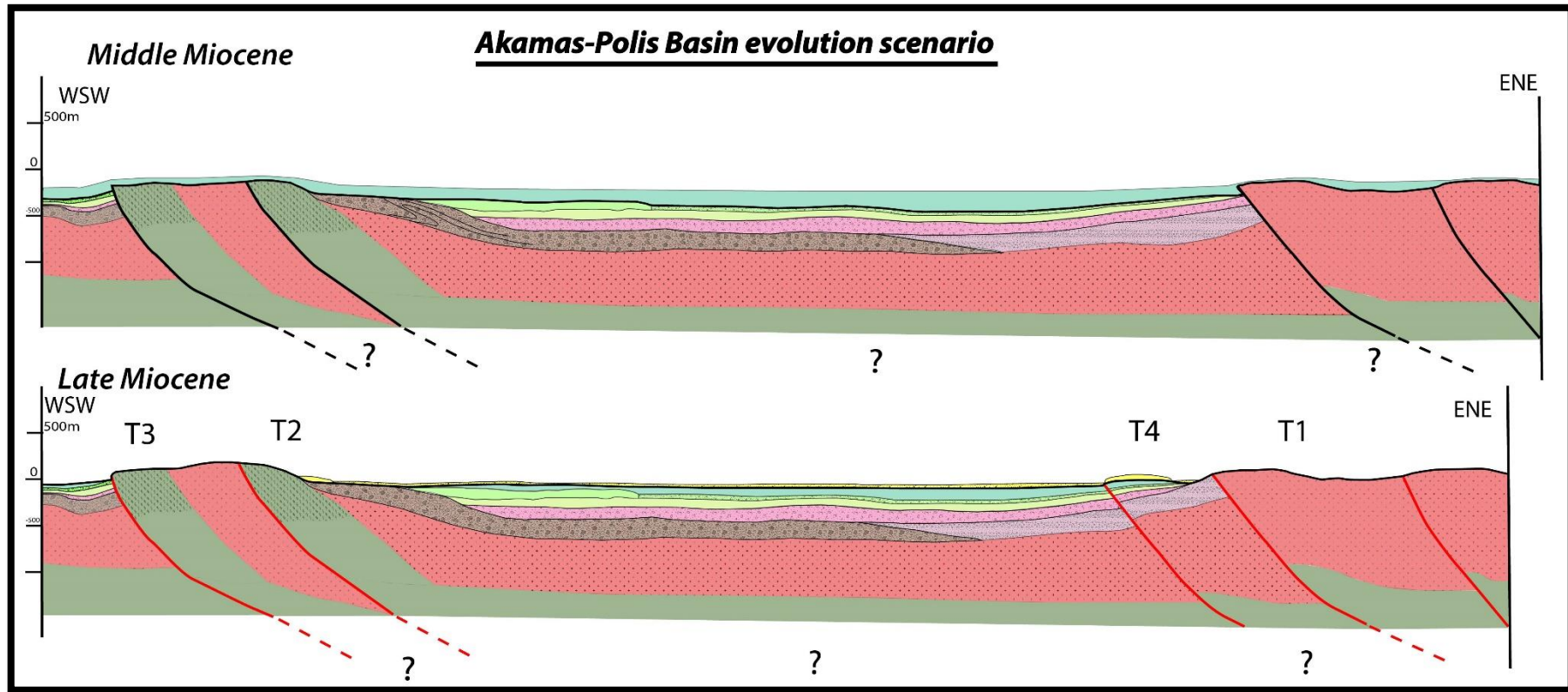


Figure 4 - 41: Reconstruction model illustrating the tectonic activity through time of the northern part of the Polis Basin (Middle-Late Miocene). Red lines indicate active thrusting, while black lines indicate inactivity. Location of cross section illustrated in Figure 4 - 36 (profile A-B). Note: Basement level and shortening rates are arbitrary. Legend as in Figure 4 - 38.

The structures modelled in the Early Miocene scenario mark the first Cenozoic tectonic phase. This major event occurred in Oligocene-Early Miocene time and is associated with the continuous convergence between the African and Eurasian continental plate, which resulted in a regional uplift and a change in the depositional environment passing from the deep pelagic chalks and cherts of the Lefkara Formation to the Early Miocene reef limestones of the Tera Member. An unconformity could exist between the two formations as it was observed from the field (Panorama view north of Pegeia village), with the patch reefs attesting underwater areas, while the karstified surface is equivalent to areas above sea level. All the thrust structures T1, T2 and T3 are proposed as active faults at this time. The activity of thrust T2 is suggested by the deposition of the Tera Member reef limestones at the western flank (Figure 4 - 40), perfectly exposed at the Androlykou quarry (Figure 4 - 5). This thrust movement results in the folding of the Mamonía Complex on the hanging wall of the T2 which places it at an adequate depth from the sea level in order to deposit the reefal limestone. East of T2, the Mamonía Complex is outcropping in accordance with the field observations from the Akamas Peninsula. In contrast it is proposed that in the center of the basin, chalks which are associated with the proximal facies of the Tera Member, are deposited due to the activity of T3 and the flexure of the basin.

A period of low tectonic movement is envisaged for the Mid-Miocene as sedimentation changes to the hemi-pelagic chalks and marls of the Pakhna formation [Lord et al., 2000]. The Pakhna deposition covers the whole area (Figure 4 - 41), possible the Troodos Mountain as well. The Late Miocene marks the second tectonic event that deformed the area. During Late Miocene T3 and T4 are envisaged to be active as reef limestones of the Koronia Member [C. Blanpied, pers. comm., 2017] are deposited near the villages of Neo Chorio Paphou (west flank) and Pelathousa (east flank) (Figure 4 - 41). The observation of Tortonian reefs on both flanks of the basin, indicate activity on existing thrusts (west flank) and out of sequence thrusting (east flank). No data exist for the underlying formations at this locality however it is proposed that a thin layer of Pakhna Formation is underlying the Koronia reefs.

During Pliocene time, the island is uplifted to its current topography with all the pre-existing thrusts active (Figure 4 - 38) in connection with the collision of the Eratosthenes micro continent with Cyprus. Pliocene thrusting of T4 uplifts the northeast flank of the Polis Basin, whereas the center of the basin is infilled by clastic sediments of the Nicosia Formation, which was confined in the center of basin as it is evidenced from the borehole data (Figure 4 - 3) and by field observations. The composition of the formation consists of clastic material eroded from the existing limestones [Lord et al., 2000]. Another result of the thrust movement of T4 is the eastward tilting of the Koronia Member reef units on the northeast flank of the Polis Basin. East of the Androlykou quarry the Pliocene Nicosia sediments juxtapose the Early Miocene reef

limestones of the Tera Member, thus prompting the proposition of a Pliocene normal fault to explain this contact. This normal fault proposed (Figure 4 - 38) in the center of the basin is connected with a gravitational process as a result of the uplift of the Akamas Peninsula, thus creating accommodation space for the deposition of the Nicosia Formation.

The second cross section C-D runs from SW to the NE and cuts the Polis Basin (Figure 4 - 36 and Figure 4 - 42). A similar approach for analyzing the evolution of the structures was undertaken for this cross section. In the NE thrust T1 is believed to be a continuation of the thrust described in cross section A-B. T4 is correlated with the thrust fault in front of Peristerona village (as in A-B) and T2 is connected to the Kathikas Thrust (Figure 4 - 42) described in section 4.2.1, which splits in two branches (Figure 4 - 42). At the center of the basin a normal fault is suggested as it was observed near the village of Pano Akourdalia (Figure 4 - 42) and a reverse fault is proposed as it was mapped in the field (Figure 4 - 42). The thickness of the beds is in accordance with the borehole data, with the location of each borehole indicated on the cross section (Figure 4 - 42).

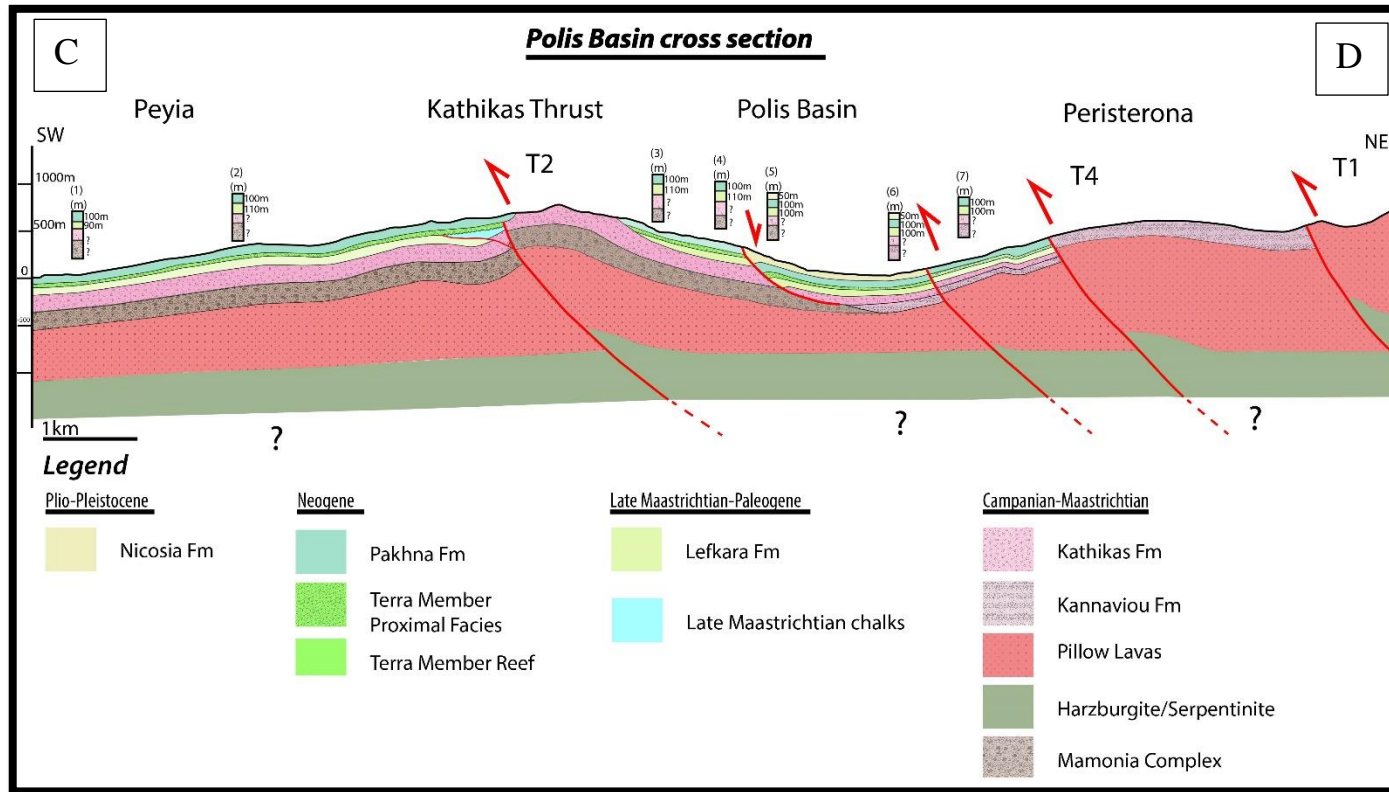


Figure 4 - 42: Cross section passing from the Pegeia village to the Troodos ophiolites illustrating the contacts and the tectonic structures of the central part of the Polis Basin. Location of cross section illustrated in Figure 4 - 36 (profile C-D). Location and description of borehole data indicated in Figure 4 - 2 and Figure 4 - 3 (boreholes 1-7). Note: Basement level and shortening rates are arbitrary.

A schematic reconstruction was carried out for the second cross section based on the same criteria discussed in the previous paragraphs and highlight at least three major tectonic events discussed (Oligocene-Early Miocene, Late Miocene, Plio-Pleistocene). It is believed that T1 extends until the central segment of the Polis Basin. Similarly as before, thrusting activity is envisaged in Campanian time with the uplift of the Troodos pillow lavas and the deposition of the Kannaviou Formation in the Polis Basin (Figure 4 - 43), in contact with the Mamonia Complex.

In Maastrichtian time, the south part of the Polis basin is infilled with the red bentonitic clays of Kathikas Formation (Figure 4 - 43). This deposition is connected with the thrusting activity of T2 further north, which results in the uplift and erosion of the Mamonia Complex at the Akamas Peninsula (Figure 4 - 39) and the deposition of the Kathikas Formation (Figure 4 - 39 and Figure 4 - 43).

During the Paleocene time deep pelagic chalks and cherts of the Lefkara Formation are deposited which suggests tectonic quiescence and subsidence of the basin (Figure 4 - 44) probably connected to thermal subsidence as it is similarly proposed in the Levant Basin. The Lefkara Formation possibly covers the whole area. The thrust fault illustrated in the reconstruction is believed to have commenced its activity prior to the big event described below for the Oligo-Miocene time.

During the Oligocene to Early Miocene time, thrust T2 is proposed for the first time, the Kathikas Formation and the Mamonia Complex are folded and Tera Member reef limestone is deposited east of T2. West of the thrusts (T2) a blind thrust is modeled uplifting Late Maastrichtian chalks. It is suggested that thrust T2 propagates towards the south and uplifts the Kathikas Formation as it is observed near the village of Kathikas (Figure 4 - 44). The clear geometry of the thrust is not observed in the field as the area is covered by the Mamonia Complex. Thus it is believed that the thrust either curves from the Akamas towards the village of Kathikas, or it is segmented into two (Figure 4 - 44). The second branch, corresponds to the thrust described north of the village of Pegeia (Panorama locality) which puts in contact Late Maastrichtian chalks with Burdigalian chalks. The hiatus is interpreted as the time of movement of the thrust.

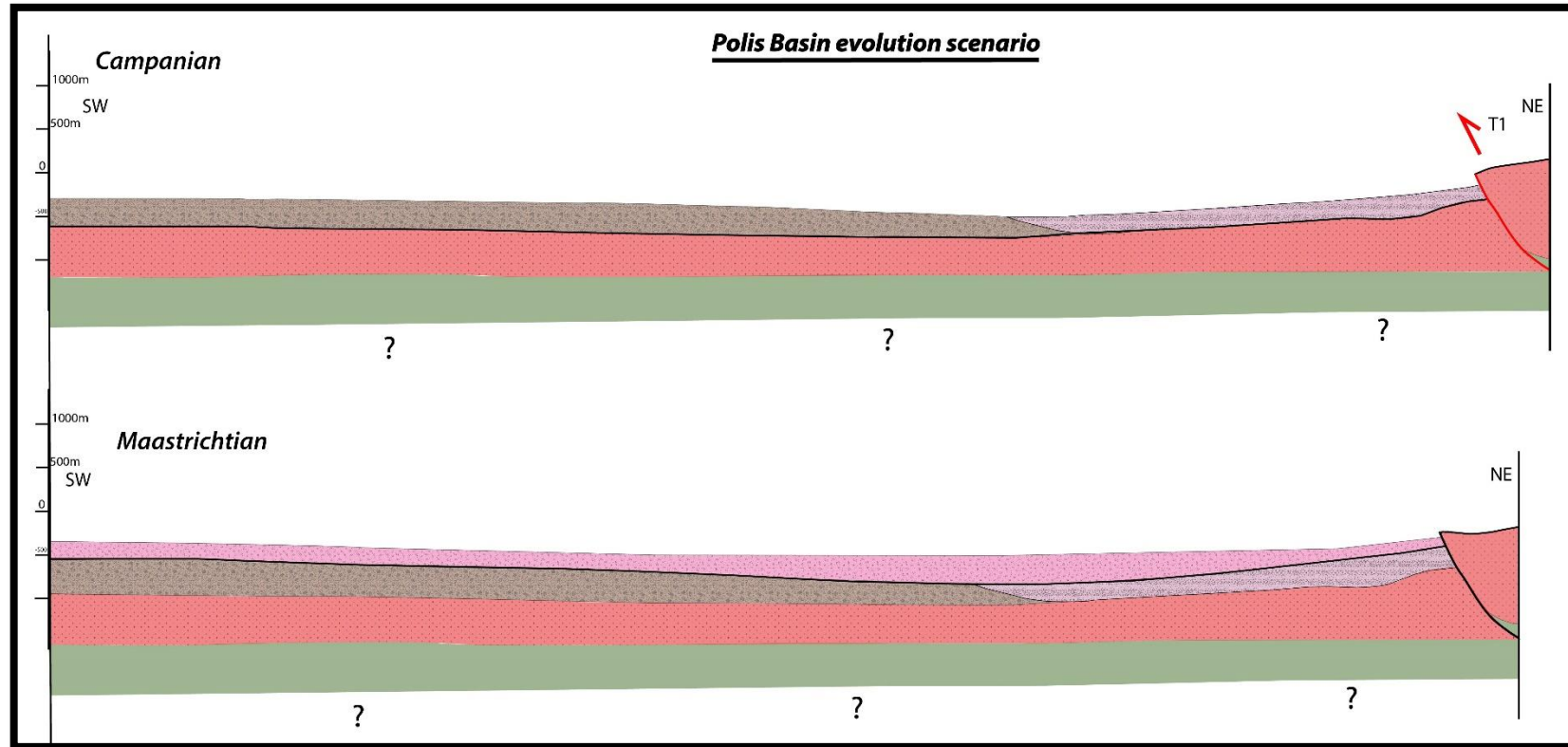


Figure 4 - 43: Reconstruction model illustrating the tectonic activity of the central part of the Polis Basin (Campanian-Maastrichtian). Red lines indicate active thrusting, while black lines indicate inactivity. Location of cross section illustrated in Figure 4 - 36 (profile C-D). Note: Basement level and shortening rate are arbitrary. Legend as in Figure 4 - 42.

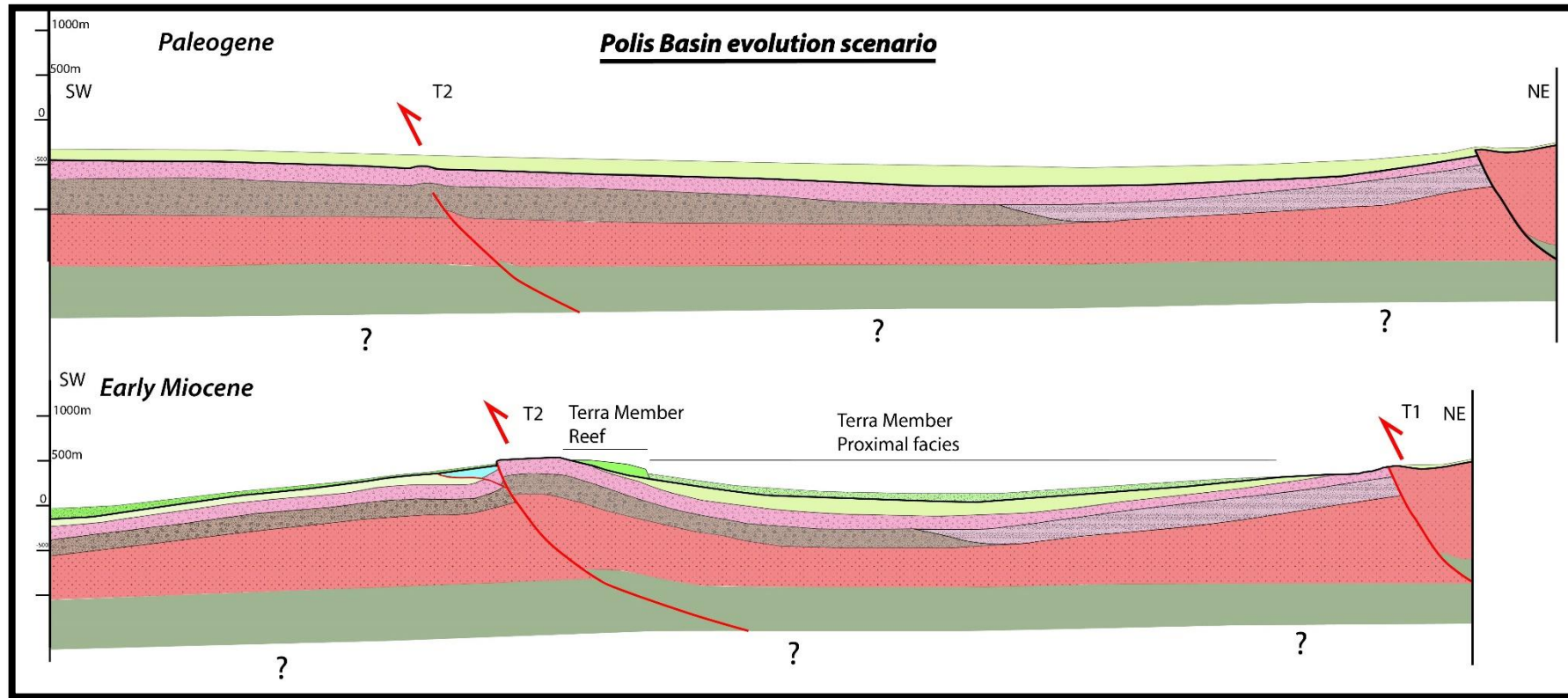


Figure 4 - 44: Reconstruction model illustrating the tectonic activity of the central part of the Polis Basin (Paleogene-Early Miocene). Red lines indicate active thrusting, while black lines indicate inactivity. Location of cross section illustrated in Figure 4 - 36 (profile C-D). Note: Basement level and shortening rate are arbitrary. Legend as in Figure 4 - 42.

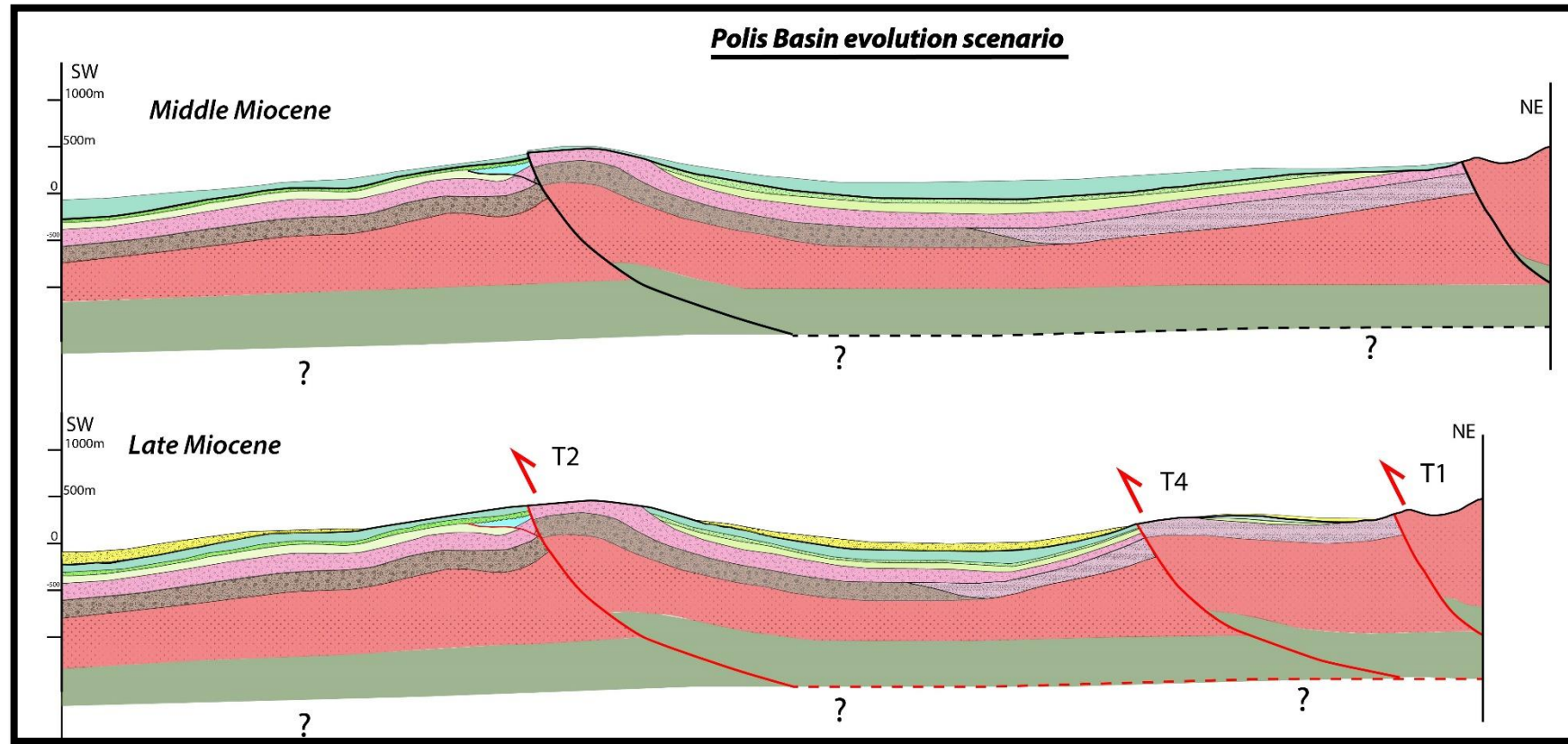


Figure 4 - 45: Reconstruction model illustrating the tectonic activity of the Polis Basin (Middle-Late Miocene). Red lines indicate active thrusting, while black lines indicate inactivity. Location of cross section illustrated in Figure 4 - 36 (profile C-D). Note: Basement level and shortening rate are arbitrary. Legend as in Figure 4 - 42.

The Middle Miocene is connected with the deposition of the Pakhna Formation which covers the whole Polis Basin, with the thicker deposits encountered at the center of the basin (Figure 4 - 45). In Late Miocene, T4 activity is proposed in connection with the deposition of the Koronia Member reef limestone near the village of Peristerona Paphou (Figure 4 - 45). The deposits at this locality have not been dated but due to its close proximity, same tectonic activity of T4 and the trend of the reefs, it is believed that they are of the same age as the reefs observed at Pelathousa.

In Pliocene a similar scenario is envisaged as that described above for the northern extend of the Polis Basin, with the uplift of the island and the erosion of the existing formations resulting in the deposition of the Nicosia Formation in the center of the basin (Figure 4 - 42). At the western flank of the Polis Basin near the village of Pano Akourdalia a normal fault was observed which cuts the Pakhna sediments. It is believed that fault F2 is related to a gravitational mechanism, due to the thick deposits of Pakhna at this locality and the vergence of the sediments towards the center of the basin (see 4.1.2, Figure 4 - 42).

### *4.5.2 Cross section in the Limassol Basin*

The cross section of the Limassol Basin was based on the synthetic stratigraphic logs created through field observations. The Pakhna Formation covers the most part of the Limassol Basin, with the Lefkara Formation outcropping just south of the Gerasa Fold and Thrust Belt, while north of the thrust fault, the Troodos ophiolites are exposed. The geometry of the beds was constructed from bed dips measured from the field (Figure 4 - 46). The thickness of the Pakhna Formation is thinning towards the north. At the southern coastline the thickness of the formation was ~650m while at the northern part of the Limassol Basin at the foothills of the Troodos Mountains this sequence is considerably reduced to ~350m [N. Papadimitriou, pers. comm., 2017]. The base of the sequence was not consistently observed, except in one location at the northern flank of the basin near the village of Koilani. The difference in thickness is herein connected with the activity of the Gerasa Fold and Thrust Belt (Figure 4 - 46) which consists the northern border of the Limassol Basin. The Gerasa Thrust was active since Oligocene to Early Miocene time (see chapter 4.4) resulting in the uplift of the northern flank of the Limassol Basin, while the southern part was deeper, allowing for the deposition of a thicker layer of Pakhna Formation. The re-activation of the Gerasa Thrust in Pliocene time is inferred by the large contrast in the dip of the beds from North (~15°) to South (~2°, almost flat). Thus from the geometry of the Limassol Basin it is proposed that this is a flexural basin created by the activity of the Gerasa Thrust (Figure 4 - 46).

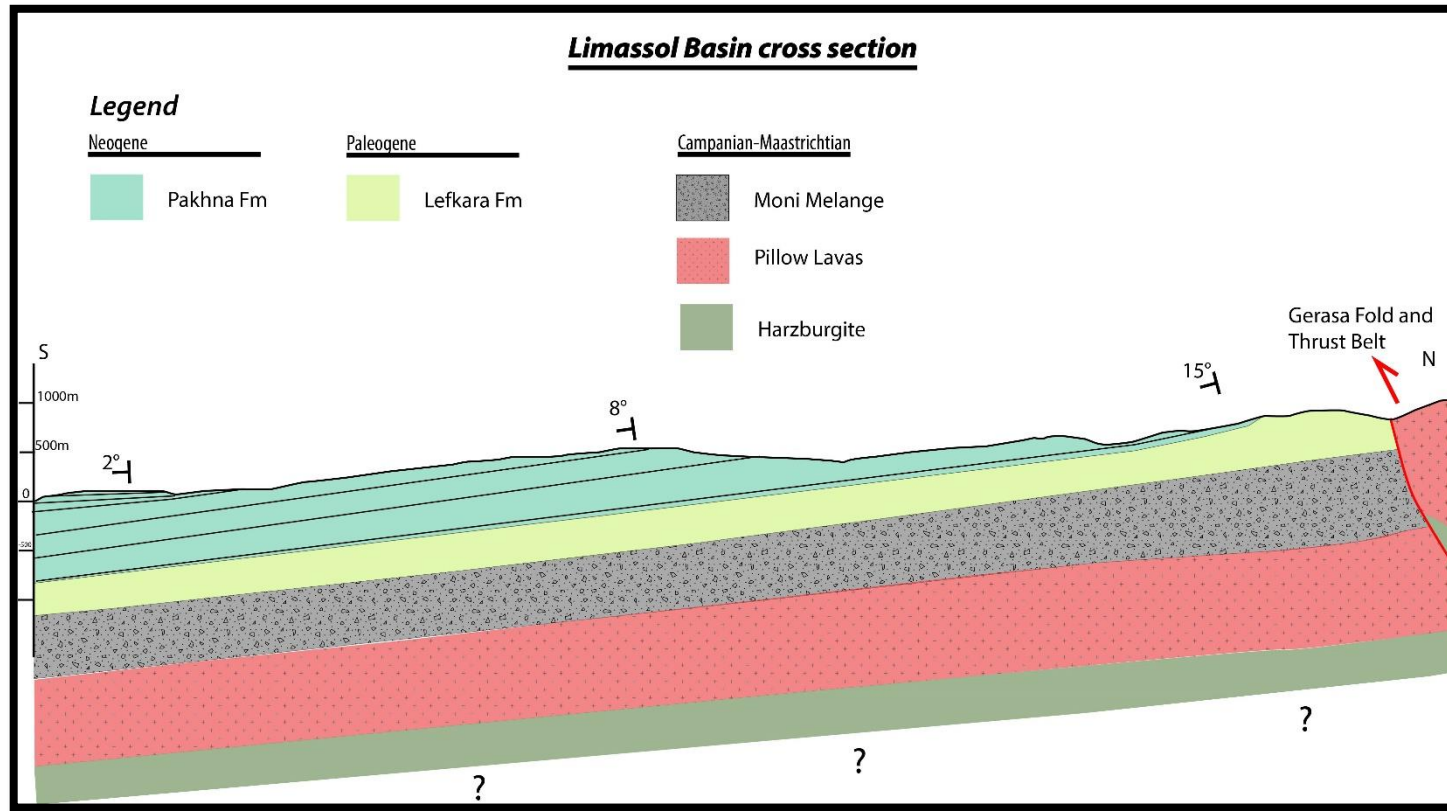


Figure 4 - 46: Cross section passing from the Paramali village to the Troodos ophiolites illustrating the contacts and the tectonic structures in the Limassol Basin. Location of cross section illustrated in Figure 4 - 2 (profile 3). Note: Basement level is arbitrary.

## 4.6 Discussion

Onshore informations acquired through field campaigns have proven useful in order to understand the tectonic evolution of the sedimentary basins and the tectonic structures on the island of Cyprus. It is with this knowledge that the timing of deformation is constrained. In this chapter different tectonic regimes are discussed as they were identified through field observations. Compressional structures were assessed, as were extensional and strike slip features. A number of major and meso-scale compressional and extensional structures were documented following the two field surveys. The new detailed maps illustrate the proposed structures which can be tied in with the cross sections and the reconstruction models.

Previous studies have described deformational events in southern Cyprus which were taken into account for the reconstruction models. These events start from the Campanian time with the juxtaposition of the Mamonia Complex with the southern part of Cyprus [Lapierre, 1975; Lapierre et al., 2008] and the creation of a suture zone as it is expressed at the Akamas Peninsula and in the Polemi Basin with the exposure of the serpentinites [Swarbrick, 1993; Swarbrick and Naylor, 1980; Bailey et al., 2000].

For the first time new data are presented herein which reinforce the proposition of an Oligocene to Early Miocene event as it is identified at the Kathikas Thrust (near the village of Pegeia) from the unconformity between the Burdigalian chalks and the underlying Late Maastrichtian chalks. In the Akamas Peninsula, the deposition of Tera Member reef carbonates (Androlykou quarry) is also connected with a tectonic uplift due to the tectonic movement of the thrusts at the high of the Akamas Peninsula. This interpretation, is in contrast with the work proposed by Payne and Robertson [1995; 2000], as they infer local normal faults which create a horst geometry for the deposition of the Tera reef limestones. In the Limassol Basin, an Oligocene to Early Miocene deformation is described on the eastern flank of the Gerasa Fault and Thrust belt as the Miocene Pakhna Formation rests unconformably on a steeply dipping Eocene Lefkara Formation or directly on the Maastrichtian Moni Formation [Eaton and Robertson, 1993]. Additionally in the Maroni Basin east of the Gerasa Fault and Thrust belt, pebbles of basalts, radiolarites and chert of the Lefkara Formation are identified in the Pakhna Formation, which is an indication of Early Miocene uplift and erosion of the eastern part of the Troodos ophiolites [Eaton and Robertson, 1993; Kinnaird, 2008]. The perceived lack of Oligocene deposits is in agreement with other authors that indicate a lack of Oligocene deposits in Syria [Al Abdala et al., 2010]. This hiatus is documented onshore Cyprus and Syria and could correspond to a regional N-S directed compressional event, probably due to the collision of the

northern part of the African plate with Cyprus [Biju-Duval et al., 1974; Sage and Letouzey, 1990] and the suture of the Zagros area [Agard et al., 2011].

Evidence of Late Miocene thrusting deformation are documented in the Polis and Limassol Basins. In the Polis Basin at the top of the Akamas Peninsula a brecciated contact between Late Miocene Koronia Member reefs and Campanian to Maastrichtian pillow lavas is identified which indicates an early Late Miocene thrust movement. In the eastern flank of the Polis Basin, the Pelathousa-Peristerona thrust is active as evidenced by the deposition of the Koronia Member reefs which are tilted towards the east and are in direct contact with the Campanian Kannaviou Formation (Figure 4 - 41). These observations of thrust displacement oppose the idea of large scale normal faults that control the evolution of the graben as it was proposed by Payne and Robertson [1995; 2000]. At the western flank of the Limassol Basin, near the village of Kouklia, folded Pakhna Formation units indicate a Late Miocene activity which is in agreement with the proposed Paphos Thrust system of Geoter [2005]. At the eastern flank of the Limassol Basin (Armenochori village), Koronia Member reef limestones are overlying the Maastrichtian Moni Formation, an indication of Late Miocene thrusting movement of the Gerasa Fault and Thrust belt, which is in agreement with data from Eaton and Robertson [1993]. At the southern part of the Limassol Basin, Eaton and Robertson [1993] propose a thrust fault which uplifts the Akrotiri High since Early Miocene time. These assumption is based on borehole data near the village of Akrotiri, where Pliocene sediments are overlying the Mamonnia Complex [Hadjistavrinou and Constantinou, 1977, Eaton and Robertson, 1993]. However the large thickness of the Pakhna Formation (~650m) at the southern part of the Limassol Basin is in contrast with this tectonic movement, therefore it is proposed herein that the thrust at Akrotiri High was active in Late Miocene time.

The Plio-Pleistocene time is envisaged as a period of tectonic uplift [Robertson, 1977; Pantazis et al., 1978; Sage and Letouzey, 1990; Orszag-Sperber et al., 1989; Follows et al., 1992; Eaton and Robertson, 1993; Kinnaird and Robertson, 2013]. The transition from the deposition of the chalks and marls of the Pakhna Formation to the calcarenites and sandstones of the Nicosia Formation is an indication of this thrusting movement. This is further documented in the southern part of the Limassol Basin (referred as the Pissouri Basin) as the Pliocene Fanglomerate is filled with ultramafic clasts eroded from the Troodos ophiolites [Stow et al., 1995]. Plio-Pleistocene thrusting in the Polis Basin is evidenced from the tilted Koronia Member reefs on the eastern flank of the basin.

Based on the field campaign observations, thrusting movements in the Polis and Limassol Basins were documented and a comparison between the two basins was undertaken. In NW Cyprus, a synthetic sedimentary log in the Pegeia area illustrates a thickness of ~150m of Pakhna Formation chinks and marls, while boreholes in the center of the Polis Basin indicate a thickness of ~100m [N. Papadimitriou, 2017, pers. comm.]. In contrast a synthetic log in the southern part of the Limassol Basin indicates a thickness of ~650m of Pakhna Formation sediments, whereas on the northern flank of the basin the thickness is reduced to ~250m [N. Papadimitriou, 2017, pers. comm.]. This large difference in sedimentary deposition in the Polis and Limassol Basin illustrates the differentiation between the two basins, which could be explained from the observed tectonic structures in both basins.

In the Polis Basin the thrust fault propagates from the foothills of the Troodos Mountains (northwestern continuation of the Gerasa Fold and Thrust belt) towards the Akamas Peninsula thrust structures near the village of Neo Chorio Paphou (towards the west), causing an uplift of the basin and restricting the depositional space of the Pakhna Formation. The close proximity and synchronous movement (Figure 4 - 40) of these two structures in Oligocene to Early Miocene, could be the reason of the reduced space in the Polis Basin. In Late Miocene time, the movement of the Pelathousa and Peristerona thrust at the eastern flank of the Polis Basin, results in the deposition and tilting of Koronia Member reef limestones and indicates an out of sequence thrusting movement. Thus the Polis Basin is considered as a piggy back basin with the infilled basin carried forward on moving thrust sheets [Ori and Friend, 1984]. The identification of serpentinites which are a product of metamorphism and migration of the deeper sitting harzburgite, at the Akamas Peninsula and at the village of Agia Varvara Paphou, are interpreted as evidence of thick skinned tectonic activity.

In contrast, in the Limassol Basin only the Gerasa Fold and Thrust belt is active in the Oligocene to Early Miocene, uplifting the Troodos Mountains and deepening the basin. A higher rate of uplift is envisaged on the southeastern part of the Gerasa Fold and Thrust belt as evidenced by the ultramafic pebbles in the Pakhna Formation in the Maronia/Psematismenos Basin. Evidence of thrust movement of the Paphos Thrust fault are observed near the village of Kouklia which is in accordance with the data presented by Geoter [2005]. The movement of the Gerasa Fold and Thrust belt in connection with the thickness of the Pakhna Formation and the Late Miocene activity of the Paphos Thrust fault, are evidence that allow the characterization of the Limassol Basin as a flexural basin, due to the activity of the large Gerasa Fault zone.

It is generally accepted that during late Neogene time both basins were uplifted and infilled by Nicosia Formation. However, a question mark still exists regarding the evolution of the basins in Messinian-Plio/Pleistocene time. At the Messinian boundary evidence of extension were recorded in the Polemi, Pissouri and Maroni/Psematismenos Basins from the studies of Weisgerber [1978], Dupoux [1983], Elion [1983], Orszag-Sperber et al., [1989]. Micro-tectonic analyses indicate that during the early Messinian the Polemi and Pissouri Basins are under an E-W extensional regime. In contrast the Maroni/Psematismenos Basin is under an NNW-SSE extension. In Late Messinian, extension was documented in a NE-SW direction affecting the Polemi and Pissouri Basins, while the Maroni/Psematismenos Basin was under an NW-SE extension. In Pleistocene time the Polemi Basin is under an NNE-SSW extension, the Pissouri Basin is under NW-SE extension while the Maroni/Psematismenos Basin is experiencing an NE-SW extension.

A tectonic evolution model of SW Cyprus is proposed (Figure 4 - 47), which encompasses all the field observations from this study and the results of previous studies. This model indicates the active structures through time while also attempting to explain the difference in sedimentation in the Polis and Limassol Basins.

In Oligocene to Early Miocene time, the Gerasa Fold and Thrust belt is active to the north of the Polis and Limassol Basins (Figure 4 - 47). To the south the Akamas thrust and the Kathikas Thrust are active, only in the Polis Basin. From the big difference in thickness of the Pakhna Formation in both basins, it is proposed that a sinistral transfer fault separates the two basins (Figure 4 - 47). This large structure could explain the thin Pakhna sediments (~200m) in the Polis Basin, compared to the thick Pakhna sediments (~650m) in the Limassol Basin. However, it was difficult to identify this large structure during the field campaign as the area is covered by the Triassic Mamonia Complex.

In Late Miocene time, the Gerasa Fold and Thrust belt is again active (Figure 4 - 47). In Polis Basin, the deformation front propagates to the south with the activity of the Paphos thrust fault, while out of sequence thrusting is identified on the eastern flank of the basin near the villages of Peristerona and Pelathousa as it is characterized by the deposition of the Tortonian Koronia Member reef.

In Plio-Pleistocene time all inland structures are active (Figure 4 - 47), as the Eratosthenes micro continent collides with Cyprus resulting in the uplift of the island. The lack of deposition of Nicosia Formation in the Limassol Basin in comparison with the Polis Basin,

could be connected with the frontal collision of the Eratosthenes micro continent with Cyprus. In the Limassol Basin the frontal collision results in a significant uplift resulting in the erosion or non-deposition of the Nicosia Formation. In the Polis Basin, this collision is oblique resulting in a less pronounced uplift and the deposition of Nicosia Formation.

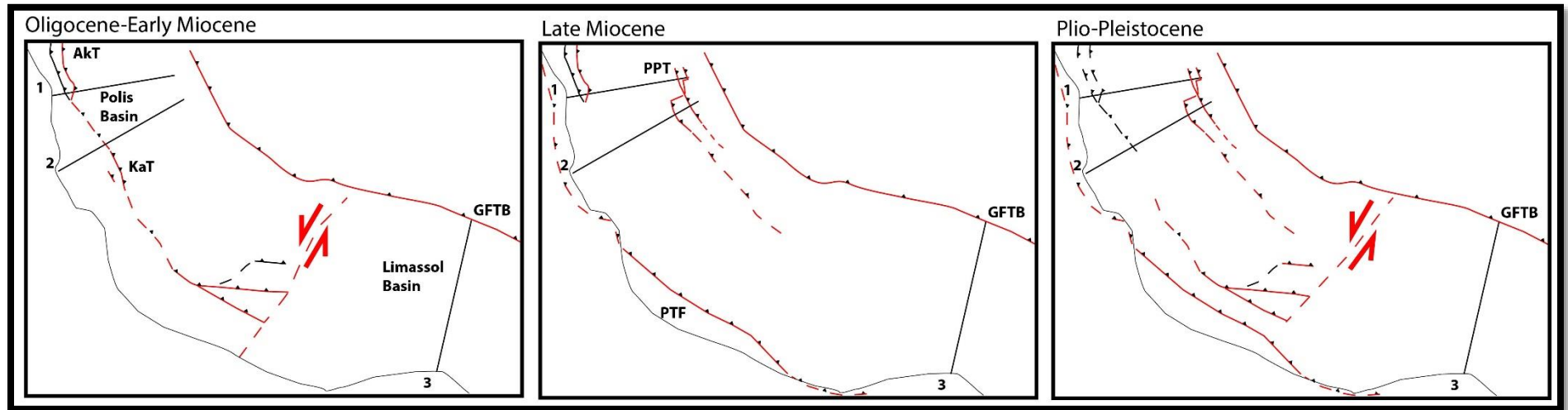


Figure 4 - 47: Simplified cartoon of the structural evolution of SW Cyprus. Red lines depict active thrust faults, while black lines depict inactive faults. Dashed lines indicate inferred faults in areas where the outcrops are covering the structures or it is difficult to observe them. Grey dashed lines indicate the limit between the two basins. Black lines with numbers indicate the cross sections discussed above. Abbreviations: Akt: Akamas Thrust; GFTB: Gerasa Fold and Thrust belt; KaT: Kathikas Thrust; PPT: Pelathousa-Peristerona Thrust; PTF: Paphos Thrust fault.



*Chapter 5*  
*Discussion*

An overview of the work undertaken throughout this project will be presented in this chapter. It focuses on the link between onshore and offshore tectonic structures, the timing of deformations and finally comparing the results herein with previous studies. The purpose of this comparison is to propose a geodynamic model on the tectonic evolution of the study area and how it is shaped through the varied lithospheric crustal configurations and the major plate boundaries in the Eastern Mediterranean region. This outcome is achieved by combining the interpretation of seismic profiles south of Cyprus and the results of onshore field campaigns which led to the creation of cross sections and reconstruction models that span since the Late Cretaceous. The aim of this geodynamic model is to comprehend the structural deformations along the Cyprus Arc system by analyzing the tectonic styles of the major plate boundaries in the Levant region. Furthermore, it could help indicate the impact of the different tectonic styles on the petroleum systems (reservoir, trap, and seal) and the timing of key deformations in order to identify prospective leads.

### **5.1 Regional structural offshore framework**

The analysis of twenty four 2D seismic profiles that cut the Cyprus Arc system provide informations that are utilized to define the deformation style along strike of this tectonic structure. These information revealed that the Cyprus Arc system includes a number of major plate structures which are: a) the Larnaca and Margat Ridges, a set of south verging thrusts active at least since Oligocene to Early Miocene time, with a re-activation in Late Miocene and Plio-Pleistocene time; and b) the Latakia Ridge, a thrust fault active at least since early Late Miocene and which is re-activated as a strike slip fault in Plio-Pleistocene time. The long lived tectonic activity evidenced from the interpretation of seismic profiles during this study, is in agreement with observations made by numerous authors which have attempted to document the offshore structures [Vidal et al, 2000; Calon et al., 2005; Hall et al., 2005; Bowman, 2011 Ghalayini et al., 2014; Montadert et al., 2014]. Calon et al., [2005] indicate a Middle Miocene to Late Miocene movement on the Larnaca Ridge. Previous studies by Hall et al. [2005] and Bowman [2011] propose the activation of the Latakia Ridge in Middle Miocene to Late Miocene time.

For the first time in this study, an Oligocene to Early Miocene deformation event is identified on the Larnaca and Margat Ridges as it was mapped in the Cyprus Basin, while no activity was observed on the Latakia Ridge during this time [Symeou et al., accepted; see chapter 3]. The acme of deformation was recorded in Middle to early Late Miocene time with on the Larnaca, Margat and Latakia Ridges [Symeou et al., accepted]. The comparison of

tectonic structures north of the Levant Basin (see chapter 4), namely the Larnaca, Margat and Latakia Ridges, has indicated a southward propagation of the deformation front as evidenced on the seismic profiles interpreted for this study [Symeou et al., accepted]. The Larnaca and Margat Ridges are active at least since Oligocene to Early Miocene time, with the activity continuing and shifting southward towards the Latakia Ridge by Middle-Late Miocene time [Symeou et al., accepted].

To the north, the Cilicia Basin is situated between the northern coast of Cyprus and the southern coast of Turkey. The Cilicia Basin (Figure 5 - 1) is considered as a Miocene piggy back basin that developed in the foredeep south of the Tauride Fold and Thrust belt [Aksu et al., 2005]. A series of south verging thrust faults are identified on the seismic profiles. The exact age of the sediments that infill this basin is unknown as no deep borehole data are available and the quality of the seismic profiles permits an interpretation only until a proposed Early Miocene horizon [Aksu et al., 2005; Blanco, 2014]. Normal faults are identified in the Messinian salt layer (Unit 2) which result from gravitational instabilities and movement of the salt deposits over the flanks of the basin [Blanco, 2014].

The indication from these observations is that plate convergence is accommodated by thrust emplacement which follows a forward propagation model, as described in other fold and thrust belts in the region like in the Cilicia Basin. It is thus the first time that the tectonic evolution of the Cyprus Basin is described by a similar model where the deformation front is migrating southward. The observations on the Margat Ridge where onlaps are recognized only from this study and the forward propagated sequence, allow for the determination of the Cyprus as a piggy back basin.

In Plio-Pleistocene time, all the structures are re-activated as a response to the westward escape of the Anatolian micro plate [McClusky et al., 2003; Le Pichon and Kreemer; 2010], and the continuous convergence of the African and Eurasian plates [McClusky et al., 2003]. At the eastern part of the Cyprus Arc system, positive flower structures are identified on the Latakia and Margat Ridges which illustrate strain partitioning and a transpressional regime [Vidal et al, 2000; Calon et al., 2005; Hall et al., 2005; Bowman, 2011; Montadert et al., 2014; Symeou et al., accepted]. At the central domain of the Eratosthenes micro continent Montadert et al., [2014] interpret the deformation in front of the Eratosthenes as a pop up structure (Figure 5 - 2), that is created from deep seated thrust faults that connect at depth with the Cyprus Arc system. In contrast in the offshore paper published from this study, it is suggested that the deformation is created by a thin skinned thrust fault with a decollement level at the base of the

Messinian salt which is in agreement with the interpretation by Reiche et al., [2015]. It is therefore proposed that the continuation of the thin skinned northward dipping thrust fault, could connect with the Cyprus Arc system, which is taken as a direct indication of the position of the Cyprus Arc system.

Plio-Pleistocene flexural basin was identified in front of the Eratosthenes micro continent which is considered as the result of the subduction of the Eratosthenes micro continent under Cyprus, while the timing of the basin constrained by stratigraphic onlaps on the northern flank of the Eratosthenes, indicative of a Plio-Pleistocene age [Montadert et al., 2014; Symeou et al., accepted]. Another flexural basin which was identified for the first time [Symeou et al., accepted] is the structure north of the Hecataeus Rise which is constrained by the Larnaca and Margat Ridges. This indicates a re-activation of the Neogene inherited faults both in a transpressive strike slip regime (Margat Ridge) and also as thrusts (Larnaca Ridge). The implication from this observation is that the deformation system resembles a strain partitioning system as it is described for an oblique convergence settings, however here it is related to the fragmentation and lateral movement of the upper plate due to the variation of the crustal nature along strike of the Cyprus Arc system [Symeou et al., accepted].

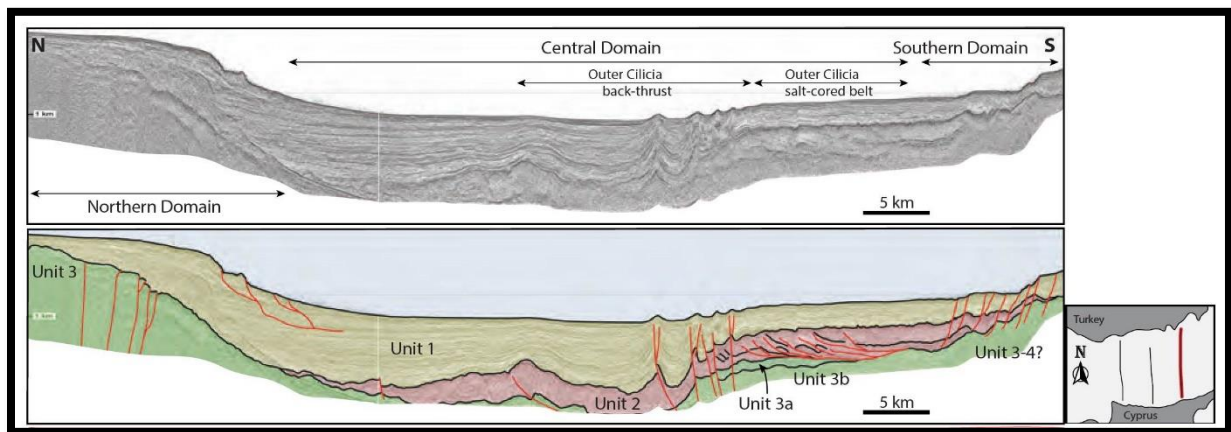


Figure 5 - 1: Un-interpreted and interpreted seismic profile in two way travel time (TWT) in the Cilicia Basin. Red line in index map illustrated the position of the profile. Unit 1 corresponds to Plio-Pleistocene clastic sediments. Unit 2 indicates Messinian salt deposits. Unit 3 corresponds to Middle to Late Miocene hemi-pelagic carbonates [Blanco, 2014].

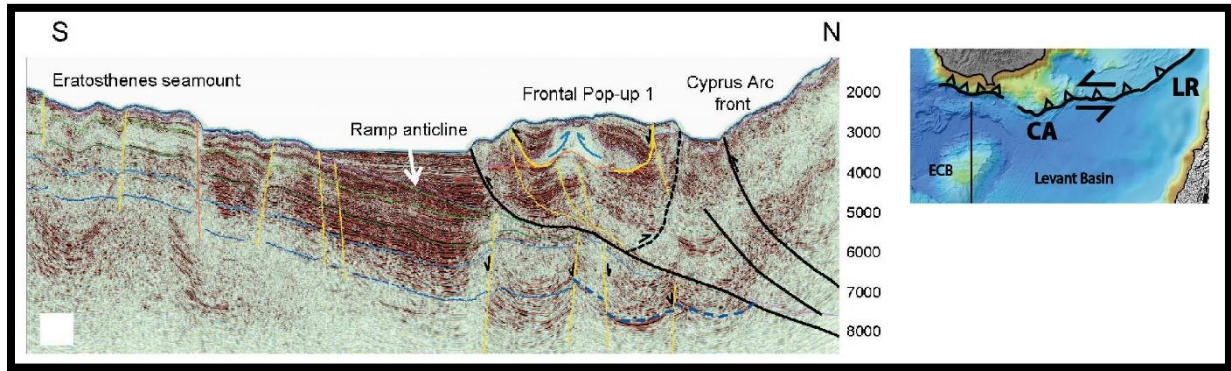


Figure 5 - 2: Interpreted seismic profile in Two-Way-Travel time (TWT) passing from the Eratosthenes micro continent towards the Cyprus Arc system. A flexural basin is documented and a pop-up structure associated with thick skinned deformation. [Montadert et al., 2014]. The black line in the inset map indicates the location of the seismic profile. Abbreviations: CA=Cyprus Arc; ECB=Eratosthenes Continental Block; LR=Latakia Ridge.

## 5.2 Structural onshore framework

Onshore Cyprus three major basins are identified: a) the Polis Basin; b) the Limassol Basin; and c) the Mesaoria Basin (see chapters 2 and 4). Prominent tectonic structures which are documented onshore are responsible for the evolution of these basins.

In southern Cyprus the Arakapas Transform fault [Simonian and Gass, 1978] is interpreted as an E-W trending fault which was active since Late Cretaceous time. The Gerasa Fold and Thrust belt is a south verging tectonic structure that runs NW-SE, parallel to the ophiolite unit and uplifts the Troodos Mountains with continuous pulses starting in Late Cretaceous time [Robertson, 1977; Swarbrick and Robertson, 1980]. Oligocene to Early Miocene deformation (Figure 5 - 3) was documented in the Limassol Basin which continued in Late Miocene as it was proposed by the Eaton and Robertson [1993]. In the Polis Basin, Late Cretaceous thrusting activity was proposed in the Akamas Peninsula [Swarbrick, 1993; Bailey et al., 2000] and on the northwestern part of the Gerasa Thrust belt [Swarbrick and Robertson, 1993].

The Mesaoria Basin is constrained by the Kyrenia Range to the north and by the Troodos Mountain to the south. It is considered as a Cenozoic foredeep basin that resulted from the thrust movement of the Kyrenia thrust and the Troodos-Larnaca culmination [Calon et al., 2005]. The continued shortening along these faults lead to the deposition of shallow marine

sediments in the center of this basin. A Middle Miocene thrust movement along the Ovgos thrust fault (Figure 5 - 4) is proposed due to the juxtaposition of the chalks and marls of the Pakhna Formation with the deep flysch sediments of the Kythrea Formation [Harrison et al., 2004; 2008]. Deep borehole data [Cleintuar et al., 1977] in the center of the basin indicate a thrusting movement of Messinian time at the Ovgos thrust fault [Harrison et al., 2004; 2008;] as the Miocene Kythrea Formation is juxtaposed with Messinian salt of the Kalavassos Formation (Figure 5 - 4).

Deformation onshore Cyprus is proposed at least since Late Cretaceous time. The initial uplift of the western part of the Troodos massif due to the activity of the Gerasa Fold and Thrust belt (NW part of the thrust), resulted in the erosion of the ophiolite units and the deposition of the Kannaviou Formation in hollows [Swarbrick and Robertson, 1980] in the Polis Basin. Thrust movements were also documented at the Akamas Peninsula, where pillow lavas and serpentinites are outcropping [Swarbrick, 1993; Bailey et al., 2000], at a distance of ~15km from the main massif.

For the first time, a Neogene thrusting deformation event is identified in the Polis Basin, near the villages of Kathikas and Pegeia (see chapter 4) where Burdigalian sediments are overlying Late Maastrichtian sediments. In Late Miocene a second tectonic pulse was identified as Late Miocene reefs of the Koronia Member were deposited on the eastern flank of the Polis Basin. It is proposed herein, that the Koronia reefs were deposited due to the thrust movement at the Pelathousa-Peristerona area. Further evidence to suggest the existence and the re-activation of this fault is the eastward tilting of the Koronia reefs in Plio-Pleistocene time. It was previously proposed that large normal faults controlled the tectonic evolution of the basin, as a result of slab roll back of the northward subducting African plate [Payne and Robertson, 1995]. This mechanism was also used to explain the deposition of the Koronia reefs by proposing antithetic normal faults which created local highs and thus determining the Polis Basin as a graben. [Payne and Robertson, 1995]. This tectonic model is contradicting with the observations made in this study, as it does not explain the Burdigalian-Late Maastrichtian unconformity or the tilting of the Koronia reefs on the western and eastern flanks of the Polis Basin respectively. It is therefore indicated that in this study the Polis Basin is considered as a piggy back basin which developed between two thick skinned thrust faults which are verging towards the west.

In the Limassol Basin, Oligo-Miocene deformations associated with thrusting activity on the Gerasa Thrust were documented for the first time in this study (see chapter 4), near the

villages of Mandria-Omodos (folded chalks and cherts of the Lefkara Formation), near Kapilio village (steeply dipping Lefkara chalks in contact with Troodos ophiolites) and near the village of Armenochori (deformation zone in the Lefkara Formation). The Late Miocene movement of the Gerasa Fold and Thrust belt was identified at the village of Armenochori, where Late Miocene Koronia Member reef units are overlying the Maastrichtian Moni Formation, which is in agreement with previous studies [Eaton and Robertson, 1993; Kinnaird, 2008]. It is proposed by Eaton and Robertson [1993], that the Akrotiri High is uplifted in Early Miocene time, however no indications of this activity were observed during this study. The large time gap between the Pliocene and Mesozoic sediments in borehole used could possible mean an uplift in Late Miocene time. Taking this into account and the thick sedimentary Pakhna sequence proposed at the southern extend of the Limassol Basin, it is herein proposed that the Limassol Basin is a flexural basin which was downthrown by the activity of the Gerasa Fold and Thrust belt.

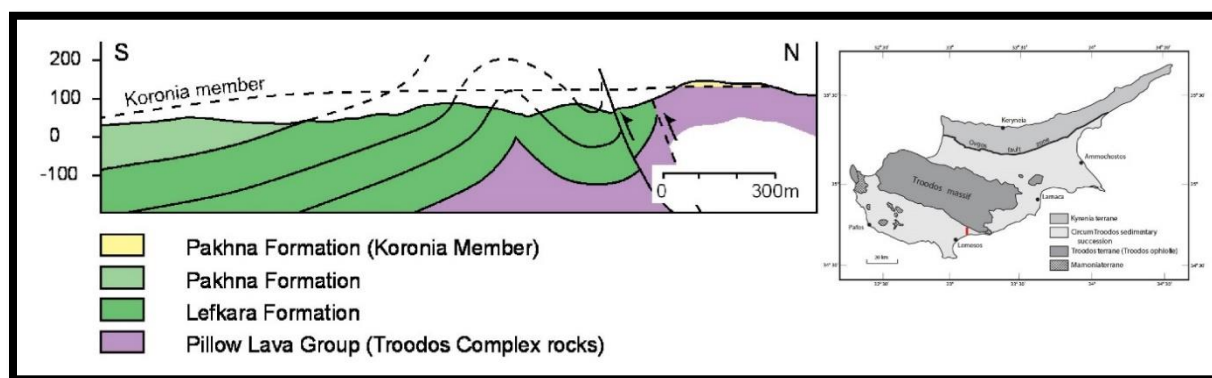


Figure 5 - 3: Simplified geological cross section through the Gerasa Fold and Thrust belt, which illustrates a stratigraphic unconformity between the Pakhna Formation and the underlying Lefkara Formation [from Kinnaird, 2008 as modified after Eaton and Robertson, 1993.] The red line on the inset map indicates the location of the cross section [map modified from Harrison et al., 2008].

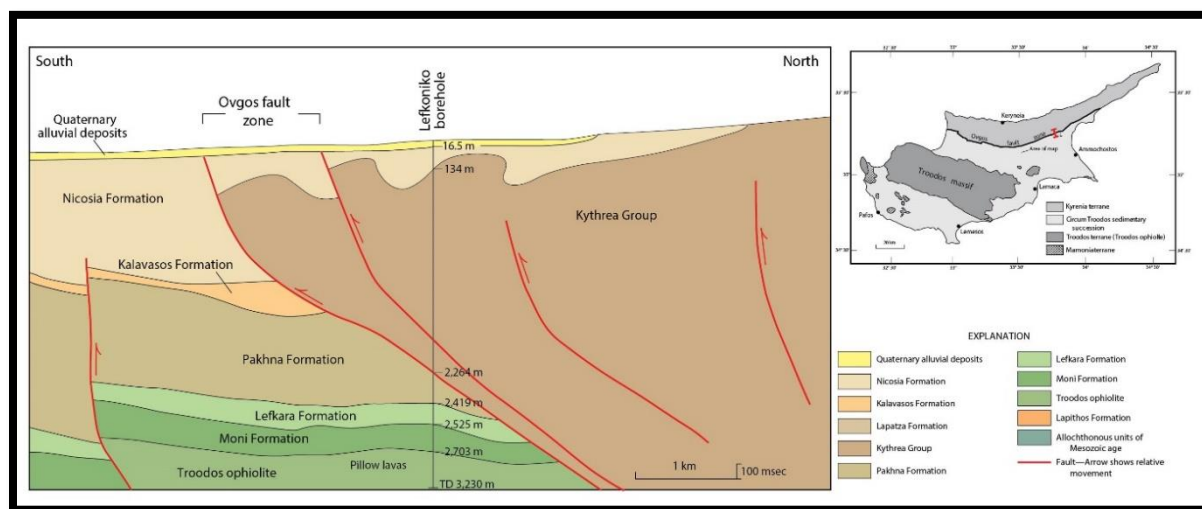


Figure 5 - 4: The Lefkoniko borehole and schematic cross section across the Ovgos thrust fault, which is considered as the boundary between the Troodos sedimentary cover and the Kyrenia terrane. True depth of the contacts are shown for the borehole. Inset map of Cyprus indicates the location of the cross section (red line). Legend explains the formations used in this cross section. [from Harrison et al., 2008]. The red line on the inset map indicates the location of the cross section [map modified from Harrison et al., 2008].

### 5.3 Regional synthesis

The complex geodynamic context of the Eastern Mediterranean originates from the breakup of Pangea, the rifting of the Tauride block in Triassic to Early Jurassic time, the creation of the Neo-Tethyan Ocean followed by the continuous convergence of the African and Eurasian plates since Late Cretaceous time. From the available data a chart was constructed which connects the recorded pulses with the geodynamic regime through time (Figure 5 - 5). A first pulse was recorded in Oligocene to Early Miocene time and it is connected with the north-south convergence between the African and Eurasian continental plates. The second pulse which is proposed herein as the strongest was identified in Late Miocene from the offshore data where a regional unconformity was identified as the Plio-Pleistocene sediments are unconformable with the underlying Messinian salt layers. The last pulse recorded in Plio-Pleistocene time is a transpressive deformation due to strain partitioning associated with the westward escape of the Anatolian micro plate.

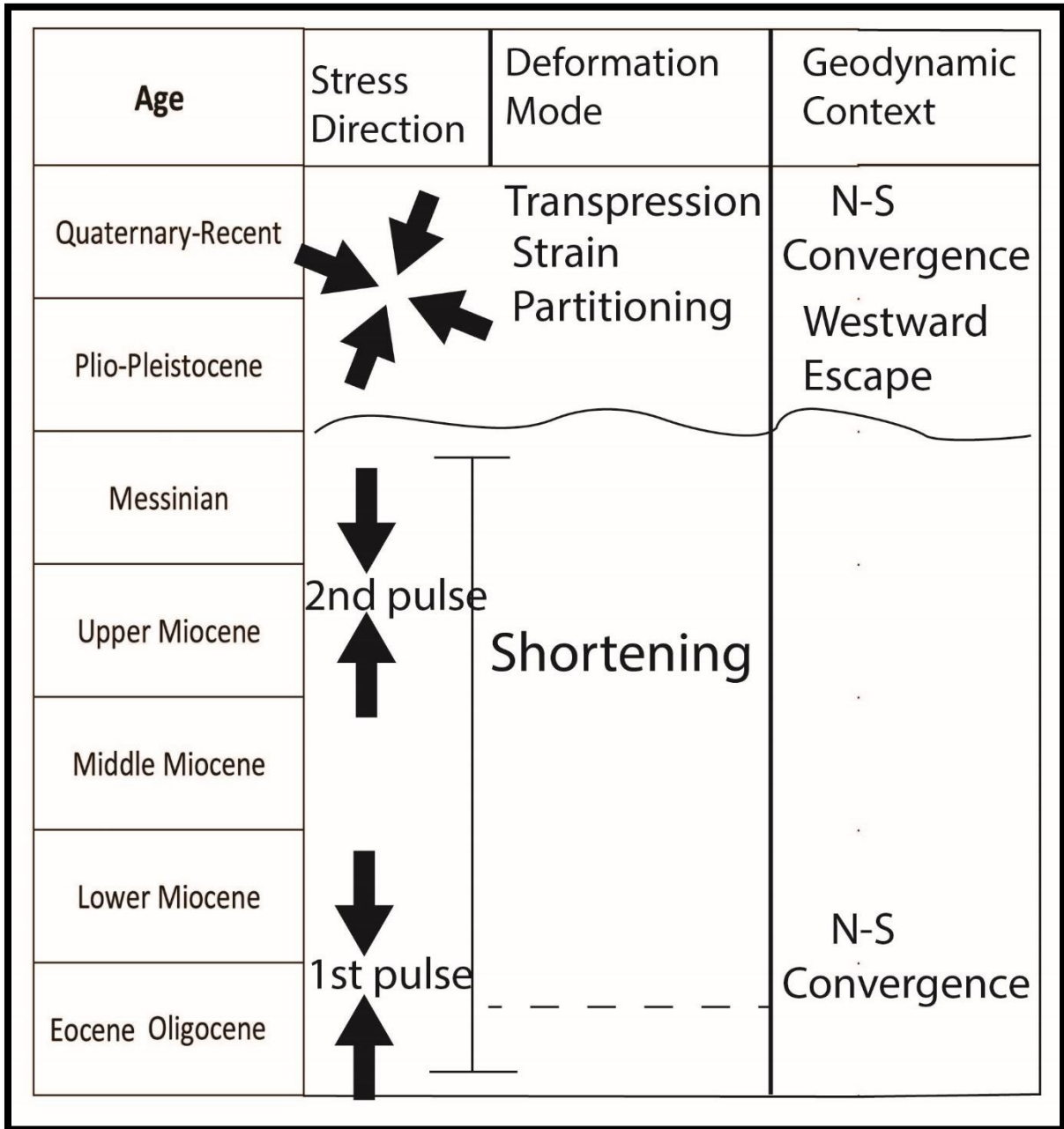


Figure 5 - 5: Deformation chart illustrating the stress direction, the deformation phase connected with the geodynamic context through time.

The major tectonic structures mapped in the region are: a) the Kyrenia Range with its eastward continuation extending to Syria where it probably joins up with the East Anatolian fault, while the western end could pass northwards into the Taurus Fold and Thrust belt; b) the

Ovgos Transform fault which could connect with the East Anatolian fault; c) the Arakapas Transform fault could be associated with the Larnaca Ridge; d) the Gerasa Fold and Thrust belt is linked with the Margat Ridge; e) the Paphos Transform fault and Akrotiri High which are possibly connected with the Latakia Ridge; and f) the Cyprus Arc system which constitutes the major boundary between Cyprus and the Levant and Herodotus Basins.

During the Oligocene to Early Miocene (Figure 5 - 6), the Kyrenia Range is active as deep flysch sediments are deposited in the Mesaoria Basin. To the south east the Larnaca and Margat Ridges are active as it identified by the creation of the flexural Cyprus Basin and the deposition of shallow sediments compared with the deep marine sediments deposited in the Levant Basin. Onshore Cyprus the active Gerasa Fold and Thrust belt results in the creation of the deep Limassol Basin while the activity of the Gerasa Fold and the Kathikas Thrust in the Polis Basin are responsible for the creation of the flexural Polis Basin. It is herein proposed that the Larnaca Ridge could connect with the Arakapas Transform Fault onshore Cyprus. The Margat Ridge stops its propagation towards the east due to the existence of a rigid body, the Hecataeus Rise which blocks the extension of the fault. This will be explained later in the text ().

In Late Miocene time the activity of the offshore Latakia Ridge and the onshore Paphos Thrust fault is an indication that the deformation front is propagating towards the south (Figure 5 - 8). This is also attested by the deposition either side of the Latakia ridge which is the major boundary between the Cyprus Basin (thin sequence of shallow sediments) and the Levant Basin (thick sequence of deep marine sediments). Out of sequence thrusting is documented from the onshore structures as it was described in chapter 4 (section 4.6 Discussion).

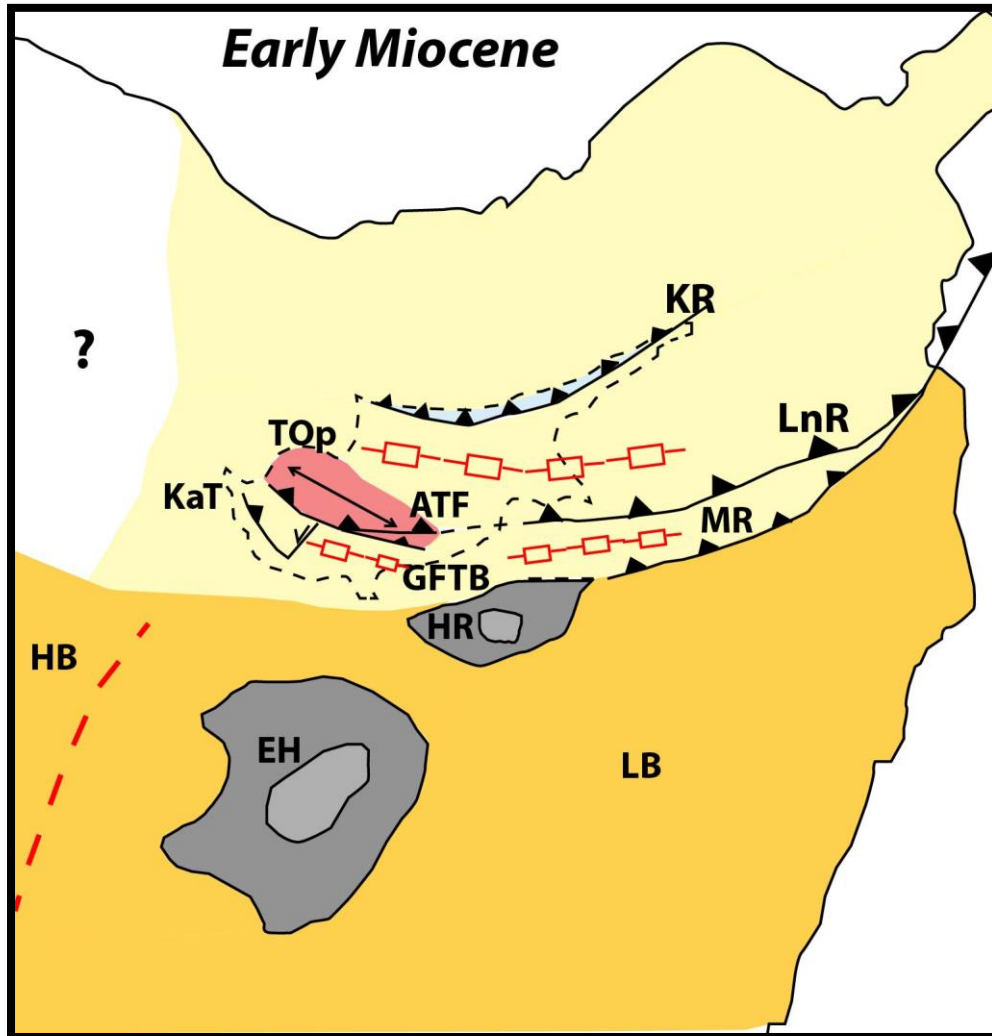


Figure 5 - 6: Oligocene to Early Miocene geodynamic evolution model of the Eastern Mediterranean region. Description of structures in Figure 5 - 7. Abbreviations: ATF: Arakapas Thrust Fault; EH: Eratosthenes High; GFTB: Gerasa Fold and Thrust Belt; HB: Herodotus Basin; HR: Hecataeus Rise; KaT: Kathikas Thrust; KR: Kyrenia Range; LB: Levant Basin; LnR: Larnaca Ridge; MR: Margat Ridge; TOp: Troodos Ophiolites.

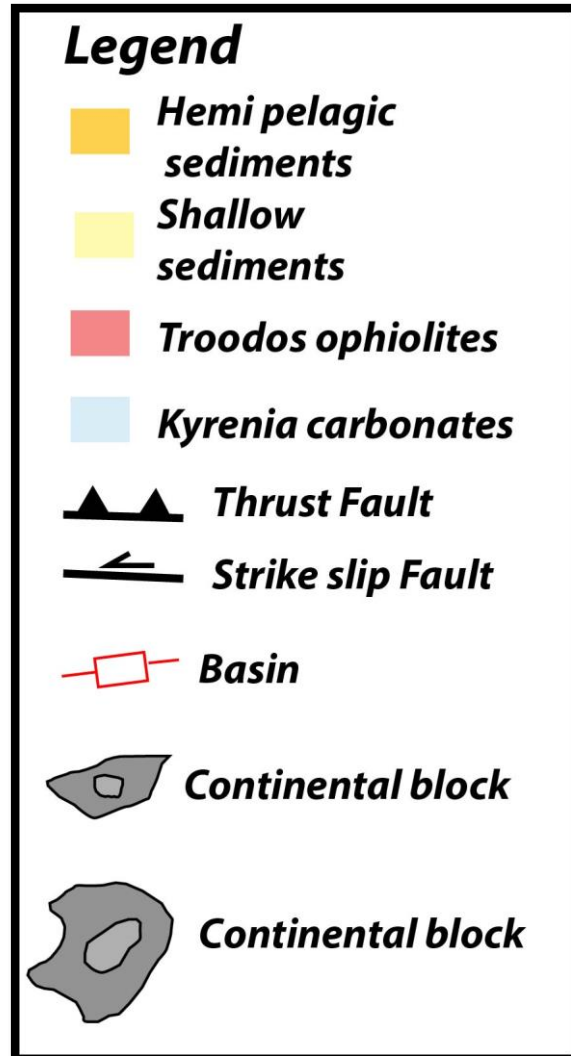


Figure 5 - 7: Legend explaining the different features illustrated in Figure 5 - 6, Figure 5 - 8, Figure 5 - 9.

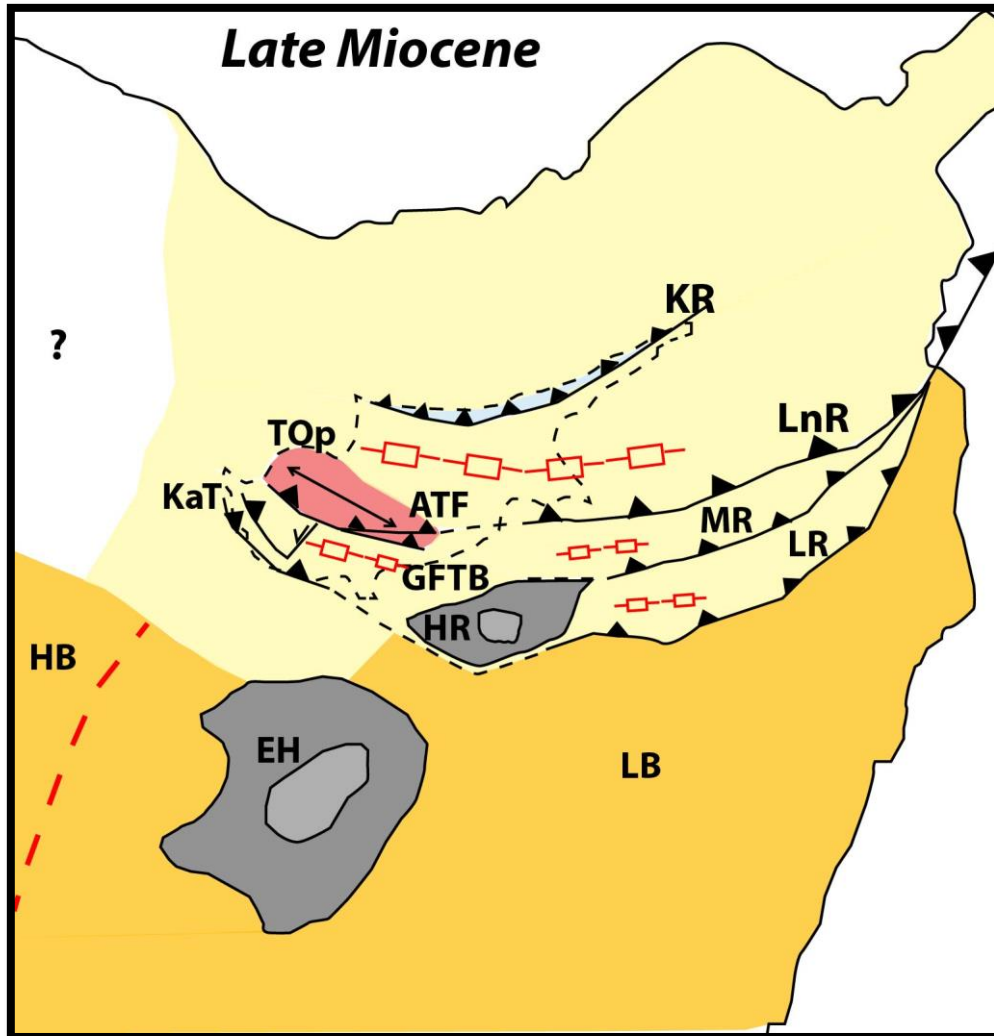


Figure 5 - 8: Late Miocene geodynamic evolution model of the Eastern Mediterranean region. Description of structures in Figure 5 - 7. Abbreviations: ATF: Arakapas Thrust Fault; EH: Eratosthenes High; GFTB: Gerasa Fold and Thrust Belt; HB: Herodotus Basin; HR: Hecataeus Rise; KaT: Kathikas Thrust; KR: Kyrenia Range; LB: Levant Basin; LnR: Larnaca Ridge; LR: Latakia Ridge; MR: Margat Ridge; TOP: Troodos Ophiolites.

In Plio-Pleistocene time, strike slip deformation is documented on the Margat and Latakia Ridge in the eastern domain, which corresponds with the westward escape of the Anatolian micro plate (Figure 5 - 9). In the central domain, compressional deformation is documented by the flexural basin created in front of the Eratosthenes micro continent which is associated with the collision of the Eratosthenes micro continent and Cyprus. It is further proposed that at this time, the Larnaca Ridge is connected onshore with the Gerasa Fold and

Thrust belt through a sinistral transfer fault, although further investigations are needed to validate this proposal.

It is important to note that the inherited structures from the Late Cretaceous emplacement of the ophiolitic belt, impact the tectonic deformation as these structures are re-activated through time.

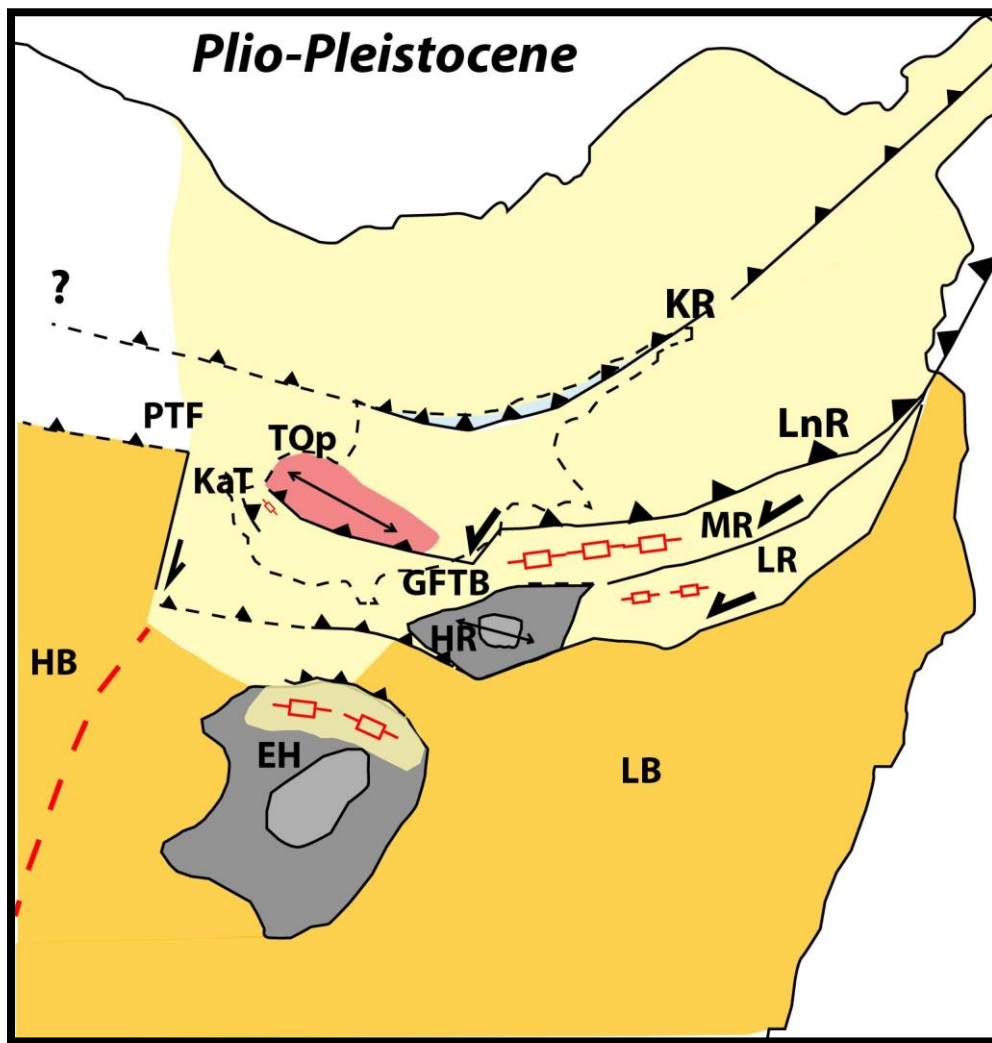


Figure 5 - 9: Plio-Pleistocene geodynamic evolution model of the Eastern Mediterranean region. Description of structures in Figure 5 - 7. Abbreviations: ATF: Arakapas Thrust Fault; EH: Eratosthenes High; GFTB: Gerasa Fold and Thrust Belt; HB: Herodotus Basin; HR: Hecataeus Rise; KaT: Kathikas Thrust; KR: Kyrenia Range; LB: Levant Basin; LnR: Larnaca Ridge; LR: Latakia Ridge; MR: Margat Ridge; TOP: Troodos Ophiolites.

In order to better constrain the geodynamic evolution models of the Eastern Mediterranean the shortening rates of the Latakia and Margat Ridges were investigated. The seismic time (in TWT) was noted at various intervals either side of the main structures. The points were picked on the already interpreted seismic horizons which are proposed in chapter 3. Then by applying the widely accepted seismic velocities for each formation, the throw of each structure was calculated. This resulted in the creation of two charts which indicate the throw of the structure in meters (vertical axis) along strike of the Cyprus Arc system (horizontal axis).

The first chart illustrates the throw along the Latakia Ridge (Figure 5 - 10). The orange lines illustrate the collective throw from Middle Miocene onwards, the red lines the collective throw from Messinian time until recent, the yellow lines indicate the throw from Pliocene onwards and the blue line indicates the current throw as it represents the seabed. The letters on the horizontal axis indicate the location of each seismic profile used to measure the time. It is worth noting that in the east, the throw of the Middle Miocene and Messinian lines is large compared with the throw of the Plio-Pleistocene to Recent lines. The large difference in throw is associated with the change in deformation style from compression in Miocene time to strike slip in Pliocene time connected with strain partitioning and the escape of the Anatolian micro plate. In contrast in the west, the throw in Miocene time gradually diminishes, while in Plio-Pleistocene time the throw is very large, which is associated with the collision of the Eratosthenes micro continent with Cyprus resulting in the uplift of the island.

The second chart illustrates the throw along the Margat Ridge (Figure 5 - 11). The throw along the ridge is indicated by the orange (Middle Miocene), red (Messinian), yellow (Plio-Pleistocene) and blue lines (Recent). A peak is identified at the center of the Margat Ridge while at the both tips of the fault the throw is reduced significantly. The diminishing throw towards the west is associated with the existence of a rigid body west of the structure. This rigid body is the Hecataeus Rise which is underlain by continental crust, acting as a physical block preventing the Margat Ridge to migrate westwards.

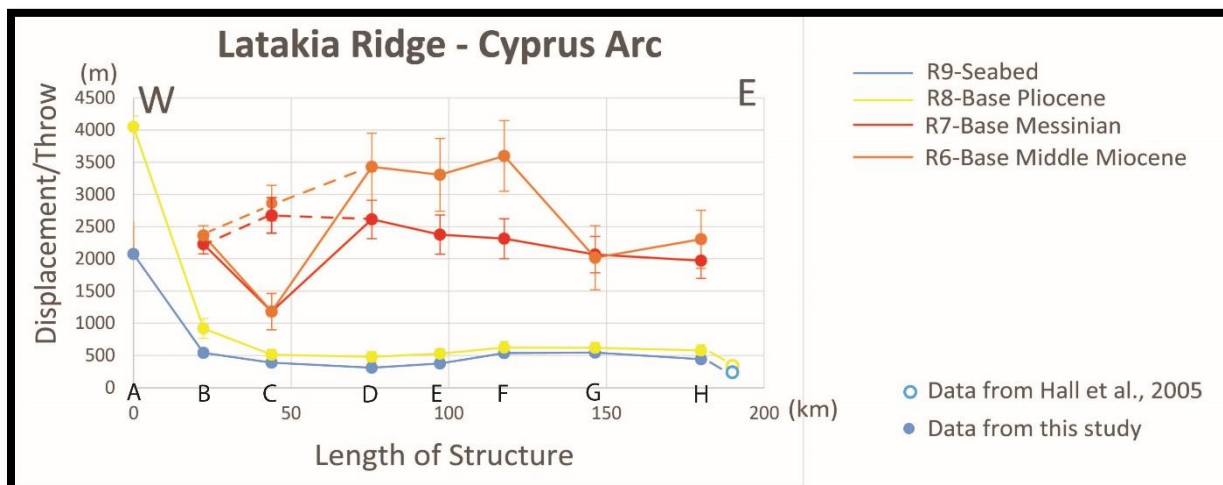


Figure 5 - 10: Illustration of the throw along strike of the Latakia Ridge. In the east the large throw between the Miocene and the Plio-Pleistocene lines indicates the transition from compression to strike slip deformation. In the west the large throw of the Plio-Pleistocene line indicates the collision between Eratosthenes micro continent and Cyprus which results in the uplift of the island.

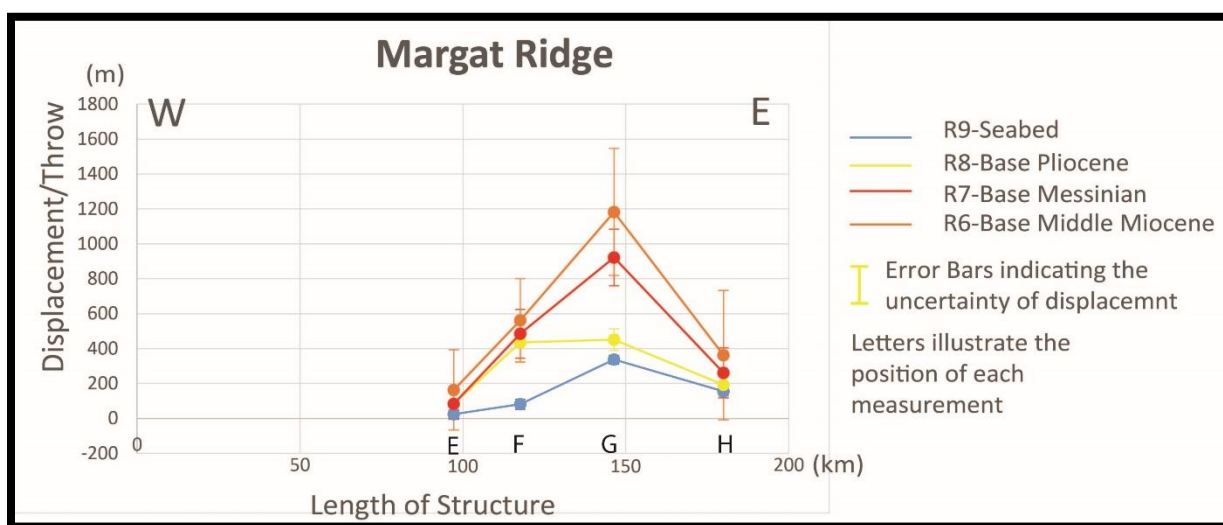


Figure 5 - 11: Illustration of the throw along strike of the Margat Ridge. The diminishing throw towards the west indicates that the structure does not extend towards the west probably due to the existence of the Hecataeus Rise, a continental block that prevents the Margat Ridge migrating towards the west.

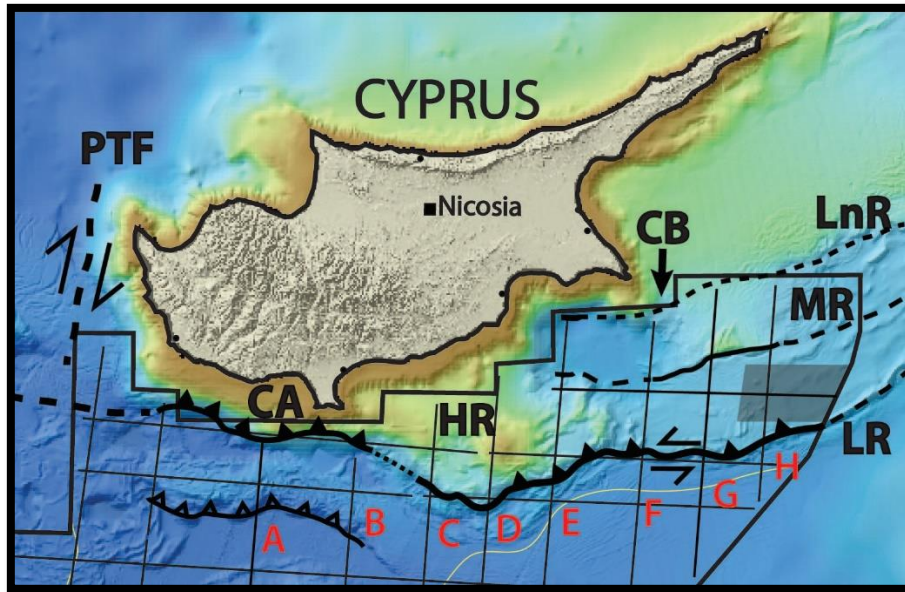


Figure 5 - 12: Location of seismic profiles utilized to create the charts in Figure 5 - 10 and in Figure 5 - 11. Abbreviations: CA: Cyprus Arc; CB: Cyprus Basin; HR: Hecataeus Rise; LnR: Larnaca Ridge; LR: Latakia Ridge; MR: Margat Ridge; PTF: Paphos Transform Fault.

#### 5.4 Assessment of impact of tectonic structures on the petroleum systems

The timing of structural deformation is very important for the identification of targets that could hold substantial hydrocarbon reserves. During the seismic interpretation and by combining discoveries mainly in the Levant Basin and the onshore observations key parameters can be addressed for the petroleum systems south of Cyprus.

Previous hydrocarbon discoveries in the Levant Basin, have focused on the Miocene sands like the Tamar and the Aphrodite fields [Roberts and Peace, 2007]. This corresponds well with the tectonic movement in Oligocene to Early Miocene time, as the uplift of the nearby continents resulted in erosion and deposition of sands in the area. The continuous convergence and the thrusting displacement can create traps as anticlines, which were drilled in the cases of Tamar and Aphrodite. Similar anticlines and small piggy back basins are identified in the Cyprus Basin. The shallow depth and the clear geometrical structures can be a nice target for exploration groups, although risks still exist as the true thickness and the basement of the Cyprus Basin is not confidently constrained due to the lack of deep borehole data.

The Eratosthenes micro continent and its surrounding fringing reefs could prove to be an important reservoir as well. Following the discovery of the Zohr field [Esestime et al., 2015], a new play of great importance was revealed. These targets around Eratosthenes, which could be Cretaceous carbonate buildups could prove valuable plays, with some structures identified S, SW and SE of the platform.

A very important element for the accumulation of hydrocarbons is the seal. In the Levant Basin, a thick layer of ~1.5-2km of Messinian salt acts a seal to the existing petroleum system. A cautious approach should be taken with regard to plays in the Cyprus Basin as the salt layer is thin or non-existent at several location due to the higher position of the basin and probably due to the relative easy way that the salt can move when under a thick package of sediments.



*Chapter 6*  
*Conclusions*

Seismic interpretation of the available 2D seismic profiles south of Cyprus and field investigations onshore southern Cyprus aided in the documentation of a plethora of tectonic structures. These informations either enhanced previous models proposed or yielded new data on the time constrain and the deformation mechanisms of the various structural elements. Some of the structures are inherited while others are of Cenozoic time. These major structures are:

### Onshore structures:

- The Gerasa Fold and Thrust belt is an inherited structure at the southern flank of the Troodos Mountain. It is the boundary between the ophiolitic unit and the Limassol and Polis sedimentary basins. It runs from NW-SE parallel to the ophiolite body and it is a southwestward verging thrust fault. Three important pulses are documented on this structure: i) a Late Cretaceous pulse inferred from the erosion of the ophiolites and the deposition of the Late Cretaceous Kannaviou and Moni Formations; ii) an Oligocene to Early Miocene movement observed from the deposition of ultrabasic pebbles of ophiolitic origin in the Miocene Pakhna Formation in the Maroni/Psematismenos Basin and from the unconformable contact between the Pakhna Formation and the underlying Eocene Lefkara Formation in the Limassol Basin; and c) a Late Miocene pulse identified by the deposition of Late Miocene Koronia Member reef carbonates on top of the Maastrichtian Moni Formation, at the eastern flank of the Limassol Basin.
- The Akamas Peninsula is constrained by two NNW-SSE thrust faults which are verging towards the west. The timing of deformation is inferred as Late Cretaceous due to the occurrence of serpentized harzburgite at this locality. An Early Miocene uplift is proposed from the deposition of the Tera Member reef carbonates which are in contact with Triassic the Mamonia Complex. Late Miocene activity is evident from the deposition of Koronia Member reef carbonates on top of the serpentinites and in contact with the Triassic Mamonia Complex.
- The Kathikas Thrust is considered as the southern continuation of the thrust faults in the Akamas Peninsula. Oligocene to Early Miocene movement is documented from the juxtaposition of the Maastrichtian Kathikas Formation next to the Eocene Lefkara Formation and from the unconformable contact between the overlying Burdigalian chinks and the Late Maastrichtian chinks. Younger thrust activity has not occurred on this thrust as the structure is sealed by the Pakhna Formation.
- The Pelathousa-Peristerona Thrust is a NW-SE trending structure which was active in Late Miocene time. This movement is evident by the juxtaposition of steeply dipping Koronia Member reef limestones next to the Campanian Kannaviou Formation. The thrust is verging towards the west.

- The Paphos Thrust fault is considered as a prolongation of the Kathikas Thrust, however only a Late Miocene movement is documented on this fault near the village of Kouklia where the Pakhna Formation chalks are folded. It is proposed that the eastward continuation of this fault connects with the Akrotiri High fault.
- The Polis Basin in the SW part of Cyprus is considered as a Late Cretaceous basin infilled with a range of sediments of relative thin thickness (Pakhna Formation ~150m) indicative of a shallow basin. It is described herein as piggy back basin created by a thick skinned mechanism, from the interaction of the NW Gerasa Fold and Thrust belt and the Akamas Peninsula Thrusts. In Late Miocene the out of sequence movement of the Pelathousa-Peristerona Thrust indicates a rather complex tectonic evolution, one not described by forward propagation.
- The Limassol Basin in south Cyprus, is considered as a deep basin as the sedimentary sequence is rather thick (Pakhna Formation ~650m). This basin is constrained by the movement of the Gerasa Fold and Thrust belt and is considered as a flexural basin. The activity of the Paphos Thrust/Akrotiri High fault confines the basin during Late Miocene time.

### Offshore Structures:

- The Larnaca and Margat Ridges are major tectonic structures active in Oligocene to Early Miocene time. The deformation is identified from stratigraphic onlaps and the creation of a flexural basin which is infilled by Middle Miocene sediments. Late Miocene activity is also observed on both structures from the variation in thickness of the Messinian salt.
- The Latakia Ridge is active in Middle to Late Miocene time as it is documented by the big change in thickness of the Middle Miocene and Messinian sediments north and south of the thrust. In Plio-Pleistocene time, positive flower structures are identified along the Latakia Ridge, which indicates the strain partitioning to a transpressive regime.
- South of Cyprus activity on the Cyprus Arc system is recorded from a flexural basin in front of the Eratosthenes micro continent, which is infilled by Plio-Pleistocene sediments. Due to the large thickness of salt deposits, the quality of the seismic profile is bad and therefore no older deformation is identified. The compressional regime identified at this location is connected with the collision between the Eratosthenes micro continent with the island of Cyprus.
- From the thrust movement, a southward propagation of the deformation front is proposed for the first time.

Along the Cyprus Arc system, a change from strike slip deformation (east) to a compressional setting (west) is identified. This change in style is attributed to the variation of the nature of the crust from east to west.

### Perspectives:

Time gaps still exist regarding the deformation timing onshore Cyprus. The similarities in facies and the difficulty to distinguish the exact boundary between the Pakhna and Lefkara Formations, was a big challenge in this study. A detailed bio stratigraphic analysis could prove valuable, as it would better constrain the activity of the various tectonic structures and eliminate uncertainty.

In order to better test the proposed models, the propagation of the deformation front and the tectonic evolution of the sedimentary basins, a balanced cross section should be created, comparing the different domains (i.e in the east: continental crust vs attenuated continental crust and in the west: continental vs continental crust . This will be important as it will test the hypothesis for the deeper parts of the basins where up until now the lack of data cannot provide a clear overview of the tectonic processes at work.

Interpretation of 3D cube seismic data could be beneficial in the investigation of the strike slip style proposed in the eastern domain, at the Latakia Ridge.

More detailed work should be pursued in the northern part of the island and in the surrounding counties, as all the areas are tied up together by a common tectonic evolution. Integration with previous and coming studies would prove important to test the proposed models and the timing of the deformation.



## *References*

Agard, P., Omrani, J., Jolivet, J., Whitechurch, H., Vrielynck, B., Spakman, W., Monie, P., Meyer, B., Wortel, R., [2011] Zagros orogeny: a subduction-dominated process, *Geol. Mag.*, p. 1-34

Aksu, A.E., Hall, J., Yaltirak, C., [2005] Miocene to Recent tectonic evolution of the eastern Mediterranean: New pieces of the old Mediterranean puzzle, *Marine Geology*, 221, p. 1-13

Al Abdalla, A., Barrier, E., Matar, A., Muller, C., [2010], Late Cretaceous to Cenozoic tectonic evolution of the NW Arabian platform in NW Syria, *in Evolution of the Levant Margin and Western Arabia Platform since the Mesozoic*, edited by Homberg, C., and Bachmann, M., *Geol. Soc. London, Spec. Publ.*, 341, p. 305-327

Angelier, J., [1990] Inversion of field data in fault tectonics to obtain the regional stress – III. A new rapid direct inversion method by analytical means, *Geophys. Jour. Intern.*, Vol. 103, p. 363-376

Baroz, F., Bernoulli, D., Biju-Duval, B., Bizon, G., Bizon, J.J., Letouzey, J., [1978] Correlations of the Neogene formations of the Florense Rise and of northern Cyprus: Paleogeographic and structural implications, doi: 10.2973/dsdp.proc. p. 903-926

Bailey, W. R., [1997] The structural evolution of a microplate suture zone, SW Cyprus, *Durham theses, Durham University*.

Bailey, W. R., Holdsworth, R. E. and Swarbrick, R. E., [2000] Kinematic history of a reactivated oceanic suture: the Mamonia complex suture zone, SW Cyprus, *Jour. Of the Geol. Soc. Of London*, Vol. 157, p. 1107-1126

Barrier, E. and Vrielynck, B., [2008], Paleotectonic maps of the Middle East: tectono sedimentary palinspastic maps from Late Norian to Pliocene, 14 maps, *Comm. la Cart. Geol. du monde*

Ben-Avraham, Z., Tibor, G., Limonov, A. F., Leybov, M. B., Ivanov, M. K., Tokarev, M. Yu., Woodside, J. M., [1995] Structure and tectonics of the eastern Cyprean Arc, *Mar. and Petrol. Geol.*, Vol. 12, p. 263-271

Ben-Avraham, Z., Ginzburg, A., Makris, J., Eppelbaum, L., [2002] Crustal structure of the Levant basin, Eastern Mediterranean, *Tectonophysics*, Vol.346, p.23-43

Bizu-Duval, B., Letouzey, J., Devaux, E., [1974] Observations géologiques dans l'île de Chypre, *Compte rendu de la mission de terrain 1973, Géologie, 18*, p. 1-16

Blanco, D., F., [2014] Orogenic Plateaus Genesis: Kinematics, Tectonics and Mechanics of the Central Anatolian plateau south margin, Turkey, *PhD thesis, University of Amsterdam* p. 1-189

Brew, G., Barazangi, M., Al-Maleh, A.K., Sawaf, T., [2001] Tectonic and Geological evolution of Syria, *GeoArabia, Vol.6, No.4*, p.573-616

Brew, G., Lupa, J., Barazangi, M., Sawaf, T., Al-Imam, A., Zaza, T., [2001b] Structure and tectonic development of the Ghab basin and the Dead Sea fault system, Syria, *Jour. Geol. Soc. London, Vol.158*, p.665-674

Bowman, S., [2011] Regional seismic interpretation of the hydrocarbon prospectivity of offshore Syria, *GeoArabia, Vol. 16, No.3*, p.95-124

Calon, T.J., Aksu, A.E. and Hall, J. [2005a] The Neogene evolution of the Outer Latakia Basin and its extension into the Eastern Mesoria Basin (Cyprus), Eastern Mediterranean. *Marine Geology, 221*, p. 61– 94.

Calon, T.J., Aksu, A.E. and Hall, J. [2005b] The Oligocene-Recent evolution of the Mesoria Basin (Cyprus) and its western marine extension, Eastern Mediterranean. *Marine Geology, 221*, p. 95– 120.

Cleintuar, M.R., Knox, G.J. and Ealey, P.J. [1977], The Geology of Cyprus and its place in the East-Mediterranean framework. *Geol. Mijnb. 56*, 66–82.

Dewey, J.F., Pitman, W.C. III, Ryan, W.B.F., Bonnin, J., [1973] Plate Tectonics and the evolution of the Alpine System, *Geol. Soc. Of America Bull., Vol. 84, No. 10*, p.3137-3180

Dilek, Y. and Altunkaynak, S., [2009], Geochemical and temporal evolution of Cenozoic magmatism in western Turkey: mantle response to collision, slab break-off and lithospheric tearing, in *Collision and Collapse at the Africa-Arabia-Eurasia Subduction Zone, edited by van Hinsbergen, D.J.J., Edwards, M.A. and Govers, R., Geol. Soc. London, Spec. Publ., 311*, p. 213-233.

Dilek, Y. and Sandvol, E., [2009], Seismic structure, crustal architecture and tectonic evolution of the Anatolian – African plate boundary and the Cenozoic orogenic belts in the Eastern Mediterranean Region, *in Ancient Orogens and Modern Analogues*, edited by Murphy, J.B., Keppie, J.D. and Hynes, A.J., *Geol. Soc. London, Spec. Publ.*, 327, p. 127-160.

Dupoux, B., [1983] Etude compare de la tectonique Neogene des bassins du sud de Chypre et du basin d'Antalya (Turquie), *These, Universite de Paris-Sud, Centre d'Orsay*, p. 1-238

Eaton, S. and Robertson, A.H.F. [1993] The Miocene Paghna Formation, southern Cyprus and its relationship to the Neogene tectonic evolution of the eastern Mediterranean, *Sedimentary Geology*, 86, p. 273-296

Elion, P., [1983] Etude structural et sedimentologique du basin Neogene de Pissouri (Chypre), *These, Universite de Paris-Sud, Centre d'Orsay*, p. 1-235

Ergun, M., Okay, S., Sari, C., Oral, E.Z., Ash, M., Hall, J., Miller, H., [2005] Gravity anomalies of the Cyprus Arc and their tectonic implications, *Marine Geology*, 221, p. 349-358

Esestine, P., Hewitt, A., Hodgson, N., [2016] Zohr – A newborn carbonate play in the Levantine Basin, East-Mediterranean, *First Break*, vol.34, p. 87-93

Faccena, C., Bellier, O., Martinod, J., Piromallo, C., Regard, V., [2006] Slab detachment beneath eastern Anatolia: A possible cause for the formation of the North Anatolian fault, *Earth and Plan. Science letters*, 242, p. 85-97

Follows, E. J., [1992] Patterns of reef sedimentation and diagenesis in Miocene of Cyprus, *Sedimentary Geology*, 79, p. 225-253

Follows, E. J., Robertson, A. H. F. and Scoffin, T. P., [1996] Tectonic controls on Miocene reefs and related carbonate facies in Cyprus, *Soc. For Sedimentary Geol.*, p. 295-315

Frizon de Lamotte, D., C. Raulin, N. Mouchot, J.-C. Wrobel-Daveau, C. Blanpied, and J.-C. Ringenbach [2011], The southernmost margin of the Tethys realm during the Mesozoic and Cenozoic: Initial geometry and timing of the inversion processes, *Tectonics*, Vol.30, TC3002, doi: 10.1029/2010TC002691

Gardosh, M. and Druckman, Y., [2006] Seismic stratigraphy, structure and tectonic evolution of the Levantine basin, offshore Israel, *in* Tectonic Development of the Eastern Mediterranean Region, *edited by* A. H. F. Robertson and D. Mountrakis, *Geol. Soc. London, Spec. Publ.*, 260, p.201-227

Gardosh, M., Garfunkel, Z., Druckman, Y., Buchbinder, B., [2010] Tethyan rifting in the Levant region and its role in early Mesozoic crustal evolution, *in* Evolution of the Levant margin and western Arabia platform since the Mesozoic, *edited by* C. Homberg and M. Bachmann, *Geol. Soc. London, Spec. Publ.*, 341, p.9-36

Garfunkel, Z. and Derin, B., [1984] Permian-early Mesozoic tectonism and continental margin formation in Israel and its implications for the history of the Eastern Mediterranean, *in* The geological evolution of the Eastern Mediterranean, *edited by* R.J. Dixon and A.H.F. Robertson, *Geol. Soc. London, Spec. Publ.*, 17, p.187-201

Garfunkel, Z., [1998] Constrains on the origin and history of the Eastern Mediterranean basin, *Tectonophysics*, 298, p.5-35

Garfunkel, Z., [2004] Origin of the Eastern Mediterranean basin: a re-evaluation, *Tectonophysics*, 391, p.11-34

Gass, I. G. and Masson-Smith, D., [1963] The geology and gravity anomalies of the Troodos massif, Cyprus, *Royal Society Publishing, Vol.* 255, p. 418-466

Geoter, [2005] Study of active tectonics in Cyprus for Seismic risk mitigation, Final Report, *Geological Survey Department of Cyprus*

Ghalayini, R., Daniel, J.M., Homberg, C., Nader, F.H., Comstock, J.E., [2014], Impact on Cenozoic strike-slip tectonics on the evolution of the northern Levant Basin (offshore Lebanon). *Tectonics*, Vol. 33, doi:10.1002/2014TC003574

Ghalayini, R., [2015] Structural modelling of the complex Cenozoic zone of the Levant Basin offshore Lebanon, *PhD thesis, University of Pierre and Marrie Curie.*

Ghalayini, R., Daniel, J.M., Homberg, C., Nader, F.H., [2016], Growth of layer-bound normal faults under a regional anisotropic stress field. *in* The Geometry and Growth of Normal Faults,

*edited by C. Childs, R.E. Holdsworth, C.A.L. Jackson, T. Manzcchi, J.J. Walsh and G. Yielding, Geol. Soc. London, Spec. Publ., 439*

Ghalayini, R., Daniel, J.M., Homberg, C., Nader, F.H., Darnault, R., Mengus, J.M., Barrier, E., [2017], The effect of the Palmyra Trough and Mesozoic structures on the Levant margin and on the evolution of the Levant restraining bend, *edited by F. Roure et al., Lithosphere Dynamics and Sedimentary Basins of the Arabian Plate and Surrounding Areas, Frontiers in Earth Sciences, DOI 10.1007/978-3-319-44726-1\_7*

Granot, R., [2016], Palaeozoic oceanic crust preserved beneath the eastern Mediterranean, *Nature Geoscience, 9, p. 701-705*

Hadjistavrinou, Y., and Constantinou, G., [1977] Hydrogeology of the Akrotiri Peninsula, *Cyprus Geol. Surv. Dept. Bull., 7*

Hall, J., Aksu, A.E., Calon, T.J., Yasar, D., [2005a] Varying tectonic control on basin development at an active microplate margin: Latakia basin, eastern Mediterranean, *Mar. Geol., 221, p.15-60*

Hall, J., Calon, T.J., Aksu, A.E., Meade, S.R., [2005b] Structural evolution of the Latakia Ridge and Cyprus basin at front of the Cyprus Arc, Eastern Mediterranean sea, *Mar. Geol., 221, p.261-297*

Hall, J., Aksu, A.E., Elitez, I., Yaltirak, C., Cifci, G., [2014] The Fethiye-Burdur fault zone: a component of upper plate extension of the subduction transform edge propagator fault linking Hellenic and Cyprus Arcs, Eastern Mediterranean, *Tectonophysics, 635, p. 80-99*

Harrison, R.W., Newell, N.L., Batihanli, H., Panayides, I., McGeehin, J.P., Mahan, S.A., Ozhur, A., Tsiolakis, E., Necdet, M., [2004] Tectonic framework and Late Cenozoic tectonic history of the northern part of Cyprus: implications for the earthquake hazards and regional tectonics, *Journ. of Asian Earth Scien., 23, p. 191-210*

Harrison, R.W., [2008], A model for the plate tectonic evolution of the Eastern Mediterranean region that emphasizes the role of transform (strike-slip) structures, *1<sup>st</sup> WSEAS International conference on Environmental and Geological Science and Engineering (EG'08) Malta, September 11-13, 2008*

Harrison, R.W., Newell, W., Panayides, I., Stone, B., Tsiolakis, E., Necdet, M., Batihanli, H., Ozgur, A., Lord, A., Berksoy, O., Zomeni, Z., Schindler, S.J., [2008], Bedrock geological map of the greater Lefkosia Area, Cyprus, *US Geological Survey Scientific Investigations Map*, 3046.

Harrison, R.W., Tsiolakis, E., Stone, B.D., Lord, A., McGeehin, J.P., Mahan, S.A., Chirico, P., [2012], Late Pleistocene and Holocene uplift history of Cyprus: implications for active tectonics along the southern margin of the Anatolian microplate, *Geol. Soc. London, Spec. Publ.*, 372, p. 561-584

Hawie, N., Gorini, C., Deschamps, R., Nader, F.H., Montadert, L., Granjeon, D., Baudin, F., [2013] Tectono-stratigraphic evolution of the northern Levant Basin (offshore Lebanon), *Mar. and Petrol. Geology*, 48, p. 392-410

Homberg, C., Barrier, E., Mroueh, M., Hamdan, W., Higazi, F., [2010] Basin tectonics during the early Cretaceous in the Levant margin, *Levant, Jour. of Geodynamics*, 47, p. 218-223

Hsu, K.J., Montadert, L., Bernoulli, D., Cita, M.B., Erickson, A., Garrison R.E., Kidd, R.B., Melieres, F., Muller, C., Wright, R., [1977] History of the Mediterranean salinity crisis, *Nature*, Vol. 267, p. 399-403

Hudec, M.R., Jackson, M.P.A., [2009], Interaction between spreading salt canopies and their peripheral thrust systems, *Jour. Of Struct. Geol.*, Vol. 31, p. 1114-1129

Inati, L., Zeyen, H., Nader, F.H., Adelinet, M., Sursock, A., Rahhal, M.E., Roure, F., [2016], Lithospheric architecture of the Levant Basin (Eastern Mediterranean region): A 2D modeling approach, *Tectonophysics*, 693, p. 143-156

Jolivet, L. and Faccenna, C., [2000] Mediterranean extension and the Africa-Eurasia collision, *Tectonics*, Vol. 19, p. 1095-1106

Kelling, G., Goccen, S. L., Floyd, P. A., Gokcen, N., [1987] Neogene tectonics and plate convergence in the eastern Mediterranean: new data from southern Turkey, *Geology*, Vol. 15, p. 425-429

Kempler, D., [1998] Eratosthenes seamount: the possible spearhead of incipient continental collision in the Eastern Mediterranean, in *Proceedings of the Ocean Drilling Program*, edited

by Robertson, A.H.F., Emeis, K.C., Richter, C., Camerlenghi, A., *Scientific Results, Vol.160*, p.709-721

Kempler, D. and Garfunkel, Z., [1991] The northeast Mediterranean triple junction from a plate kinematic point of view, *Bull. Tech. Univ. Instabul, Vol. 44*, p. 425-454

Kempler, D. and Garfunkel, Z., [1994] Structures and kinematics in the northeastern Mediterranean: A study of an irregular plate boundary, *Tectonophysics, 234*, p. 19-32

Kinnaird, T.C., [2008] Tectonic and sedimentary response to oblique and incipient continental-continental collision the easternmost Mediterranean (Cyprus), *unpublished Phd thesis, University of Edinburgh*

Kinnaird, T.C., Robertson, A.H.F., Morris, A., [2011] Time of uplift of the Troodos massif (Cyprus) constrained by sedimentary and magnetic polarity evidence, *J. Geol. Soc., V. 168*, p.457-470

Kinnaird, T.C., Robertson, A.H.F., [2013] Tectonic and sedimentary response to subduction and incipient continental collision in southern Cyprus, easternmost Mediterranean region, *Geol. Soc. London, Spec. Publ. 373*, p.585-614

Klimke, J., Ehrhardt, A., [2014] Impact and implication of the Afro-Eurasian collision south of Cyprus from reflection seismic data, *Tectonophysics, 626*, p.105-119

Lapierre, H., [1971] Geological map of Polis – Paphos Area

Lapierre, H., [1975] Les formations sedimentaires et eruptives des nappes de Mamonia et leurs relations avec le massif du Troodos (Chypre occidentale), *Memoires de la societe geologique de France, 123*, p. 1-132

Lapierre, H., Bosch, D., Narros, A., Mascle, G.H., Tardy, M., Demant, A., [2007] The Mamonia Complex (SW Cyprus) revisited: remnant of Late Triassic intra-oceanic volcanism along the Tethyan southwestern passive margin, *Geol. Mag., 144(1)*, p.1-19

Le Pichon, X. and Kreemer, C., [2010] The Miocene-to-Present kinematic evolution of the Eastern Mediterranean and Middle East and its implications for Dynamics, *Annual. Rev. Earth Planet, Sci.* 2010, 38, p. 323-351, doi:10.1146/annurev-earth-040809-152419

Lord, A. R., Panayides, I., Urquhart, E., Xenophontos, C., [2000], A biochronostratigraphical framework for the Late Cretaceous-Recent circum Troodos sedimentary sequence, Cyprus, in *Proceedings of the third international conference on the Geology of Eastern Mediterranean*, edited by Panayides, I., Xenophontos, C. and Malpas, J., [2000], p. 289-297

Lord, A. R., Harrison, R., W., BouDagher-Fadel, M., Stone, B., D., Varol, O., [2009] Miocene mass transport sediments, Troodos massif, Cyprus, *Proceedings of the Geolo. Assoc.*, 120, p. 133-138

Makris, J., Ben-Avraham, Z., Behle, A., Ginzburg, A., Giese, P., Steinmetz L., Whitmarsh, R.B., Eleftheriou, S., [1983] Seismic refraction profiles between Cyprus and Israel and their interpretation, *Geoph. J. of the Royal Astronomical Society*, 75, p.575-591

Malpas, J., Calon, T. and Squires, G., [1993] The development of a Late Cretaceous microplate suture zone in SW Cyprus, in *Magnetic Processes and Plate Tectonics*, edited by Prichard, H. M., Alabaster, T., Harris, N. B. W. and Neary, C. R., *Geol. Soc. Special Publ.*, Vol. 76, p 177-195

Mantis, M., [1971] Paleontological evidence defining the age of the Troodos Pillow Lava series in Cyprus, *Kypriakos Logos*, Vol. III., no. 15-16, p. 202-208

Mantis, M., [1977] The stratigraphy of a deep borehole at palia Lemesos area, *Bull. Of Cyprus Geographical Assoc.*, p. 3-16

McCallum, J.E., Scrutton, R.A., Robertson, A.H.F., Ferrari, W., [1993] Seismostratigraphy and Neogene-Recent depositional history of the south central continental margin of Cyprus, *Marine and Petroleum Geology*, Vol. 10, p. 426-438

McClusky, S., Balassanian, S., Barka, A., Demir, C., Ergintav, S., Georgiev, I., Gurkan, O., Hamburger, M., Hurst, K., Kahle, H., Kastens, K., Kekelidze, G., King, R., Kotzev, V., Lenk, O., Mahmoud, S., Mishin, A., Nadariya, M., Ouzounis, A., Paradissis, D., Peter, Y., Prilepin, M., Reilinger, R., Sanli, I., Seeger, H., Tealeb, A., Toksoz, M.N. and Veis, G., [2000] Global

Positioning System constraints on plate kinematics and dynamics in the eastern Mediterranean and Caucasus, *Jour. Of Geoph. Research*, Vol. 105, No. B3, p. 5695-5719

McClusky, S., Reilinger, R., Mahmoud, S., Ben Sari, D., Tealeb, A., [2003], GPS constraints on Africa (Nubia) and Arabia plate motions, *Geophys. J. Int.*, Vol. 155, p. 126-138

Montadert, L., Lie, O., Semb, P.H., Kassinis, S., [2010] New seismic may put offshore Cyprus hydrocarbon prospects in the spotlight, *First Break*, Vol.28 April 2010, p.91-101

Montadert, L., Nicolaides, S., Semb, H.P., Lie, O., [2014] Petroleum Systems Offshore Cyprus, in *Petroleum systems of the Tethyan region*, edited by L. Marlow, C. Kendall and L. Yose, *AAPG memoir 106*, p.301-334

Morris, A., Anderson, M.W., Inwood, J., Robertson, A.H.F., [2006] Paleomagnetic insights into the evolution of Neotethyan oceanic crust in the eastern Mediterranean, in *Tectonic Development of the Eastern Mediterranean Region*, edited by A. H. F. Robertson and D. Mountrakis, *Geol. Soc. London, Spec. Publ.*, 260, p.351-372

Moustafa, A. R., [2010] Structural setting and tectonic evolution of the North Sinai folds, Egypt, in *Evolution of the Levant margin and western Arabia platform since the Mesozoic*, edited by C. Homberg and M. Bachmann, *Geol. Soc. London, Spec. Publ.*, 341, p.37-63

Mukasa, S. B. and Ludden, J. N., [1987] Uranium-lead isotopic ages of plagiogranites from the Troodos ophiolite, Cyprus and their tectonic significance, *Geology*, Vol. 15, p. 825-828

Netzeband, G., Gohl, K., Hubscher C., Ben-Avraham, Z., Dehghani, G., Gajewski, D., Liersch, P., [2006] The Levantine basin – crustal structure and origin, *Tectonophysics*, 418, p.167-188

Ori, G. G. and Friend, P. F., [1984] Sedimentary basins formed and carried piggy back on active thrust sheets, *Geology*, Vol. 12, p. 475-478

Orszag-Sperber, F., Rouchy, J. M., Elion, P., [1989] The sedimentary expression of regional tectonic events during the Miocene-Pliocene transition in the southern Cyprus basins, *Geol. Mag.*, 126, p. 291-299

Pantazis, T.M., [1978], Cyprus Evaporites, *Initial reports of the deep sea drilling project, Vol. 42, part 2*, p. 1185-1194

Papadimitriou, E.E. and Karakostas, V.G., [2006] Earthquake generation in Cyprus revealed by the evolving stress field, *Tectonophysics*, 423, p. 61-72

Papazachos, B.C. and Papaioannou, CH. A., [1999] Lithospheric boundaries and plate motions in the Cyprus area, *Tectonophysics*, 308, p. 193-204

Payne, A.S. and Robertson, A.H.F., [1995] Neogene supra-subduction zone extension in the Polis graben system, westCyprus, *J. Geol. Soc. London*, 152, p.613-628

Payne, A.S., and Robertson, A.H.F.,[2000] Structural evolution and regional significance of the Polis graben system, western Cyprus, *in Proceedings of the Third Internal Conference on the geology of the EasternMediterranean, edited by Panayides, I., Xenophontos, C. and Malpas,J.,Cyprus Geological Survey Department, Nicosia.*

Petit, J. P., [1987] Criteria for the sense of movement on fault surfaces in brittle rocks, *Jour. Of Struct. Geol., Vol. 9*, p. 597-608

Prichard, H. M. and Maliotis, G., [1998] Gold mineralization associated with low-temperature, off-axis, fluid activity in the Troodos ophiolite, Cyprus, *Journ. Of the Geol. Soc. Of London, Vol. 155*, p. 223-231

Reiche, S. and Hubscher, C., [2015] The Hecataeus Rise, easternmost Mediterranean: A structural record of Miocene-Quaternary convergence and incipient continent-continent collision at the African-Anatolian plate boundary, *Marine Petrol. Geol.*, 67, p. 368-388

Reilinger, R., McClusky, S., Vernant, P., Lawrence, S., Ergintav, S., Cakmak, R., Ozener, H., Kadirov, F., Guliev, I., Stepanyan, R., Nadariya, M., Hahubia, G., Mahmoud., S., Sakr, K., ArRajehi, A., Paradissis, D., Al-Aydrus, A., Prilepin, M., Guseva, T., Evren, E., Dmitrotsa, A., Filikov, S.V., Gomez, F., Al-Ghazzi, R., Karam, G., [2006], GPS constraints on continental deformation in the Africa-Arabia-Eurasia continental collision zone and implications for the dynamics of plate interactions, *J. Geophys. Res.*, 111, B05411, doi:10.1029/2005JB004051

Ricou, L. E., [1971], Le croissant péri-arabe: Une ceinture de nappes mises en place au Crétacé supérieur, *Rev. Geogr. Phys. Geol. Dyn.*, 13, p. 327-350

Ricou, L. E., Argyridis, I., Marcoux, J., [1975] L'axe calcaire du Taurus, un alignement de fenêtres arabo-africaines sous des nappes radiolaritiques, ophiolitiques et métamorphiques, *Bull. De la Soc. De Geol. de France*, 16, p. 107-111

Roberts, G. and Peace, D., [2007] Hydrocarbon plays and prospectivity of the Levantine basin, offshore Lebanon and Syria from modern seismic data, *GeoArabia*, Vol. 12, No.3, p.99-124

Robertson, A.H., [1975] Cyprus umbers: basalt-sediment relationships on the Mesozoic ocean ridge, *Journ. Of Geol. Soc. Of London*, Vol. 131, p. 511-531

Robertson, A.H., [1976] Origins of ochres and umbers: evidence from Skouriotissa, Troodos massif, Cyprus, *extract from transactions section b of the institution of Mining and Metallurgy*, Vol. 85, p. 244-251

Robertson, A.H., [1977] Tertiary uplift history of the Troodos massif, Cyprus, *Geol. Soc. Of America Bulletin*, Vol. 88, p.1763-1772

Robertson, A.H.F. and Dixon, J.E., [1984] Introduction: aspects of the geological evolution of the Eastern Mediterranean, *Geol. Soc. London, Spec. Publ.*, 17, p.1-74

Robertson, A.H.F., [1990] Tectonic evolution of Cyprus, *in Ophiolites: Oceanic Crustal Analogues*, edited by Malpas, J., Moores, E.M., Panayiotou, A., Xenophontos, C., *Geological Survey Department, Nicosia, Cyprus*, p. 235-252

Robertson, A.H.F., Kidd, R.B., Ivanov, M.K., Limonov, A.F., Woodside, J.M., Galindo-Zalvidar, J., Nieto, L., Scientific Party of the 1993 'TTR-3' cruise, [1995] Eratosthenes Seamount: collisional processes in the easternmost Mediterranean in relation to the Plio-Quaternary uplift of southern Cyprus, *Terra Nova*, 7, p. 254-264

Robertson, A.H.F., [1998] Late Miocene paleo-environments and tectonic setting of the southern margin of the Cyprus and the Eratosthenes seamount, *in Proceedings of the Ocean Drilling Program*, edited by Robertson, A.H.F., Emeis, K.C., Richter, C., Camerlenghi, A., *Scientific Results*, Vol.160, p.453-463

Robertson, A.H.F., [1998] Formation and destruction of the Eratosthenes seamount, Eastern Mediterranean sea and implications for collisional processes, *in* Proceedings of the Ocean Drilling Program, *edited by* Robertson, A.H.F., Emeis, K.C., Richter, C., Camerlenghi, A., *Scientific Results, Vol.160*, p.681-699

Robertson, A.H.F., [1998] Mesozoic-Tertiary tectonic evolution of the easternmost Mediterranean area: integration of marina and land evidence, *in* Proceedings of the Ocean Drilling Program, *edited by* Robertson, A.H.F., Emeis, K.C., Richter, C., Camerlenghi, A., *Scientific Results, Vol.160*, p.723-782

Robertson, A.H.F., [1998] Tectonic significance of the Eratosthenes seamount: a continental fragment in the process of collision with a subduction zone in the eastern Mediterranean (Ocean Drilling Program Leg 160), *Tectonophysics*, 298, p.63-82

Robertson, A.H.F., [2007] Overview of tectonic settings related to the rifting and the opening of Mesozoic ocean basins in the Eastern Tethys: Oman, Himalayas and Eastern Mediterranean regions, *in* Imaging, Mapping and Modelling Continental Lithosphere Extension and Breakup, *edited by* Kamer, G.D., Manatschal, G., Pinheiro, L.M., *Geol. Soc. London, Spec. Publ.*, 282, p.325-388

Robertson, A.H.F., Parlak, O., Ustaomer, T., [2012] Overview of the Paleozoic-Neogene evolution of the Neotethys in the Eastern Mediterranean region (southern Turkey, Cyprus, Syria), *Petrol. Geos.*, *Vol.18*, p.381-404

Sage, L., Letouzey, J., [1990] Convergence of the African and Eurasian Plate in the Eastern Mediterranean, *in* Petroleum and tectonics in mobile belts, *edited by* Letouzey, J. and Editions Technip, Paris, p. 49-68

Schattner, U., [2010] What triggered the early-to-mid Pleistocene tectonic transition across the entire eastern Mediterranean?, *Earth and Planetary Science Letters*, 289, p.539-548

Segev, A., Schattner, U., Lyakhovsky, V., [2011], Middle-Late Eocene structure of the southern Levant continental margin – Tectonic motion versus global sea-level change, *Tectonophysics*, 499, p. 165-177

Simonian, K.O., Gass, I.G., [1978] Arakapas fault belt, Cyprus: A fossil transform fault, *Geo. Soc. of America Bull.*, 89, p. 1220-1230

Stampfli, G.M. and Borel, G.D., [2002] A plate tectonic model for the Paleozoic and Mesozoic constrained by dynamic plate boundaries and restored synthetic oceanic isochrones, *Earth and Planetary Science Letters*, 196, p. 17-33

Stow, D., A., V., Braakenburg, N. E., Xenophontos, [1995] The Pissouri Basin fan-delta complex, southwestern Cyprus, *Sedimentary Geology*, 98, p. 245-262

Swarbrick, R. E, and Naylor, M. A., [1980] The Kathikas melange, SW Cyprus: Late Cretaceous submarine debris flows, *Sedimentology*, 27, p. 62-78

Swarbrick, R. E. and Robertson, A. F., [1980] Revised stratigraphy of the Mesozoic rocks of southern Cyprus, *Geol. Mag.*, 117, p. 547-563

Swarbrick, R. E., [1993] Sinistral strike slip and transpressional tectonics in an ancient oceanic setting: the Mamonia complex, southwest Cyprus, *Jour. Of the Geol. Soc. London*, Vol. 150, p. 381-392

Turner, W. M., [1992] Geological map of Akamas – Polis area, *Sheet III, IV*.

Urquhart, E. and Banner, F. T., [1994] Biostratigraphy of the supra-ophiolite sediments of the Troodos massif, Cyprus: the Cretaceous Perapedhi, Kannaviou, Moni and Kathikas Formations, *Geol. Mag.*, Vol. 131, p. 499-518

Vidal, N., Alvarez-Marron, J., Klaeschen, D., [2000a] The structure of the Africa-Anatolia plate boundary in the eastern Mediterranean, *Tectonics*, Vol. 19, No. 4, p.723-739

Vidal, N., Klaeschen, D., Kopf, A., Docherty, C., Von Huene, R., Krasheninnikov, V.A., [2000b] Seismic images at the convergence zone from south of Cyprus to the Syrian coast, eastern Mediterranean, *Tectonophysics*, 329, p. 157-170

Wdowinski, S., Ben-Avraham, Z., Arvidsson, R., Ekstrom, G., [2006] Seismotectonics of the Cyprian Arc, *Geophys. J. Int.*, 164, p. 176-181

Weisgerber, F., [1978] Stratigraphie et sedimentology du Miocene terminal et tu Pliocene inferieur au sud de Chypre: la bordure meridionale du massif du Troodos, *CES Geologie-Physique*, p. 1-175

Welford, J.K., Hall, J., Hubscher, C., Reiche, S., Louden, K., [2015] Crustal seismic velocity structure from the Eratosthenes seamount to Hecataeus Rise across the Cyprus Arc, eastern Mediterranean, *Geophys. J. Int.*, 200, p.933-951

Woodside, J., [1977] Tectonic elements and crust of the eastern Mediterranean sea, *Marine Geophysical Researches*, 3, p.317-354

Woodside, J.M., Mascle, J., Zitter, T.A.C., Limonov, A.F., Ergun, M., Volkonskaia, A., shipboard scientists of the Prismed II Expedition [2002] The Florense Rise, the western bend of the Cyprus Arc, *Marine Geol. Vol. 185*, p. 177-194

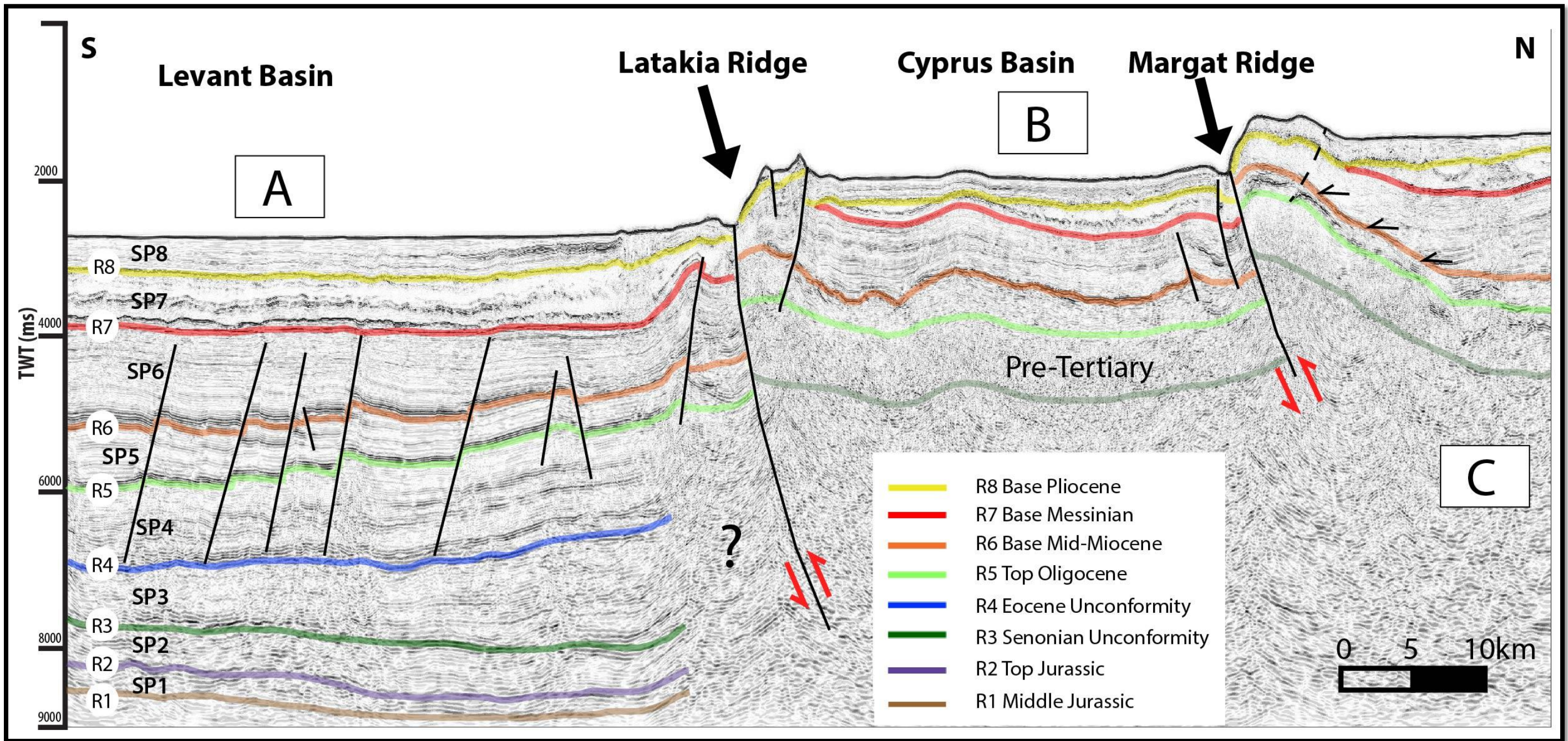
Zitter, T. A. C., Woodside, J. M., Mascle, J., [2000] Neotectonic accommodation between Hellenic and Cyprus Arcs, *Geology and Petroleum Geology of Mediterranean Basins, 1-4 October 2000, Malt*

Zitter, T.A.C., Woodside, J.M., Mascle, J., [2003] The Anaximander Mountains: a clue to the tectonics of southwest Anatolia, *Geol. Journal*, 38, p. 375-394

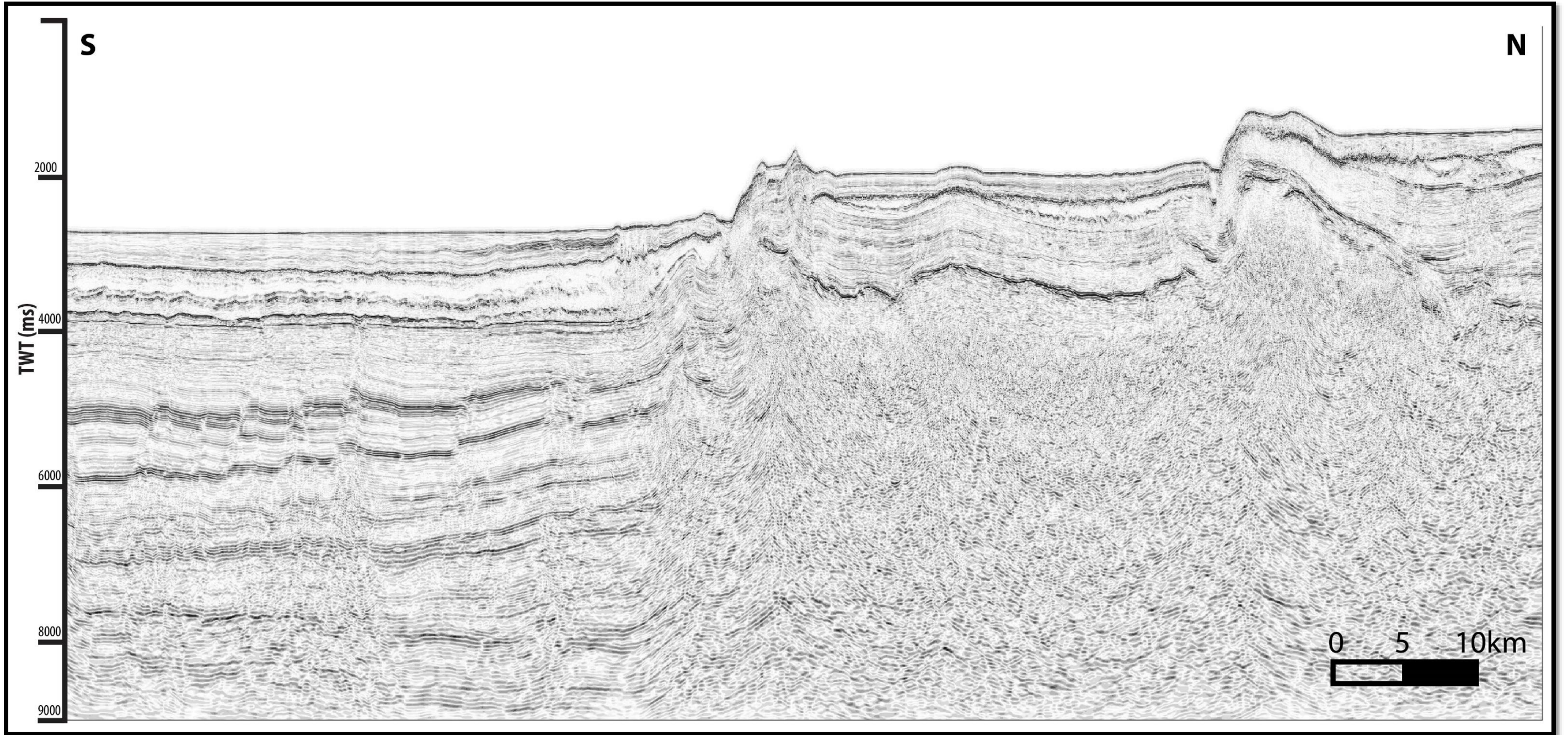
Zomeni, Z., and Georgiadou, I., [2015] Geological map of Pegeia – Steni Area, *Sheet 16 I & II*

Zomeni, Z., and Tsiolakis, E., [2008] Geological map of Pafos – Kallepeia Area, *Sheet 16 III & IV*.

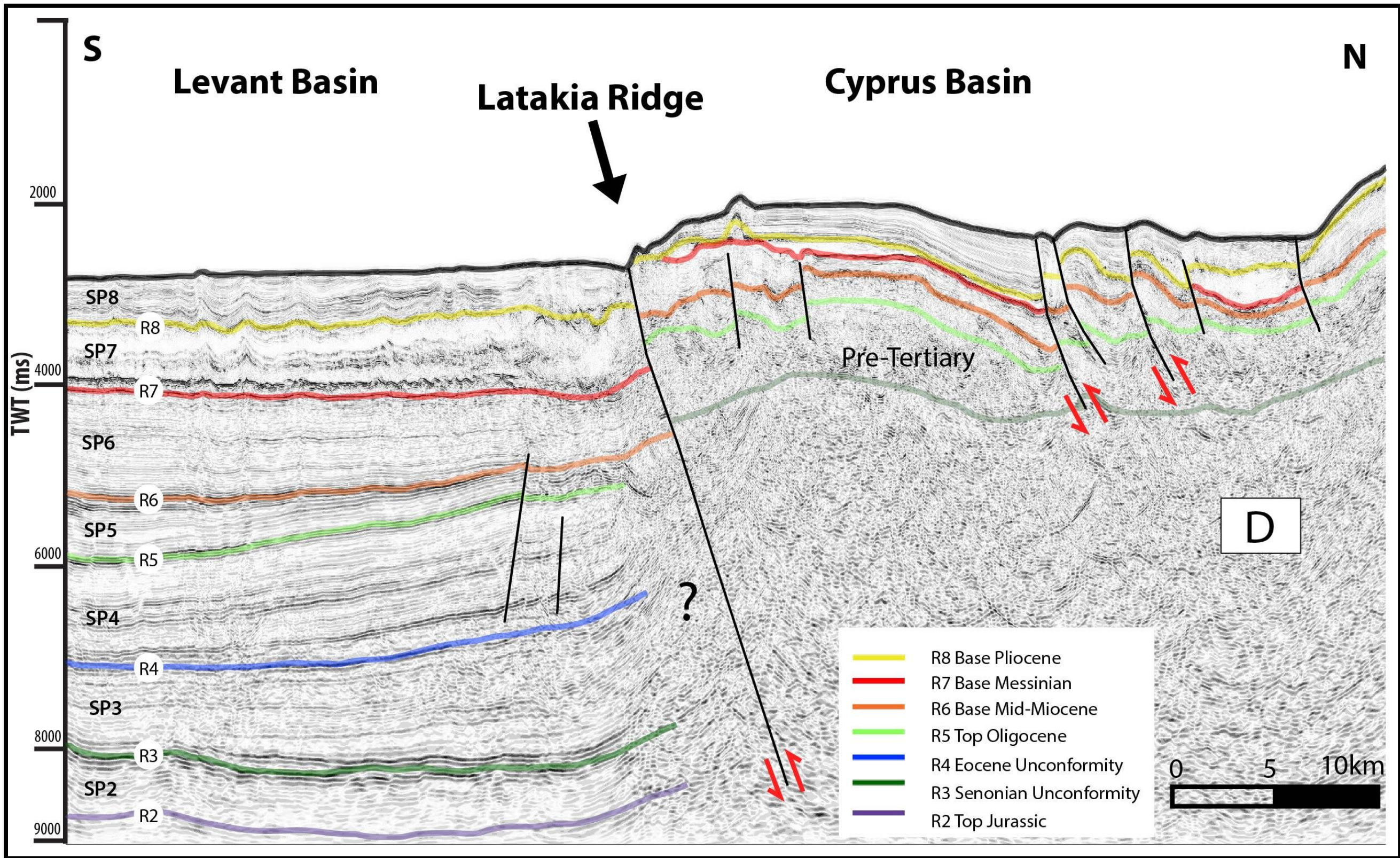
# *Appendix*



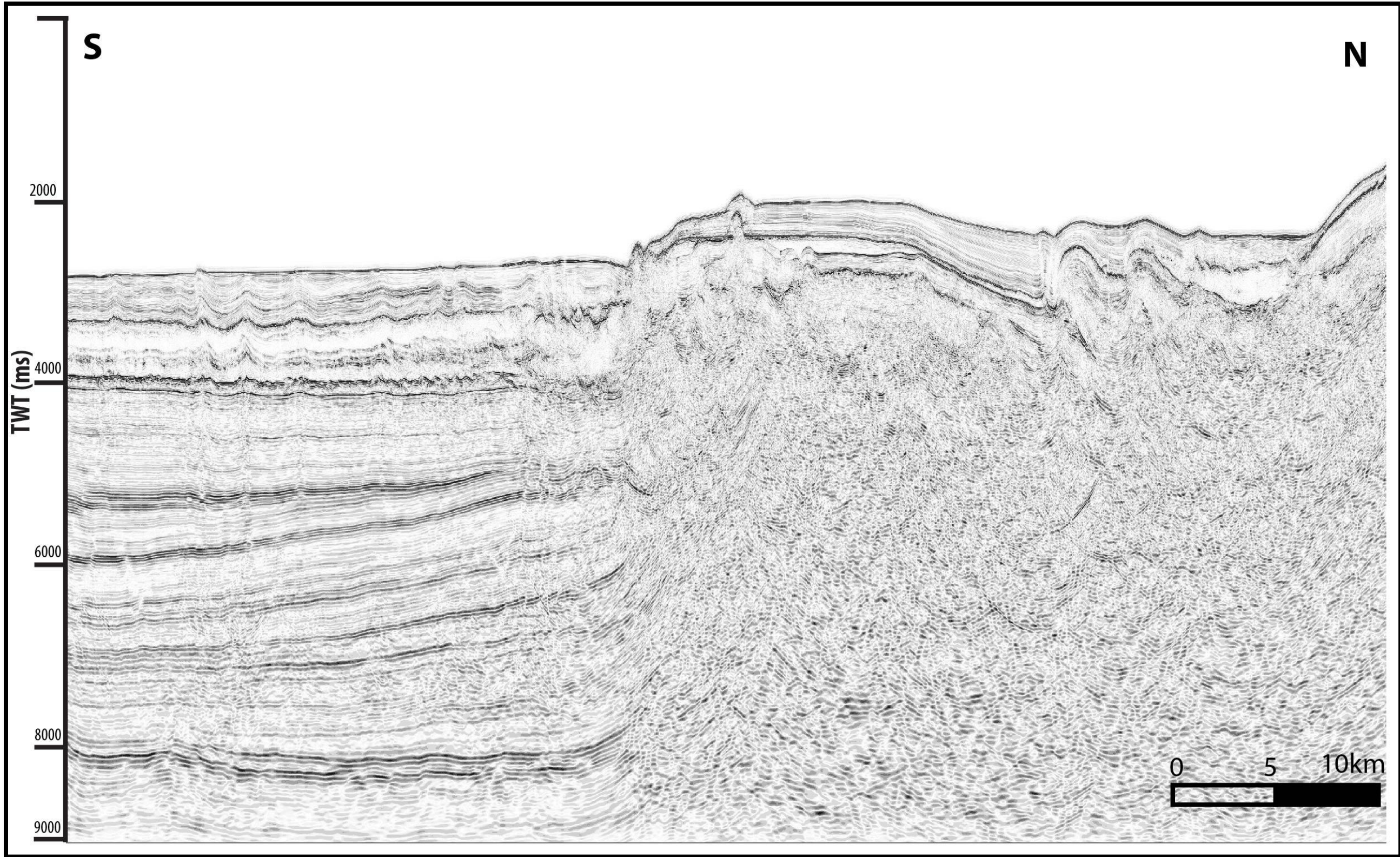
Interpreted Seismic profile 6063. As illustrated in Chapter 3, Figure 3 - 9.



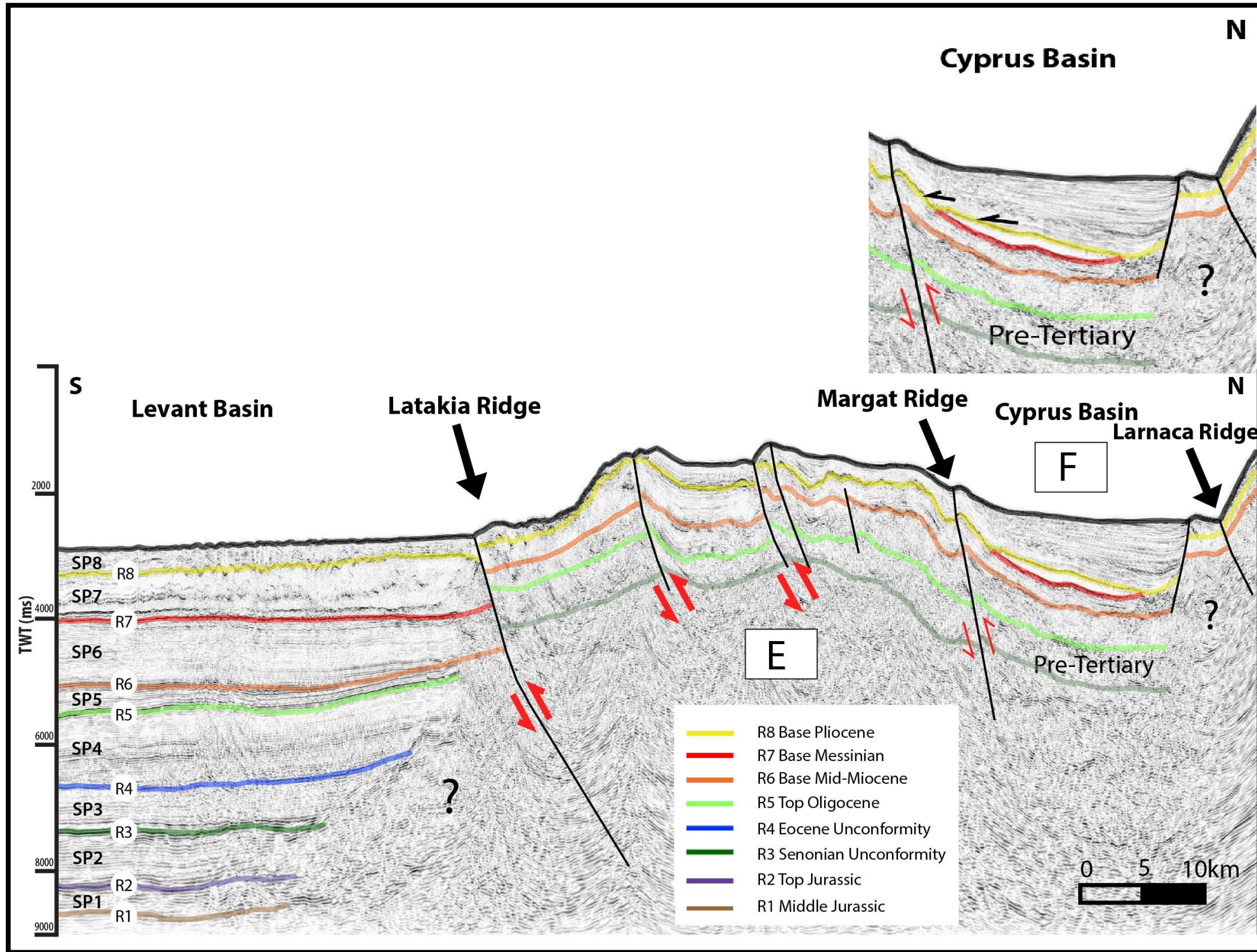
Un-interpreted Seismic profile 6063. As illustrated in Chapter 3, Figure 3 - 9.



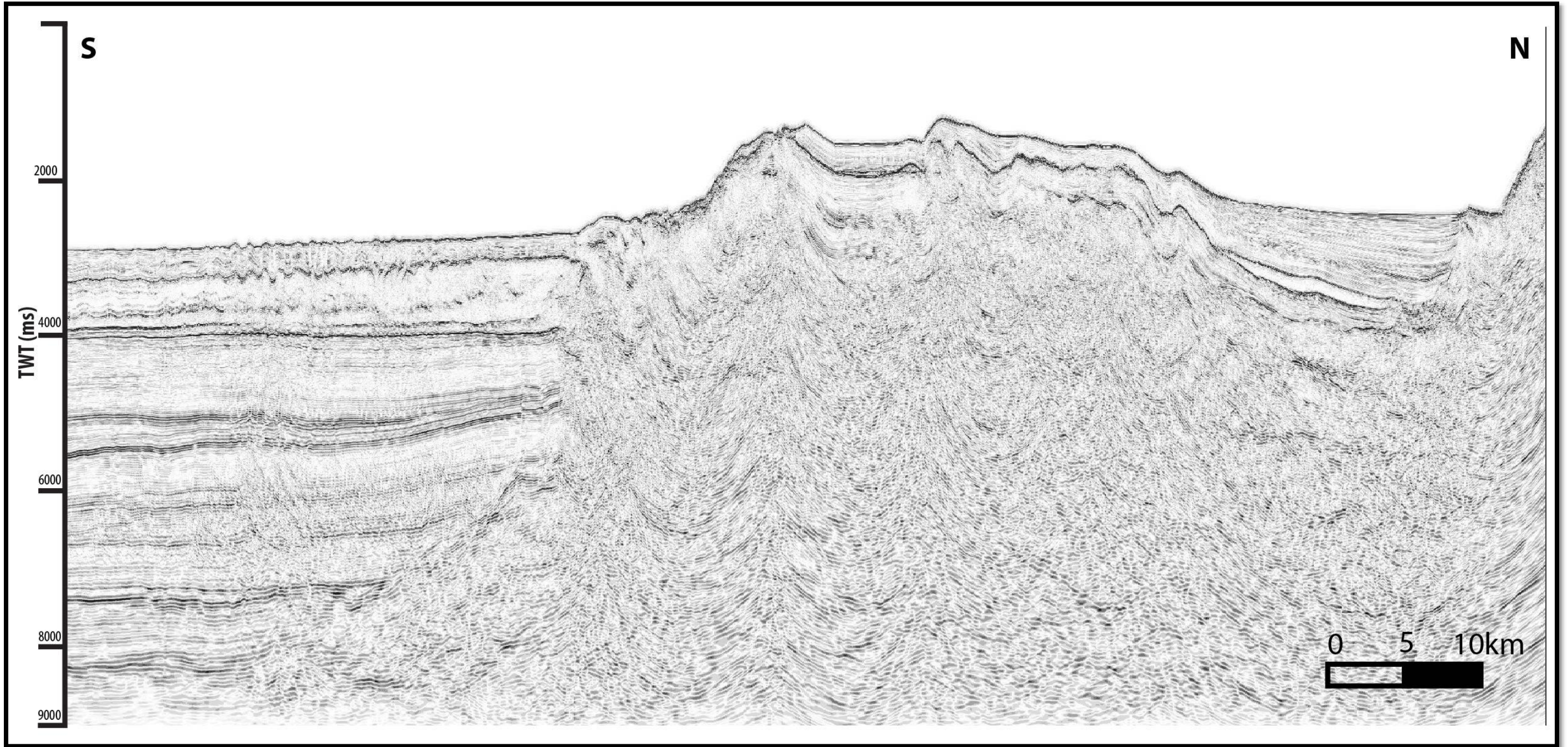
Interpreted seismic profile 6061. As illustrated in Chapter 3, Figure 3 - 10.



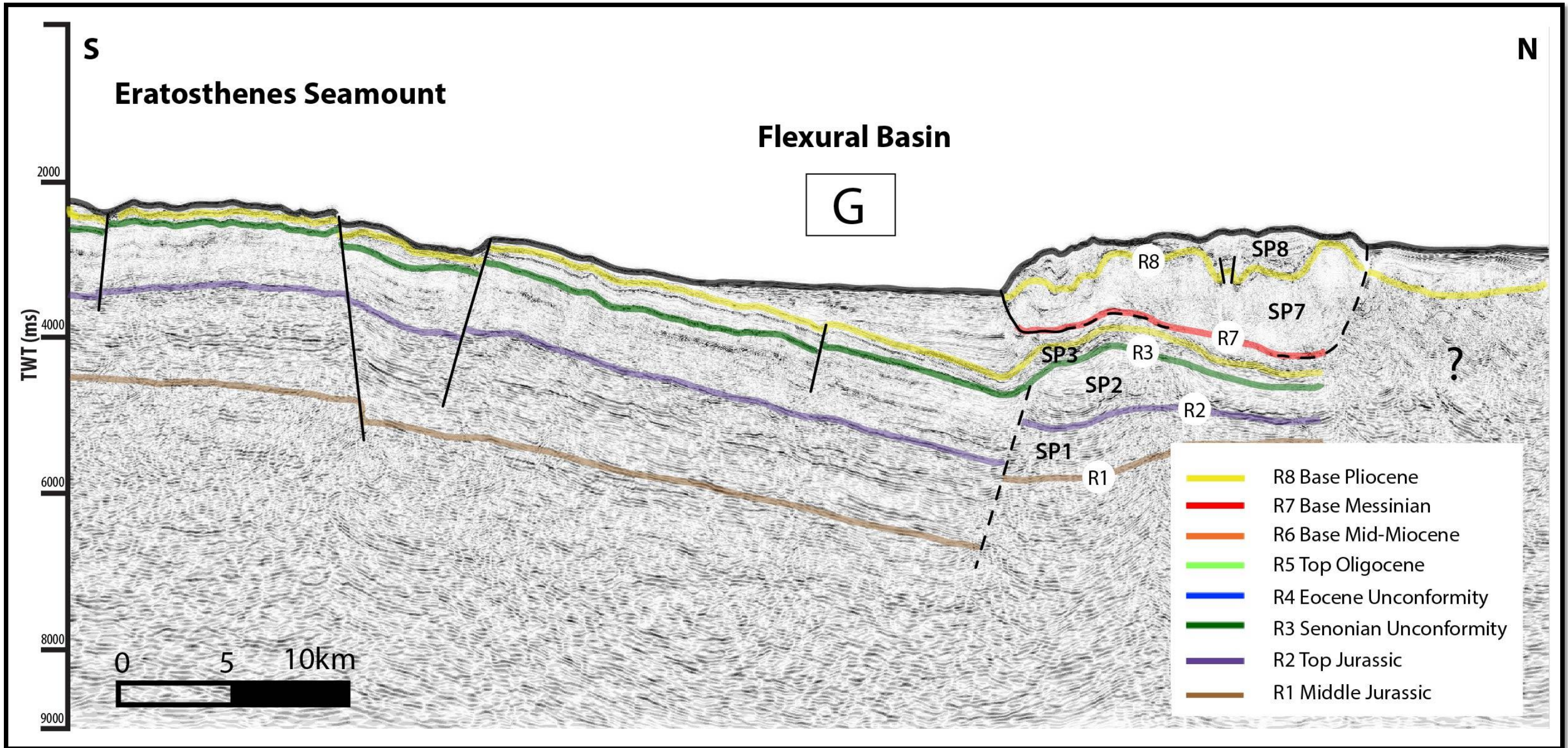
Un-interpreted seismic profile 6061. As illustrated in Chapter 3, Figure 3 - 10.



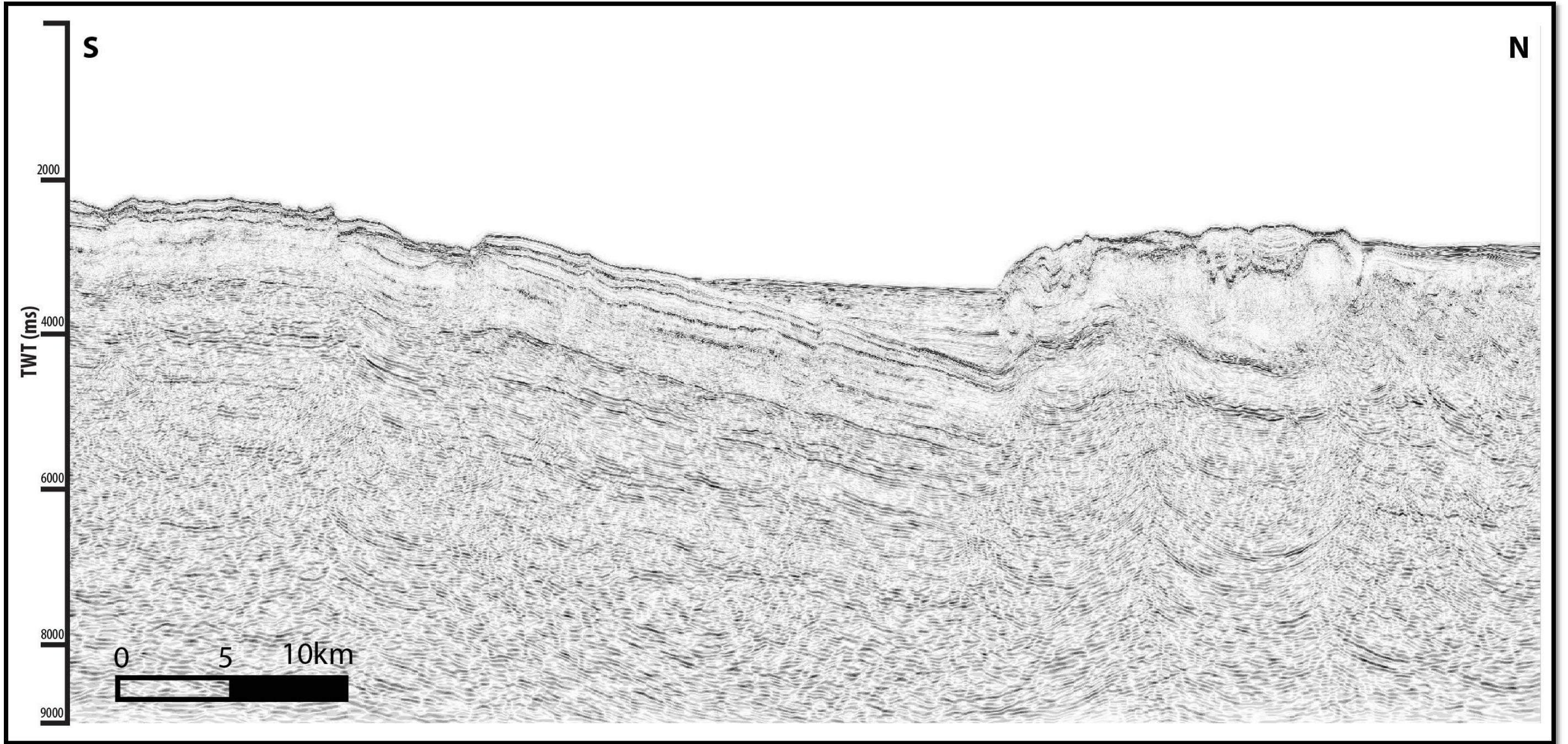
Interpreted seismic profile 6053. As illustrated in Chapter 3, Figure 3 - 12.



Un-interpreted seismic profile 6053. As illustrated in Chapter 3, Figure 3 - 12.



Interpreted seismic profile 6015. As illustrated in Chapter 3, Figure 3 - 13.



Un-interpreted seismic profile 6015. As illustrated in Chapter 3, Figure 3 - 13.

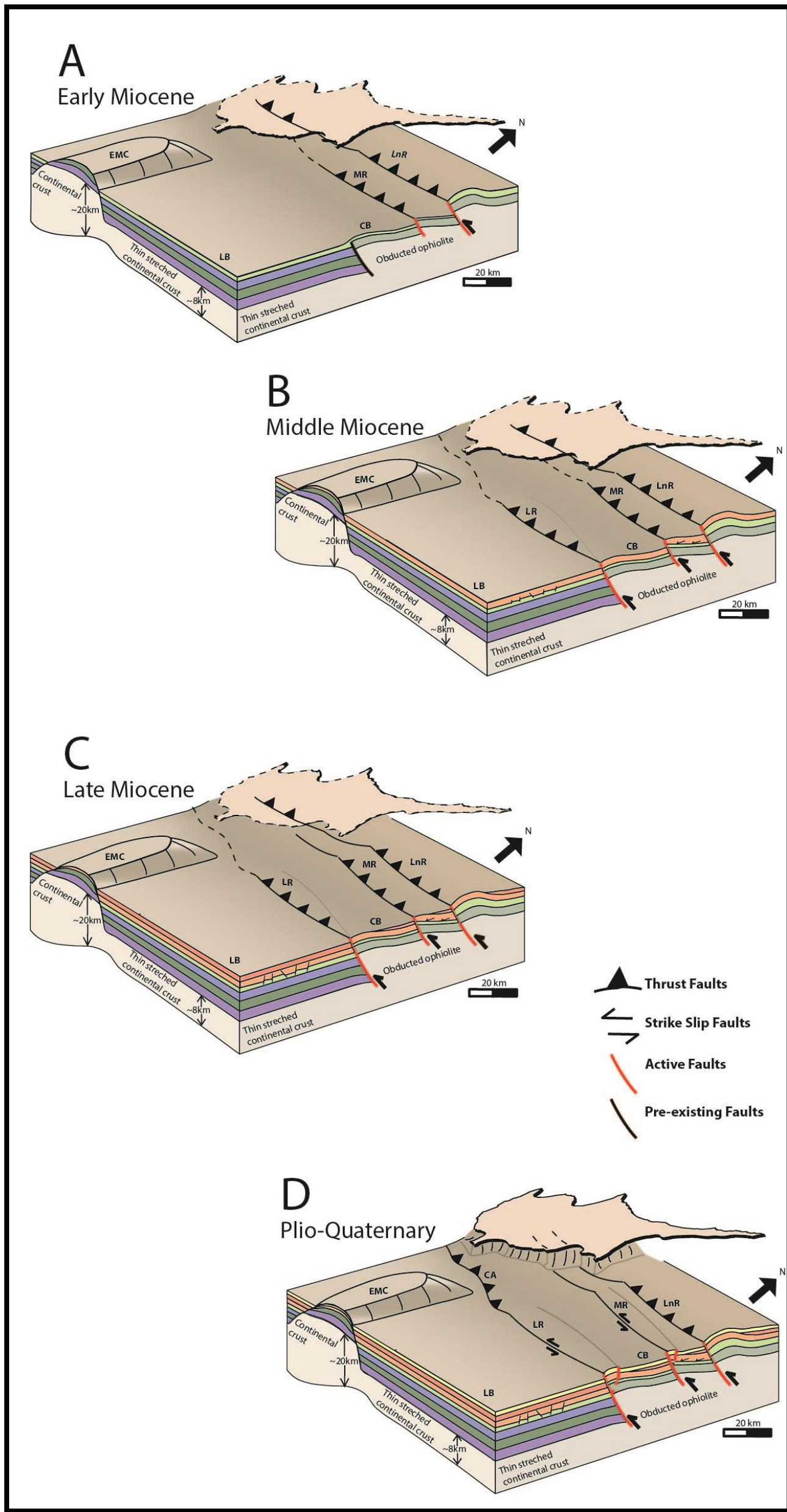


Figure 3 - 15 original size in text.

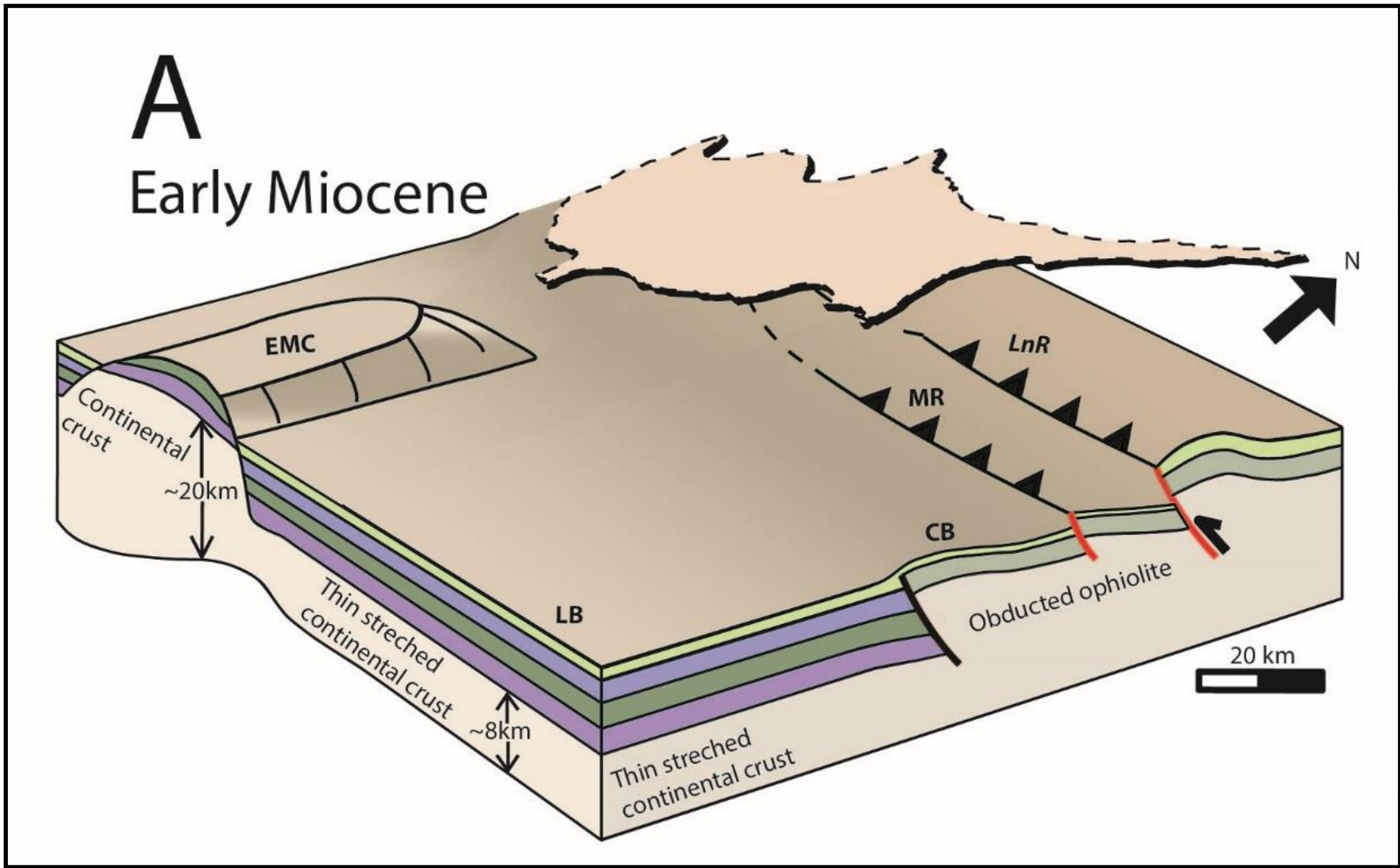


Figure 3 - 15 A: Early Miocene expanded

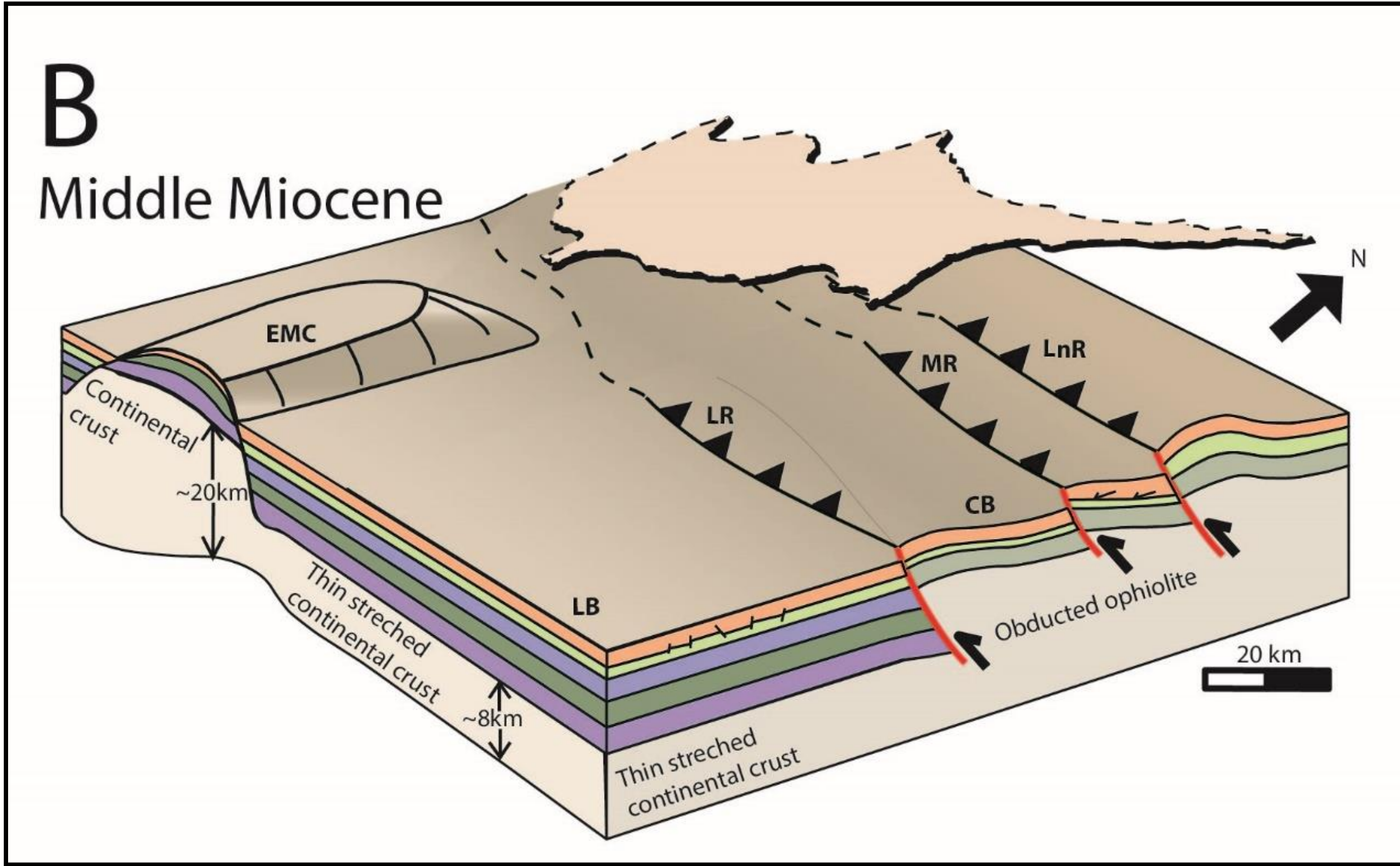


Figure 3 - 15 B: Middle Miocene expanded

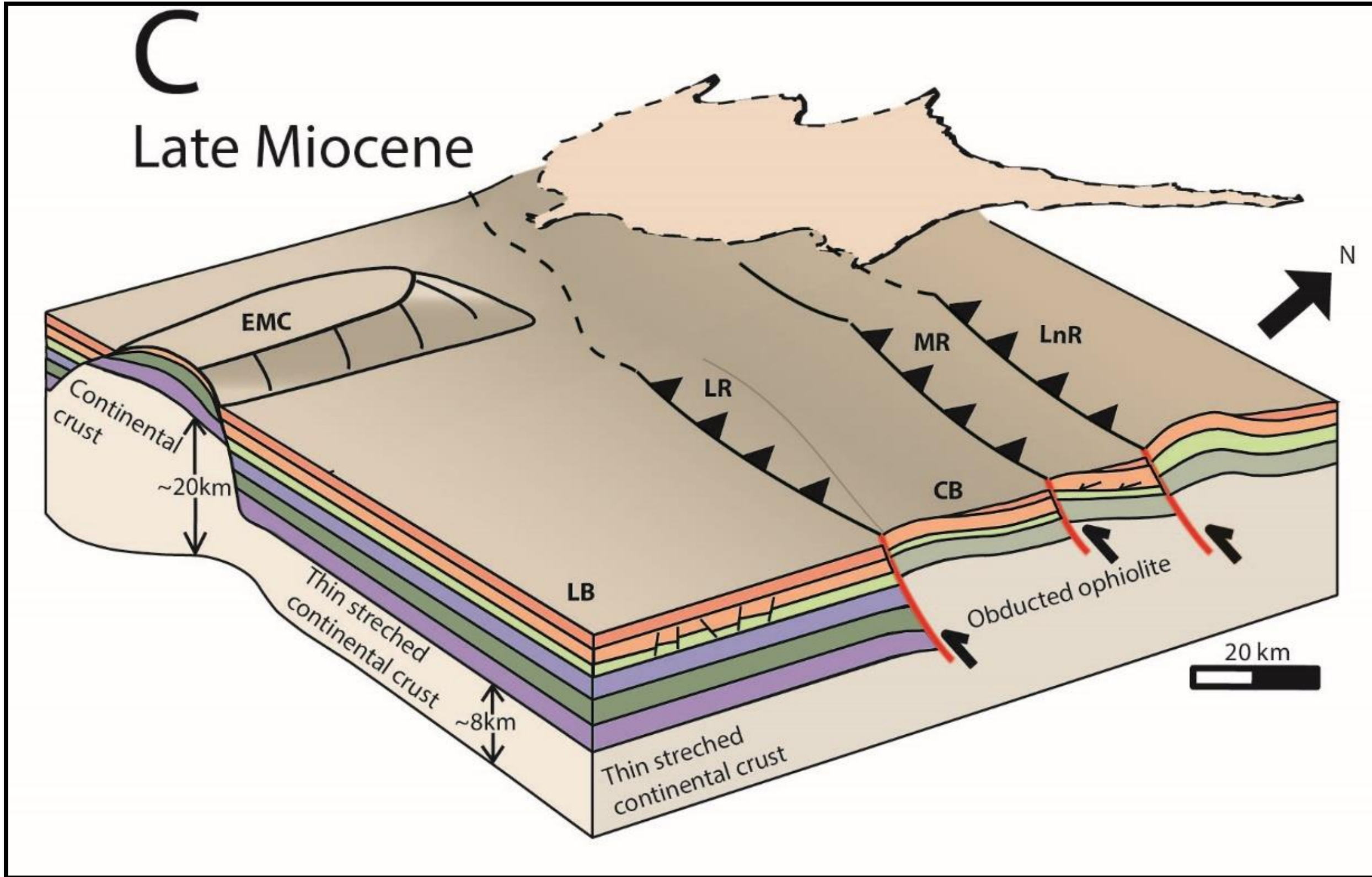


Figure 3 - 15 C: Late Miocene expanded

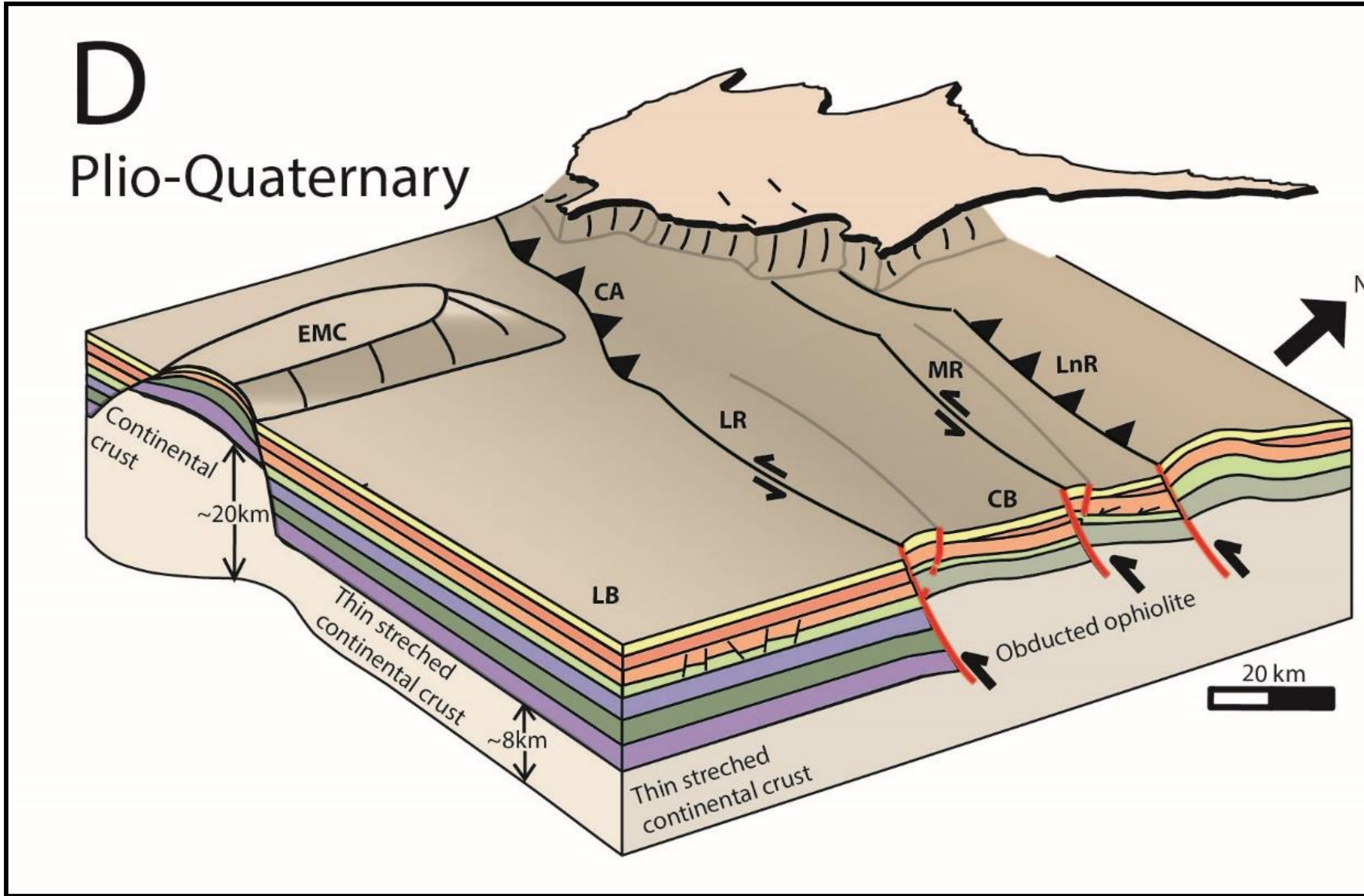


Figure 3 - 15 D: Plio-Pleistocene expanded